



SATHYABAMA

INSTITUTE OF SCIENCE AND TECHNOLOGY
(DEEMED TO BE UNIVERSITY)

Accredited "A" Grade by NAAC | 12B Status by UGC | Approved by AICTE

www.sathyabama.ac.in

SCHOOL OF ELECTRICAL AND ELECTRONICS ENGINEERING

DEPARTMENT OF ELECTRICAL AND ELECTRONICS ENGINEERING

UNIT – I - Electric Vehicle – SEE1628/SEEA3028

1.1 General Description of Vehicle Movement

Figure 1.1 shows the forces acting on a vehicle moving up a grade. The tractive effort, F_t , in the contact area between tires of the driven wheels and the road surface propels the vehicle forward. It is produced by the power plant torque and is transferred through transmission and final drive to the drive wheels. While the vehicle is moving, there is resistance that tries to stop its movement. The resistance usually includes tire rolling resistance, aerodynamic drag, and uphill resistance. According to Newton's second law, vehicle acceleration can be written as

$$\frac{dV}{dt} = \frac{\Sigma F_t - \Sigma F_{tr}}{\delta M}, \quad (1.1)$$

where V is vehicle speed, ΣF_t is the total tractive effort of the vehicle, ΣF_{tr} is the total resistance, M_V is the total mass of the vehicle, and δ is the mass factor, which is an effect of rotating components in the power train. Equation

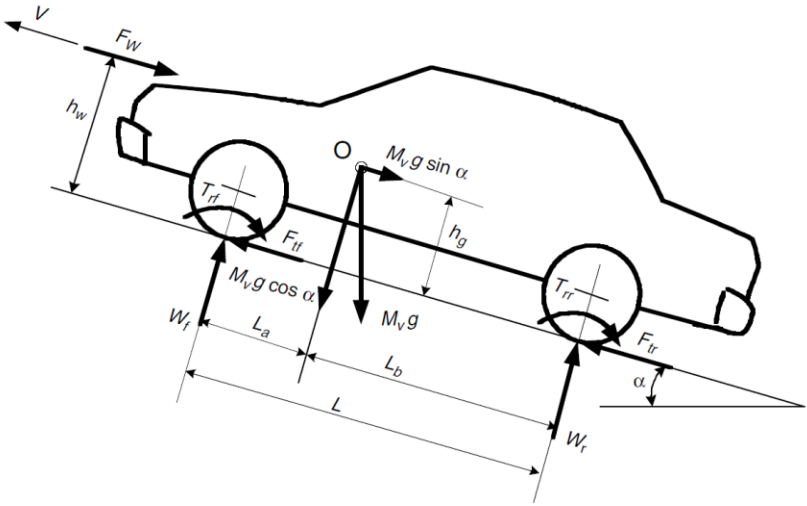


Figure 1.1
Forces acting on a vehicle

(1.1) indicates that speed and acceleration depend on tractive effort, resistance, and vehicle mass.

1.1.1 Vehicle Resistance

As shown in Figure 1.1, vehicle resistance opposing its movement includes rolling resistance of the tires, appearing in Figure 1.1 as rolling resistance torque T_{rf} and T_{rr} , aerodynamic drag, F_w , and grading resistance (the term $M_v g \sin \alpha$ in Figure 1.1). All of the resistances will be discussed in detail in the following sections.

Rolling Resistance

The rolling resistance of tires on hard surfaces is primarily caused by hysteresis in the tire materials. This is due to the deflection of the carcass while the tire is rolling. The hysteresis causes an asymmetric distribution of ground reaction forces. The pressure in the leading half of the contact area is larger than that in the trailing half, as shown in Figure 1.2(a). This phenomenon results in the ground reaction force shifting forward. This forwardly shifted ground reaction force, with the normal load acting on the wheel center, creates a moment, that opposes the rolling of the wheel. On soft surfaces, the rolling resistance is primarily caused by deformation of the ground surface as shown in Figure 1.2(b). The ground reaction force almost completely shifts to the leading half.

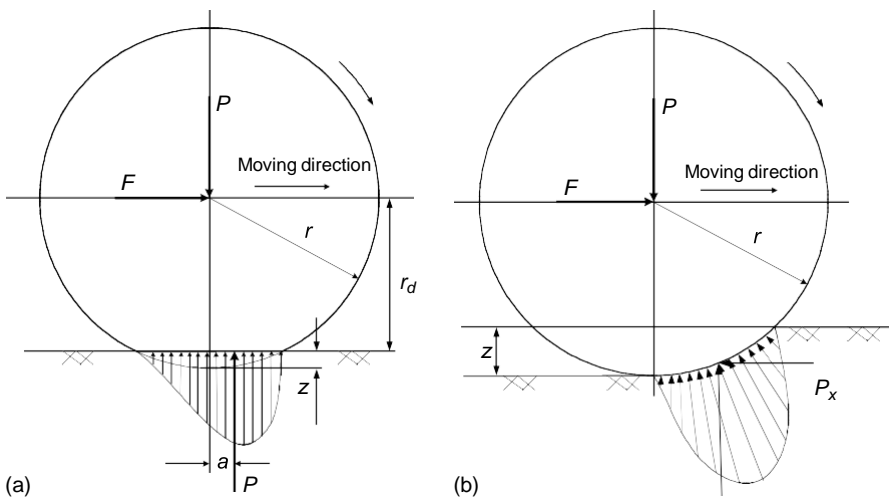


Figure 1.2

Tire deflection and rolling resistance on a (a) hard and (b) soft road surface

The moment produced by the forward shift of the resultant ground reaction force is called the rolling resistant moment, as shown in Figure 1.2(a), and can be expressed as

$$T_r = Pa. \tag{1.2}$$

To keep the wheel rolling, a force F , acting on the center of the wheels, is required to balance this rolling resistant moment. This force is expressed as

$$F = \frac{T_r}{r_d} = \frac{Pa}{r_d} = Pf_r \tag{1.3}$$

where r_d is the effective radius of the tire and $f_r = a/r_d$ is called the rolling resistance coefficient. In this way, the rolling resistant moment can be replaced equivalently by a horizontal force acting on the wheel center in the opposite direction of the movement of the wheel. This equivalent force is called rolling resistance with a magnitude of

$$F_r = Pf_r \tag{1.4}$$

where P is the normal load, acting on the center of the rolling wheel. When a vehicle is operated on a slope road, the normal load, P , should be replaced by the component, which is perpendicular to the road surface. That is,

$$F_r = Pf_r \cos \alpha, \tag{1.5}$$

where α is the road angle (refer to Figure 1.1).

The rolling resistance coefficient, f_r , is a function of the tire material, tire structure, tire temperature, tire inflation pressure, tread geometry, road roughness, road material, and the presence or absence of liquids on the road. The typical values of rolling resistance coefficients on various roads are given in Table 1.1.

TABLE 1.1
Rolling Resistance Coefficients

Conditions	Rolling resistance coefficient
Car tires on concrete or asphalt	0.013
Car tires on rolled gravel	0.02
Tar macadam	0.025
Unpaved road	0.05
Field	0.1–0.35
Truck tires on concrete or asphalt	0.006–0.01
Wheels on rail	0.001–0.002

the rolling resistance coefficient of passenger cars on concrete road may be calculated from the following equation:

$$f_r = f_0 + f_s \left(\frac{V}{100} \right)^{2.5} \quad (1.6)$$

where V is vehicle speed in km/h, and f_0 and f_s depend on inflation pressure of the tire.

In vehicle performance calculation, it is sufficient to consider the rolling resistance coefficient as a linear function of speed. For the most common range of inflation pressure, the following equation can be used for a passenger car on concrete road:

$$f_r = 0.01 \left(1 + \frac{V}{100} \right). \quad (1.7)$$

This equation predicts the values of f_r with acceptable accuracy for speeds up to 128 km/h.

Aerodynamic Drag

A vehicle traveling at a particular speed in air encounters a force resisting its motion. This force is referred to as aerodynamic drag. It mainly results from two components: shape drag and skin friction.

Shape drag: The forward motion of the vehicle pushes the air in front of it. However, the air cannot instantaneously move out of the way and its pressure is thus increased, resulting in high air pressure. In addition, the air behind the vehicle cannot instantaneously fill the space left by the forward motion of the vehicle. This creates a zone of low air pressure. The motion has therefore created two zones of pressure that oppose the motion of a vehicle by pushing it forward (high pressure in front) and pulling it backward (low pressure in the back) as shown in Figure 1.3. The resulting force on the vehicle is the shape drag.

Skin friction: Air close to the skin of the vehicle moves almost at the speed of the vehicle while air far from the vehicle remains still. In between, air

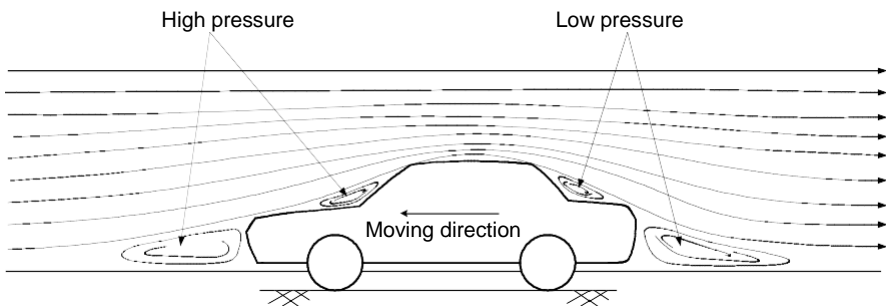


Figure 1.3
Shape drag

molecules move at a wide range of speeds. The difference in speed between two air molecules produces a friction that results in the second component of aerodynamic drag.

Aerodynamic drag is a function of vehicle speed V , vehicle frontal area A_f , shape of the vehicle, and air density ρ . Aerodynamic drag is expressed as

$$F_w = \frac{1}{2} \rho A_f C_D (V + V_w)^2, \tag{1.8}$$

where C_D is the aerodynamic drag coefficient that characterizes the shape of the vehicle and V_w is the component of wind speed on the vehicle's moving direction, which has a positive sign when this component is opposite to the vehicle speed and a negative sign when it is in the same direction as vehicle speed. The aerodynamic drag coefficients for a few types of vehicle body shapes are shown in Figure 1.4.

Grading Resistance

When a vehicle goes up or down a slope, its weight produces a component, which is always directed to the downward direction, as shown in Figure 2.5. This component either opposes the forward motion (grade climbing) or

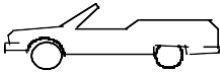

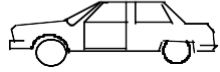
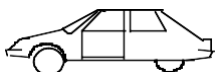


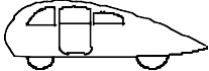
Vehicle Type	Coefficient of Aerodynamic Resistance
 Open convertible	0.5–0.7
 Van body	0.5–0.7
 Ponton body	0.4–0.55
 Wedge-shaped body; headlamps and bumpers are integrated into the body, covered underbody, optimized cooling air flow	0.3–0.4
 Headlamp and all wheels in body, covered underbody	0.2–0.25
 K-shaped (small breakway section)	0.23
 Optimum streamlined design	0.15–0.20
Trucks, road trains	0.8–1.5
Buses	0.6–0.7
Streamlined buses	0.3–0.4
Motorcycles	0.6–0.7

Figure 1.4
Indicative drag coefficients for different body shapes

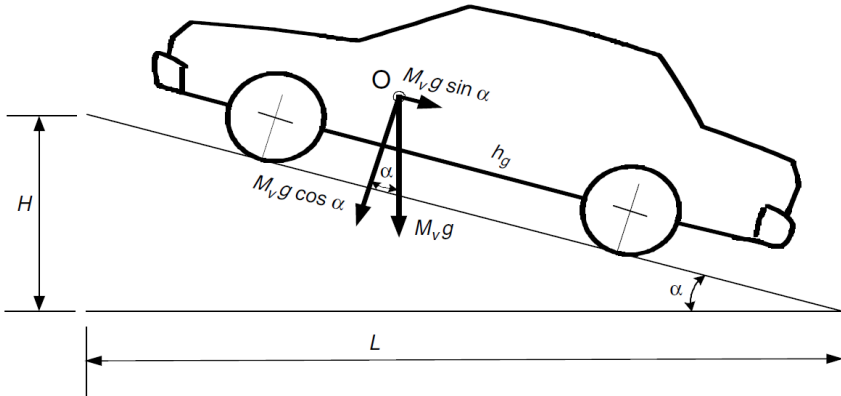


Figure 1.5
Automobile climbing a grade

helps the forward motion (grade descending). In vehicle performance analysis, only uphill operation is considered. This grading force is usually called grading resistance. The grading resistance, from Figure 1.5, can be expressed as

$$F_g = M_v g \sin \alpha. \quad (1.9)$$

To simplify the calculation, the road angle, α , is usually replaced by grade value when the road angle is small. As shown in Figure 2.5, the grade is defined as

$$i = \frac{H}{L} = \tan \alpha \approx \sin \alpha. \quad (1.10)$$

In some literature, the tire rolling resistance and grading resistance together are called road resistance, which is expressed as

$$F_{rd} = F_f + F_g = M_v g (f_r \cos \alpha + \sin \alpha). \quad (1.11)$$

When the road angle is small, the road resistance can be simplified as

$$F_{rd} = F_f + F_g = M_v g (f_r + i). \quad (1.12)$$

1.2 Dynamic Equation

In the longitudinal direction, the major external forces acting on a two-axle vehicle, as shown in Figure 1.1, include the rolling resistance of front and rear tires F_{rf} and F_{rr} , which are represented by rolling resistance moment T_{rf} and T_{rr} , aerodynamic drag F_w , grading resistance F_g ($M_v g \sin \alpha$), and tractive

effort of the front and rear tires, F_{tf} and F_{tr} . F_{tf} is zero for a rear-wheel driven vehicle, whereas F_{tr} is zero for a front-wheel-driven vehicle. The dynamic equation of vehicle motion along the longitudinal direction is expressed by

$$M_v \frac{dV}{dt} = (F_{tf} + F_{tr}) - (F_{rf} + F_{rr} + F_w + F_g), \quad (1.13)$$

where dV/dt is the linear acceleration of the vehicle along the longitudinal direction and M_v is the vehicle mass. The first term on the right-hand side of (1.13) is the total tractive effort and the second term is the resistance. To predict the maximum tractive effort that the tire-ground contact can support, the normal loads on the front and rear axles have to be determined. By summing the moments of all the forces about point R (center of the tire-ground area), the normal load on the front axle W_f can be determined as

$$W_f = \frac{M_v g L_b \cos \alpha - (T_{rf} + T_{rr} + F_w h_w + M_v g h_g \sin \alpha + M h_g dV/dt)}{L} \quad (1.14)$$

Similarly, the normal load acting on the rear axle can be expressed as

$$W_r = \frac{M_v g L_a \cos \alpha - (T_{rf} + T_{rr} + R_w h_w + M_v g h_g \sin \alpha + M_v h_g dV/dt)}{L} \quad (1.15)$$

For passenger cars, the height of the center of application of aerodynamic resistance, h_w , is assumed to be near the height of the center of gravity of the vehicle, h_g . Equations (1.14) and (1.15) can be simplified as

$$W_f = \frac{L_b}{L} M_v g \cos \alpha - \frac{h_g}{L} \left(F_w + F_g + M_v g f_r \frac{r_d}{h_g} \cos \alpha + M_v \frac{dV}{dt} \right) \quad (1.16)$$

$$W_r = \frac{L_a}{L} M_v g \cos \alpha + \frac{h_g}{L} \left(F_w + F_g + M_v g f_r \frac{r_d}{h_g} \cos \alpha + M_v \frac{dV}{dt} \right) \quad (1.17)$$

where r_d is the effective radius of the wheel. Referring to (1.5) and (1.13), (1.16) and (1.17) can be rewritten as

$$W_f = \frac{L_b}{L} M_v g \cos \alpha - \frac{h_g}{L} \left(F_t - F_r \left(1 - \frac{r_d}{h_g} \right) \right) \quad (1.18)$$

$$W_r = \frac{L_a}{L} M_v g \cos \alpha + \frac{h_g}{L} \left(F_t - F_r \left(1 - \frac{r_d}{h_g} \right) \right) \quad (1.19)$$

where $F_t = F_{tf} + F_{tr}$ is the total tractive effort of the vehicle and F_r is the total rolling resistance of the vehicle. The maximum tractive effort that the tire-ground contact can support (any small amount over this maximum tractive effort will cause the tire to spin on

the ground) is usually described by the product of the normal load and coefficient of road adhesion μ or referred to as frictional coefficient in some literatures For a front-wheel-driven vehicle,

$$F_{t\max} = \mu W_f = \mu \left[\frac{L_b}{L} M_v g \cos \alpha - \frac{h_g}{L} \left(F_{t\max} - F_r \left(1 - \frac{r_d}{h_g} \right) \right) \right] \quad (1.20)$$

$$F_{t\max} = \frac{\mu M_v g \cos \alpha [L_b + f_r (h_g - r_d)] / L}{1 + \mu h_g / L} \quad (1.21)$$

where f_r is the coefficient of the rolling resistance. For a rear-wheel-driven vehicle,

$$F_{t\max} = \mu W_r = \mu \left[\frac{L_a}{L} M_v g \cos \alpha - \frac{h_g}{L} \left(F_{t\max} - F_r \left(1 - \frac{r_d}{h_g} \right) \right) \right] \quad (1.22)$$

$$F_{t\max} = \frac{\mu M_v g \cos \alpha [L_a + f_r (h_g - r_d)] / L}{1 + \mu h_g / L} \quad (1.23)$$

In vehicle operation, the maximum tractive effort on the driven wheels, transferred from the power plant through transmission, should not exceed the maximum values that are limited by the tire–ground cohesion in (1.21) and (1.23). Otherwise, the driven wheels will spin on the ground, leading to vehicle instability.

1.3 Tire–Ground Adhesion and Maximum Tractive Effort

When the tractive effort of a vehicle exceeds the limitation of the maximum tractive effort due to the adhesive capability between the tire and the ground, the drive wheels will spin on the ground. Actually, the adhesive capability between the tire and the ground is sometimes the main limitation of vehicle performance. This is especially true when the vehicle drives on wet, icy, snow-covered, or soft soil roads. In this case, a tractive torque on the drive wheel would cause the wheel to have significant slipping on the ground. The maximum tractive effort on the driven wheel depends on the longitudinal force that the adhesive capability between the tire and ground can supply, rather than the maximum torque that the engine can supply. Experimental results show that, on various types of ground, the maximum tractive effort of the drive wheel closely relates to the slipping of the running wheel. The slip, s , of a tire is usually defined as

$$s = \left(1 - \frac{V}{r\omega} \right) \times 100\% = \left(1 - \frac{r_e}{r} \right) \times 100\%, \quad (1.24)$$

where V is the translatory speed of the tire center, ω is the angular speed of the tire, r is the rolling radius of the free rolling tire, and r_e is the effective rolling radius of the tire, defined as the ratio of the translatory speed of the tire center to the angular speed of the tire. In traction, the speed V is less than $r\omega$, therefore, the slip of the tire has a positive value between 0 and 1.0.

During braking, however, the tire slip would be defined as

$$s = \left(1 - \frac{r\omega}{V}\right) \times 100\% = \left(1 - \frac{r}{r_e}\right) \times 100\%, \tag{1.25}$$

which has a positive value between 0 and 1.0, similar to traction. The maximum traction effort of a tire corresponding to a certain tire slip is usually expressed as

$$F_x = P\mu, \tag{1.26}$$

where P is the vertical load of the tire and μ is the tractive effort coefficient, which is a function of tire slip. The tractive effort coefficient and tire slip always have a relationship as shown in Figure 1.6.

In the small slip range (section OA in Figure 1.6), the tractive effort is almost linearly proportional to the slip value. This small slip is caused by the elasticity of the tire rather than the relative slipping between the tire and the ground at the contact patch, as shown in Figure 1.7. Because of the nearly linear elastic property of the tire, the tractive effort–slip curve is almost linear. A further increase in wheel torque and tractive force results in part of the tire tread sliding on the ground. Under these circumstances, the relationship between tractive force and slip is nonlinear. This corresponds to section AB of the curve as shown in Figure 1.6. The peak tractive effort is reached at a slip of 15–20%. A further increase in slip beyond this

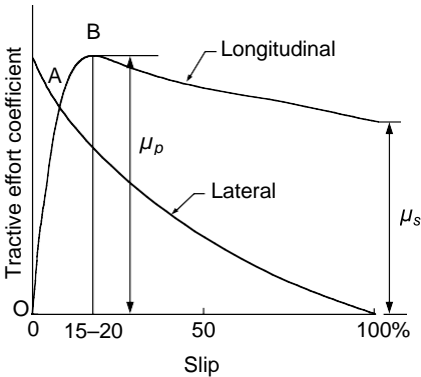


FIGURE 1.6
Variation of tractive effort coefficient with longitudinal slip of a tire

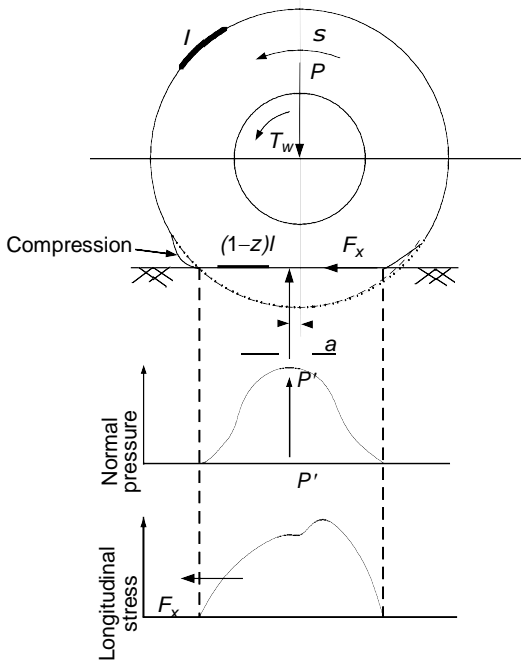


FIGURE 1.7
Behavior of a tire under the action of driving torque

TABLE 1.2
Average Values of Tractive Effort Coefficient on Various Roads

Roads Surface	Peak Values, μ_p	Sliding Values, μ_s
Asphalt and concrete (dry)	0.8–0.9	0.75
Concrete (wet)	0.8	0.7
Asphalt (wet)	0.5–0.7	0.45–0.6
Grave	0.6	0.55
Earth road (dry)	0.68	0.65
Earth road (wet)	0.55	0.4–0.5
Snow (hard packed)	0.2	0.15
Ice	0.1	0.07

results in an unstable condition. The tractive effort coefficient falls rapidly from the peak value to the purely sliding value as shown in Figure 1.6. For normal driving, the slip of the tire must be limited in a range less than 15–20%. Table 1.2 shows the average values of tractive effort coefficients on various roads.

1.4 Power Train Tractive Effort and Vehicle Speed

An automotive power train, as shown in Figure 1.8, consists of a power plant (engine or electric motor), a clutch in manual transmission or a torque converter in automatic transmission, a gearbox (transmission), final drive,

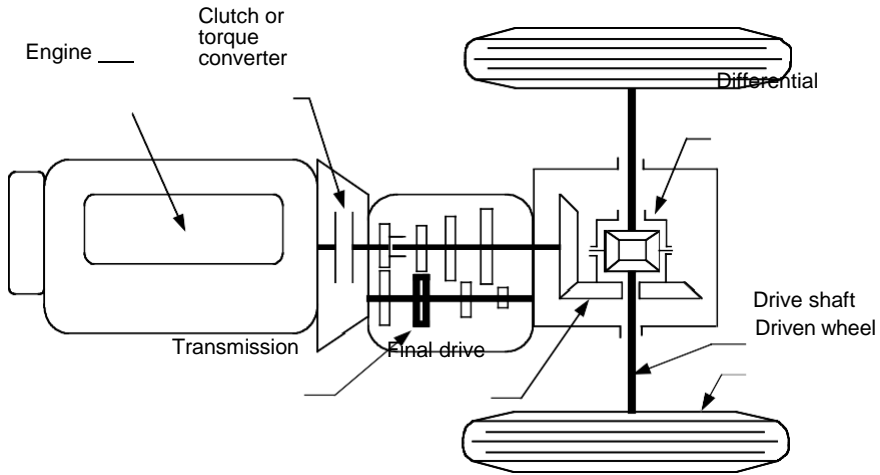


Figure 1.8
 Conceptual illustration of an automobile power train

differential, drive shaft, and driven wheels. The torque and rotating speed of the power plant output shaft are transmitted to the drive wheels through the clutch or torque converter, gearbox, final drive, differential, and drive shaft. The clutch is used in manual transmission to couple the gearbox to or decouple it from the power plant. The torque converter in automatic transmission is a hydrodynamic device, functioning as the clutch in manual transmission with a continuously variable gear ratio. The gearbox supplies a few gear ratios from its input shaft to its output shaft for the power plant torque–speed profile to match the requirements of the load. The final drive is usually a pair of gears that supply a further speed reduction and distribute the torque to each wheel through the differential.

The torque on the driven wheels, transmitted from the power plant, is expressed as

$$T_w = i_g i_0 \eta_t T_p \tag{1.27}$$

where i_g is the gear ratio of the transmission defined as $i_g = N_{in} / N_{out}$ (N_{in} — input rotating speed, N_{out} — output rotating speed), i_0 is the gear ratio of the final drive, η_t is the efficiency of the driveline from the power plant to the driven wheels, and T_p is the torque output from the power plant.

The tractive effort on the driven wheels, as shown in Figure 1.9, can be expressed as

$$F_t = \frac{T_w}{r_d} = \frac{T_p i_g i_0 \eta_t}{r_d}$$

Substituting (1.27) into (1.28) yields the following result:

(1.28)

(1.29)

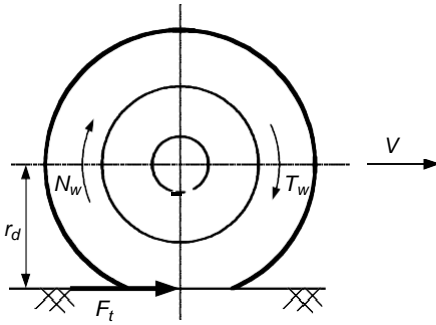


FIGURE 1.9
Tractive effort and torque on a driven wheel

The friction in the gear teeth and the friction in the bearings create losses in mechanical gear transmission. The following are representative values of the mechanical efficiency of various components:

- Clutch: 99%
- Each pair of gears: 95–97%
- Bearing and joint: 98–99%

The total mechanical efficiency of the transmission between the engine output shaft and drive wheels or sprocket is the product of the efficiencies of all the components in the driveline. As a first approximation, the following average values of the overall mechanical efficiency of a manual gear-shift transmission may be used:

- Direct gear: 90%
- Other gear: 85%
- Transmission with a very high reduction ratio: 75–80%

The rotating speed (rpm) of the driven wheel can be expressed as

$$N_w = \frac{N_p}{i_g i_0}, \quad (1.30)$$

where N_p is the output rotating speed (rpm). The translational speed of the wheel center (vehicle speed) can be expressed as

$$V = \frac{\pi N_w r_d}{30} \text{ (m/s)}. \quad (1.31)$$

Substituting (2.30) into (2.31) yields

$$V = \frac{\pi N_p r_d}{30 i_g i_0} \text{ (m/s)}. \quad (2.32)$$

1.5 Vehicle Power Plant and Transmission Characteristics

There are two limiting factors to the maximum tractive effort of a vehicle. One is the maximum tractive effort that the tire–ground contact can support (equation [1.21] or [1.23]) and the other is the tractive effort that the power plant

torque with given driveline gear ratios can provide (equation [1.29]). The smaller of these two factors will determine the performance potential of the vehicle. For on-road vehicles, the performance is usually limited by the second factor. In order to predict the overall performance of a vehicle, its power plant and transmission characteristics must be taken into consideration.

Power Plant Characteristics

For vehicular applications, the ideal performance characteristic of a power plant is the constant power output over the full speed range. Consequently, the torque varies with speed hyperbolically as shown in Figure 1.10. At low speeds, the torque is constrained to be constant so as not to be over the maxima limited by the adhesion between the tire-ground contact area. This constant power characteristic will provide the vehicle with a high tractive effort at low speeds, where demands for acceleration, drawbar pull, or grade climbing capability are high.

Since the internal combustion engine and electric motor are the most commonly used power plants for automotive vehicles to date, it is appropriate to review the basic features of the characteristics that are essential to predicating vehicle performance and driveline design. Representative characteristics of a gasoline engine in full throttle and an electric motor at full load are shown in Figure 1.11 and Figure 1.12, respectively. The internal combustion engine usually has torque-speed characteristics far from the ideal performance characteristic required by traction. It starts operating smoothly at idle speed. Good combustion quality and maximum engine torque are reached at an intermediate engine speed. As the speed increases further, the mean effective pressure decreases because of the growing losses in the air-induction manifold and a decline in engine torque. Power output, however, increases to its maximum at a certain high speed. Beyond this point, the engine torque decreases more rapidly with increasing speed. This results in the decline of engine power output. In vehicular applications, the maximum permissible

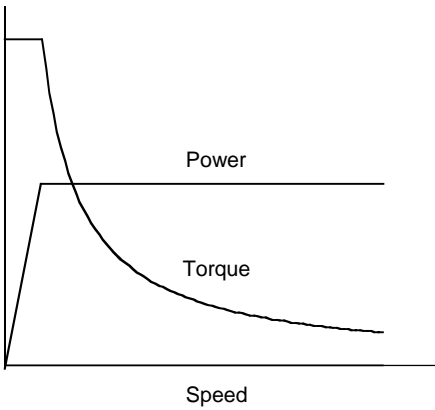


Figure 1.10
Ideal performance characteristics for a vehicle traction power plant

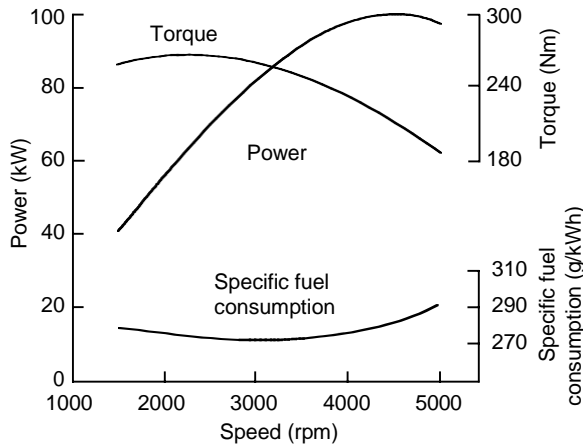


Figure 1.11
Typical performance characteristics of gasoline engines

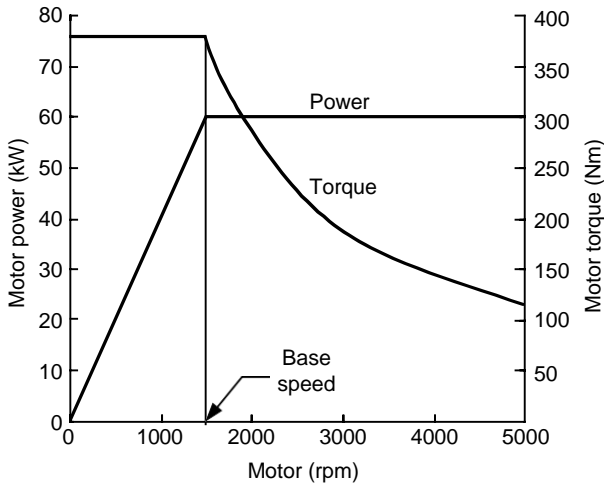


Figure 1.12
Typical performance characteristics of electric motors for traction

speed of the engine is usually set just a little above the speed of the maximum power output. The internal combustion engine has a relatively flat torque–speed profile (compared with an ideal one), as shown in Figure 1.11. Consequently, a multi-gear transmission is usually employed to modify it, as shown in Figure 1.13.

Electric motors, however, usually have a speed–torque characteristic that is much closer to the ideal, as shown in Figure 1.12. Generally, the electric motor starts from zero speed. As it increases to its base speed, the voltage increases to its rated value while the flux remains constant. Beyond the base speed, the

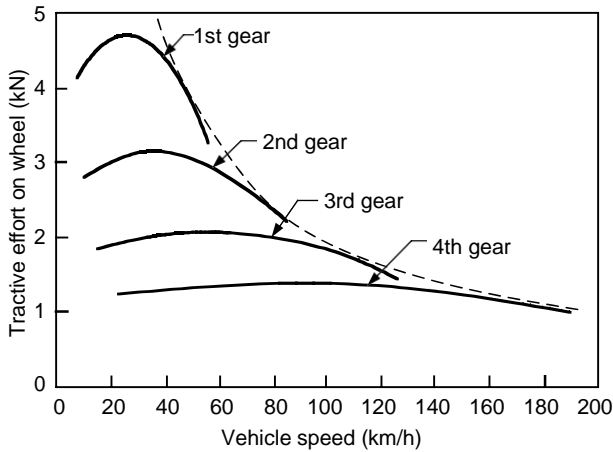


Figure 1.13
Tractive effort of internal combustion engine and a multigear transmission vehicle vs. vehiclespeed

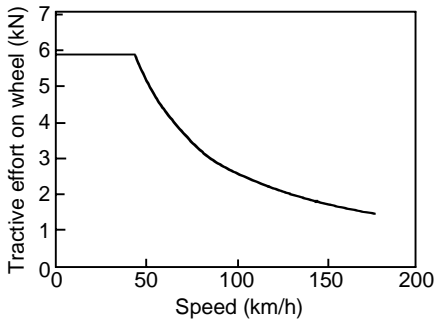


Figure 1.14
Tractive effort of a single-gear electric vehicle vs. vehicle speed

voltage remains constant and the flux is weakened. This results in constant output power while the torque declines hyperbolically with speed. Since the speed–torque profile of an electric motor is close to the ideal, a single-gear or double-gear transmission is usually employed, as shown in Figure 2.14.

Transmission Characteristics

The transmission requirements of a vehicle depend on the characteristics of the power plant and the performance requirements of the vehicle. As mentioned previously, a well-controlled electric machine such as the power plant of an electric vehicle will not need a multigear transmission. However, an internal combustion engine must have a multigear or continuously varying transmission to multiply its torque at low speed. The term transmission here includes all those systems employed for transmitting engine power to the drive wheels. For automobile applications, there are usually two basic types of transmission: manual gear transmission and hydrodynamic transmission.

Manual Gear Transmission

Manual gear transmission consists of a clutch, gearbox, final drive, and drive shaft as shown in Figure 1.8. The final drive has a constant gear reduction ratio or a differential gear ratio. The common practice of requiring direct drive (nonreducing) in the gearbox to be in the highest gear determines this ratio. The gearbox provides a number of gear reduction ratios ranging from three to five for passenger cars and more for heavy commercial vehicles that are powered with gasoline or diesel engines.

The maximum speed requirement of the vehicle determines the gear ratio of the highest gear (i.e., the smallest ratio). On the other hand, the gear ratio of the lowest gear (i.e., the maximum ratio) is determined by the requirement of the maximum tractive effort or the gradeability. Ratios between them should be spaced in such a way that they will provide the tractive effort-speed characteristics as close to the ideal as possible, as shown in Figure 1.15. In the first iteration, gear ratios between the highest and the lowest gear may be selected in such a way that the engine can operate in the same speed range for all the gears. This approach would benefit the fuel economy and performance of the vehicle. For instance, in normal driving, the proper gear can be selected according to vehicle speed to operate the engine in its optimum speed range for fuel-saving purposes. In fast acceleration, the engine can be operated in its speed range with high power output. This approach is depicted in Figure 1.16.

For a four-speed gearbox, the following relationship can be established (see Figure 1.16):

$$\frac{i_{g1}}{i_{g2}} = \frac{i_{g2}}{i_{g3}} = \frac{i_{g3}}{i_{g4}} = K_g \tag{1.33}$$

where i_{g1} , i_{g2} , i_{g3} , and i_{g4} are the gear ratios for the first, second, third, and fourth gear, respectively. In a more general case, if the ratio of the highest

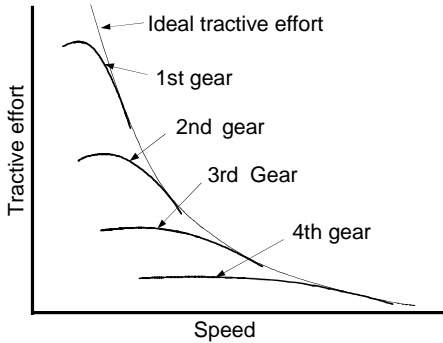


FIGURE 1.15
Tractive effort characteristics of a gasoline engine-powered vehicle

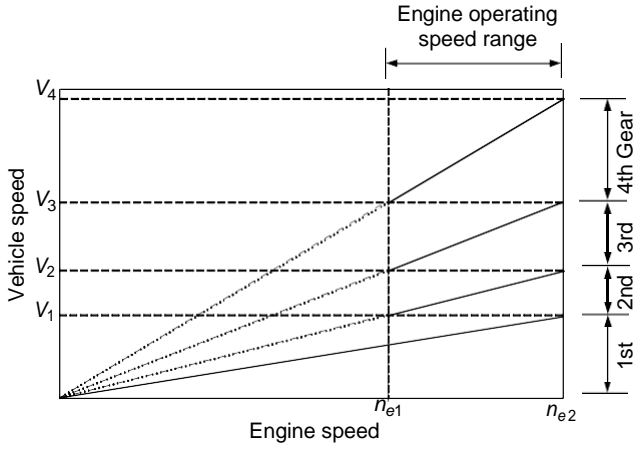


FIGURE 1.16
 Demonstration of vehicle speed range and engine speed range for each gear

gear, i_{gn} (smaller gear ratio), and the ratio of the lowest gear, i_{g1} (largest gear ratio), have been determined and the number of the gear n_g is known, the factor K_g can be determined as

$$K = \left(\frac{i_{g1}}{i_{gn}} \right)^{(n_g-1)}, \quad (1.35)$$

and each gear ratio can be obtained by

$$\begin{aligned} i_{gn-1} &= K_g i_{gn} \\ i_{gn-2} &= K_g^2 i_{gn} \\ &\vdots \\ i_{g2} &= K_g^{n_g-1} i_{gn}. \end{aligned} \quad (1.36)$$

For passenger cars, to suit changing traffic conditions, the step between the ratios of the upper two gears is often a little closer than that based on (1.36). That is,

$$\frac{i_{g1}}{i_{g2}} > \frac{i_{g2}}{i_{g3}} > \frac{i_{g3}}{i_{g4}}. \quad (1.37)$$

This, in turn, affects the selection of the ratios of the lower gears. For commercial vehicles, however, the gear ratios in the gearbox are often arranged based on (1.37).

Figure 1.17 shows the tractive effort of a gasoline engine vehicle with four-gear transmission and that of an electric vehicle with single-gear transmission. It is clear that electric machines with favorable torque–speed characteristics can satisfy tractive effort with simple single-gear transmission.

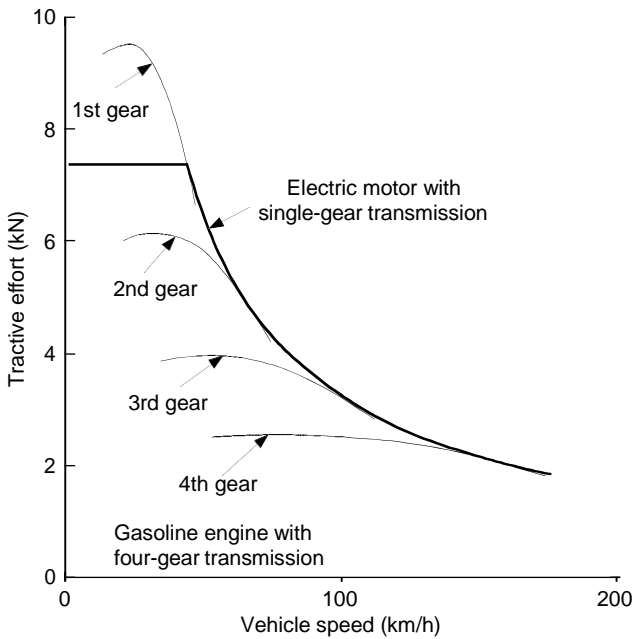


FIGURE 1.17

Tractive efforts of a gasoline engine vehicle with four-gear transmission and an electric vehicle with single-gear transmission

Hydrodynamic Transmission

Hydrodynamic transmissions use fluid to transmit power in the form of torque and speed and are widely used in passenger cars. They consist of a torque converter and an automatic gearbox. The torque converter consists of at least three rotary elements known as the impeller (pump), the turbine, and the reactor, as shown in Figure 2.18. The impeller is connected to the engine shaft and the turbine is connected to the output shaft of the converter, which in turn is coupled to the input shaft of the multispeed gearbox. The reactor is coupled to external housing to provide a reaction on the fluid circulating in the converter. The function of the reactor is to enable the turbine to develop an output torque higher than the input torque of the converter, thus producing torque multiplication. The reactor is usually mounted on a free wheel (one-way clutch) so that when the starting period has been completed and the turbine speed is approaching that of the pump, the reactor is in free rotation. At this point, the converter operates as a fluid coupled with a ratio of output torque to input torque that is equal to 1.0.

The major advantages of hydrodynamic transmission may be summarized as follows:

- When properly matched, the engine will not stall.
- It provides flexible coupling between the engine and the driven wheels.

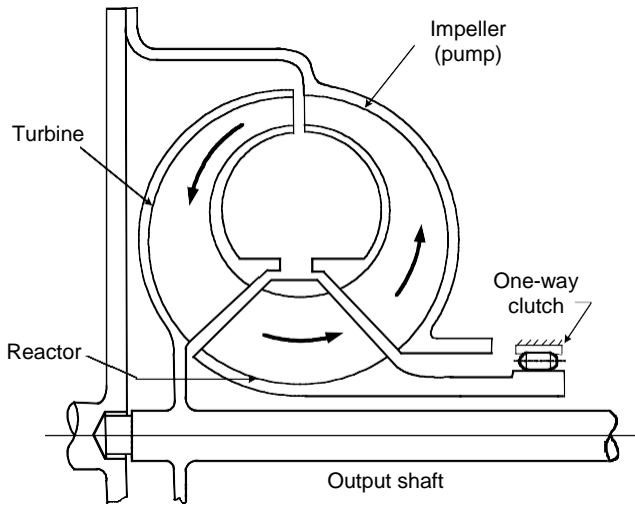


FIGURE 1.18
Schematic view of a torque converter

Together with a suitably selected multispeed gearbox, it provides torque-speed characteristics that approach the ideal. The major disadvantages of hydrodynamic transmission are its low efficiency in a stop-go driving pattern and its complex construction.

The performance characteristics of a torque converter are described in terms of the following four parameters:

1. *Speed ratio*

$$C_{sr} = \frac{\text{output_speed}}{\text{input_speed}}, \quad (1.38)$$

which is the reciprocal of the gear ratio mentioned before.

2. *Torque ratio*

$$C_{tr} = \frac{\text{output_torque}}{\text{input_torque}}. \quad (1.39)$$

3. *Efficiency*

$$= \frac{\text{output_speed} \times \text{output_torque}}{\text{input_speed} \times \text{input_torque}} = \quad (1.40)$$

4. *Capacity factor (size factor)*

$$K_{tc} = \frac{\text{speed}}{\sqrt{\text{torque}}}. \quad (1.41)$$

The capacity factor, K_c , is an indicator of the ability of the converter to absorb or transmit torque, which is proportional to the square of the rotary speed.

Typical performance characteristics of the torque converter are shown in Figure 1.19, in which torque ratio, efficiency, and input capacity factor — that is the ratio of input speed to the square root of input torque — are plotted against speed ratio. The torque ratio has the maximum value at stall condition, where the output speed is zero. The torque ratio decreases as the speed ratio increases (gear ratio decreases) and the converter eventually acts as a hydraulic coupling with a torque ratio of 1.0. At this point, a small difference between the input and output speed exists because of the slip between the impeller (pump) and the turbine. The efficiency of the torque converter is zero at stall condition and increases with increasing speed ratio (decrease in the gear ratio). It reaches the maximum when the converter acts as a fluid coupling (torque ratio equal to 1.0).

To determine the actual operating condition of the torque converter, the engine operating point has to be specified because the engine drives the torque converter. To characterize the engine operating condition for the purpose of determining the combined performance of the engine and the converter, an engine capacity factor, $K_{e'}$, is introduced and defined as

$$K_{e'} = \frac{n_e}{\sqrt{T_e}} \tag{1.42}$$

where n_e and T_e are engine speed and torque, respectively. The variation of the capacity factor with speed for a typical engine is shown in Figure 2.20. To achieve proper matching, the engine and the torque converter should have a similar range in the capacity factor.

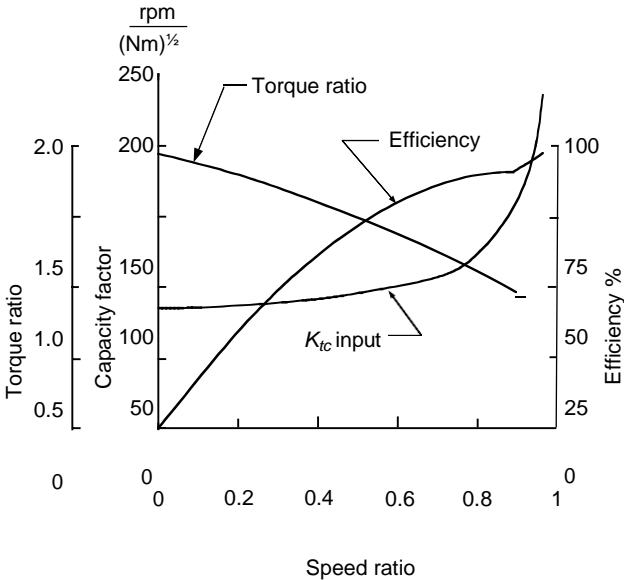


FIGURE 1.19

Performance characteristics of a torque converter

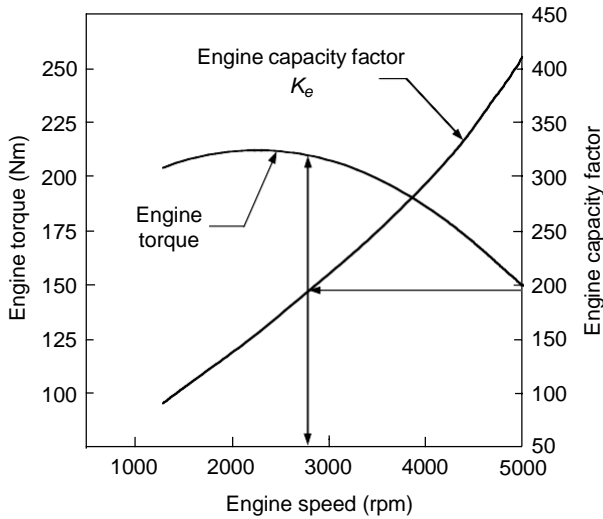


Figure 1.20
Capacity factor of a typical engine

The engine shaft is usually connected to the input shaft of the torque converter, as mentioned above. That is,

$$K_e = K_c. \quad (1.43)$$

The matching procedure begins with specifying the engine speed and engine torque. Knowing the engine operating point, one can determine the engine capacity factor, K_e (see Figure 1.21). Since $K_e = K_c$ the input capacity factor of the torque converter corresponding to the specific engine operating point is then known. As shown in Figure 2.20, for a particular value of the input capacity factor of the torque converter, K_{ic} , the converter speed ratio, C_{srr} and torque ratio, C_{trr} can be determined from the torque converter performance characteristics. The output torque and output speed of the converter are then given by

$$T_{tc} = T_e C_{tr} \quad (1.44)$$

and

$$n_{tc} = n_e C_{srr} \quad (1.45)$$

where T_{tc} and n_{tc} are the output torque and output speed of the converter, respectively.

Since the torque converter has a limited torque ratio range (usually less than 2), a multispeed gearbox is usually connected to it. The gearbox comprises several planetary gear sets and is automatically shifted. With the gear

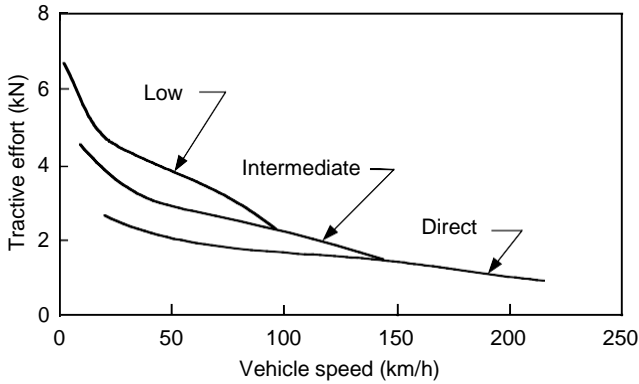


FIGURE 1.21
Tractive effort–speed characteristics of a passenger car with automatic transmission

ratios of the gearbox, the tractive effort and speed of the vehicle can be calculated (see [1.27] and [1.32]) by

$$F = \frac{T_e C_{tr} i_g i_0 \eta_t}{r}$$

and

$$V = \frac{\pi n_e C_{sr} r}{30 i_g i_0} \text{ (m/s)} = 0.377 \frac{n_e C_{sr} r}{i_t} \text{ (km/h)}. \quad (1.47)$$

Figure 1.21 shows the variation of the tractive effort with speed for a passenger car equipped with a torque converter and a three-speed gearbox.

Continuously Variable Transmission

A continuously variable transmission (CVT) has a gear ratio that can be varied continuously within a certain range, thus providing an infinity of gear ratios. This continuous variation allows for the matching of virtually any engine speed and torque to any wheel speed and torque. It is therefore possible to achieve an ideal torque–speed profile (constant power profile) because any engine power output to the transmission can be applied at any speed to the wheels.

The commonly used CVT in automobiles uses a pulley and belt assembly. One pulley is connected to the engine shaft, while the other is connected to the output shaft. The belt links the two pulleys. The distance between the two half pulleys can be varied, thus varying the effective diameter on which the belt grips. The transmission ratio is a function of the two effective diameters:

$$i_g = \frac{D_2}{D_1'} \quad (1.48)$$

where D_1 and D_2 are the effective diameters of the output pulley and input pulley, respectively.

Until recently, this implementation was affected by the limited belt–pulley adhesive contact. The design has been improved by the use of metallic belts that provide better solidity and improved contact. Furthermore, an interesting concept has been developed and is being used by Nissan. This concept uses three friction gears: one is connected to the engine shaft, another to the output shaft, while the third gear grips on the particular profile of the other two gears. It can be rotated to grip on different effective diameters, therefore achieving a variable gear ratio.

1.6 Vehicle Performance

The performance of a vehicle is usually described by its maximum cruising speed, gradeability, and acceleration. The predication of vehicle performance is based on the relationship between tractive effort and vehicle speed discussed in Sections 2.5 and 2.6. For on-road vehicles, it is assumed that the maximum tractive effort is limited by the maximum torque of the power plant rather than the road adhesion capability. Depicted tractive effort (equation [2.29] or [2.46]) and resistance ($F_r + F_w + F_g$) on a diagram are helpful for vehicle performance analysis as shown in Figure 2.22 and

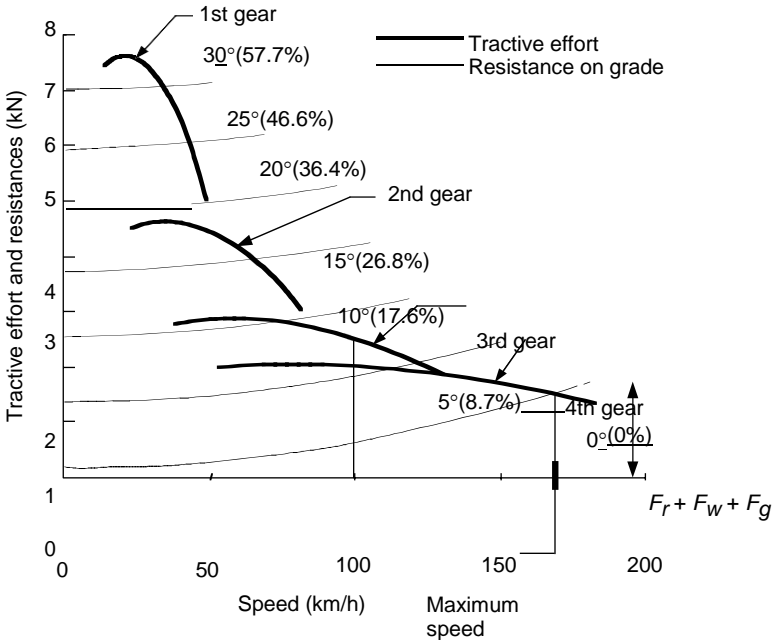


FIGURE 1.22 Tractive effort of a gasoline engine-powered vehicle with multispeed transmission and its resistance

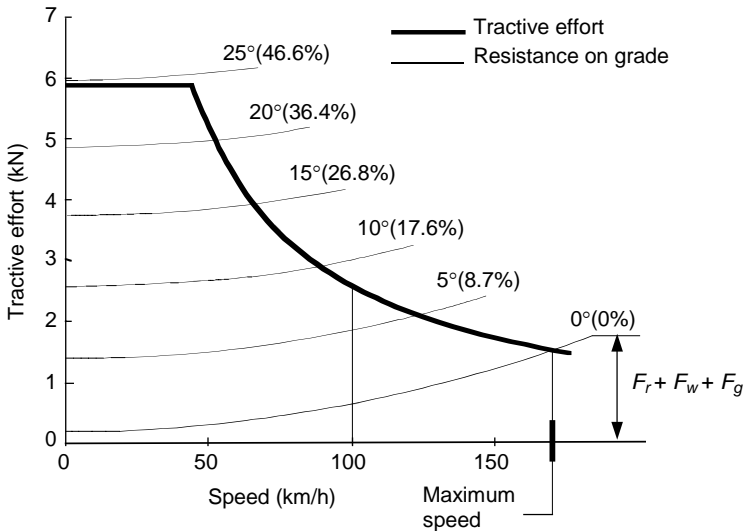


FIGURE 1.23
Tractive effort of an electric motor-powered vehicle with single-speed transmission and its resistance

Figure 1.23 for a gasoline engine-powered, four-gear manual transmission vehicle and an electric motor-powered, single-gear transmission vehicle, respectively.

Maximum Speed of a Vehicle

The maximum speed of a vehicle is defined as the constant cruising speed that the vehicle can develop with full power plant load (full throttle of the engine or full power of the motor) on a flat road. The maximum speed of a vehicle is determined by the equilibrium between the tractive effort of the vehicle and the resistance or the maximum speed of the power plant and gear ratios of the transmission. The tractive effort and resistance equilibrium can be expressed as

$$\frac{T_p i_g i_t \eta_t}{r_d} = M_v g f_r \cos \alpha + \frac{1}{2} \rho_a C_D A_f V^2. \quad (1.49)$$

This equation indicates that the vehicle reaches its maximum speed when the tractive effort, represented by the left-hand-side term in (2.49), equals the resistance, represented by the right-hand-side terms. The intersection of the tractive effort curve and the resistance curve represents the maximum speed of the vehicle, as shown in Figure 2.22 and Figure 2.23.

It should be noted that for some vehicles, no intersection exists between the effort curve and the resistance curve, because of a large power plant or large gear ratio. In this case, the maximum speed of the vehicle can be

determined by the maximum speed of the power plant. Using (1.32) or (1.47), the maximum speed of the vehicle can be written as

$$V_{max} = \frac{\pi n_{p,max} r_d}{30 i_{g,min}} \text{ (m/s)}, \tag{1.50}$$

where $n_{p,max}$ and $i_{g,min}$ are the maximum speed of the engine (electric motor) and the minimum gear ratio of the transmission, respectively.

1.3.1 Gradeability

Gradeability is usually defined as the grade (or grade angle) that the vehicle can overcome at a certain constant speed, for instance, the grade at a speed of 100 km/h (60 mph). For heavy commercial vehicles or off-road vehicles, the gradeability is usually defined as the maximum grade or grade angle in the whole speed range.

When the vehicle drives on a road with relative small grade and constant speed, the tractive effort and resistance equilibrium can be written as

$$\frac{T_p i_0 i_g \eta_t}{r_d} = M_v g f_r + \frac{\rho_a C_D A_f V^2}{2} + M_v g i. \tag{1.51}$$

Thus,

$$i = \frac{(T_p i_0 i_g \eta_t / r_d) - M_v g f_r - (1/2) \rho_a C_D A_f V^2}{M_v g} = d - f_r, \tag{1.52}$$

where

$$d = \frac{F_t - F_w}{M_v g} = \frac{(T_p i_0 i_g \eta_t / r_d) - (1/2) \rho_a C_D A_f V^2}{M g} \tag{1.53}$$

is called the performance factor. While the vehicle drives on a road with a large grade, the gradeability of the vehicle can be calculated as

$$\sin \alpha = \frac{d - f_r \sqrt{1 - d^2 + f_r^2}}{1 + f_r^2}. \tag{1.54}$$

The gradeability of the vehicle can also be obtained from the diagram in Figure 1.22 or Figure 1.23, in which the tractive effort and resistance are plotted.

Acceleration Performance

The acceleration performance of a vehicle is usually described by its acceleration time and the distance covered from zero speed to a certain high speed (zero to 96 km/h or 60 mph, for example) on level ground. Using Newton's second law (equation [2.13]), the acceleration of the vehicle can be written as

$$a = \frac{dV}{dt} = \frac{F_t - F_f - F_w}{M_v \delta} = \frac{(T_p i_0 i_g \eta_t / r_d) - M_v g f_r - (1/2) \rho_a C_D A_f V^2}{M_v \delta} = \frac{g}{\delta} (d - f_r), \quad (2.55)$$

where δ is called the mass factor, considering the equivalent mass increase due to the angular moments of the rotating components. The mass factor can be written as

$$\delta = 1 + \frac{I_w}{M_v r_d^2} = \frac{i_0^2 i_g^2 I_p}{M_v r^2} \tag{1.56}$$

where I_w is the total angular moment of the wheels and I_p is the total angular moment of the rotating components associated with the power plant. Calculation of the mass factor, δ , requires knowing the values of the mass moments of inertia of all the rotating parts. In the case where these values are not known, the mass factor, δ , for a passenger car would be estimated using the following empirical relation:

$$\delta = 1 + \delta_1 + \delta_2 i_g^2 i_0^2 \tag{1.57}$$

where δ_1 represents the second term on the right-hand side of equation (1.56), with a reasonable estimate value of 0.04, and δ_2 represents the effect of the power plant-associated rotating parts, and has a reasonable estimate value of 0.0025.

Figure 1.24 and Figure 1.25 show the acceleration along with vehicle speed for a gasoline engine-powered vehicle with four-gear transmission and an electric motor-powered vehicle with single-gear transmission.

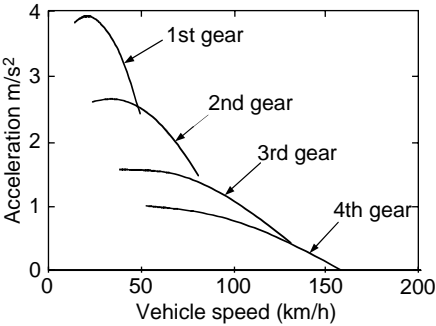


Figure 1.24
Acceleration of a gasoline engine-powered vehicle with four-gear transmission

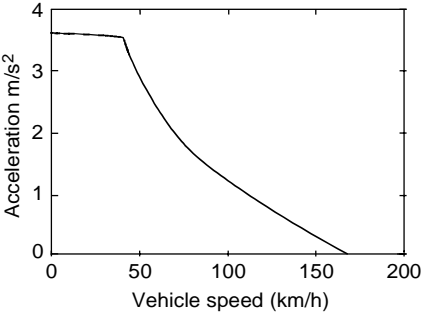


Figure 1.25
Acceleration of an electric machine-powered vehicle with single-gear transmission

From (1.55), the acceleration time, t_a , and distance, S_a , from low speed V_1 to high speed V_2 can be written, respectively, as

$$t_a = \int_{V_1}^{V_2} \frac{M_v \delta V}{(T_p i_g i_0 \eta_t / r_d) - M_v g f_r - (1/2) \rho_a C_D A_f V^2} dV \quad (1.58)$$

$$S_a = \int_{V_1}^{V_2} \frac{M_v \delta}{(T_p i_g i_0 \eta_t / r_d) - M_v g f_r - (1/2) \rho_a C_D A_f V^2} dV. \quad (1.59)$$

In (1.58) and (1.59), the torque of the power plant, T_p , is a function of speed (see Figure 1.11 and Figure 1.12), which in turn is a function of vehicle speed (see [1.23] and [1.37]) and gear ratio of the transmission. This makes it difficult to solve (1.58) and (1.59) analytically; therefore, numeral methods are usually used. Figure 1.26 and Figure 1.27 show the acceleration time and

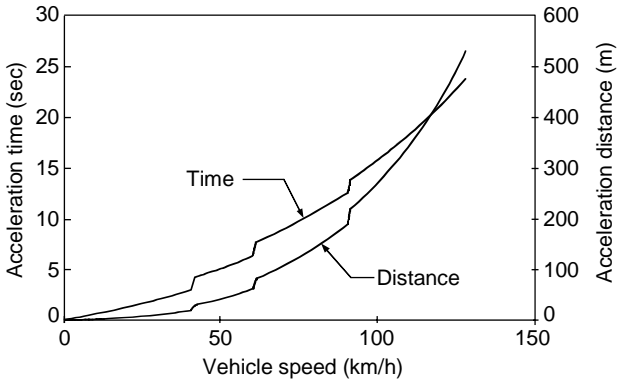


Figure 2.26 Acceleration time and distance along with vehicle speed for a gasoline engine-powered passenger car with four-gear transmission

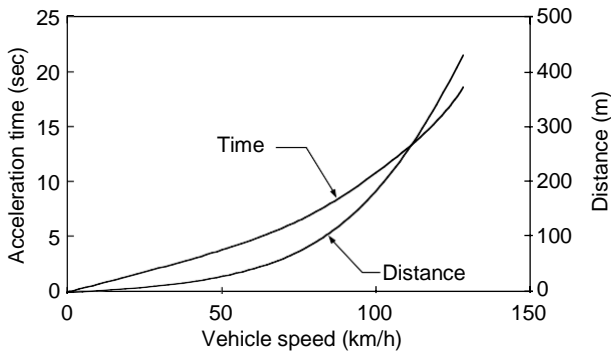


Figure 2.27 Acceleration time and distance along with vehicle speed for an electric machine-powered passenger car with single-gear transmission

distance along with vehicle speed for a gasoline engine-powered and an electric machine-powered electric vehicle, respectively.

2.8 Braking Performance

The braking performance of a vehicle is undoubtedly one of the most important characteristics that affect vehicle safety. In urban driving, a significant amount of energy is consumed in braking. In recent years, more and more electric drives have been involved in vehicle traction, such as electric vehicles, hybrid electric vehicles, and fuel cell-powered vehicles. The electrification of the vehicle drive train makes it feasible to recover some of the energy lost in braking. This technology is usually referred to as regenerative braking. A well-designed regenerative braking system not only improves vehicle efficiency but also potentially improves braking performance. In this section, a method of approach to the analysis of braking performance will be presented, which aims to help the designing of regenerative braking systems.

Braking Force

Figure 1.34(a) shows a wheel during braking. The brake pad is pressed against the brake plate, thus developing a frictional torque on the brake plate. This braking torque results in a braking force in the tire – ground contact area. It is just this braking force that tries to stop the vehicle. The braking force can be expressed as

$$F_b = \frac{T_b}{r_d}. \quad (1.66)$$

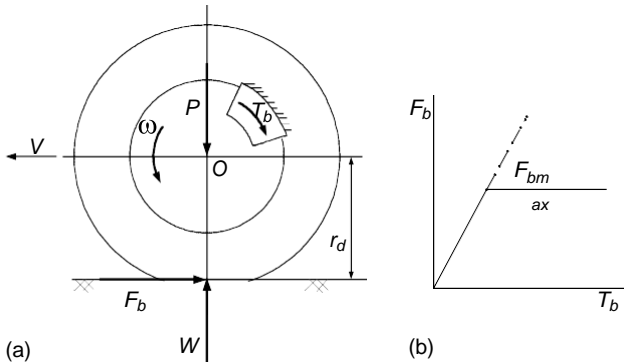


Figure 1.34

(a) Braking torque and braking force, and (b) relationship between braking torque and braking force

The braking force increases with an increase in braking torque. However, when the braking force reaches the maximum braking force that the tire-ground adhesion can support, it will not increase further, although the braking torque may still increase as shown in Figure 1.34(b). This maximum braking force limited by the adhesive capability can be expressed as

$$F_{b \max} = \mu_b W, \quad (1.67)$$

where μ_b is the adhesive coefficient of the tire-ground contact. Similar to the traction case (Figure 1.8), the adhesive coefficient varies with the slipping of the tire. There exists a maximum value in the slip range of 15–20%, declining somewhat at 100% slip.

Braking Distribution on Front and Rear Axles

Figure 1.35 shows the forces acting on a vehicle during braking on a flat road. Rolling resistance and aerodynamic drag are ignored in this figure, because they are quite small compared to the braking forces. j is the deceleration of the vehicle during braking, which can be easily expressed as

$$j = \frac{F_{bf} + F_{br}}{M_v}, \quad (1.68)$$

where F_{bf} and F_{br} are the braking forces acting on front and rear wheels, respectively.

The maximum braking force is limited by the tire-ground adhesion and is proportional to the normal load acting on the tire. Thus, the actual braking force developed by the brake torque should also be proportional to the normal load so that both the front and the rear wheels obtain their maximum braking force at the same time. During braking, there is load transfer from the rear axle to the front axle. By considering the equilibrium of moments

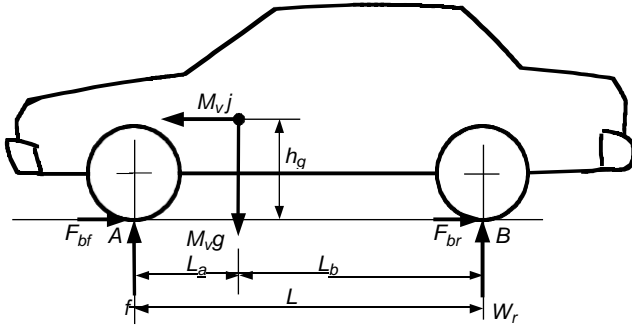


Figure 1.35

Force acting on a vehicle during braking on a flat road

about the front and rear tire-ground contact points A and B, the normal loads on the front and rear axles, W_f and W_r , can be expressed as

$$W_f = \frac{M_v g}{L} \left(L_b + h_g \frac{j}{g} \right) \quad (1.69)$$

$$W_r = \frac{M_v g}{L} \left(L_a - h_g \frac{j}{g} \right) \quad (1.70)$$

where j is the deceleration of the vehicle.

The braking forces of the front and rear axle should be proportional to their normal load, respectively; thus, one obtains

$$\frac{F_{bf}}{F_{br}} = \frac{W_f}{W_r} = \frac{L_b + h_g j/g}{L_a - h_g j/g} \quad (1.71)$$

Combining (1.68) and (1.71), the ideal braking forces on the front and rear axle can be obtained as shown in Figure 1.36, where j represents the maximum acceleration that a vehicle can obtain on the road with an adhesive coefficient μ . The ideal braking force distribution curve (simply, I curve) is a nonlinear hyperbolic curve. If it is desired for the front and rear wheels to lock up at the same time on any road, the braking force on the front and rear axle must closely follow this curve.

In vehicle design, the actual braking forces on the front and rear axle are usually designed to have a fixed linear proportion. This proportion is represented by the ratio of the front axle braking force to the total braking force of the vehicle, that is

$$\beta = \frac{F_{bf}}{F_b}, \quad (1.72)$$

where F_b is the total braking force of the vehicle ($F_b = F_{bf} + F_{br}$). With β being the actual braking force on the front and rear axle, this can be expressed as

$$F_{bf} = \beta F_b. \tag{1.73}$$

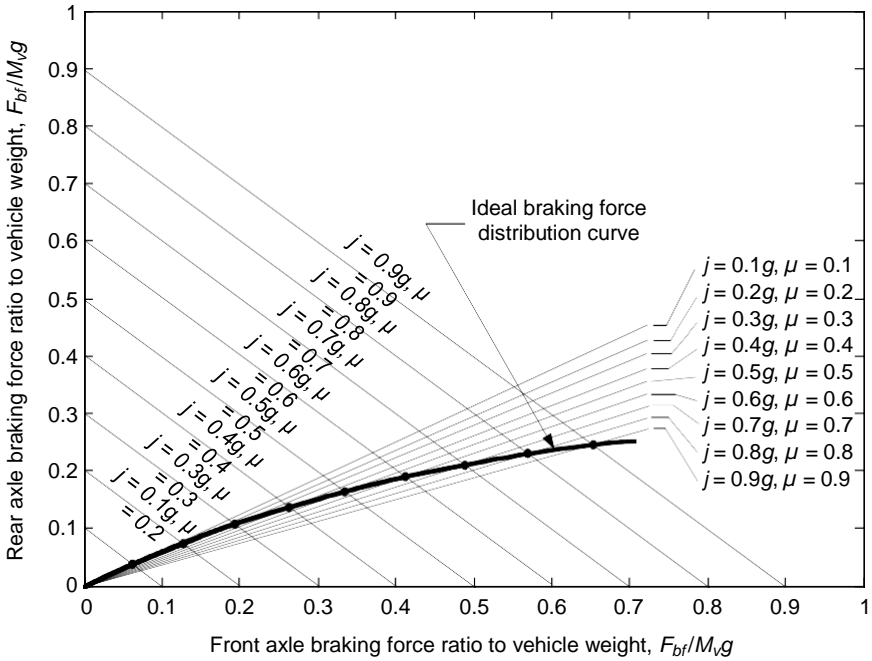


Figure 1.36

Ideal braking force distribution curve on the front and rear axles

and

$$F_{br} = (1 - \beta)F_b \quad (1.74)$$

Thus, one obtains

$$\frac{F_{bf}}{F_{br}} = \frac{\beta}{1 - \beta}$$

Figure 1.37 shows the ideal and actual braking force distribution curves (labeled I and β curves). It is clear that only one intersection point exists, at which the front and rear axles lock up at the same time. This point represents one specific road adhesive coefficient, μ_0 . Referring to (1.71), in which j/g is replaced by μ_0 , and (1.75), one can obtain

$$\frac{\beta}{1 - \beta} = \frac{L_b + \mu_0 h_g}{L_a - \mu_0 h_g} \quad (1.76)$$

From (1.75), one can obtain μ_0 or β by

$$\mu_0 = \frac{L\beta - L_b}{h_g}$$

$$\beta = \frac{\mu_0 h_g + L_b}{L}$$

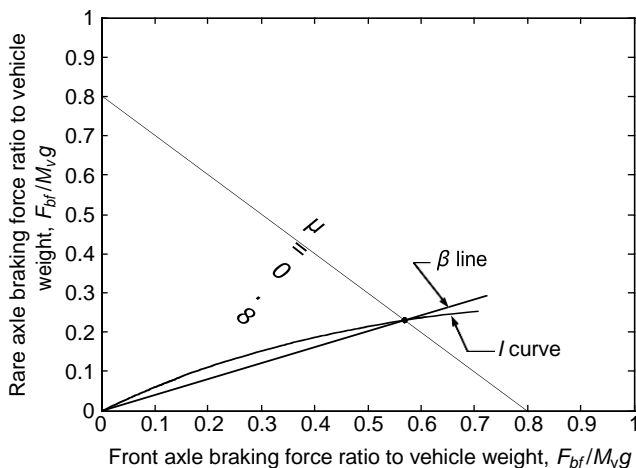


Figure 1.37
Ideal and actual braking force distribution curves

During braking on roads with an adhesive coefficient that is less than μ_0 (the region in which the β curve is below the I curve), the front wheels lock up first, whereas when the road adhesive coefficient is larger than μ_0 (the region in which the β curve is above the I curve), the rear wheels lock up first.

When the rear wheels lock up first, the vehicle will lose directional stability, as shown in Figure 1.38. The figure shows the top view of a two-axle vehicle acted upon by the braking force and the inertia force. When the rear wheels lock, the capability of the rear tires to resist lateral forces is reduced to zero (refer to Figure 1.7). If some slight lateral movement of the rear wheels is initiated by side wind, road camber, or centrifugal force, a yawing moment due to the inertia force about the yaw center of the front axle will develop. As the yaw motion progresses, the moment arm of the inertia force increases, resulting in an increase in yaw acceleration. As the rear end of the vehicle swings around 90° , the moment arm gradually decreases and eventually the vehicle rotates 180° with the rear end leading the front end.

The lockup of front wheels will cause a loss of directional control, and the driver will no longer be able to exercise effective steering. It should be pointed out, however, that front wheel lockup does not cause directional instability. This is because whenever the lateral movement of the front wheels occurs, a self-correcting moment due to the inertial force of the vehicle about the yaw center of the rear axle develops. Consequently, it tends to bring the vehicle back to a straight-line path. Figure 1.39 shows the measured angular deviation of a vehicle when the front and rear wheels do not lock at the same instant.¹

Loss of steering control may be detected more readily by the driver and control may be regained by the release or partial release of the brakes. Contrary to the case of front wheel lockup, when rear wheels lock and the

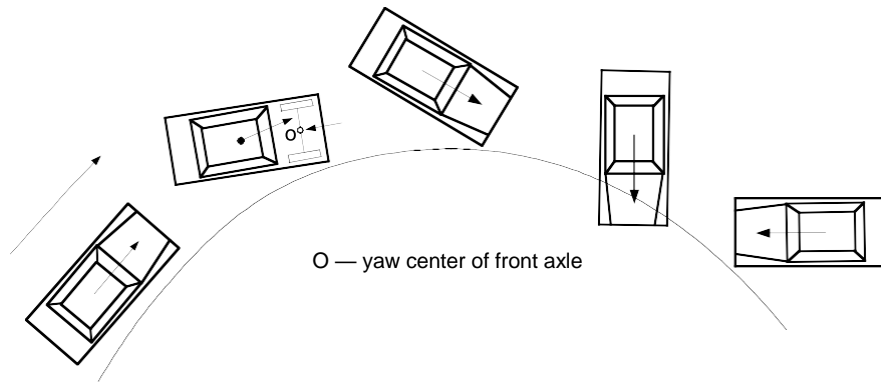


Figure 1.38
Loss of directional stability due to the lockup of rear wheels

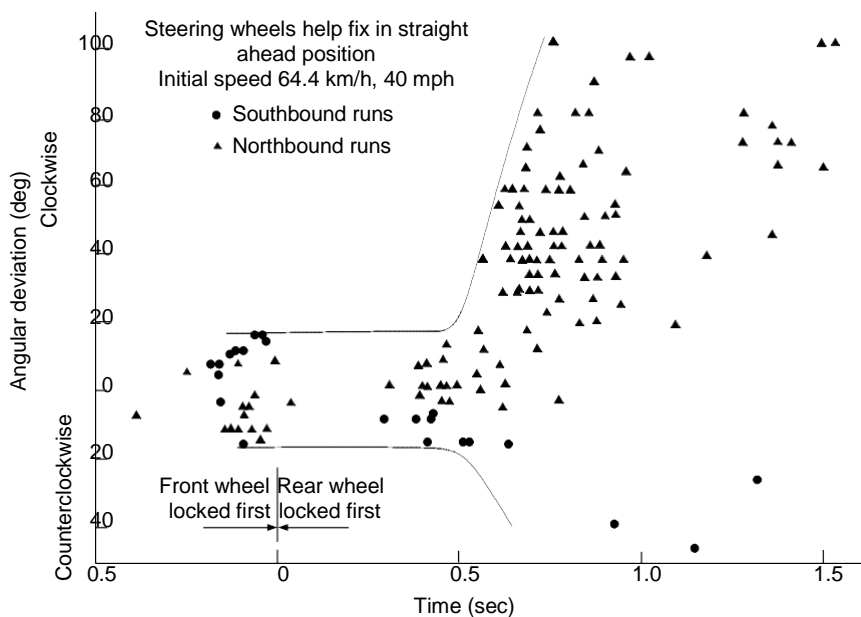


Figure 1.39
Angular deviation of a car when all four wheels do not lock at the same instant

angular deviation of the vehicle exceeds a certain level, control cannot be regained even by complete release of the brakes and by the most skilful driving. This suggests that rear wheel lockup is a more critical situation, particularly on a road with a low adhesive coefficient. Since on slippery surfaces the value of the braking force is low, the kinetic energy of the vehicle will dissipate at a low rate and the vehicle will experience a serious loss of directional stability over a considerable distance. Therefore, designers of vehicle brake systems must ensure that rear wheels do not lock up first.

The antilock braking system (ABS), developed in recent years, can effectively prevent wheels from locking up. This system employs speed sensors to detect the wheel rotating speed. When a wheel lockup is detected, the braking pressure control system reduces the pressure and brings the wheel back to its rotation.³

References

- [1] J.Y. Wong, *Theory of Ground Vehicles*, John Wiley & Sons, New York, 1978.
- [2] Bosch, *Automotive Handbook*, by Robert Bosch GmbH, Stuttgart, 2000.
- [3] S. Mizutani, *Car Electronics*, Sankaido Co., Warrendale, PA, 1992.

Question Bank

PART A

Q.No	Questions	CO (L)
1.	Identify the different factors effect the movement of vehicle.	CO1(L3)
2.	Organize the building blocks of automobile power train system.	CO1(L3)
3.	Apply the basic automobile knowledge to write the expression for dynamic equation of vehicle.	CO1(L3)
4.	Apply the basic automobile knowledge to write the expression for road resistance.	CO1(L3)
5.	Identify the different components of aerodynamic drag.	CO1(L3)
6.	Compare the gasoline engine and electric motor from its tractive effort characteristics.	CO1(L4)
7.	Analyze the different factor involved in the braking performance of the vehicle.	CO1(L3)
8.	Analyze the different factor involved in the vehicle performance	CO1(L4)
9.	Compare gear ratio and final drive from its operation.	CO1(L4)
10.	Choose the condition to achieve directional instability of the vehicle.	CO1(L3)
11.	Judge how to obtain the gear ratio from gear ratio factor.	CO1(L5)
12.	Justify why gradeability test is very important in the vehicle performance.	CO1(L5)

PART – B

Q.No	Questions	CO (L)
1	Construct the concept of power train system of a vehicle with neat sketch also to derive the expression for vehicle speed.	CO1(L3)
2	Justify what are the parameters affect the performance of the vehicle. Deliver the feature of the any one performance factor with required dynamic equation.	CO1(L5)
3	Justify what are the parameters affect the braking performance of the vehicle. Deliver the feature of the any one performance factor with required dynamic equation.	CO1(L5)
4	Develop the expression for the gear ratio of each gear from manual gear transmission.	CO1(L3)
5	Analyze the forces which resist the movement of the vehicle with neat sketch also to derive the expression for each.	CO1(L4)
6	Analyze the operation of hydrodynamic transmission from its performance characteristics	CO1(L4)



SATHYABAMA

INSTITUTE OF SCIENCE AND TECHNOLOGY
(DEEMED TO BE UNIVERSITY)

Accredited "A" Grade by NAAC | 12B Status by UGC | Approved by AICTE

www.sathyabama.ac.in

SCHOOL OF ELECTRICAL AND ELECTRONICS ENGINEERING

DEPARTMENT OF ELECTRICAL AND ELECTRONICS ENGINEERING

UNIT – II - Electric Vehicle – SEE1628/SEEA3028

EV Types, EV Configurations, Energy Sources, Motors Used, Charging Systems, Power Conversion Techniques, Technological Problems, Control Algorithms, Trends and Future Developments

1. Introduction

In recent times, electric vehicles (EV) are gaining popularity, and the reasons behind this are many. The most eminent one is their contribution in reducing greenhouse gas (GHG) emissions. In 2009, the transportation sector emitted 25% of the GHGs produced by energy related sectors [1]. EVs, with enough penetration in the transportation sector, are expected to reduce that figure, but this is not the only reason bringing this century old and once dead concept back to life, this time as a commercially viable and available product. As a vehicle, an EV is quiet, easy to operate, and does not have the fuel costs associated with conventional vehicles. As an urban transport mode, it is highly useful. It does not use any stored energy or cause any emission while idling, is capable of frequent start-stop driving, provides the total torque from the startup, and does not require trips to the gas station. It does not contribute either to any of the smog making the city air highly polluted. The instant torque makes it highly preferable for motor sports. The quietness and low infrared signature makes it useful in military use as well. The power sector is going through a changing phase where renewable sources are gaining momentum. The next generation power grid, called 'smart grid' is also being developed. EVs are being considered a major contributor to this new power system comprised of renewable generating facilities and advanced grid systems [2,3]. All these have led to a renewed interest and development in this mode of transport.

The idea to employ electric motors to drive a vehicle surfaced after the innovation of the motor itself. From 1897 to 1900, EVs became 28% of the total vehicles and were preferred over the internal combustion engine (ICE) ones [1]. But the ICE types gained momentum afterwards, and with very low oil prices, they soon conquered the market, became much more mature and advanced, and EVs got lost into oblivion. A chance of resurrection appeared in the form of the EV1 concept from General Motors, which was launched in 1996, and quickly became very popular. Other leading carmakers, including Ford, Toyota, and Honda brought out their own EVs as well. Toyota's highly successful Prius, the first commercial hybrid electric vehicle (HEV), was launched in Japan in 1997, with 18,000 units sold in the first year of production [1]. Today, almost none of those twentieth century EVs exist; an exception can be Toyota Prius, still going strong in a better and evolved form. Now the market is dominated by Nissan Leaf, Chevrolet Volt, and Tesla Model S; whereas the Chinese market is in the grip of BYD Auto Co., Ltd (Xi'an National Hi-tech Industrial Development Zone, Xi'an, China).

EVs can be considered as a combination of different subsystems. Each of these systems interact with each other to make the EV work, and there are multiple technologies that can be employed to operate the subsystems. In Figure 1, key parts of these subsystems and their contribution to the total system is demonstrated. Some of these parts have to work extensively with some of the others, whereas some have to interact very less. Whatever the case may be, it is the combined work of all these systems that make an EV operate.

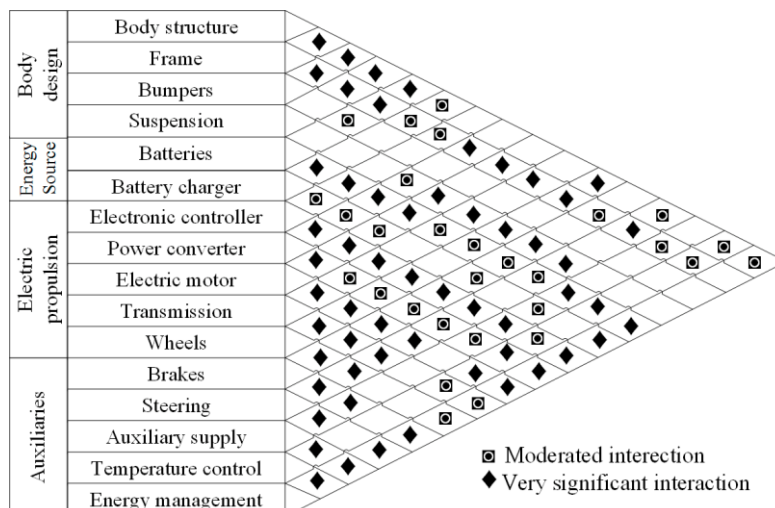


Figure 1. Major EV subsystems and their interactions. Some of the subsystems are very closely related while some others have moderated interactions. Data from [4].

There are quite a few configurations and options to build an EV with. EVs can be solely driven with stored electrical power, some can generate this energy from an ICE, and there are also some

vehicles that employ both the ICE and the electrical motors together. The general classification is discussed in Section 2, whereas different configurations are described in Section 3. EVs use different types of energy storage to store their power. Though batteries are the most used ones, ultracapacitors, flywheels and fuel cells are also up and coming as potential energy storage systems (ESS). Section 4 is dedicated to these energy sources. The types of motors that have been used in EVs and can be used in future are discussed in Section 5. Different charging voltages and charger configurations can be used in charging the vehicles. Wireless charging is also being examined and experimented with to increase convenience. These charger standards, configurations and power conversion systems are demonstrated in Sections 6–8 discusses the effects EVs create in different sectors. Being a developing technology, EVs still have many limitations that have to be overcome to enable them to penetrate deeper into the market. These limitations are pointed out in Section 9 along with probable solutions. Section 10 summed up some strategies used in EVs to enable proper use of the available power. Section 11 presented different types of control algorithms used for better driving assistance, energy management, and charging. The current state of the global EV market is briefly presented in Section 12, followed by Section 13 containing the trends and sectors that may get developed in the future. Finally, the ultimate outcomes of this paper is presented in Section 14. The topics covered in this paper have been discussed in different literatures. Over the years, a number of publications have been made discussing different aspects of EV technology. This paper was created as an effort to sum up all these works to demonstrate the state-of-the-art of the system and to position different technologies side by side to find out their merits and demerits, and in some cases, which one of them can make its way to the future EVs.

2. EV Types

EVs can run solely on electric propulsion or they can have an ICE working alongside it. Having only batteries as energy source constitutes the basic kind of EV, but there are kinds that can employ other energy source modes. These can be called hybrid EVs (HEVs). The International Electrotechnical Commission's Technical Committee 69 (Electric Road Vehicles) proposed that vehicles using two or more types of energy source, storage or converters can be called as an HEV as long as at least one of those provide electrical energy [4]. This definition makes a lot of combinations possible for HEVs like ICE and battery, battery and flywheel, battery and capacitor, battery and fuel cell, etc. Therefore, the common population and specialists both started calling vehicles with an ICE and electric motor combination HEVs, battery and capacitor ones as ultra-capacitor-assisted EVs, and the ones with battery and fuel cell FCEVs [2–4]. These terminologies have become widely accepted and according to this norm, EVs can be categorized as follows:

- (1) Battery Electric Vehicle (BEV)
- (2) Hybrid Electric Vehicle (HEV)
- (3) Plug-in Hybrid Electric Vehicle (PHEV)
- (4) Fuel Cell Electric Vehicle (FCEV)

2.1. Battery Electric Vehicle (BEV)

EVs with only batteries to provide power to the drive train are known as BEVs. BEVs have to rely solely on the energy stored in their battery packs; therefore the range of such vehicles depends directly on the battery capacity. Typically they can cover 100 km–250 km on one charge [5], whereas the top-tier models can go a lot further, from 300 km to 500 km [5]. These ranges depend on driving condition and style, vehicle configurations, road conditions, climate, battery type and age. Once depleted, charging the battery pack takes quite a lot of time compared to refueling a conventional ICE vehicle. It can take as long as 36 h completely replenish the batteries [6,7], there are far less time consuming ones as well, but none is comparable to the little time required to refill a fuel tank.

Charging time depends on the charger configuration, its infrastructure and operating power level. Advantages of BEVs are their simple construction, operation and convenience. These do not produce any greenhouse gas (GHG), do not create any noise and therefore beneficial to the environment. Electric propulsion provides instant and high torques, even at low speeds. These advantages, coupled with their limitation of range, makes them the perfect vehicle to use in urban areas; as depicted in Figure 2, urban driving requires running at slow or medium speeds, and these ranges demand a lot of torque. Nissan Leaf and Teslas are some high-selling BEVs these days, along with some Chinese vehicles. Figure 3 shows basic configuration for BEVs: the wheels are driven by electric motor(s) which is run by batteries through a power converter circuit.

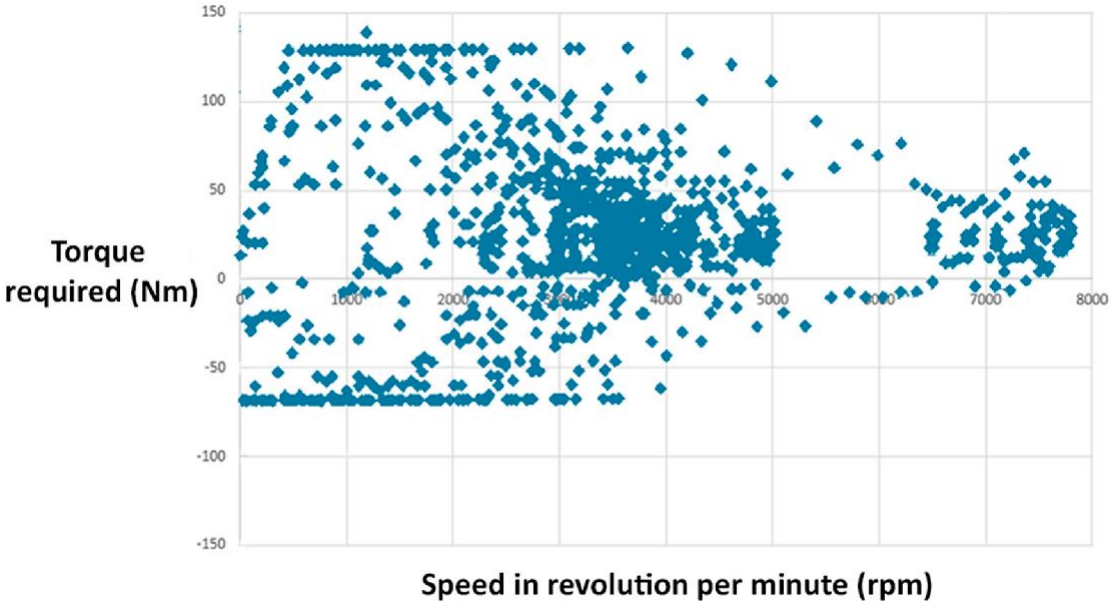


Figure 2. Federal Urban Driving Schedule torque-speed requirements. Most of the driving is done in the 2200 to 4800 rpm range with significant amount of torque. Lower rpms require torques as high as 125 Nm; urban vehicles have to operate in this region regularly as they face frequent start-stops. Data from [4].

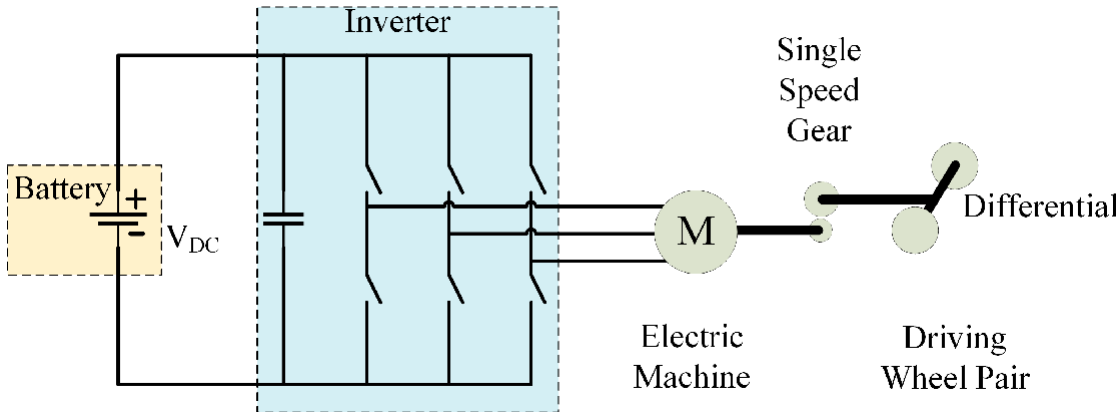
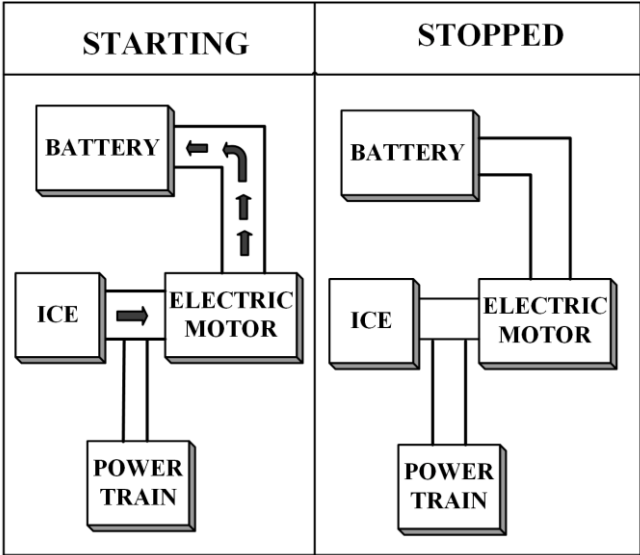


Figure 3. BEV configuration. The battery’s DC power is converted to AC by the inverter to run the motor. Adapted from [5].

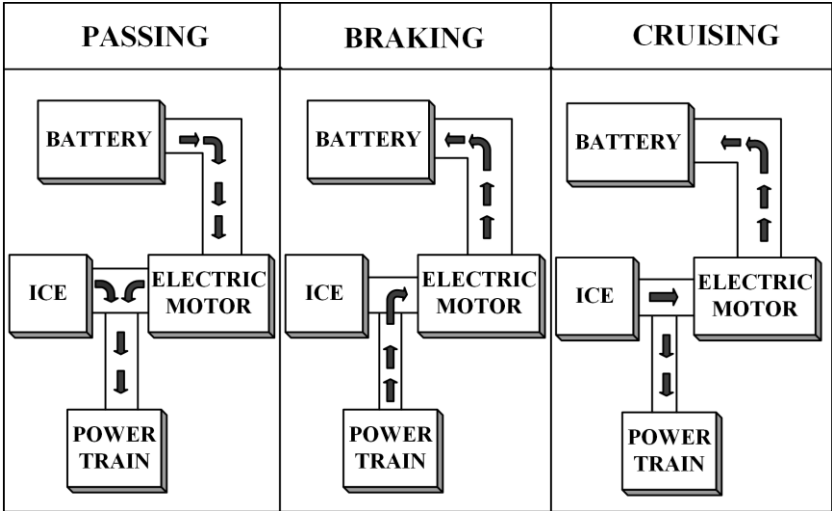
2.2. Hybrid Electric Vehicle (HEV)

HEVs employ both an ICE and an electrical power train to power the vehicle. The combination of these two can come in different forms which are discussed later. An HEV uses the electric propulsion system when the power demand is low. It is a great advantage in low speed conditions like urban areas; it also reduces the fuel consumption as the engine stays totally off during idling

periods, for example, traffic jams. This feature also reduces the GHG emission. When higher speed is needed, the HEV switches to the ICE. The two drive trains can also work together to improve the performance. Hybrid power systems are used extensively to reduce or to completely remove turbo lag in turbocharged cars, like the Acura NSX. It also enhances performance by filling the gaps between gear shifts and providing speed boosts when required. The ICE can charge up the batteries, HEVs can also retrieve energy by means of regenerative braking. Therefore, HEVs are primarily ICE driven cars that use an electrical drive train to improve mileage or for performance enhancement. To attain these features, HEV configurations are being widely adopted by car manufacturers. Figure 4 shows the energy flows in a basic HEV. While starting the vehicle, the ICE may run the motor as a generator to produce some power and store it in the battery. Passing needs a boost in speed, therefore the ICE and the motor both drives the power train. During braking the power train runs the motor as generator to charge the battery by regenerative braking. While cruising, ICE runs the both the vehicle and the motor as generator, which charges the battery. The power flow is stopped once the vehicle stops. Figure 5 shows an example of energy management systems used in HEVs. The one demonstrated here splits power between the ICE and the electric motor (EM) by considering the vehicle speed, driver’s input, state of charge (SOC) of battery, and the motor speed to attain maximum fuel efficiency.



(a) Direction of power flow during starting and when stopped.



(b) Direction of power flow during passing, braking and cruising.

Figure 4. Power flow among the basic building blocks of an HEV during various stages of a drive cycle. Adapted from [8].

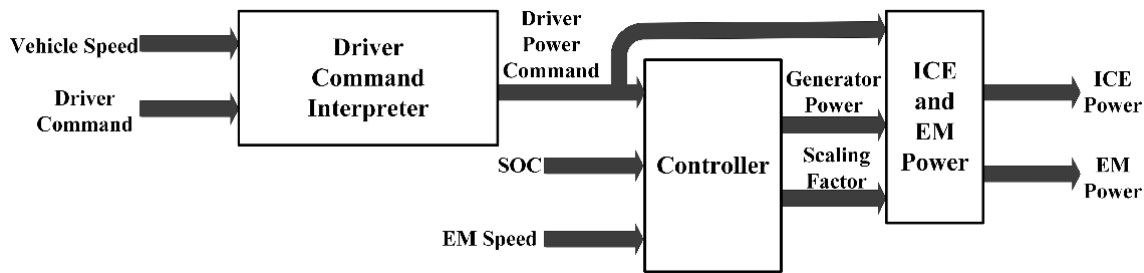


Figure 5. Example of energy management strategy used in HEV. The controller splits power between the ICE and the motor by considering different input parameters. Adapted from [8].

2.3. Plug-In Hybrid Electric Vehicle (PHEV)

The PHEV concept arose to extend the all-electric range of HEVs [9–14]. It uses both an ICE and an electrical power train, like a HEV, but the difference between them is that the PHEV uses electric propulsion as the main driving force, so these vehicles require a bigger battery capacity than HEVs. PHEVs start in ‘all electric’ mode, runs on electricity and when the batteries are low in charge, it calls on the ICE to provide a boost or to charge up the battery pack. The ICE is used here to extend the range. PHEVs can charge their batteries directly from the grid (which HEVs cannot); they also have the facility to utilize regenerative braking. PHEVs’ ability to run solely on electricity for most of the time makes its carbon footprint smaller than the HEVs. They consume less fuel as well and thus reduce the associated cost. The vehicle market is now quite populated with these, Chevrolet Volt and Toyota Prius sales show their popularity as well.

2.4. Fuel Cell Electric Vehicle (FCEV)

FCEVs also go by the name Fuel Cell Vehicle (FCV). They got the name because the heart of such vehicles is fuel cells that use chemical reactions to produce electricity [15]. Hydrogen is the fuel of choice for FCVs to carry out this reaction, so they are often called ‘hydrogen fuel cell vehicles’. FCVs carry the hydrogen in special high pressure tanks, another ingredient for the power generating process is oxygen, which it acquires from the air sucked in from the environment. Electricity generated from the fuel cells goes to an electric motor which drives the wheels. Excess energy is stored in storage systems like batteries or supercapacitors [2,3,16–18]. Commercially available FCVs like the Toyota Mirai or Honda Clarity use batteries for this purpose. FCVs only produce water as byproduct of its power generating process which is ejected out of the car through the tailpipes. The configuration of an FCV is shown in Figure 6. An advantage of such vehicles is they can produce their own electricity which emits no carbon, enabling it to reduce its carbon footprint further than any other EV. Another major advantage of these are, and maybe the most important one right now, refilling these vehicles takes the same amount of time required to fill a conventional vehicle at a gas pump. This makes adoption of these vehicles more likely in the near future [2–4,19]. A major current obstacle in adopting this technology is the scarcity of hydrogen fuel stations, but then again, BEV or PHEV charging stations were not a common scenario even a few years back. A report to the U.S. Department of Energy (DOE) pointed to another disadvantage which is the high cost of fuel cells, that cost more than \$200 per kW, which is far greater than ICE (less than \$50 per kW) [20,21]. There are also concerns regarding safety in case of flammable hydrogen leaking out of the tanks. If these obstacles were eliminated, FCVs could really represent the future of cars. The possibilities of using this technology in supercars is shown by Pininfarina’s H2 Speed (Figure 7). Reference [22] compared BEVs and FCEVs in different aspects, where FCEVs appeared to be better than BEVs in many ways; this comparison is shown in Figure 8. In this figure, different costs and cost associated issues of BEV and FCEV: weight, required storage volume, initial GHG emission, required natural gas energy, required wind energy, incremental costs, fueling infrastructure cost per car, fuel cost per kilometer, and incremental life cycle cost are all compared for 320 km (colored blue) and 480 km (colored green) ranges. The horizontal axis shows the attribute ratio of BEV to FCEV. As having a less value in these attributes indicates an advantage, any value higher than one in the horizontal axis will declare FCEVs

superior to BEVs in that attribute. That being said, BEVs only appear better in the fields of required wind energy and fuel cost per kilometer. Fuel cost still appears to be one of the major drawbacks of FCEVs, as a cheap, sustainable and environment-friendly way of producing hydrogen is still lacking, and the refueling infrastructure lags behind that of BEVs; but these problems may no longer prevail in the near future.

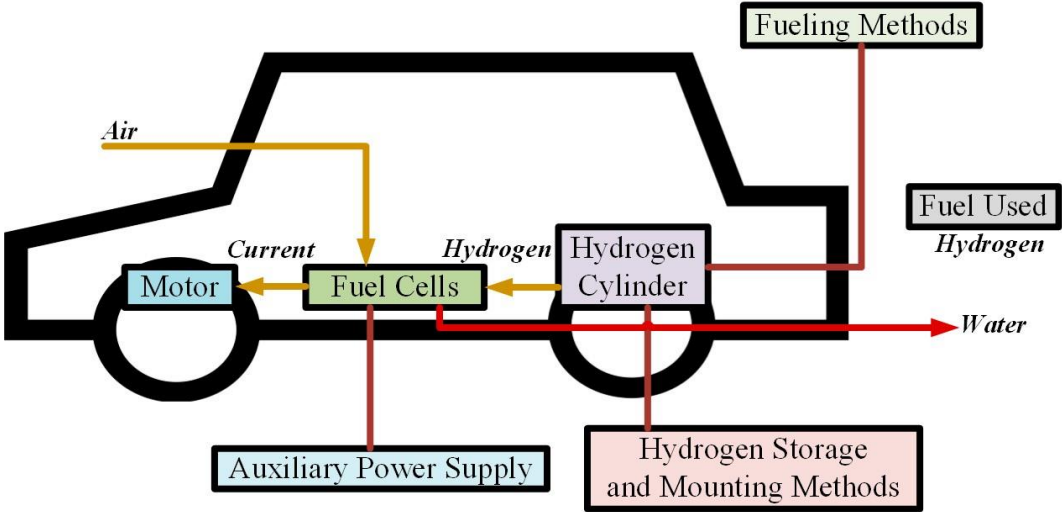


Figure 6. FCEV configuration. Oxygen from air and hydrogen from the cylinders react in fuel cells to produce electricity that runs the motor. Only water is produced as by-product which is released in the environment.



Figure 7. Pininfarina H2 Speed, a supercar employing hydrogen fuel cells.

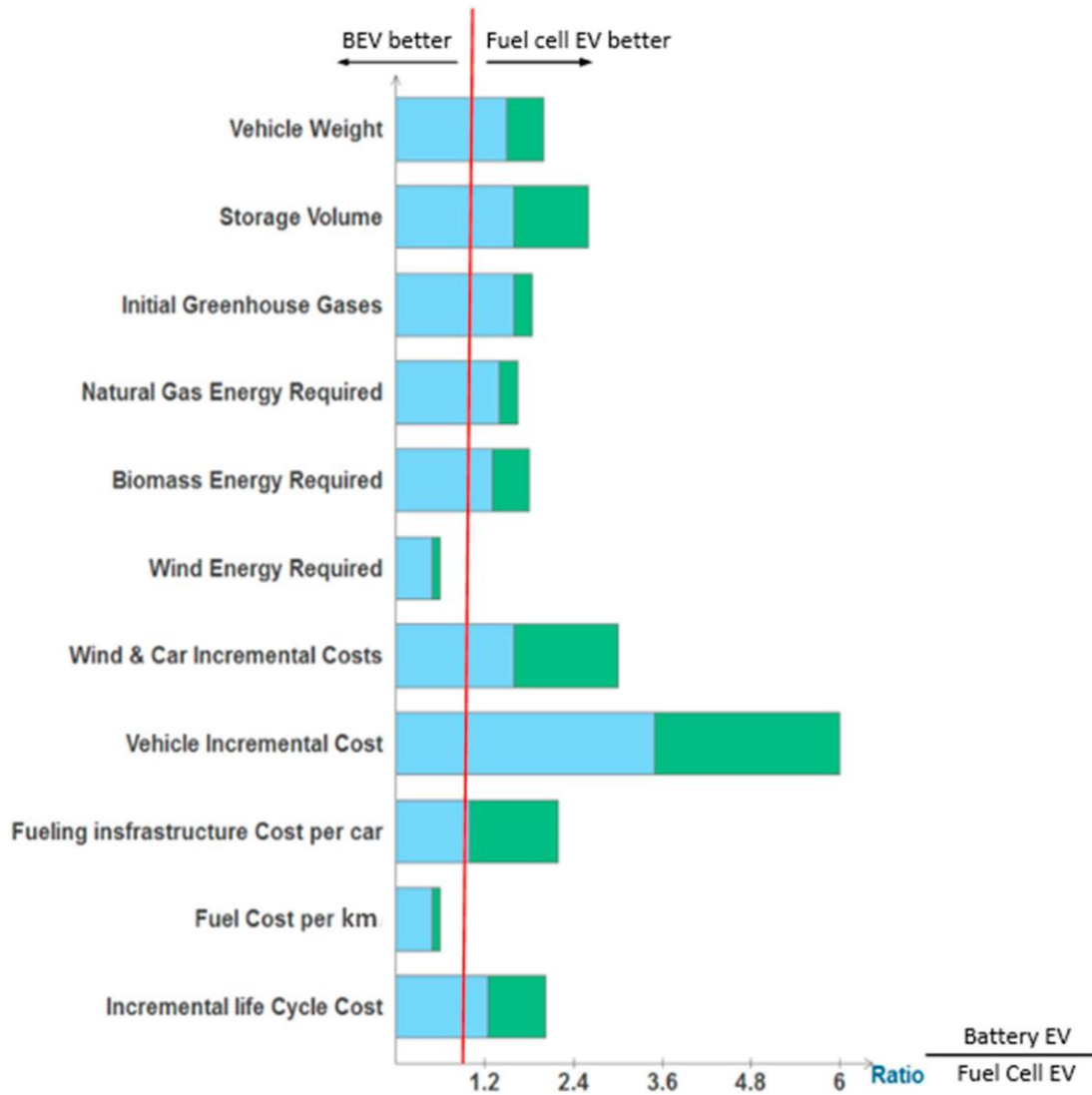


Figure 8. Advanced battery EV attribute and fuel cell EV attribute ratio for 320 km (colored blue) and 480 km (colored green) ranges, with assumptions of average US grid mix in 2010–2020 time-range and all hydrogen made from natural gas (values greater than one indicate a fuel cell EV advantage over the battery EV). Data from [22].

Rajashekara predicted a slightly different future for FCVs in [23]. He showed a plug-in fuel cell vehicle (PFCV) with a larger battery and smaller fuel cell, which makes it battery-dominant car. According to [23], if hydrogen for such vehicles can be made from renewable sources to run the fuel cells and the energy to charge the batteries comes from green sources as well, these PFCVs will be the future of vehicles. The FCVs we see today will not have much appeal other than some niche markets. Figure 9 shows a basic PFCV configuration. Table 1 compares the different vehicle types in terms of driving component, energy source, features, and limitations.

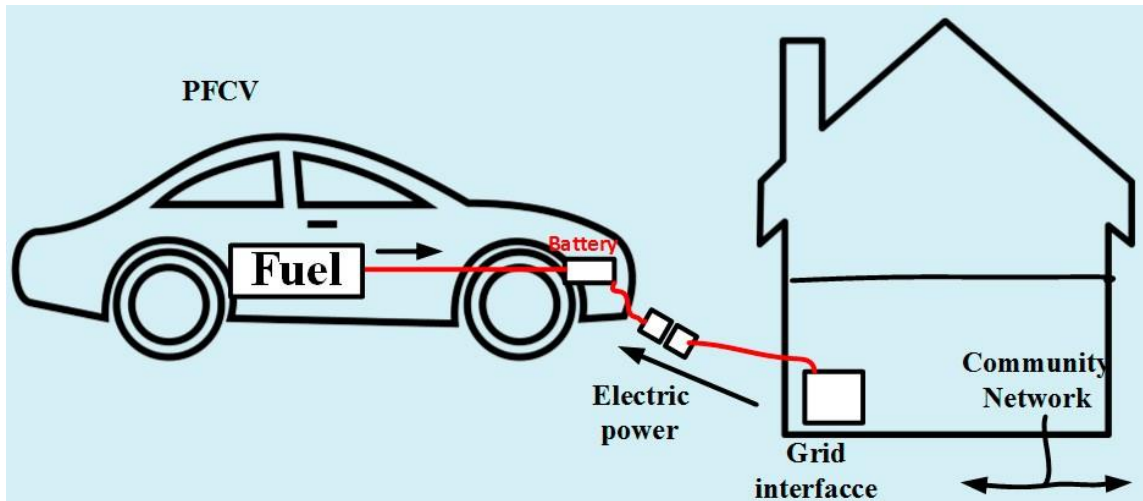


Figure 9. PFCV configuration. In addition to the fuel cells, this arrangement can directly charge the battery from a power outlet.

Table 1. Comparison of different vehicle types. Adapted from [4].

EV Type	Driving Component	Energy Source	Features	Problems
BEV	• Electric motor	• Battery • Ultracapacitor	<ul style="list-style-type: none"> • No emission • Not dependent on oil • Range depends largely on the type of battery used • Available commercially 	<ul style="list-style-type: none"> • Battery price and capacity • Range • Charging time • Availability of charging stations • High price
HEV	• Electric motor • ICE	• Battery • Ultracapacitor • ICE	<ul style="list-style-type: none"> • Very little emission • Long range • Can get power from both electric supply and fuel • Complex structure having both electrical and mechanical drivetrains • Available commercially 	<ul style="list-style-type: none"> • Management of the energy sources • Battery and engine size optimization
FCEV	• Electric motor	• Fuel cell	<ul style="list-style-type: none"> • Very little or no emission • High efficiency • Not dependent on supply of electricity • High price • Available commercially 	<ul style="list-style-type: none"> • Cost of fuel cell • Feasible way to produce fuel • Availability of fueling facilities

3. EV Configurations

An electric vehicle, unlike its ICE counterparts, is quite flexible [4]. This is because of the absence of intricate mechanical arrangements that are required to run a conventional vehicle. In an EV, there is only one moving part, the motor. It can be controlled by different control arrangements and techniques. The motor needs a power supply to run which can be from an array of sources. These two components can be placed at different locations on the vehicle and as long as they are connected through electrical wires, the vehicle will work. Then again, an EV can run solely on electricity, but an ICE and electric motor can also work in conjunction to turn the wheels. Because of such flexibility, different configurations emerged which are adopted according to the type of vehicle. An EV can be considered as a system incorporating three different subsystems [4]: energy source, propulsion and auxiliary. The energy source subsystem includes the source, its refueling system and energy management system. The propulsion subsystem has the electric motor, power converter, controller, transmission and the driving wheels as its components. The auxiliary subsystem is comprised of auxiliary power supply, temperature control system and the power steering unit. These subsystems are shown in Figure 10.

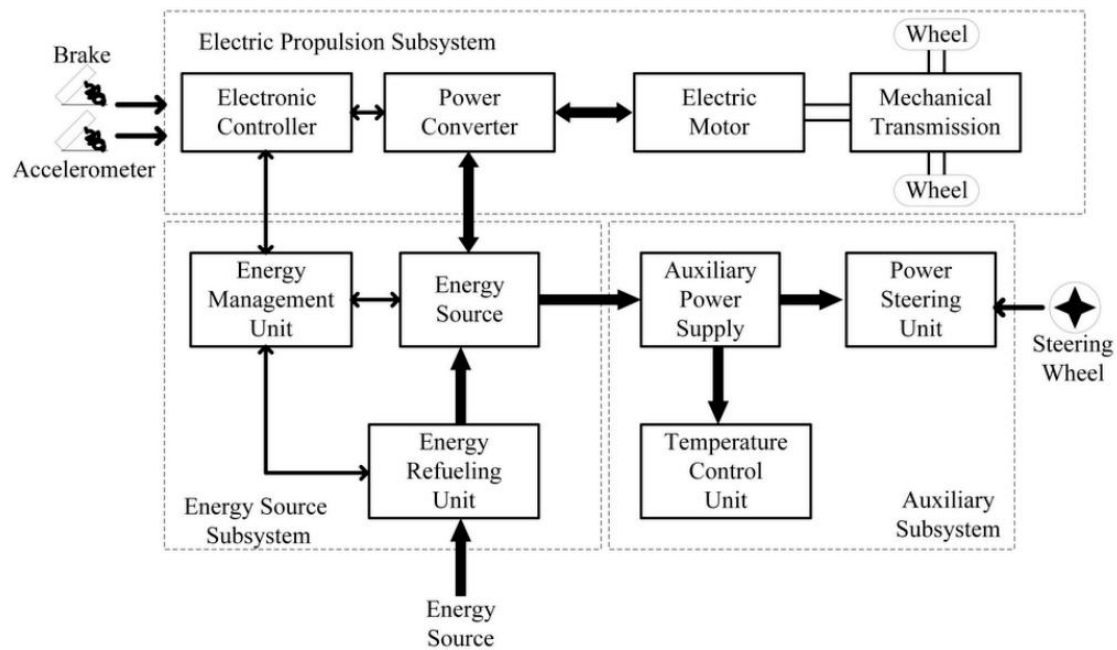


Figure 10. EV subsystems. Adapted from [4].

The arrows indicate the flow of the entities in question. A backward flow of power can be created by regenerative actions like regenerative braking. The energy source has to be receptive to store the energy sent back by regenerative actions. Most of the EV batteries along with capacitors/flywheels (CFs) are compatible with such energy regeneration techniques [4].

3.1. General EV Setup

EVs can have different configurations as shown in [4]. Figure 11a shows a front-engine front-wheel drive vehicle with just the ICE replaced by an electric motor. It has a gearbox and clutch that allows high torque at low speeds and low torque at high speeds. There is a differential as well that allows the wheels to rotate at different speeds. Figure 11b shows a configuration with the clutch omitted. It has a fixed gear in place of the gearbox which removes the chance of getting the desired torque-speed characteristics. The configuration of Figure 11c has the motor, gear and differential as a single unit that drives both the wheels. The Nissan Leaf, as well as the Chevrolet Spark, uses an electric motor mounted at the front to drive the front axle. In Figure 11d,e, configurations to obtain differential action by using two motors for the two wheels are shown. Mechanical interaction can be further reduced by placing the motors inside the wheels to produce an 'in-wheel drive'. A planetary gear system is employed here because advantages like high speed reduction ratio and inline arrangement of input and output shafts. Mechanical gear system is totally removed in the last configuration (Figure 11f) by mounting a low-speed motor with an outer rotor configuration on the wheel rim. Controlling the motor speed thus controls the wheel speed and the vehicle speed.

EVs can be built with rear wheel drive configuration as well. The single motor version of the Tesla Model S uses this configuration (Figure 12). The Nissan Blade Glider is a rear wheel drive EV with in-wheel motor arrangement. The use of in-wheel motors enables it to apply different amount of torques at each of the two rear wheels to allow better cornering.

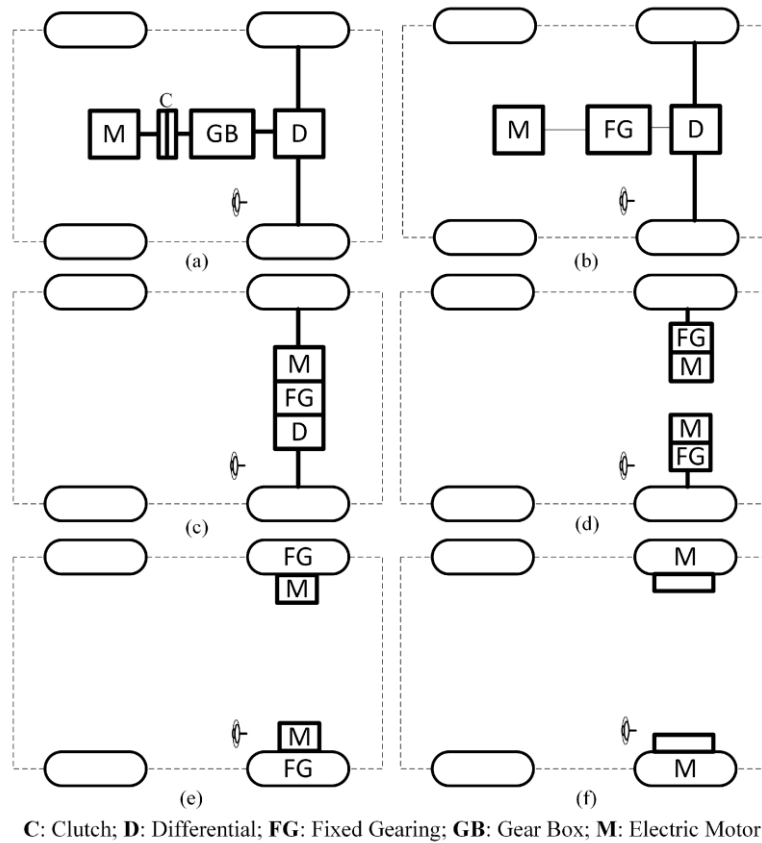


Figure 11. Different front wheel drive EV configurations. (a) Front-wheel drive vehicle with the ICE replaced by an electric motor; (b) Vehicle configuration with the clutch omitted; (c) Configuration with motor, gear and differential combined as a single unit to drive the front wheels; (d) Configuration with individual motors with fixed fearing for the front wheels to obtain differential action; (e) Modified configuration of Figure 11d with the fixed gearing arrangement placed within the wheels; (f) Configuration with the mechanical gear system removed by mounting a low-speed motor on the wheel rim. Adapted from [4].

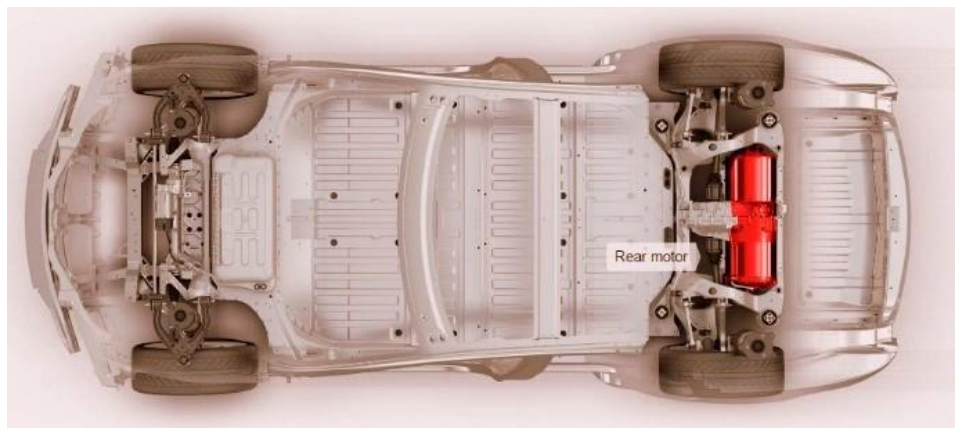


Figure 12. Tesla Model S, rear wheel drive configuration [22,24]. (Reprint with permission [24]; 2017, Tesla.)

For more control and power, all-wheel drive (AWD) configurations can also be used, though it comes with added cost, weight and complexity. In this case, two motors can be used to drive the front and the rear axles. An all-wheel drive configuration is shown in Figure 13. AWD configurations are useful to provide better traction in slippery conditions, they can also use torque vectoring for better cornering performance and handling. AWD configuration can also be realized for in-wheel motor systems. It can prove quite useful for city cars like the Hiriko Fold (Figure 14) which has steering

actuator, suspension, brakes and a motor all integrated in each wheel. Such arrangements can provide efficient all wheel driving, all wheel steering along with ease of parking and cornering.

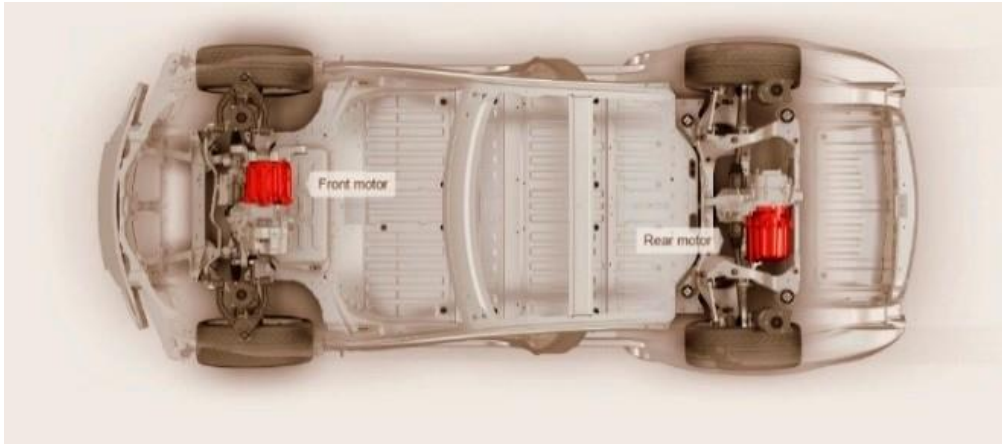


Figure 13. Tesla Model S, all-wheel drive configuration [24]. (Reprint with permission [24]; 2017, Tesla.)9442679129



Figure 14. Hiriko Fold—a vehicle employing in-wheel motors.

In-wheel motor configurations are quite convenient in the sense that they reduce the weight of the drive train by removing the central motor, related transmission, differential, universal joints and drive shaft [25]. They also provide more control, better turning capabilities and more space for batteries, fuel cells or cargo, but in this case the motor is connected to the power and control systems through wires that can get damaged because of the harsh environment, vibration and acceleration, thus causing serious trouble. Sato et al., proposed a wireless in-wheel motor system (W-IWM) in [26] which they had implemented in an experimental vehicle (shown in Figure 15). Simply put, the wires are replaced by two coils which are able to transfer power in-between them. Because of vibrations caused by road conditions, the motor and the vehicle can be misaligned and can cause variation in the secondary side voltage. In-wheel motor configurations are shown in Figure 16, whereas the efficiencies at different stages of such a system are shown in Figure 17. In conditions like this, magnetic resonance coupling is preferred for wireless power transfer [27] as it can overcome the problems associated with such misalignments [28]. The use of a hysteresis comparator and applying the secondary inverter power to a controller to counter the change in secondary voltage was also proposed in [28]. Wireless power transfer (WPT) employing magnetic resonance coupling in a series-parallel arrangement can provide a transmitting efficiency of 90% in both directions at 2 kW [29]. Therefore, W-IWM is compliant with regenerative braking as well.



Figure 15. Experimental vehicle with W-IWM system by Sato et al. [26]. (Reprint with permission [26]; 2015, IEEE.)

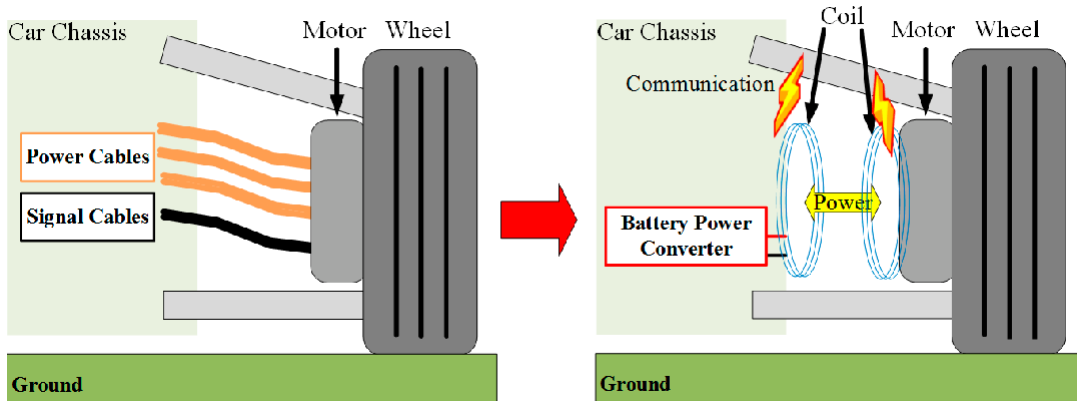


Figure 16. Conventional and wireless IWM. In the wireless setup, coils are used instead of wires to transfer power from battery to the motor. Adapted from [26].

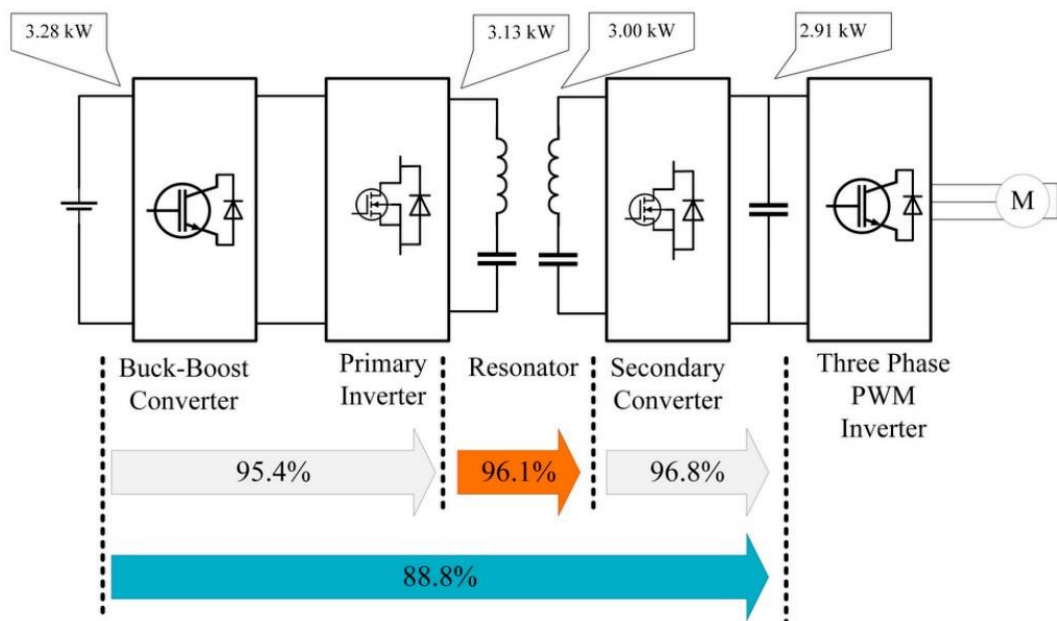


Figure 17. W-IWM setup showing efficiency at 100% torque reference. Adapted from [26].

3.2. HEV Setup

HEVs use both an electrical propulsion system and an ICE. Various ways in which these two can be set up to spin the wheels creates different configurations that can be summed up in four categories [4]:

- (1) Series hybrid
- (2) Parallel hybrid
- (3) Series-parallel hybrid
- (4) Complex hybrid

3.2.1. Series Hybrid

This configuration is the simplest one to make an HEV. Only the motor is connected to the wheels here, the engine is used to run a generator which provides the electrical power. It can be put as an EV that is assisted by an ICE generator [4]. Series hybrid drive train is shown in Figure 18. Table 2 shows the merits and demerits of this configuration.

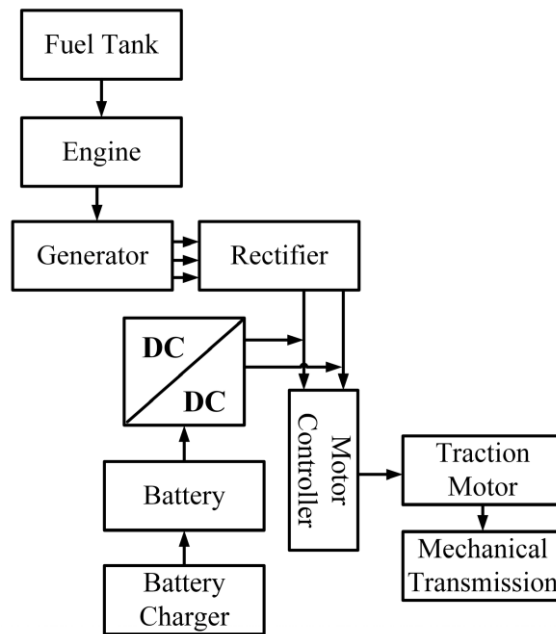


Figure 18. Drive train of series hybrid system. The engine is used to generate electricity only and supply to the motor through a rectifier. Power from the battery goes to the motor through a DC-DC converter [30].

Table 2. Advantages and limitations of series hybrid configuration. Adapted from [8].

Advantages	Efficient and optimized power-plant
	Possibilities for modular power-plant
	Optimized drive line
	Possibility of swift 'black box' service exchange
	Long lifetime
	Mature technology
	Fast response
Limitations	Capable of attaining zero emission
	Large traction drive system
	Requirement of proper algorithms
Multiple energy conversion steps	

3.2.2. Parallel Hybrid

This configuration connects both the ICE and the motor in parallel to the wheels. Either one of them or both take part in delivering the power. It can be considered as an IC engine vehicle with electric assistance [4]. The energy storages in such a vehicle can be charged by the electric motor by means of regenerative braking or by the ICE when it produces more than the power required to drive the wheels. Parallel hybrid drive train is shown in Figure 19. Table 3 shows the merits and demerits of this configuration, while Table 4 compares the series and the parallel systems.

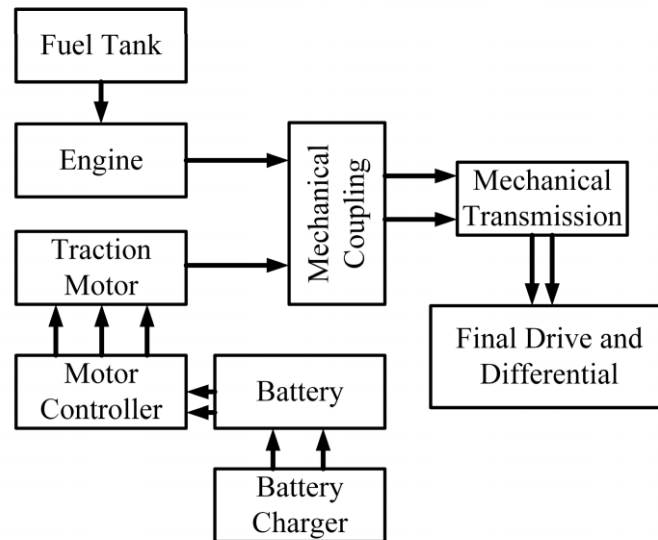


Figure 19. Drive train of parallel hybrid system. The engine and the motor both can run the can through the mechanical coupling [30].

Table 3. Advantages and limitations of parallel hybrid configuration. Adapted from [30].

Advantages	Capable of attaining zero emission
	Economic gain
Limitations	More flexibility
	Expensive
	Complex control
	Requirement of proper algorithms
	<u>Need of high voltage to ensure efficiency</u>

Table 4. Comparison of parallel and series hybrid configurations. Data from [8].

Parameters	Parallel HEV	Series HEV
Voltage	14 V, 42 V, 144 V, 300 V	216 V, 274 V, 300 V, 350 V, 550 V, 900 V
Power requirement	3 KW–40 KW	>50 KW
Relative gain in fuel economy (%)	5–40	>75

3.2.3. Series-Parallel Hybrid

In an effort to combine the series and the parallel configuration, this system acquires an additional mechanical link compared to the series type, or an extra generator when compared to the parallel type. It provides the advantages of both the systems but is more costly and complicated nonetheless. Complications in drive train are caused to some extent by the presence of a planetary gear unit [30]. Figure 20 shows a planetary gear arrangement: the sun gear is connected to the generator, the output shaft of the motor is connected to the ring gear, the ICE is coupled to the planetary carrier, and the pinion gears keep the whole system connected. A less complex alternative to this system is to use a transmutor, which is a floating-stator electric machine. In this system the engine is attached to the stator, and the rotor stays connected to the drive train wheel through the gears. The motor speed is the relative speed between the rotor and the stator and controlling it adjusts

the engine speed for any particular vehicle speed [30]. Series-parallel hybrid drive train with planetary gear system is shown in Figure 21; Figure 22 shows the system with a transmotor.

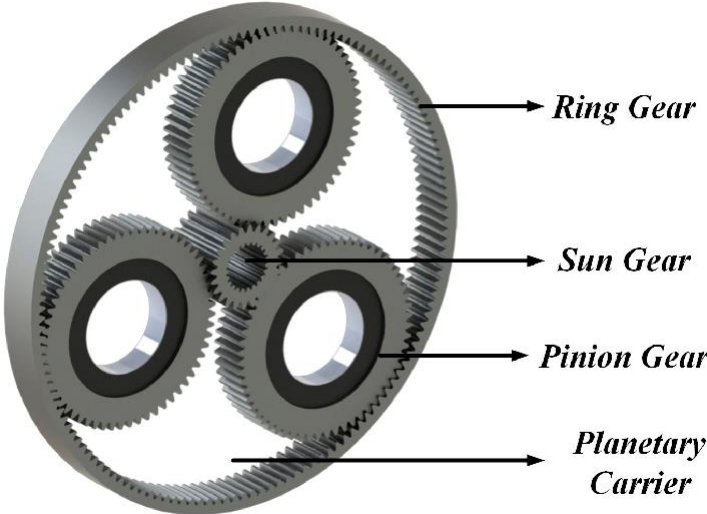


Figure 20. Planetary gear system [31].

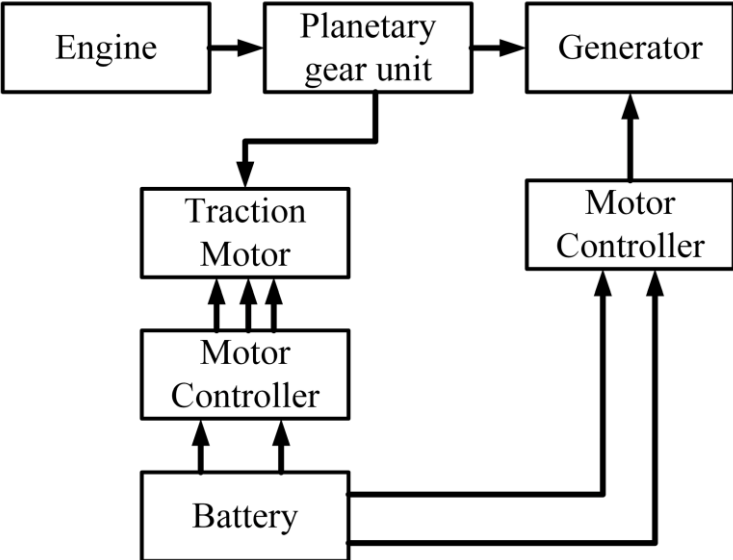


Figure 21. Drive train of series-parallel hybrid system using planetary gear unit. The planetary gear unit combines the engine, the generator and the motor [30].

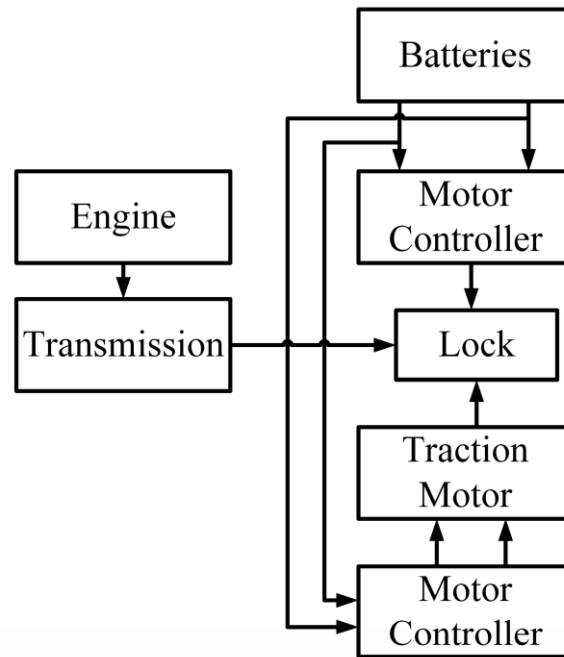


Figure 22. Drive train of series-parallel hybrid system using transmotor. The planetary gear system is absent in this arrangement [30].

3.2.4. Complex Hybrid

This system has one major difference with the series-parallel system, that is, it allows bidirectional flow of power whereas the series-parallel can provide only unidirectional power flow. However, using current market terminologies, this configuration is denoted as series-parallel system too. High complexity and cost are drawbacks of this system, but it is adopted by some vehicles to use dual-axle propulsion [4]. Constantly variable transmission (CVT) can be used for power splitting in a complex hybrid system or choosing between the power sources to drive the wheels. Electric arrangements can be used for such processes and this is dubbed as e-CVT, which has been developed and introduced by Toyota Motor Co. (Toyota City, Aichi Prefecture 471-8571, Japan). CVTs can be implemented hydraulically, mechanically, hydro-mechanically or electromechanically [32]. Two methods of power splitting—input splitting and complex splitting are shown in [32]. Input splitting got the name as it has a power split device placed at the transmission input. This system is used by certain Toyota and Ford models [32]. Reference [32] also showed different modes of these two splitting mechanisms and provided descriptions of e-CVT systems adopted by different manufacturers which are shown in Figures 23 and 24. Such power-split HEVs require two electric machines, wheels, an engine and a planetary gear (PG), combining all of them can be done in twenty-four different ways. If another PG is used, that number gets greater than one thousand. An optimal design incorporating a single PG is proposed in [31]. Four-wheel drive (4WD) configurations can benefit from using a two-motor hybrid configuration as it nullifies the need of a power transmission system to the back wheels (as they get their own motor) and provides the advantage of energy reproduction by means of regenerative braking [33]. Four-wheel drive HEV structure is shown in Figure 25. A stability enhancement scheme for such a configuration by controlling the rear motor is shown in [33].

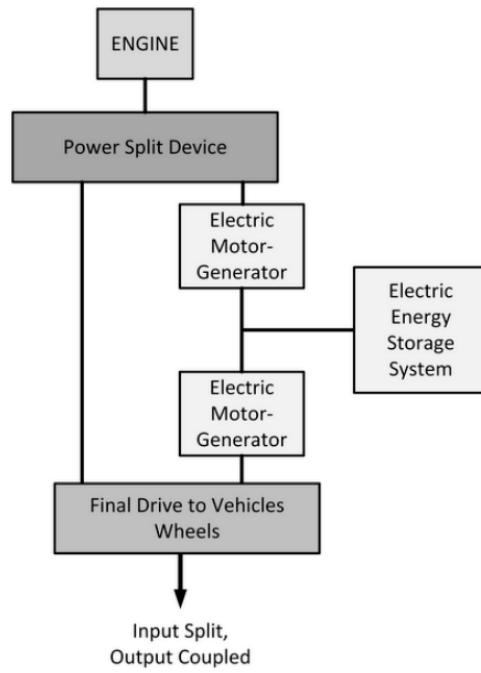


Figure 23. Input split e-CVT system. Adapted from [32].

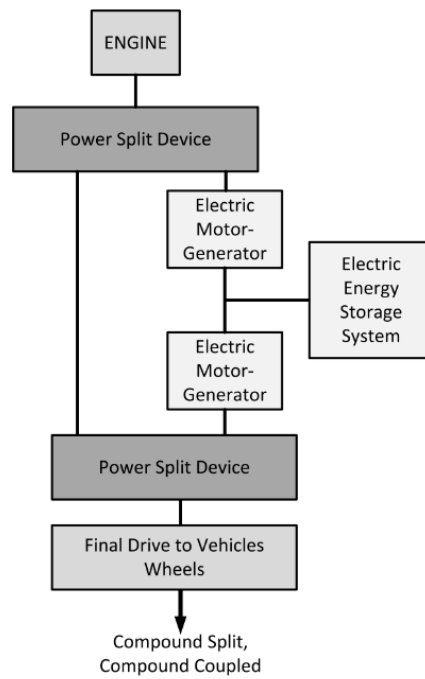


Figure 24. Compound split e-CVT system. Adapted from [32].

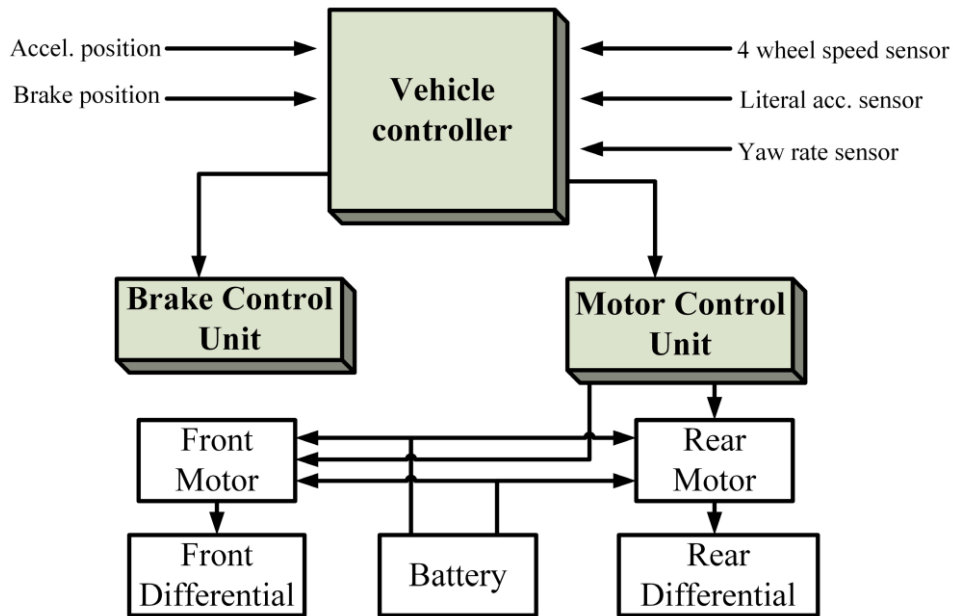


Figure 25. Structure for four-wheel drive HEV [32]. This particular system uses a vehicle controller which employs a number of sensors to perceive the driving condition and keeps the vehicle stable by controlling the brake control and the motor control units.

4. Energy Sources

EVs can get the energy required to run from different sources. The criteria such sources have to satisfy are mentioned in [4], high energy density and high power density being two of the most important ones [30]. There are other characteristics that are sought after to make a perfect energy source, fast charging, long service and cycle life, less cost and maintenance being a few of them. High specific energy is required from a source to provide a long driving range whereas high specific power helps to increase the acceleration. Because of the diverse characteristics that are required for the perfect source, quite a few sources or energy storage systems (ESS) come into discussion; they are also used in different combinations to provide desired power and energy requirements [4].

4.1. Battery

Batteries have been the major energy source for EVs for a long time; though of course, was time has gone by, different battery technologies have been invented and adopted and this process is still going on to attain the desired performance goals. Table 5 shows the desired performance for EV batteries set by the U.S. Advanced Battery Consortium (USABC).

Table 5. Performance goal of EV batteries as set by USABC. Data from [4].

	Parameters	Mid-Term	Long-Term
Primary goals	Energy density (C/3 discharge rate) (Wh/L)	135	300
	Specific energy (C/3 discharge rate) (Wh/kg)	80 (Desired: 100)	200
	Power density (W/l)	250	600
	Specific power (80% DOD/30 s) (W/kg)	150 (Desired: 200)	400
	Lifetime (year)	5	10
	Cycle life (80% DOD) (cycles)	600	1000
	Price (USD/kWh)	<150	<100
	Operating temperature (°C)	-30 to 65	-40 to 84
	Recharging time (hour)	<6	3 to 6
	Fast recharging time (40% to 80% SOC) (hour)	0.25	
Secondary goals	Self-discharge (%)	<15 (48 h)	<15 (month)
	Efficiency (C/3 discharge, 6 h charge) (%)	75	80
	Maintenance	No maintenance	No maintenance

	Resistance to abuse	Tolerance	Tolerance
	Thermal loss	3.2 W/kWh	3.2 W/kWh

Some of the prominent battery types are: lead-acid, Ni-Cd, Ni-Zn, Zn/air, Ni-MH, Na/S, Li-polymer and Li-ion batteries. Yong et al., also showed a battery made out of graphene for EV use whose advantages, structural model and application is described in [34]. Different battery types have their own pros and cons, and while selecting one, these things have to be kept in mind. In [35], Khaligh et al., provided key features of some known batteries which are demonstrated in Table 6. In Table 7, common battery types are juxtaposed to relative advantage of one battery type over the others.

Table 6. Common battery types, their basic construction components, advantages and disadvantages. Data from [35–44].

Battery Type	Components	Advantage	Disadvantage
4.1.1. Lead-acid	<ul style="list-style-type: none"> Negative active material: spongy lead Positive active material: lead oxide Electrolyte: diluted sulfuric acid 	<ul style="list-style-type: none"> Available in production volume Comparatively low in cost Mature technology as used for over fifty years 	<ul style="list-style-type: none"> Cannot discharge more than 20% of its capacity Has a limited life cycle if operated on a deep rate of SOC (state of charge) Low energy and power density Heavier May need maintenance
NiMH (Nickel-Metal Hydride)	<ul style="list-style-type: none"> Electrolyte: alkaline solution Positive electrode: nickel hydroxide Negative electrode: alloy of nickel, titanium, vanadium and other metals. 	<ul style="list-style-type: none"> Double energy density compared to lead-acid Harmless to the environment Recyclable Safe operation at high voltage Can store volumetric power and energy Cycle life is longer Operating temperature range is long Resistant to over-charge and discharge 	<ul style="list-style-type: none"> Reduced lifetime of around 200–300 cycles if discharged rapidly on high load currents Reduced usable power because of memory effect
Li-Ion (Lithium-Ion)	<ul style="list-style-type: none"> Positive electrode: oxidized cobalt material Negative electrode: carbon material Electrolyte: lithium salt solution in an organic solvent 	<ul style="list-style-type: none"> High energy density, twice of NiMH Good performance at high temperature Recyclable Low memory effect High specific power High specific energy Long battery life, around 1000 cycles 	<ul style="list-style-type: none"> High cost Recharging still takes quite a long time, though better than most batteries
Ni-Zn (Nickel-Zinc)	<ul style="list-style-type: none"> Positive electrode: nickel oxyhydroxide Negative electrode: zinc 	<ul style="list-style-type: none"> High energy density High power density Uses low cost material Capable of deep cycle Friendly to environment Usable in a wide temperature range from -10 °C to 50 °C 	<ul style="list-style-type: none"> Fast growth of dendrite, preventing use in vehicles
Ni-Cd (Nickel-Cadmium)	<ul style="list-style-type: none"> Positive electrode: nickel hydroxide Negative electrode: cadmium 	<ul style="list-style-type: none"> Long lifetime Can discharge fully without being damaged Recyclable 	<ul style="list-style-type: none"> Cadmium can cause pollution in case of not being properly disposed of Costly for vehicular application

Table 7. Cross comparison of different battery types to show relative advantages. Adapted from [45].

Advantages Over	Lead-Acid	Ni-Cd (Nickel-Cadmium)	NiMH (Nickel-Metal Hydride)	Li-Ion (Lithium-Ion)	
				Conventional	Polymer
Lead-acid		<ul style="list-style-type: none"> • Volumetric energy density • Gravimetric energy density • Range of operating temperature • Rate of self-discharge reliability 	<ul style="list-style-type: none"> • Volumetric energy density • Gravimetric energy density • Rate of self-discharge 	<ul style="list-style-type: none"> • Volumetric energy density • Gravimetric energy density • Rate of self-discharge 	<ul style="list-style-type: none"> • Volumetric energy density • Gravimetric energy density • Rate of self-discharge • Design features
	Ni-Cd (Nickel-Cadmium)	<ul style="list-style-type: none"> • Output voltage • Cost • Higher cyclability 		<ul style="list-style-type: none"> • Volumetric energy density • Gravimetric energy density • Rate of self-discharge • Output voltage 	<ul style="list-style-type: none"> • Volumetric energy density • Gravimetric energy density • Rate of self-discharge • Design features
NiMH (Nickel-Metal Hydride)	<ul style="list-style-type: none"> • Output voltage • Cost • Higher cyclability 	<ul style="list-style-type: none"> • Range of operating temperature • Cost • Higher cyclability • Rate of self-discharge 		<ul style="list-style-type: none"> • Volumetric energy density • Gravimetric energy density • Range of operating temperature 	<ul style="list-style-type: none"> • Volumetric energy density • Gravimetric energy density • Range of operating temperature • Rate of self-discharge • Design features
Li-Ion (conventional)	<ul style="list-style-type: none"> • Cost • Safety • Higher cyclability • Re-cyclability 	<ul style="list-style-type: none"> • Range of operating temperature • Cost • Safety • Higher cyclability • Recyclability 	<ul style="list-style-type: none"> • Cost • Safety • Rate of discharge • Re-cyclability 		<ul style="list-style-type: none"> • Volumetric energy density • Gravimetric energy density (potential) • Cost • Design features • Safety
Li-Ion (polymer)	<ul style="list-style-type: none"> • Cost • Higher cyclability 	<ul style="list-style-type: none"> • Range of operating temperature • Higher cyclability • Cost 	<ul style="list-style-type: none"> • Volumetric energy density • Cost • Higher cyclability 	<ul style="list-style-type: none"> • Range of operating temperature • Higher cyclability 	
Absolute advantages	<ul style="list-style-type: none"> • Cost • Higher cyclability 	<ul style="list-style-type: none"> • Cost • Range of operating temperature 	<ul style="list-style-type: none"> • Volumetric energy density 	<ul style="list-style-type: none"> • Volumetric energy density • Gravimetric energy density • Range of operating temperature • Rate of self-discharge • Output voltage 	<ul style="list-style-type: none"> • Volumetric energy density • Gravimetric energy density • Range of operating temperature • Rate of self-discharge • Output voltage • Design features

The battery packs used in EVs are made of numerous battery cells (Figure 26). The Tesla Model S, for example, has 7104 Li-Ion cells in the 85 kWh pack. All these cells are desired to have the same SOC at all times to have the same degradation rate and same capacity over the lifetime, preventing premature end of life (EOL) [46]. A power electronic control device, called a cell voltage equalizer, can achieve this feat by taking active measures to equalize the SOC and voltage of each cell. The equalizers can be of different types according to their construction and working principle. Resistive equalizers keep all the cells at the same voltage level by burning up the extra power at cells with higher voltages. Capacitive equalizers, on the other hand, transfers energy from the higher energy cells to the lower energy ones by switching capacitors. Inductive capacitors can be of different configurations: basic, Cuk, and single of multiple transformer based; but all of them transfer energy from higher energy cells to the ones with lower energy by using inductors [46–52]. All these configurations have their own merits and demerits, which are shown in Table 8; the schematics are shown in Figures 27 and 28. Table 9 shows comparisons between the equalizer types.

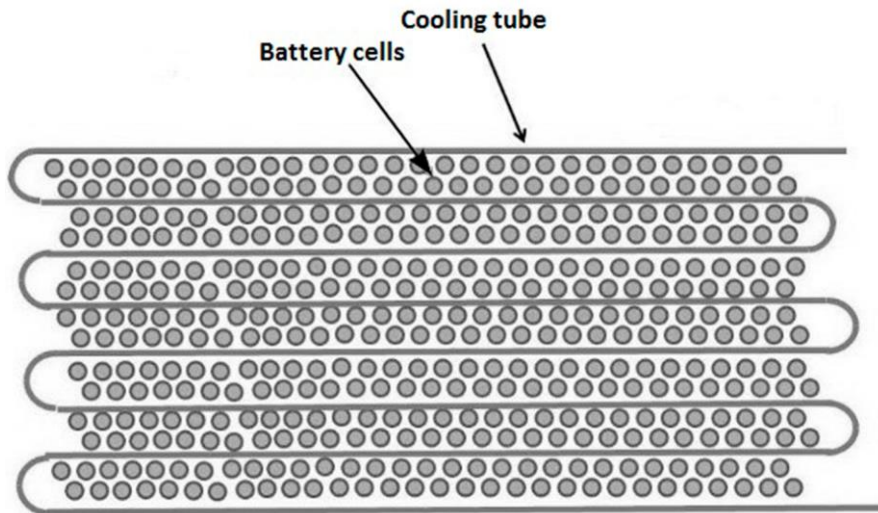


Figure 26. Battery cell arrangement in a battery pack. Cooling tubes are used to dissipate the heat generated in the battery cells.

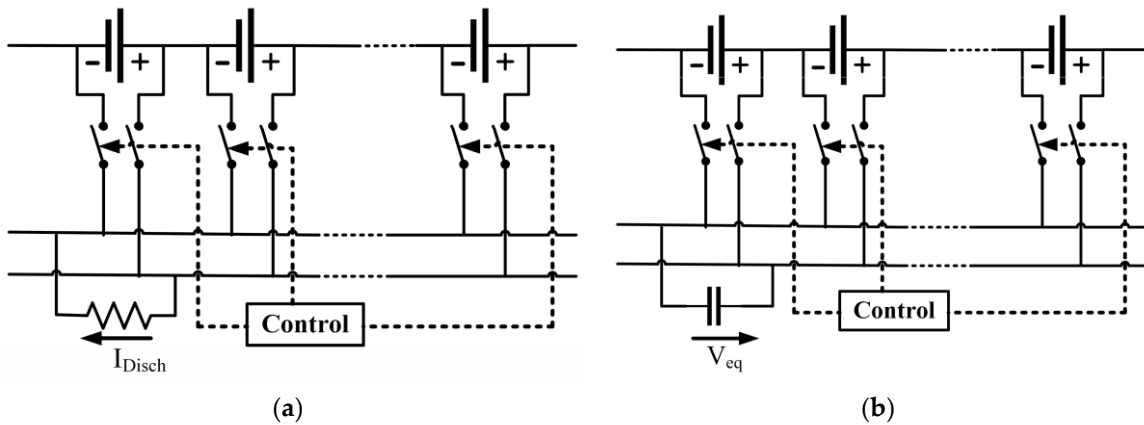
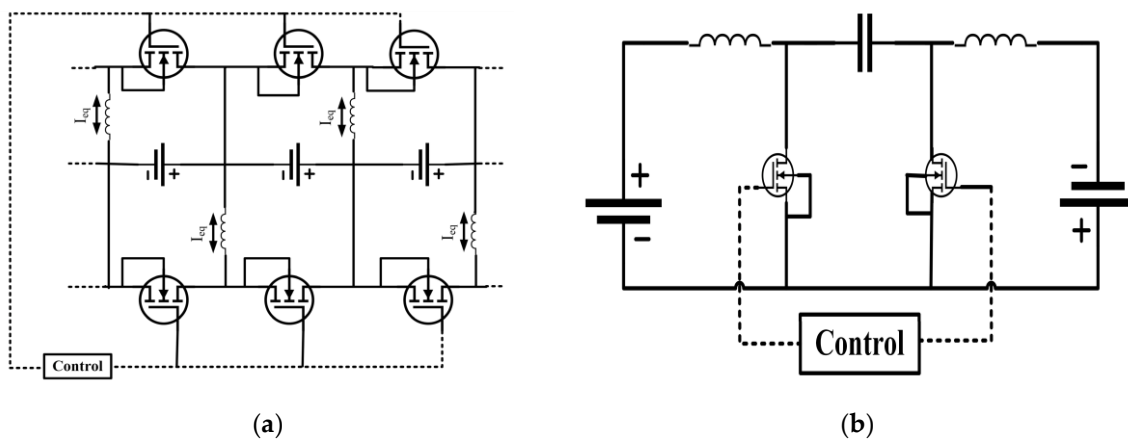


Figure 27. Equalizer configurations: (a) Resistive equalizer, extra power from any cell is burned up in the resistance; (b) Capacitive equalizer, excess energy is transferred to lower energy cells by switching of capacitors.



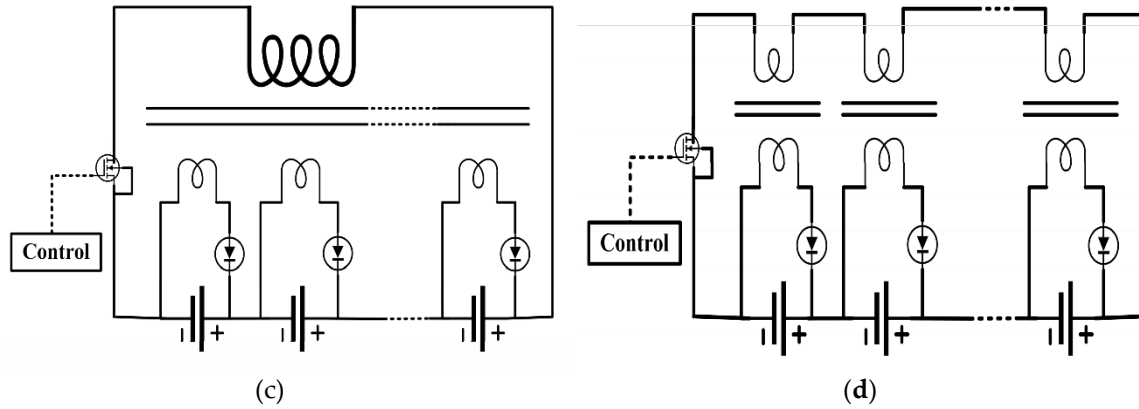


Figure 28. Inductive equalizer configurations: (a) Basic; (b) Cuk; (c) Transformer based; (d) Multiple transformers based. Excess energy is transferred to lower energy cells by using inductors.

Table 8. Advantages and disadvantages of different equalizer types. Data from [46–52].

Equalizer Type	Advantage	Disadvantage
Resistive	<ul style="list-style-type: none"> • Cheapest, widely utilized for laptop batteries 	<ul style="list-style-type: none"> • Inherent heating problem • Low equalizing current (300–500) mA • Only usable in the last stages of charging and floatation • Efficiency is almost 0% • All equalizing current transforms into heat for EV application, therefore not recommended
Capacitive	<ul style="list-style-type: none"> • Better current capabilities than resistive equalizers • No control issue • Simple implementation 	<ul style="list-style-type: none"> • Unable to control inrush current • Potentially harmful current ripples can flow for big cell voltage differences • Cannot provide any required voltage difference which is essential for SOC equalization
Basic Inductive	<ul style="list-style-type: none"> • Relatively simple • Capable of transporting high amount of energy • Can handle complex control schemes like voltage difference control and current limitation • Can compensate for internal resistance of cells • Increased equalizing current • Not dependent on cell voltage 	<ul style="list-style-type: none"> • Requires additional components to prevent ripple currents • Needs two switches in addition to drivers and controls in each cell • Current distribution is highly concentrated in neighboring cells because of switching loss
Cuk Inductive	<ul style="list-style-type: none"> • Has all the advantages of inductive equalizers • Can accommodate complex control and withstand high current 	<ul style="list-style-type: none"> • Additional cost of higher voltage and current rated switches, power capacitors • Subjected to loss caused by series capacitor • A little less efficient than typical inductive equalizers • Faces problems during distributing equalizing currents all over the cell string • May need additional processing power
Transformer based Inductive	<ul style="list-style-type: none"> • Theoretically permits proper current distribution in all cells without addition control or loss 	<ul style="list-style-type: none"> • Complex transformer with multiple secondary, which is very much challenging to mass produce • Not an option for EV packs • Cannot handle complex control algorithms
Multiple transformer based Inductive	<ul style="list-style-type: none"> • Separate transformers are used which are easier for mass production 	<ul style="list-style-type: none"> • Still difficult to build with commercial inductors without facing voltage and current imbalance

Table 9. Comparison of equalizers; a \uparrow sign indicates an advantage whereas the \downarrow signs indicate drawbacks. Adapted from [46].

Equalizer Type	Equalizer Current	Current Distribution	Current Control	Current Ripple	Manufacture	Cost	Control
Resistive	$\downarrow\downarrow$	N/A	\uparrow	$\uparrow\uparrow\uparrow$	$\uparrow\uparrow\uparrow$	$\uparrow\uparrow$	$\uparrow\uparrow\uparrow$
Capacitive	\downarrow	\uparrow	$\downarrow\downarrow$	$\downarrow\downarrow$	$\uparrow\uparrow$	$\uparrow\uparrow$	$\uparrow\uparrow$
Basic Inductive	$\uparrow\uparrow$	\uparrow	\uparrow	$\uparrow\uparrow$	\uparrow	\downarrow	\downarrow
Cuk	$\uparrow\uparrow$	\uparrow	\uparrow	$\uparrow\uparrow\uparrow$	\downarrow	$\downarrow\downarrow$	\downarrow
Transformer	\uparrow	$\uparrow\uparrow\uparrow$	$\downarrow\downarrow$	$\downarrow\downarrow$	$\downarrow\downarrow$	$\downarrow\downarrow$	$\uparrow\uparrow$

Lithium-ion batteries are being used everywhere these days. It has replaced the lead-acid counterpart and became a mature technology itself. Their popularity can be justified by the fact that best-selling EVs, for example, Nissan Leaf and Tesla Model S—all use these batteries [53,54]. Battery parameters of some current EVs are shown in Table 10. Lithium batteries also have lots of scope to improve [55]. Better battery technologies have been discovered already, but they are not being pursued because of the exorbitant costs associated with their research and development, so it can be said that, lithium batteries will dominate the EV scene for quite some time to come.

Table 10. Battery parameters of some current EVs. Data from [5].

Model	Total Energy (kWh)	Usable Energy (kWh)	Usable Energy (%)
i3	22	18.8	85
C30	24	22.7	95
B-Class	36	28	78
e6	61.4	57	93
RAV4	41.8	35	84

4.2. Ultracapacitors (UCs)

UCs have two electrodes separated by an ion-enriched liquid dielectric. When a potential is applied, the positive electrode attracts the negative ions and the negative electrode gathers the positive ones. The charges get stored physically stored on electrodes this way and provide a considerably high power density. As no chemical reactions take place on the electrodes, ultracapacitors tend to have a long cycle life; but the absence of any chemical reaction also makes them low in energy density [35]. The internal resistance is low too, making it highly efficient, but it also causes high output current if charged at a state of extremely low SOC [56,57]. A UC's terminal voltage is directly proportional to its SOC; so it can also operate all through its voltage range [35]. Basic construction of an UC cell is shown in Figure 29. EVs go through start/stop conditions quite a lot, especially in urban driving situations. This makes the battery discharge rate highly changeable. The average power required from batteries is low, but during acceleration or conditions like hill-climb a high power is required in a short duration of time [4,35]. The peak power required in a high-performance electric vehicle can be up to sixteen times the average power [4]. UCs fit in perfectly in such a scenario as it can provide high power for short durations. It is also fast in capturing the energy generated by regenerative braking [2,35]. A combined battery-UC system (as shown in Figure 30) negates each other's shortcomings and provides an efficient and reliable energy system. The low cost, load leveling capability, temperature adaptability and long service life of UCs make them a likable option as well [4,30].

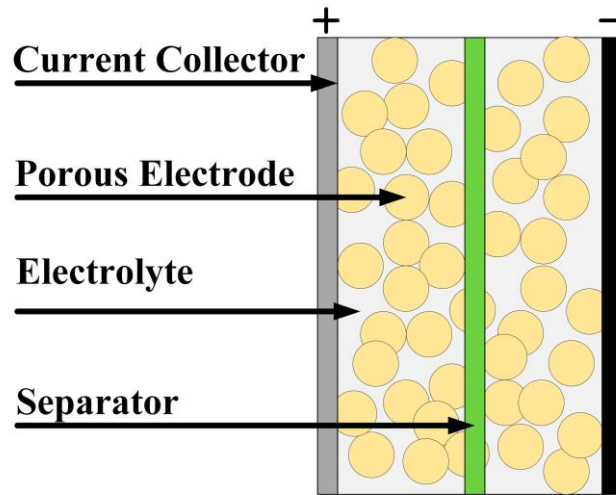


Figure 29. An UC cell; a separator keeps the two electrodes apart [58].

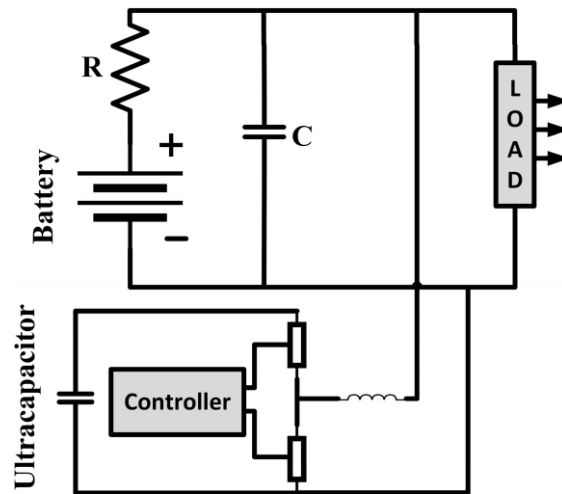


Figure 30. Combination of battery and UC to complement each-other's shortcomings [59].

4.3. Fuel Cell (FC)

Fuel cells generate electricity by electrochemical reaction. An FC has an anode (A), a cathode (C) and an electrolyte (E) between them. Fuel is introduced to the anode, gets oxidized there, the ions created travel through the electrolyte to the cathode and combine with the other reactant introduced there. The electrons produced by oxidation at the anode produce the electricity. Hydrogen is used in FCEVs because of its high energy content, and the facts it is non-polluting (producing only water as exhaust) and abundant in Nature in the form of different compounds such as hydrocarbons [4]. Hydrogen can be stored in different methods for use in EVs [4]; commercially available FCVs like the Toyota Mirai use cylinders to store it. The operating principle of a general fuel cell is demonstrated in Figure 31, while Figure 32 shows a hydrogen fuel cell. According to the material used, fuel cells can be classified into different types. A comparison among them is shown in Table 11. The chemical reaction governing the working of a fuel cell is stated below:



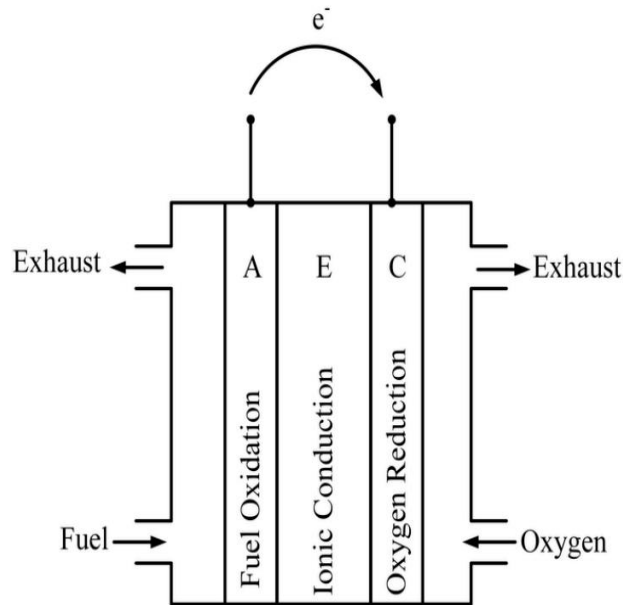


Figure 31. Working principle of fuel cell. Fuel and oxygen is taken in, exhaust and current is generated as the products of chemical reaction. Adapted from [4].

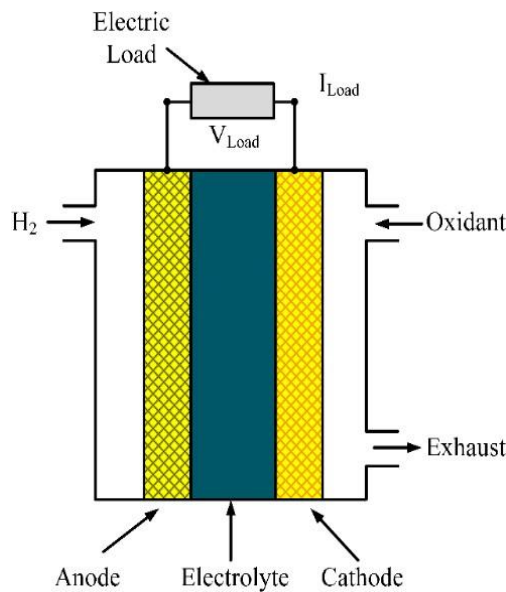


Figure 32. Hydrogen fuel cell configuration. Hydrogen is used as the fuel which reacts with oxygen and produces water and current as products. Adapted from [35].

Table 11. Comparison of different fuel cell configurations. Data from [2].

	PAFC	AFC	MCFC	SOFC	SPFC	DMFC
Working temp. (°C)	150–210	60–100	600–700	900–1000	50–100	50–100
Power density (W/cm ²)	0.2–0.25	0.2–0.3	0.1–0.2	0.24–0.3	0.35–0.6	0.04–0.25
Estimated life (kh)	40	10	40	40	40	10
Estimated cost (USD/kW)	1000	200	1000	1500	200	200

PAFC: Phosphoric acid fuel cell; AFC: Alkaline fuel cell; SOFC: Solid oxide fuel cell; SPFC: Solid polymer fuel cell, also known as proton exchange membrane fuel cell.

Fuel cells have many advantages for EV use like efficient production of electricity from fuel, noiseless operation, fast refueling, no or low emissions, durability and the ability to provide high density current output [24,60]. A main drawback of this technology is the high price. Hydrogen also

have lower energy density compared to petroleum derived fuel, therefore larger fuel tanks are required for FCEVs, these tanks also have to be capable enough to contain the hydrogen properly and to minimize risk of any explosion in case of an accident. FC's efficiency depends on the power it is supplying; efficiency generally decreases if more power is drawn. Voltage drop in internal resistances cause most of the losses. Response time of FCs is comparatively higher to UCs or batteries [35]. Because of these reasons, storage like batteries or UCs is used alongside FCs. The Toyota Mirai uses batteries to power its motor and the FC is used to charge the batteries. The batteries receive the power reproduced by regenerative braking as well. This combination provides more flexibility as the batteries do not need to be charged, only the fuel for the FC has to be replenished and it takes far less time than recharging the batteries.

4.4. Flywheel

Flywheels are used as energy storage by using the energy to spin the flywheel which keeps on spinning because of inertia. The flywheel acts as a motor during the storage stage. When the energy is needed to be recovered, the flywheel's kinetic energy can be used to rotate a generator to produce power. Advanced flywheels can have their rotors made out of sophisticated materials like carbon composites and are placed in a vacuum chamber suspended by magnetic bearings. Figure 33 shows a flywheel used in the Formula One (F1) racing kinetic energy recovery system (KERS). The major components of a flywheel are demonstrated in Figure 34. Flywheels offer a lot of advantages over other storage forms for EV use as they are lighter, faster and more efficient at absorbing power from regenerative braking, faster at supplying a huge amount of power in a short time when rapid acceleration is needed and can go through a lot of charge-discharge cycles over their lifetime. They are especially favored for hybrid racecars which go through a lot of abrupt braking and acceleration, which are also at much higher g-force than normal commuter cars. Storage systems like batteries or UCs cannot capture the energy generated by regenerative braking in situations like this properly. Flywheels, on the other hand, because of their fast response, have a better efficiency in similar scenarios, by making use of regenerative braking more effectively; it reduces pressure on the brake pads as well. The Porsche 911GT3R hybrid made use of this technology. Flywheels can be made with different materials, each with their own merits and demerits. Characteristics of some these materials are shown in Table 12; among the ones displayed in the table, carbon T1000 offers the highest amount of energy density, but it is much costlier than the others. Therefore, there remains a trade-off between cost and performance.

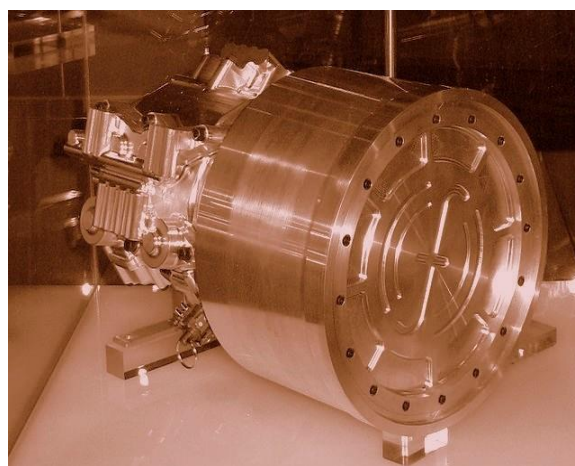


Figure 33. A flywheel used in the Formula One racing kinetic energy recovery system (KERS).

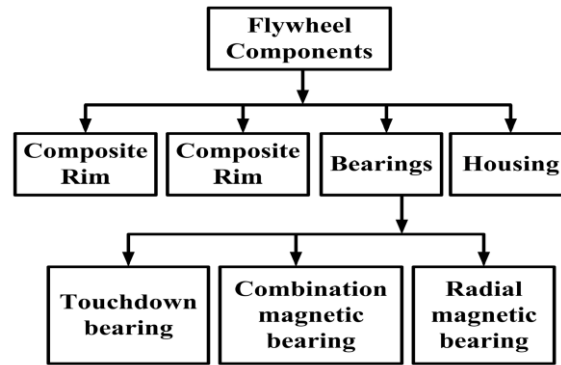


Figure 34. Basic flywheel components. The flywheel is suspended in its housing by bearings, and is connected to a motor-generator to store and supply energy [61].

Table 12. Characteristics of different materials used for flywheels [62].

Material	Density (kg/m ³)	Tensile Strength (mpa)	Max Energy Density (mj/kg)	Cost (USD/kg)	
Monolithic material	4340 steel	7700	1520	0.19	1
	E-glass	2000	100	0.05	11
	S2-glass	1920	1470	0.76	24.6
Composites	Carbon	1520	1950	1.28	101.8
	Carbon	1510	1650	1.1	31.3

Currently, no single energy source can provide the ideal characteristics, i.e., high value of both power and energy density. Table 13 shows a relative comparison of the energy storages to demonstrate this fact. Hybrid energy storages can be used to counter this problem by employing one source for high energy density and another for high power density. Different combinations are possible to create this hybrid system. It can be a combination of battery and ultracapacitor, battery and flywheel, or fuel cell and battery [4]. Table 14 shows the storage systems used by some current vehicles.

Table 13. Relative energy and power densities of different energy storage systems [63].

Storage	Energy Density	Power Density
Battery	High	Low
Ultracapacitor	Low	High
Fuel cell	High	Low
Flywheel	Low	High

Table 14. Vehicles using different storage systems.

Storage System	Vehicles Using the System
Battery	Tesla Model S, Nissan Leaf
Fuel cell + battery	Toyota Mirai, Honda Clarity
Flywheel	Porsche 911GT3R Hybrid

5. Motors Used

The propulsion system is the heart of an EV [64–69], and the electric motor sits right in the core of the system. The motor converts electrical energy that it gets from the battery into mechanical energy which enables the vehicle to move. It also acts as a generator during regenerative action which sends energy back to the energy source. Based on their requirement, EVs can have different numbers

of motors: the Toyota Prius has one, the Acura NSX has three—the choice depends on the type of the vehicle and the functions it is supposed to provide. References [4,23] listed the requirements for a motor for EV use which includes high power, high torque, wide speed range, high efficiency, reliability, robustness, reasonable cost, low noise and small size. Direct current (DC) motor drives demonstrate some required properties needed for EV application, but their lack in efficiency, bulky structure, lack in reliability because of the commutator or brushes present in them and associated maintenance requirement made them less attractive [4,30]. With the advance of power electronics and control systems, different motor types emerged to meet the needs of the automotive sector, induction and permanent magnet (PM) types being the most favored ones [23,30,70].

5.1. Brushed DC Motor

These motors have permanent magnets (PM) to make the stator; rotors have brushes to provide supply to the stator. Advantages of these motors can be the ability to provide maximum torque in low speed. The disadvantages, on the other hand, are its bulky structure, low efficiency, heat generated because of the brushes and associated drop in efficiency. The heat is also difficult to remove as it is generated in the center of the rotor. Because of these reasons, brushed DC motors are not used in EVs any more [70].

5.2. Permanent Magnet Brushless DC Motor (BLDC)

The rotor of this motor is made of PM (most commonly NdFeB [4]), the stator is provided an alternating current (AC) supply from a DC source through an inverter. As there are no windings in the rotor, there is no rotor copper loss, which makes it more efficient than induction motors. This motor is also lighter, smaller, better at dissipating heat (as it is generated in the stator), more reliable, has more torque density and specific power [4]. But because of its restrained field-weakening ability, the constant power range is quite short. The torque also decreases with increased speed because of back EMF generated in the stator windings. The use of PM increases the cost as well [30,70]. However, enhancement of speed range and better overall efficiency is possible with additional field windings [4,71]. Such arrangements are often dubbed PM hybrid motors because of the presence of both PM and field windings. But such arrangements too are restrained by complexity of structure; the speed ratio is not enough to meet the needs of EV use, specifically in off-roaders [30]. PM hybrid motors can also be constructed using a combination of reluctance motor and PM motor. Controlling the conduction angle of the power converter can improve the efficiency of PM BLDCs as well as speed range, reaching as high as four times the base speed, though the efficiency may decrease at very high speed resulting from demagnetization of PM [4]. Other than the PM hybrid configurations, PM BLDCs can be buried magnet mounted—which can provide more air gap flux density, or surface magnet mounted—which require less amount of magnet. BLDCs are useful for use in small cars requiring a maximum 60 kW of power [72]. The characteristics of PM BLDCs are shown in Figure 35.

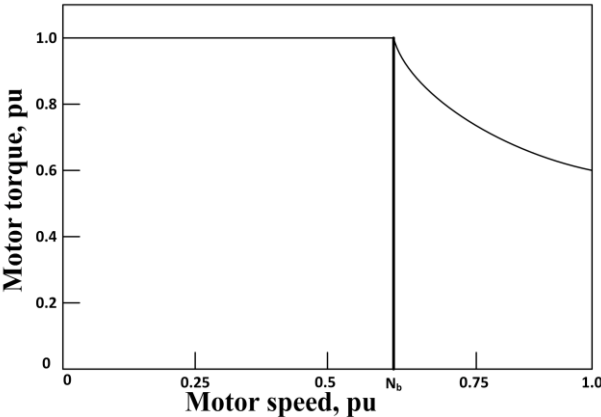


Figure 35. Characteristics of a Permanent Magnet Brushless DC Motor. The torque remains constant at the maximum right from the start, but starts to decrease exponentially for speeds over the base speed.

5.3. Permanent Magnet Synchronous Motor (PMSM)

These machines are one of the most advanced ones, capable of being operated at a range of speeds without the need of any gear system. This feature makes these motors more efficient and compact. This configuration is also very suitable for in-wheel applications, as it is capable of providing high torque, even at very low speeds. PMSMs with an outer rotor are also possible to construct without the need of bearings for the rotor. But these machines' only notable disadvantage also comes in during in-wheel operations where a huge iron loss is faced at high speeds, making the system unstable [73]. NdFeB PMs are used for PMSMs for high energy density. The flux linkages in the air-gap are sinusoidal in nature; therefore, these motors are controllable by sinusoidal voltage supplies and vector control [70]. PMSM is the most used motor in the BEVs available currently; at least 26 vehicle models use this motor technology [5].

5.4. Induction Motor (IM)

Induction motors are used in early EVs like the GM EV1 [23] as well as current models like the Teslas [54,74]. Among the different commutatorless motor drive systems, this is the most mature one [2]. Vector control is useful to make IM drives capable of meeting the needs of EV systems. Such a system with the ability to minimize loss at any load condition is demonstrated in [75]. Field orientation control can make an IM act like a separately excited DC motor by decoupling its field control and torque control. Flux weakening can extend the speed range over the base speed while keeping the power constant [30], field orientation control can achieve a range three to five times the base speed with an IM that is properly designed [76]. Three phase, four pole AC motors with copper rotors are seen to be employed in current EVs. Characteristics of IM are shown in Figure 36.

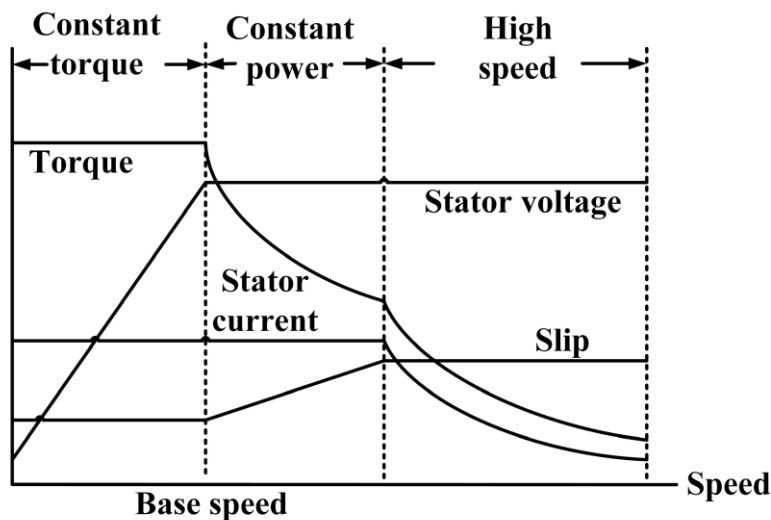


Figure 36. Induction motor drive characteristics. Maximum torque is maintained till base speed, and then decreases exponentially. Adapted from [4].

5.5. Switched Reluctance Motor (SRM)

SRMs, also known as doubly salient motor (because of having salient poles both in the stator and the rotor) are synchronous motors driven by unipolar inverter-generated current. They demonstrate simple and robust mechanical construction, low cost, high-speed, less chance of hazards, inherent long constant power range and high power density useful for EV applications. PM is not required for such motors and that facilitates enhanced reliability along with fault tolerance. On the

downside, they are very noisy because of the variable torque nature, have low efficiency, and are larger in size and weight when compared to PM machines. Though such machines have a simple construction, their design and control are not easy resulting from fringe effect of slots and poles and high saturation of the pole-tips [4,23,30,70]. Because of such drawbacks, these machines did not advance as much as the PM or induction machines. However, because of the high cost rare-rare earth materials needed in PM machines, interest in SRMs are increasing. Advanced SRMs like the one demonstrated by Nidec in 2012 had almost interior permanent machine (IPM)-like performance, with a low cost. Reducing the noise and torque ripple are the main concerns in researches associated with SRMs [23]. One of the configurations that came out of these researches uses a dual stator system, which provides low inertia and noise, superior torque density and increased speed-range compared to conventional SRMs [77,78]. Design by finite element analysis can be employed to reduce the total loss [79], control by fuzzy sliding mode can also be employed to reduce control chattering and motor nonlinearity management [80].

5.6. Synchronous Reluctance Motor (SynRM)

A Synchronous Reluctance Motor runs at a synchronous speed while combining the advantages of both PM and induction motors. They are robust and fault tolerant like an IM, efficient and small like a PM motor, and do not have the drawbacks of PM systems. They have a control strategy similar to that of PM motors. The problems with SynRM can be pointed as the ones associated with controllability, manufacturing and low power factor which hinder its use in EVs. However, researches have been going on and some progress is made as well, the main area of concern being the rotor design. One way to improve this motor is by increasing the saliency which provides a higher power factor. It can be achieved by axially or transversally laminated rotor structures, such an arrangement is shown in Figure 37. Improved design techniques, control systems and advanced manufacturing can help it make its way into EV applications [23].



Figure 37. SynRM with axially laminated rotor [23].

5.7. PM Assisted Synchronous Reluctance Motor

Greater power factors can be achieved from SynRMs by integrating some PMs in the rotor, creating a PM assisted Synchronous Reluctance Motor. Though it is similar to an IPM, the PMs used are fewer in amount and the flux linkages from them are less too. PMs added in the right amount to the core of the rotor increase the efficiency with negligible back EMF and little change to the stator. This concept is free from the problems associated with demagnetization resulting from overloading and high temperature observed in IPMs. With a proper efficiency optimization technique, this motor

can have the performance similar to IPM motors. A PM-assisted SynRM suitable for EV use was demonstrated by BRUSA Elektronik AG (Sennwald, Switzerland). Like the SynRM, PM-assisted SynRMs can also get better with improved design techniques, control systems and advanced manufacturing systems [23]. A demonstration of the rotor of PM-assisted SynRM is shown in Figure 38.

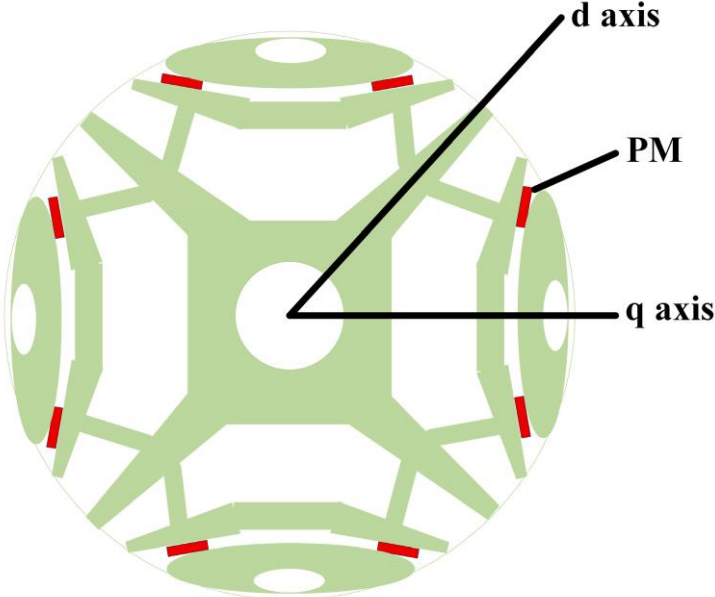


Figure 38. Permanent magnet (PM) assisted SynRM. Permanent magnets are embedded in the rotor [23].

5.8. Axial Flux Ironless Permanent Magnet Motor

According to [70], this motor is the most advanced one to be used in EVs. It has an outer rotor with no slot; use of iron is avoided here as well. The stator core is absent too, reducing the weight of the machine. The air gap here is radial field type, providing better power density. This motor is a variable speed one too. One noteworthy advantage of this machine is that the rotors can be fitted on lateral sides of wheels, placing the stator windings on the axle centrally. The slot-less design also improves the efficiency by minimizing copper loss as there is more space available [70].

Power comparison of three different motor types is conducted in Table 15. Table 16 compares torque densities of three motors. Table 17 summarizes the advantages and disadvantages of different motor types, and shows some vehicles using different motor technologies.

Table 15. Power comparison of different motors having the same size. Data from [72].

Motor Type	Power (kW)		Base Speed	Maximum Speed
	HEV	BEV		
IM	57	93	3000	12,000
SRM	42	77	2000	12,000
BLDC	75	110	4000	9000

Table 16. Typical torque density values of some motors. Data from [30].

Motor Type	Torque/Volume (Nm/m ³)	Torque/Cu Mass (Nm/kg Cu)
PM motor	28860	28.7–48
IM	4170	6.6
SRM	6780	6.1

Table 17. Advantages, disadvantages and usage of different motor types.

Motor Type	Advantage	Disadvantage	Vehicles Used In
Brushed DC Motor	<ul style="list-style-type: none"> • Maximum torque at low speed • No rotor copper loss • More efficiency than induction motors 	5.8.1. Bulky structure	Fiat Panda Elettra (Series DC motor), Conceptor G-Van (Separately excited DC motor)
		5.8.2. Low efficiency	
		5.8.3. Heat generation at brushes	
		5.8.4. Short constant power range	
Permanent Magnet Brushless DC Motor (BLDC)	<ul style="list-style-type: none"> • Lighter • Smaller • Better heat dissipation • More reliability • More torque density • More specific power 	<ul style="list-style-type: none"> • Decreased torque with increase in speed • High cost because of PM 	Toyota Prius (2005)
Permanent Magnet Synchronous Motor (PMSM)	<ul style="list-style-type: none"> • Operable in different speed ranges without using gear systems • Efficient • Compact • Suitable for in-wheel application • High torque even at very low speeds 	<ul style="list-style-type: none"> • Huge iron loss at high speeds during in-wheel operation 	Toyota Prius, Nissan Leaf, Soul EV
Induction Motor (IM)	<ul style="list-style-type: none"> • The most mature commutatorless motor drive system • Can be operated like a separately excited DC motor by employing field orientation control 		Tesla Model S, Tesla Model X, Toyota RAV4, GM EV1
Switched Reluctance Motor (SRM)	<ul style="list-style-type: none"> • Simple and robust construction • Low cost • High speed • Less chance of hazard • Long constant power range • High power density 	<ul style="list-style-type: none"> • Very noisy • Low efficiency • Larger and heavier than PM machines • Complex design and control 	Chloride Lucas
Synchronous Reluctance Motor (SynRM)	<ul style="list-style-type: none"> • Robust • Fault tolerant • Efficient • Small 	<ul style="list-style-type: none"> • Problems in controllability and manufacturing • Low power factor 	
PM assisted Synchronous Reluctance Motor	<ul style="list-style-type: none"> • Greater power factor than SynRMs • Free from demagnetizing problems observed in IPM 		BMW i3
Axial Flux Ironless Permanent Magnet Motor	<ul style="list-style-type: none"> • No iron used in outer rotor • No stator core • Lightweight • Better power density • Minimized copper loss • Better efficiency • Variable speed machine • Rotor is capable of being fitted to the lateral side of the wheel 		Renovo Coupe

6. Charging Systems

For charging of EVs, DC or AC systems can be used. There are different current and voltage configurations for charging, generally denoted as ‘levels’. The time required for a full charge depends on the level being employed. Wireless charging has also been tested and researched for quite a long time. It has different configurations as well. The charging standards are shown in Table 18. The safety standards that should be complied by the chargers are the following [46]:

- SAE J2929: Electric and Hybrid Vehicle Propulsion Battery System Safety Standard
- ISO 26262: Road Vehicles—Functional safety

- ISO 6469-3: Electric Road Vehicles—Safety Specifications—Part 3: Protection of Persons Against Electric Hazards

- ECE R100: Protection against Electric Shock
- IEC 61000: Electromagnetic Compatibility (EMC)
- IEC 61851-21: Electric Vehicle Conductive Charging system—Part 21: Electric Vehicle Requirements for Conductive Connection to an AC/DC Supply
- IEC 60950: Safety of Information Technology Equipment
- UL 2202: Electric Vehicle (EV) Charging System Equipment
- FCC Part 15 Class B: The Federal Code of Regulation (CFR) FCC Part 15 for EMC Emission Measurement Services for Information Technology Equipment.
- IP6K9K, IP6K7 protection class
- -40 °C to 105 °C ambient air temperature

Table 18. Charging standards. Data from [81].

Standard	Scope	
IEC 61851: Conductive charging system	IEC 61851-1	Defines plugs and cables setup
	IEC 61851-23	Explains electrical safety, grid connection, harmonics, and communication architecture for DCFC station (DCFCS)
	IEC 61851-24	Describes digital communication for controlling DC charging
IEC 62196: Socket outlets, plugs, vehicle inlets and connectors	IEC 62196-1	Defines general requirements of EV connectors
	IEC 62196-2	Explains coupler classifications for different modes of charging
	IEC 62196-3	Describes inlets and connectors for DCFCS
IEC 60309: Socket outlets, plugs, and couplers	IEC 60309-1	Describes CS general requirements
	IEC 60309-2	Explains sockets and plugs sizes having different number of pins determined by current supply and number of phases, defines connector color codes according to voltage range and frequency.
IEC 60364	Explains electrical installations for buildings	
SAE J1772: Conductive charging systems	Defines AC charging connectors and new Combo connector for DCFCS	
SAE J2847: Communication	SAE J2847-1	Explains communication medium and criteria for connecting EV to utility for AC level 1&2 charging
	SAE J2847-2	Defines messages for DC charging
SAE J2293	SAE J2293-1	Explains total EV energy transfer system, defines requirements for EVSE for different system architectures
SAE J2344	Defines EV safety guidelines	
SAE J2954: Inductive charging	Being developed	

6.1. AC Charging

AC charging system provides an AC supply that is converted into DC to charge the batteries. This system needs an AC-DC converter. According to the SAE EV AC Charging Power Levels, they can be classified as below:

- Level 1: The maximum voltage is 120 V, the current can be 12 A or 16 A depending on the circuit ratings. This system can be used with standard 110 V household outlets without requiring any special arrangement, using on-board chargers. Charging a small EV with this arrangement can take 0.5–12.5 h. These characteristics make this system suitable for overnight charging [5,46,81].
- Level 2: Level 2 charging uses a direct connection to the grid through an Electric Vehicle Service Equipment (EVSE). On-board charger is used for this system. Maximum system ratings are 240V, 60 A and 14.4 kW. This system is used as a primary charging method for EVs [46,81].
- Level 3: This system uses a permanently wired supply dedicated for EV charging, with power ratings greater than 14.4 kW. ‘Fast chargers’—which recharge an average EV battery pack in no more than 30 min, can be considered level 3 chargers. All level 3 chargers are not fast chargers

though [46,82]. Table 19 shows the AC charging characteristics defined by Society of Automotive Engineers (SAE).

Table 19. SAE (Society of Automotive Engineers) AC charging characteristics. Data from [44,80].

AC Charging System	Supply Voltage (V)	Maximum Current (A)	Branch Circuit Breaker Rating (A)	Output Power Level (kW)
Level 1	120 V, 1-phase	12	15	1.08
	120 V, 1-phase	16	20	1.44
Level 2	208 to 240 V, 1-phase	16	20	3.3
	208 to 240 V, 1-phase	32	40	6.6
	208 to 240 V, 1-phase	≤80	Per NEC 635	≤14.4
Level 3	208/480/600 V	150–400	150	3

6.2. DC Charging

DC systems require dedicated wiring and installations and can be mounted at garages or charging stations. They have more power than the AC systems and can charge EVs faster. As the output is DC, the voltage has to be changed for different vehicles to suit the battery packs. Modern stations have the capability to do it automatically [46]. All DC charging systems has a permanently connected Electric Vehicle Service Equipment (EVSE) that incorporates the charger. Their classification is done depending on the power levels they supply to the battery:

- Level 1: The rated voltage is 450 V with 80 A of current. The system is capable of providing power up to 36 kW.
- Level 2: It has the same voltage rating as the level 1 system; the current rating is increased to 200A and the power to 90 kW.
- Level 3: Voltage in this system is rated to 600 V. Maximum current is 400 A with a power rating of 240 kW. Table 20 shows the DC charging characteristics defined by Society of Automotive Engineers (SAE).

Table 20. SAE (Society of Automotive Engineers) DC charging characteristics. Data from [46].

DC Charging System	DC Voltage Range (V)	Maximum Current (A)	Power (kW)
Level 1	200–450	≤80	≤36
Level 2	200–450	≤200	≤90
Level 3	200–600	≤400	≤240

6.3. Wireless Charging

Wireless charging or wireless power transfer (WPT) enjoys significant interest because of the conveniences it offers. This system does not require the plugs and cables required in wired charging systems, there is no need of attaching the cable to the car, low risk of sparks and shocks in dirty or wet environment and less chance of vandalism. Forerunners in WPT research include R&D centers and government organizations like Phillips Research Europe, Energy Dynamic Laboratory (EDL), US DOT, DOE; universities including the University of Tennessee, the University of British Columbia, Korea Advance Institute of Science and Technology (KAIST); automobile manufacturers including Daimler, Toyota, BMW, GM and Chrysler. The suppliers of such technology include Witricity, LG, Evatran, HaloIPT (owned by Qualcomm), Momentum Dynamics and Conductix-Wampfler [27]. However, this technology is not currently available for commercial EVs because of the health and safety concerns associated with the current technology. The specifications are determined by different standardization organizations in different countries: Canadian Safety Code 6 in Canada [83], IEEE C95.1 in the USA [84], ICNIRP in Europe [85] and ARPANSA in Australia [86]. There are different technologies that are being considered to provide WPT facilities. They differ in the operating frequency, efficiency, associated electromagnetic interference (EMI), and other factors.

Inductive power transfer (IPT) is a mature technology, but it is only contactless, not wireless. Capacitive power transfer (CPT) has significant advantage at lower power levels because of low cost and size, but not suitable for higher power applications like EV charging. Permanent magnet coupling power transfer (PMPT) is low in efficiency, other factors are not favorable as well. Resonant inductive power transfer (RIPT) as well as On-line inductive power transfer (OLPT) appears to be the most promising ones, but their infrastructure may not allow them to be a viable solution. Resonant antennae power transfer (RAPT) is made on a similar concept as RIPT, but the resonant frequency in this case is in MHz range, which is capable of damage to humans if not shielded properly. The shielding is likely to hinder range and performance; generation of such high frequencies is also a challenge for power electronics [87]. Table 21 compares different wireless charging systems in terms of performance, cost, size, complexity, and power level. Wireless charging for personal vehicles is unlikely to be available soon because of health, fire and safety hazards, misalignment problems and range. Roads with WPT systems embedded into them for charging passing vehicles also face major cost issues [27]. Only a few wireless systems are available now, and those too are in trial stage. WiTricity is working with Delphi Electronics, Toyota, Honda and Mitsubishi Motors. Evatran is collaborating with Nissan and GM for providing wireless facilities for Nissan Leaf and Chevrolet Volt models. However, with significant advance in the technology, wireless charging is likely to be integrated in the EV scenario, the conveniences it offers are too appealing to overlook.

Table 21. Comparison of wireless charging systems.

Wireless Charging System	Performance			Cost	Volume/Size	Complexity	Power Level
	Efficiency	EMI	Frequency				
Inductive							
power transfer (IPT)	Medium	Medium	10–50 kHz	Medium	Medium	Medium	Medium/High
Capacitive power transfer (CPT)	Low	Medium	100–500 kHz	Low	Low	Medium	Low
Permanent magnet coupling power transfer (PMPT)	Low	High	100–500 kHz	High	High	High	Medium/Low
Resonant inductive power transfer (RIPT)	Medium	Low	1–20 MHz	Medium	Medium	Medium	Medium/Low
On-line inductive power transfer (OLPT)	Medium	Medium	10–50 kHz	High	High	Medium	High
Resonant antennae power transfer (RAPT)	Medium	Medium	100–500 kHz	Medium	Medium	Medium	Medium/Low

For the current EV systems, on-board AC systems are used for the lowest power levels, for higher power, DC systems are used. DC systems currently have three existing standards [16]:

- Combined Charging System (CCS)
- CHAdeMO (CHARGE de MOVE, meaning: ‘move by charge’)
- Supercharger (for Tesla vehicles)

The powers offered by CCS and CHAdeMO are 50 kW and 120 kW for the Supercharger system [88,89]. CCS and CHAdeMO are also capable of providing fast charging, dynamic charging and vehicle to infrastructure (V2X) facilities [6,90]. Most of the EV charging stations at this time provides level 2 AC charging facilities. Level 3 DC charging network, which is being increased rapidly, is also

available for Tesla cars. The stations may provide the CHAdeMO standard or the CCS, therefore, a vehicle has to be compatible with the configuration provided to be charged from the station. The CHAdeMO system is favored by the Japanese manufacturers like Nissan, Toyota and Honda whereas the European and US automakers, including Volkswagen, BMW, General Motors and Ford, prefer the CCS standard. Reference [5] discusses the charging systems used by current EVs along with the time required to get them fully charged.

7. Power Conversion Techniques

Batteries or ultracapacitors (UC) store energy as a DC charge. Normally they have to obtain that energy from AC lines connected to the grid, and this process can be wired or wireless. To deliver this energy to the motors, it has to be converted back again. These processes work in the reverse direction as well i.e., power being fed back to the batteries (regenerative braking) or getting supplied to grid when the vehicle in idle (V2G) [91]. Typical placement of different converters in an EV is shown in Figure 39 along with the power flow directions. This conversion can be DC-DC or DC-AC. For all this conversion work required to fill up the energy storage of EVs and then to use them to propel the vehicle, power converters are required [72], and they come in different forms. A detailed description of power electronics converters is provided in [92]. Further classification of AC-AC converters is shown in [93]. A detailed classification of converters is shown in Figure 40.

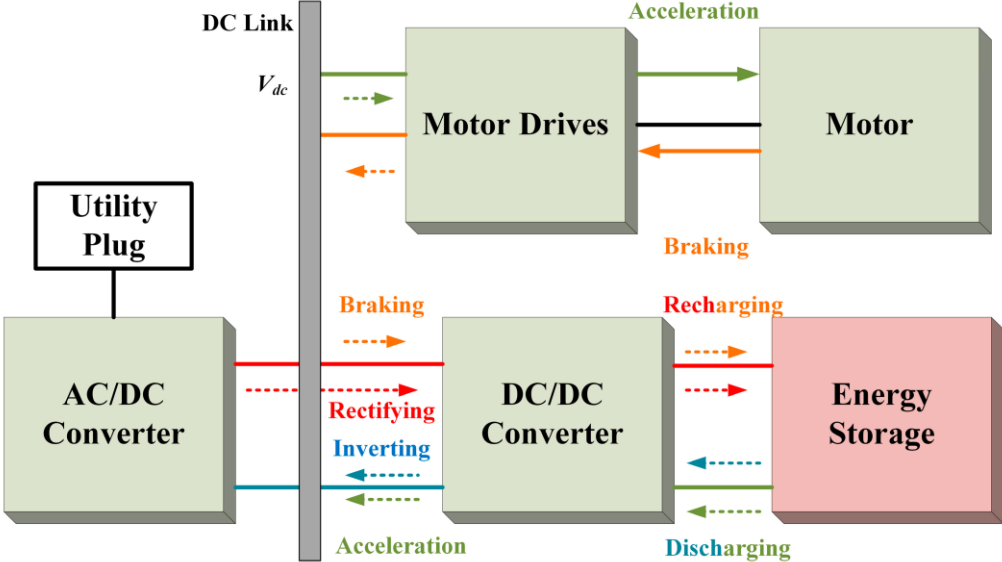


Figure 39. Typical placements of different converters in an EV. AC-DC converter transforms the power from grid to be stored in the storage through another stage of DC-DC conversion. Power is supplied to the motor from the storage through the DC-DC converter and the motor drives [72].

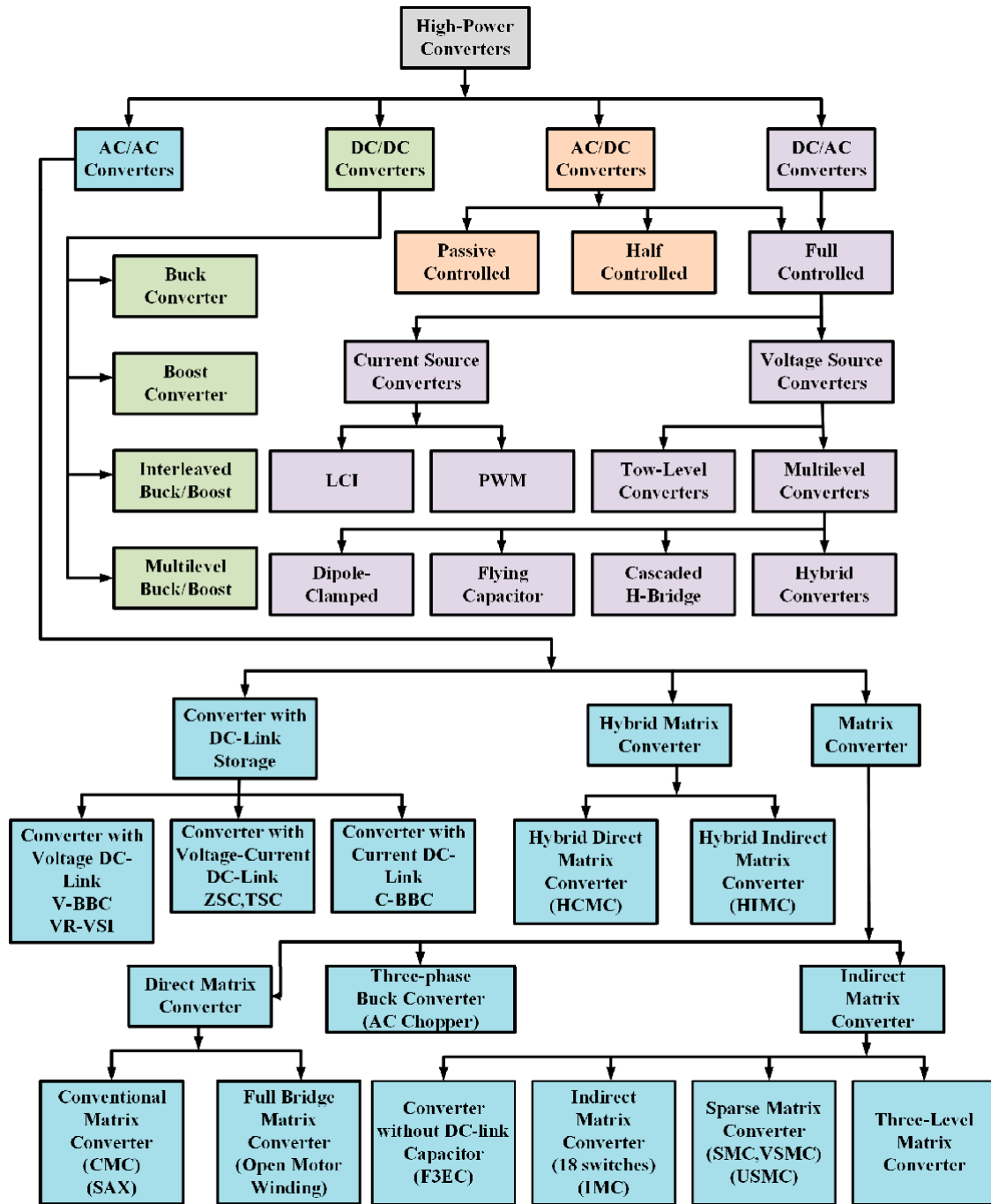


Figure 40. Detailed classification of converters. Data from [92,93].

7.1. Converters for Wired Charging

DC-DC boost converter is used to drive DC motors by increasing the battery voltage up to the operating level [72]. DC-DC converters are useful to combine a power source with a complementing energy source [94]. Figure 41 shows a universal DC-DC converter used for DC-DC conversion. It can be used as a boost converter for battery to DC link power flow and as a buck converter when the flow is reversed. The operating conditions and associated switching configuration is presented in Table 22. DC-DC boost converters can also use a digital signal processor [95].

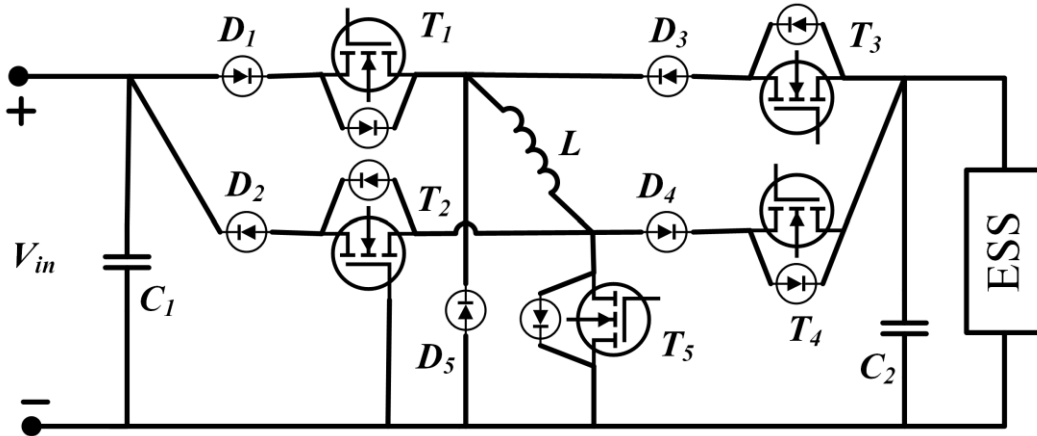


Figure 41. Universal DC-DC converter [72].

Table 22. Operating conditions for universal DC-DC converter. Adapted from [88].

Direction	Mode	T ₁	T ₂	T ₃	T ₄	T ₅
V _{dc} to V _{batt}	Boost	On	Off	Off	On	PWM
V _{dc} to V _{batt}	Buck	PWM	Off	Off	On	Off
V _{batt} to V _{dc}	Boost	Off	On	On	Off	PWM
V _{batt} to V _{dc}	Buck	Off	On	PWM	Off	Off

According to [72], dual inverter is the most updated technology to drive AC motors like permanent magnet synchronous motors (PMSMs), shown in Figure 42. For dual voltage source applications, the system of Figure 43 is used [96]. These inverters operate on space vector PWM. For use on both PMSMs and induction motors (IMs), a bidirectional stacked matrix inverter can be used; such a system is shown in Figure 44.

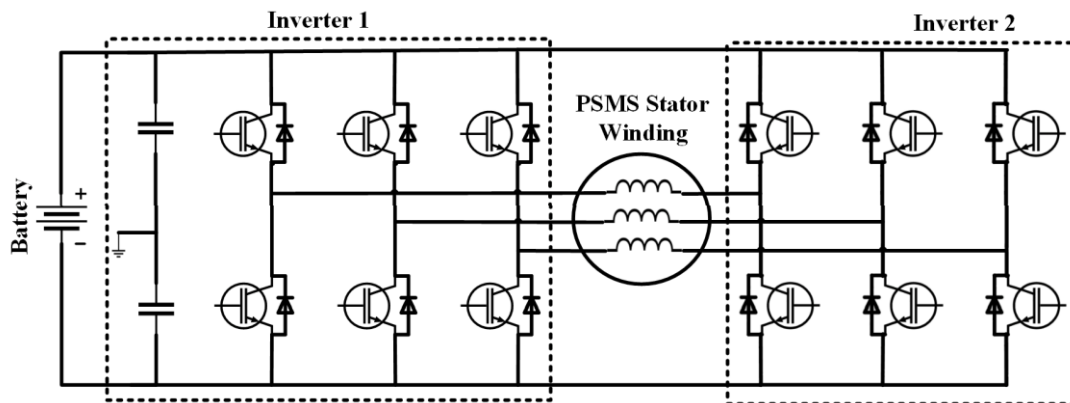


Figure 42. Dual inverter for single source [72].

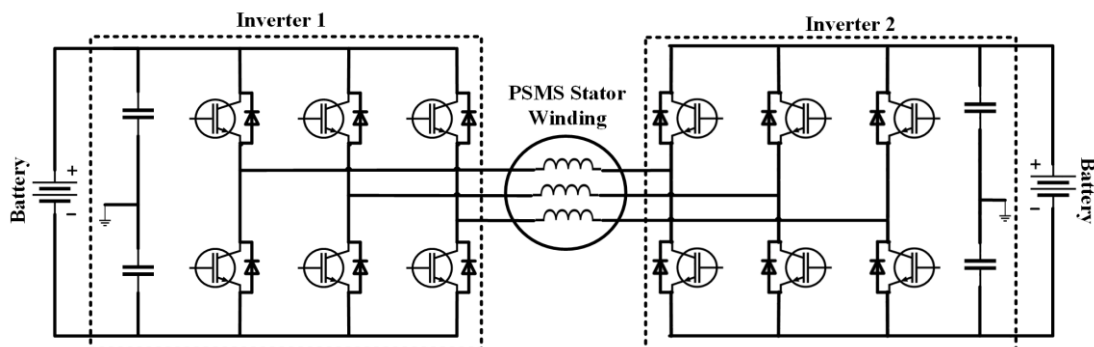


Figure 43. Dual inverter with dual sources [72].

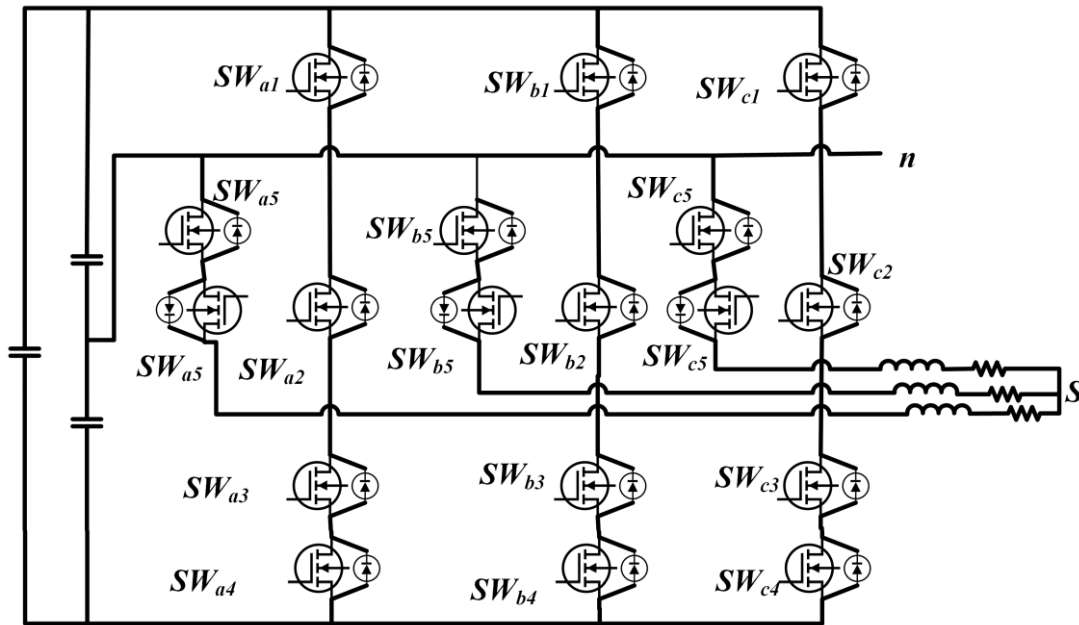


Figure 44. Novel stacked matrix inverter as shown in [97].

Some notable conventional DC-DC converters are: phase-shift full-bridge (PSFB), inductor-inductor-capacitor (LLC), and series resonant converter (SRC). A comparison of components used in these three converters is presented in [98], which is demonstrated here in Table 23. The DC-DC converters used are required to have low cost, weight and size for being used in automobiles [99]. Interleaved converters are a preferable option regarding these considerations, it offers some other advantages as well [100–103], though using it may increase the weight and volume of the inductors compared to the customary single-phase boost converters [99]. To solve this problem, Close-Coupled Inductor (CCI) and Loosely-Coupled Inductor (LCI) integrated interleaved converters have been proposed in [99]. In [48] converters for AC level-1 and level-2 chargers are shown by Williamson et al., who stated that Power Factor Correction (PFC) is a must to acquire high power density and efficiency. Two types of PFC technique are shown here: single-stage approach and two-stage approach. The first one suits for low-power use and charge only lead-acid batteries because of high low frequency ripple. To avoid these problems, the second technique is used.

Table 23. Comparison of components used in PSFB, LLC and SRC converter. Adapted from [98].

Item	PSFB	LLC	SRC
Number of switch blocks	4	4	4
Number of diode blocks	4	4	4
Number of transformers	1	1	2
Number of inductors	1	0	0
Additional capacitor	Blocking capacitor	-	-
Output filter size	Small	-	Large

In [34], Yong et al., presented the front end AC-DC converters. The Interleaved Boost PFC Converter (Figure 45) has a couple of boost converters connected in parallel and working in 180° out of phase [104–106]. The ripple currents of the inductors cancel each other. This configuration also provides twice the effective switching frequency and provides a lower ripple in input current, resulting in a relatively small EMI filter [103,107]. In Bridgeless/Dual Boost PFC Converter (Figure 46), the gating signals are made identical here by tying the power-train switches. The MOSFET gates are not made decoupled. Rectifier input bridge is not needed here. The Bridgeless Interleaved Boost PFC Converter (Figure 47) is proposed to operate above the 3.5 kW level. It has two MOSFETS and uses two fast diodes; the gating signals have a phase difference of 180°.

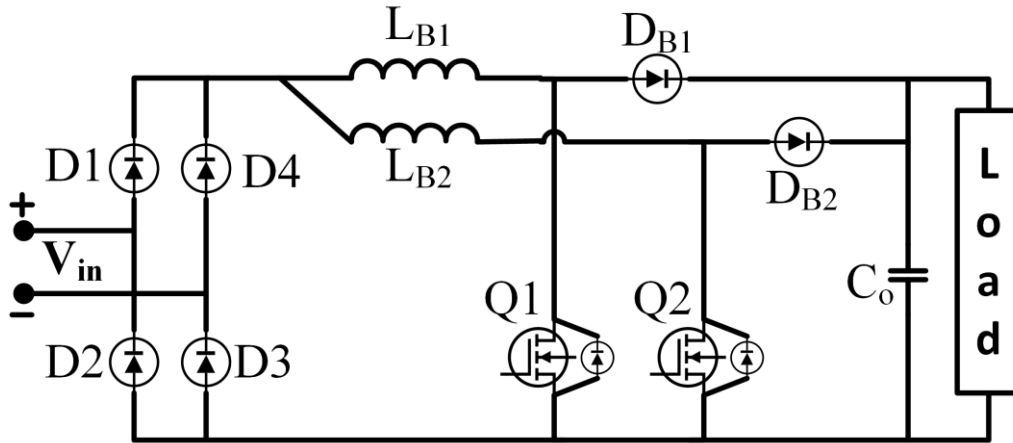


Figure 45. Interleaved Boost PFC Converter [46].

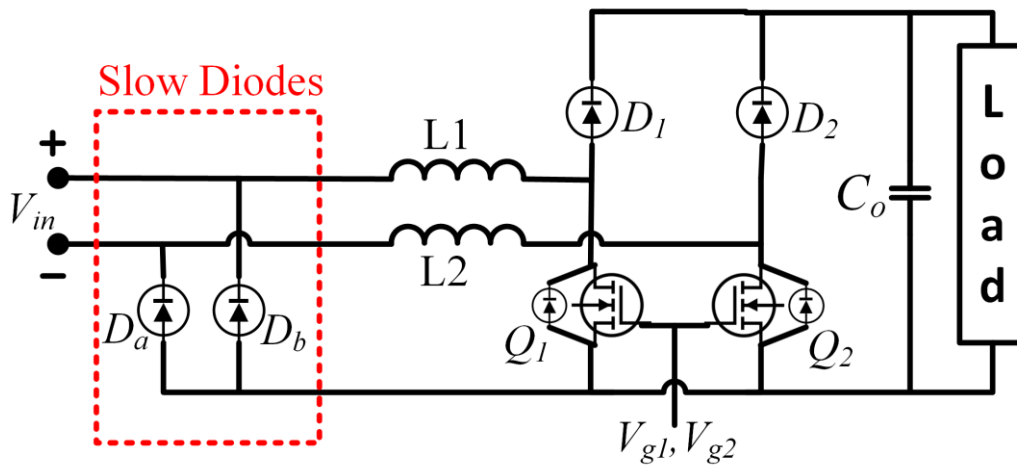


Figure 46. Bridgeless/Dual Boost PFC Converter. Adapted from [46].

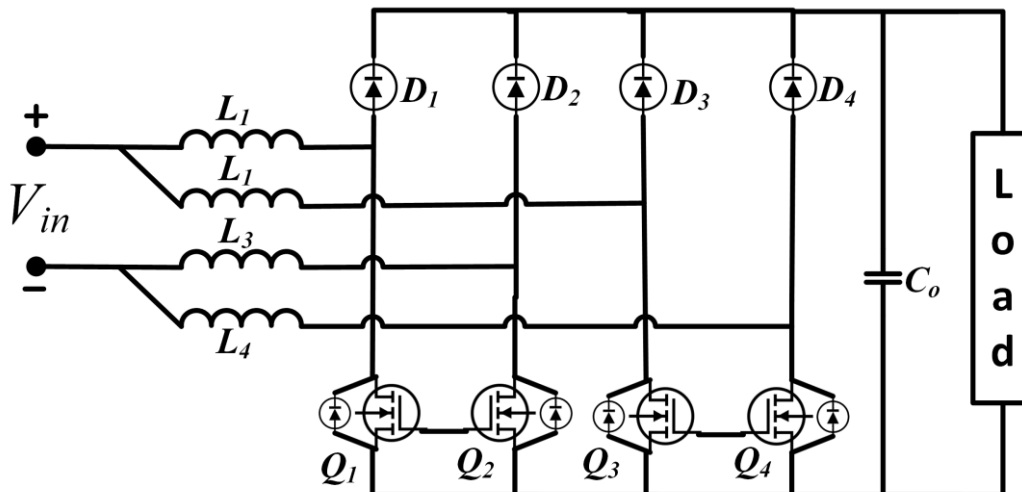


Figure 47. Bridgeless Interleaved Boost PFC Converter [46].

Williamson et al., presented some isolated DC-DC converter topologies in [44]. The ZVS FB Converter with Capacitive Output Filter (Figure 48) can achieve high efficiency as it uses zero voltage switching (ZVS) along with the capacitive output filters which reduces the ringing of diode rectifiers. The trailing edge PWM full-bridge system proposed in [107]. The Interleaved ZVS FB Converter with

Voltage Doubler (Figure 49) further reduces the voltage stress and ripple current on the capacitive output filter, it reduces the cost too. Interleaving allows equal power and thermal loss distribution in each cell. The number of secondary diodes is reduced significantly by the voltage doubler rectifier at the output [34]. Among its operating modes, DCM (discontinuous conduction mode) and BCM (boundary conduction mode) are preferable. The Full Bridge LLC Resonant Converter (Figure 50) is widely used in telecom industry for the benefits like high efficiency at resonant frequency. But unlike the telecom sector, EV applications require a wide operating range. Reference [41] shows a design procedure for such configurations for these applications.

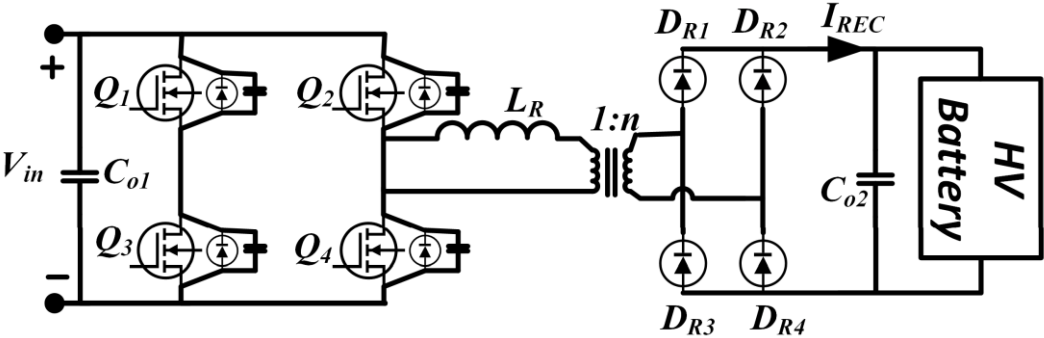


Figure 48. ZVS FB Converter with Capacitive Output Filter [46].

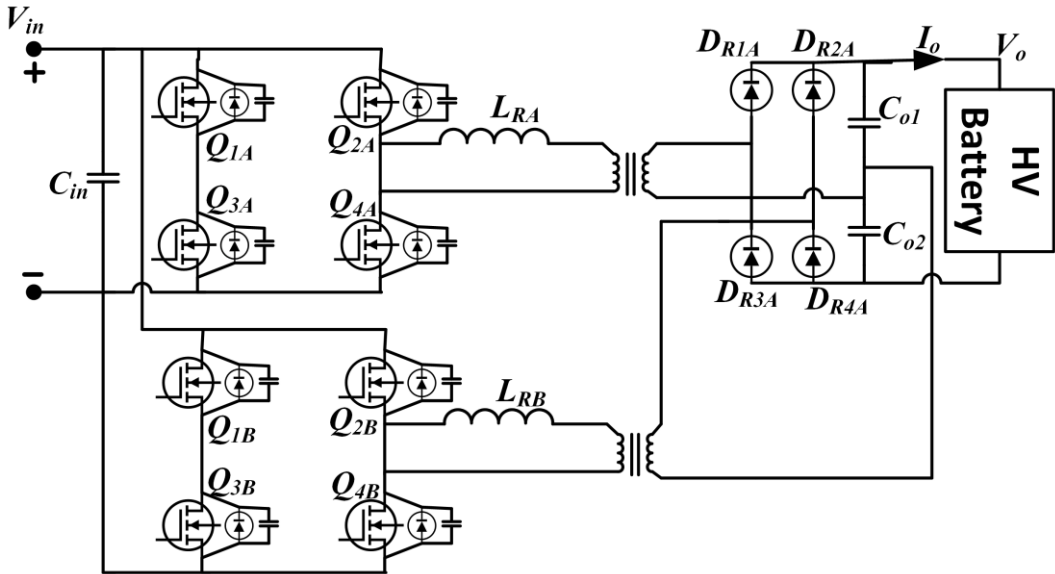


Figure 49. Interleaved ZVS FB Converter with Voltage Doubler [46].

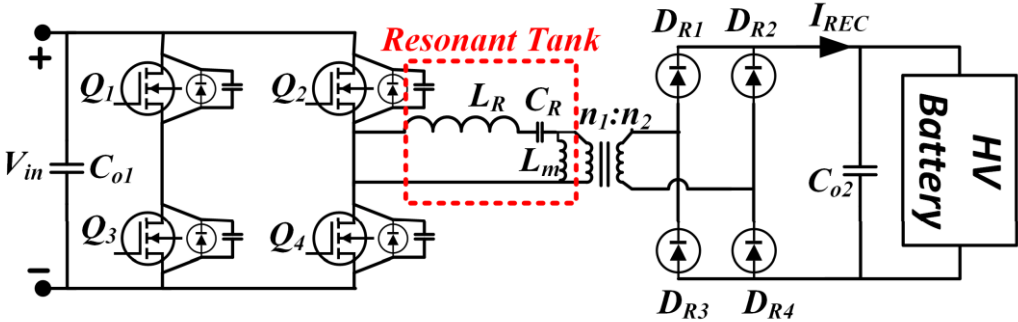


Figure 50. Full Bridge LLC Resonant Converter. Adapted from [46].

Balch et al., showed converter configurations that are used in different types of EVs in [42]. In Figure 51, a converter arrangement for a BEV is shown. An AC-DC charger is used for charging the battery pack here while a two-quadrant DC-DC converter is used for power delivery to the DC bus from the battery pack. This particular example included an ultracapacitor as well. An almost similar arrangement was shown in [42] for PHEVs (Figure 52) where a bidirectional DC-DC converter was used between the DC bus and the battery pack to facilitate regeneration. Use of integrated converter in PHEV is shown in Figure 53. Figure 54 shows converter arrangement for a PFCV; this configuration is quite similar to one shown for BEV, but it contains an additional boost converter to adjust the power produced by the fuel cell stack to be sent to the DC bus.

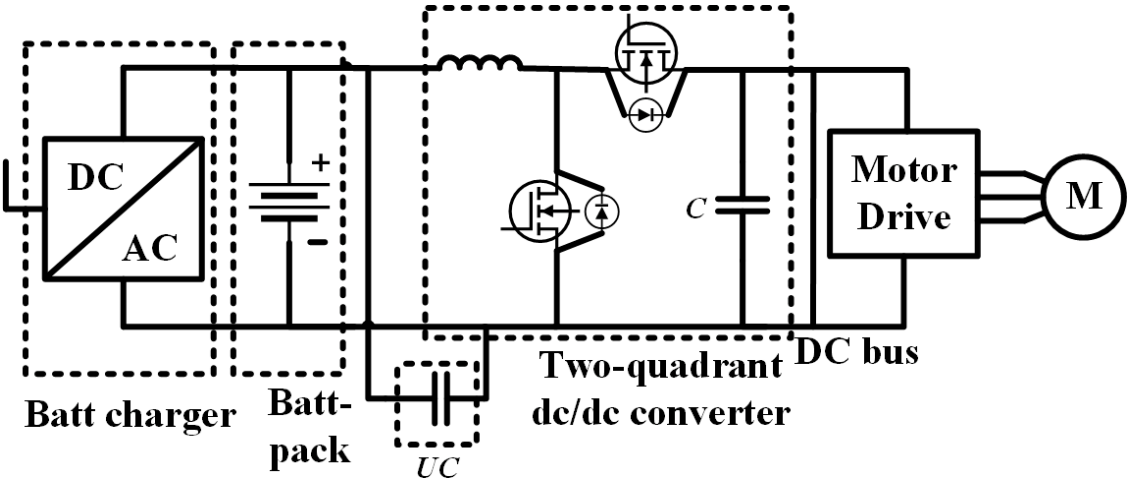


Figure 51. Converter placement in a pure EV [35]. The charger has an AC-DC converter to supply DC to the battery from the grid, whereas the DC-DC converter converts the battery voltage into a value required to drive the motor.

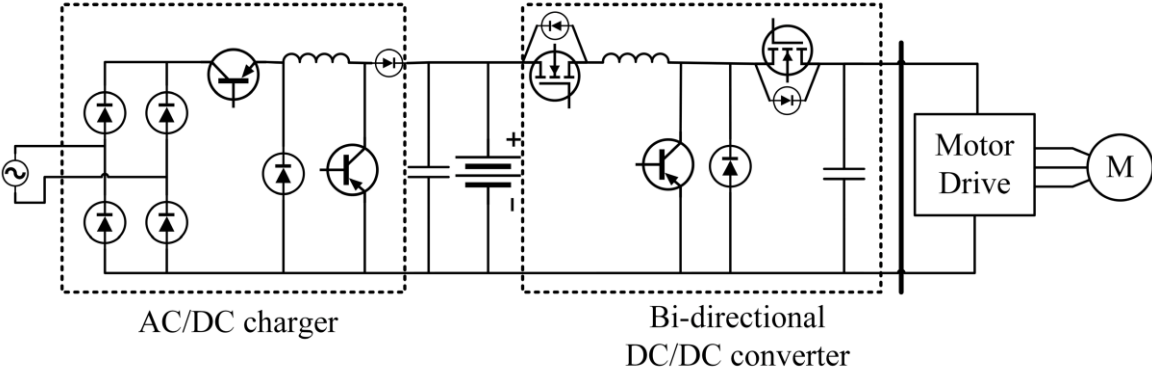


Figure 52. Cascaded converter to use in PHEV. Adapted from [35]. A bidirectional DC-DC converter is used between the DC bus and the battery pack to allow regenerated energy to flow back to the battery from the motor.

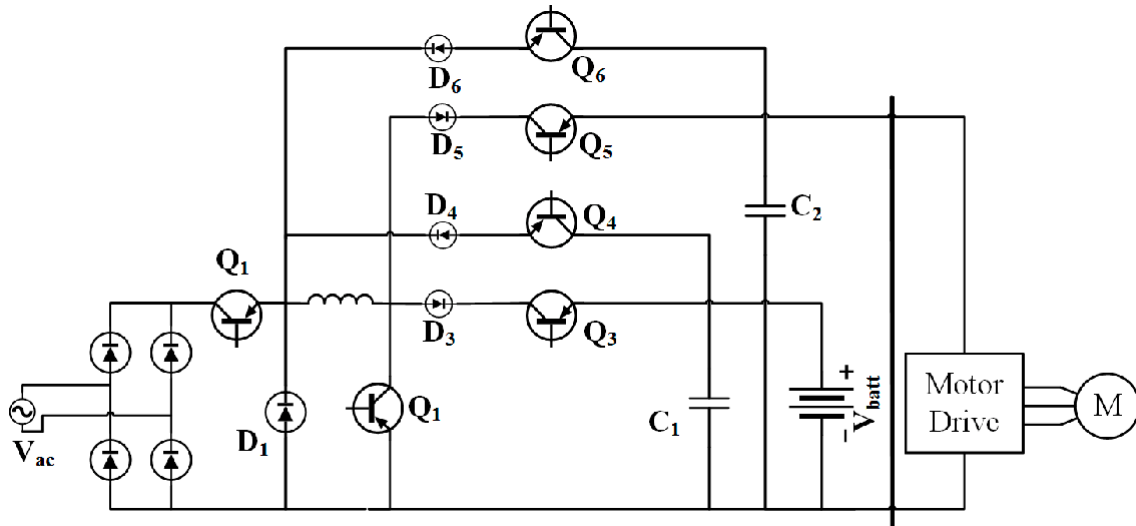


Figure 53. Integrated converter used in PHEV [35].

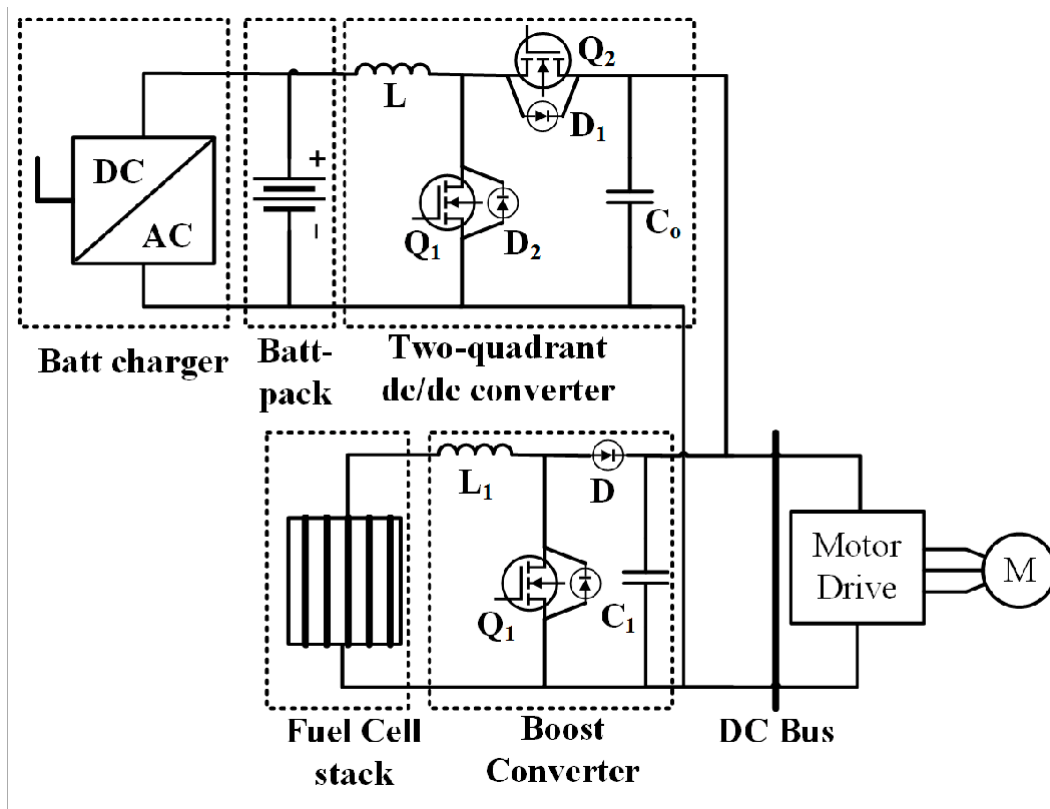


Figure 54. Converter arrangement in PFCV. Adapted from [35]. An AC-DC converter is used to convert the power from the grid; DC-DC converter is used for power exchange between the DC bus and battery; boost converter is used to make the voltage generated from the fuel cell stack suitable for the DC bus.

Bidirectional converters allow transmission of power from the motors to the energy sources and also from vehicle to grid. Novel topologies for bidirectional AC/DC-DC/DC converters to be used in PHEVs are being researched [103,108–112], such a configuration is shown in Figure 55. Kok et al., showed different DC-DC converter arrangements for EVs using multiple energy sources in [94] which are presented in Figure 56. The first system has both battery and ultracapacitor added in cascade, while the second one has them connected in parallel. The third one shows a system employing fuel cells, and battery for backup. In [113], Koushki et al., classified bidirectional AC-DC converters into two main groups: Low frequency AC-High frequency AC-DC (Figure 57), and Low

frequency AC-DC- High frequency AC-DC (Figure 58). The first kind can also be called single-stage converters where the latter may be described as two-stage, which can be justified from their topologies. Converters employed for EV application are compiled in Table 24. From this table, it is evident that step down converters are required for charging the batteries from a higher voltage grid voltage, bidirectional converters are needed for providing power flow in both directions, and specialized converters such as the last three, are needed for better charging performances.

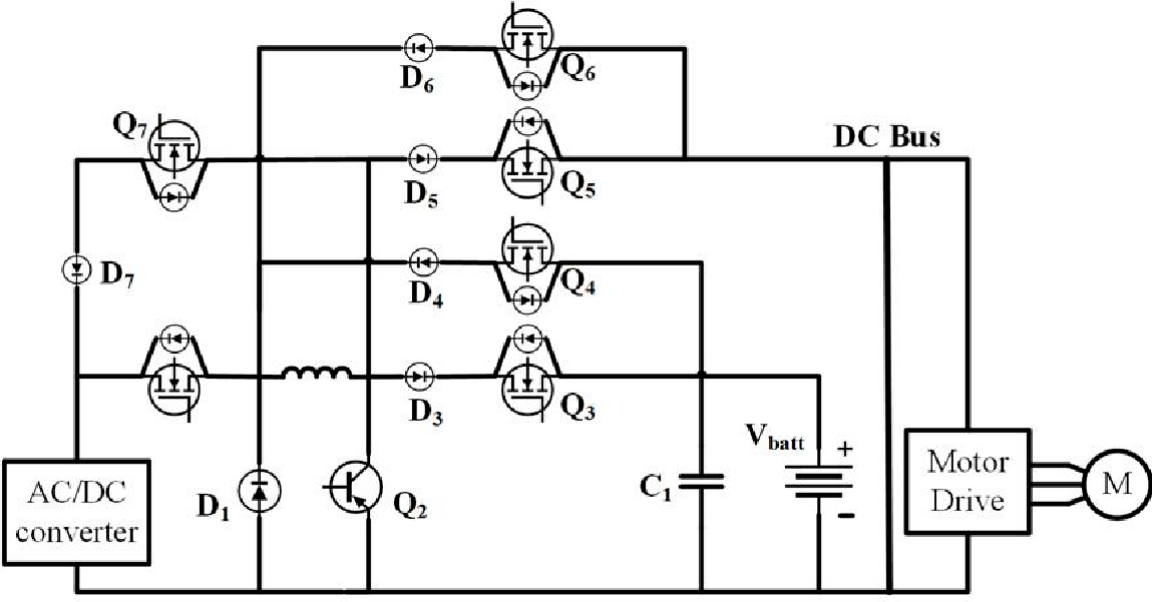
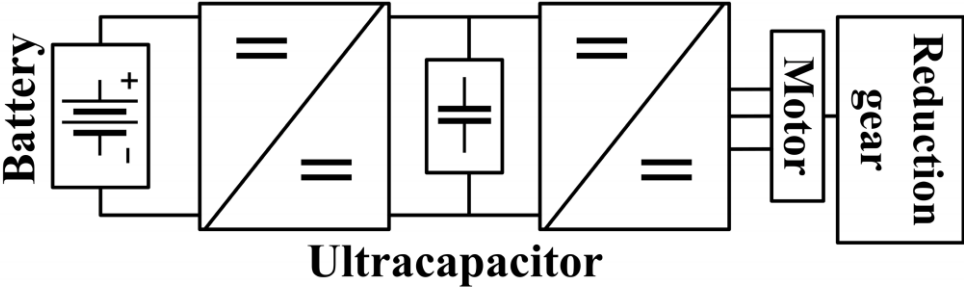
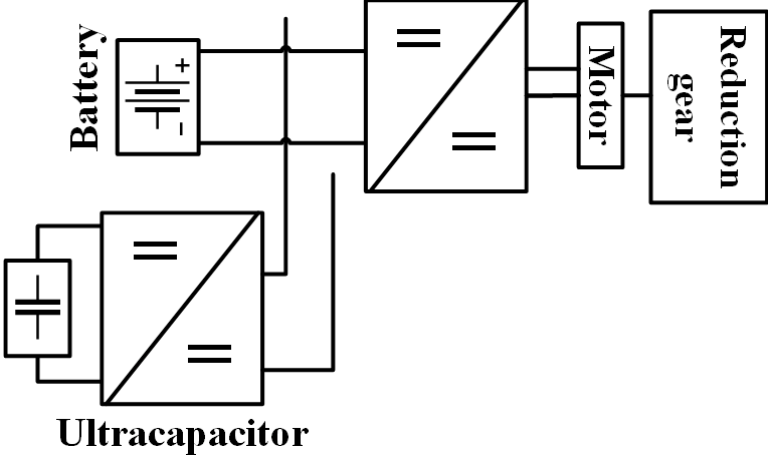


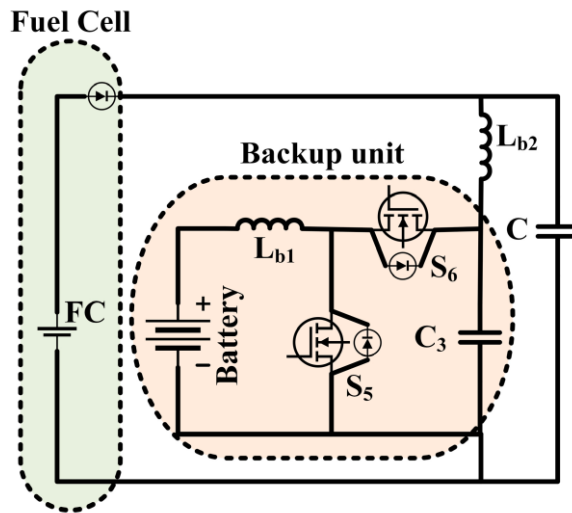
Figure 55. Integrated bidirectional AC/DC-DC/DC converter [33].



(a)



(b)



(c)

Figure 56. Converter arrangements as shown in [94]: (a) Cascaded connection; (b) Parallel connection; (c) Fuel cell with battery backup. Adapted from [94].

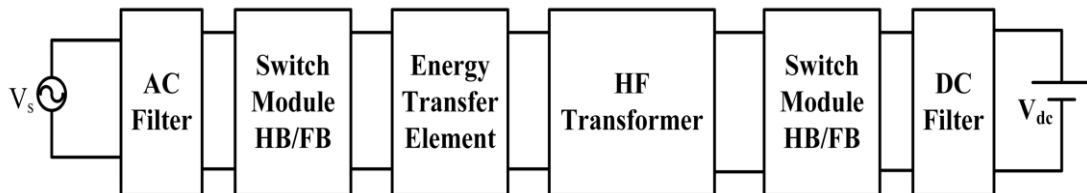


Figure 57. Low frequency AC-High frequency AC-DC converter, also called single-stage converter [113].

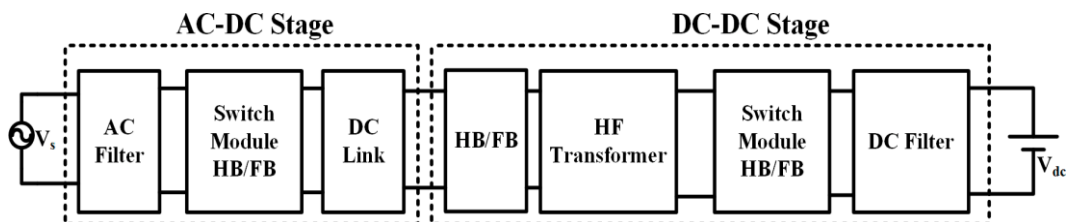


Figure 58. Low frequency AC-DC-High frequency AC-DC converter, also called two-stage converter. Adapted from [113].

Table 24. Converters with EV application displaying their key features and uses in EVs.

Configuration	Reference	Operation	Key Features	Application in EV
Buck converter	Bose [92]	Step down	Can operate in continuous or discontinuous mode	Sending power to the battery
Buck-Boost converter	Bose [92]	Step up and step down	Two quadrant operation of chopper	Regenerative action
Interleaved Boost PFC converter	Williamson et al. [46]	Step up with power factor correction	Relatively small input EMI filter	Charging
Bridgeless/Dual Boost PFC Converter	Williamson et al. [46]	Step up with power factor correction	Does not require rectifier input bridge	Charging

ZVS FB Converter with Capacitive Output Filter	Williamson et al. [46]	AC-DC conversion	Zero voltage switching	Charging
---	---------------------------	------------------	------------------------	----------

AC-DC converters are used to charge the batteries from AC supply-lines; DC-DC converters are required for sending power to the motors from the batteries. The power flow can be reversed in case of regenerative actions or V2G. Bidirectional converters are required in such cases. Different converter configurations have different advantages and shortcomings which engendered a lot of research and proliferation of hybrid converter topologies.

7.2. Systems for Wireless Charging

Wireless charging or wireless power transfer (WPT) uses a principle similar to transformer. There is a primary circuit at the charger end, from where the energy is transferred to the secondary circuit located at the vehicle. In case of inductive coupling, the voltage obtained at the secondary side is:

$$v_2 = L_2(di_2/dt) + M(di_1/dt) \tag{2}$$

M is the mutual inductance and can be calculated by:

$$M = k\sqrt{L_1L_2} \tag{3}$$

The term k here is the coupling co-efficient; L_1 and L_2 are the inductances of primary and secondary circuit. Figure 59 shows the 'double D' arrangement for WPT which demonstrates the basic principle of wireless power transfer by means of flux linkages. A variety of configurations can be employed for wireless power transfer; some of them meet a few desired properties to charge vehicles. Inductive WPT, shown in Figure 60a, is the most rudimentary type, transfer power from one coil to another just like the double D system. Capacitive WPT (Figure 60b) uses a similar structure as the inductive system, but it has two coupling transformers at its core. Low frequency permanent magnet coupling power transfer (PMPT) is shown in Figure 60c; it uses a permanent magnet rotor to transmit power, another rotor placed in the vehicle acts as the receiver. Resonant antennae power transfer (RAPT) (Figure 60d) uses resonant antennas for wireless transfer of power. Resonant inductive power transfer (RIPT), shown in Figure 60e, uses resonance circuits for power transfer. Online power transfer (OLPT) has a similar working principle as RIPT, it can be used in realizing roadways that can charge vehicles wirelessly by integrating the transmitter with the roadway (pilot projects using similar technology placed them just beneath the road surface), and equipping vehicles with receivers to collect power from there. Schematic for this system is shown in Figure 60f. Characteristics of these systems are shown in Table 25.

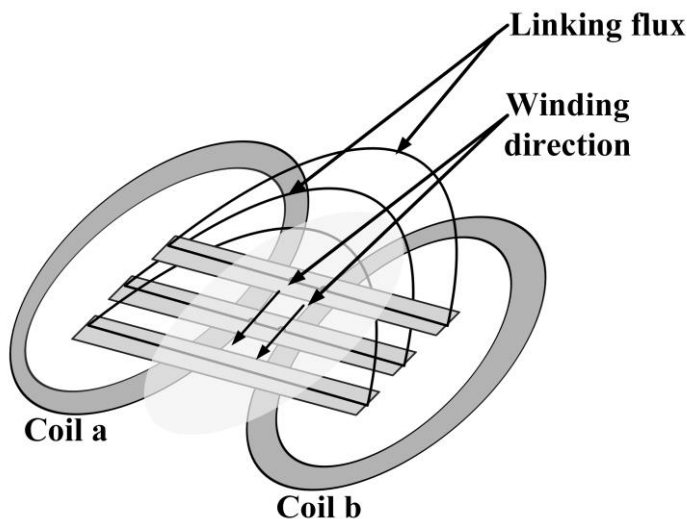


Figure 59. Double D arrangement for WPT. Fluxes generated in one coil cut the other one and induces a voltage there, enabling power transfer between the coils without any wired connection [27].

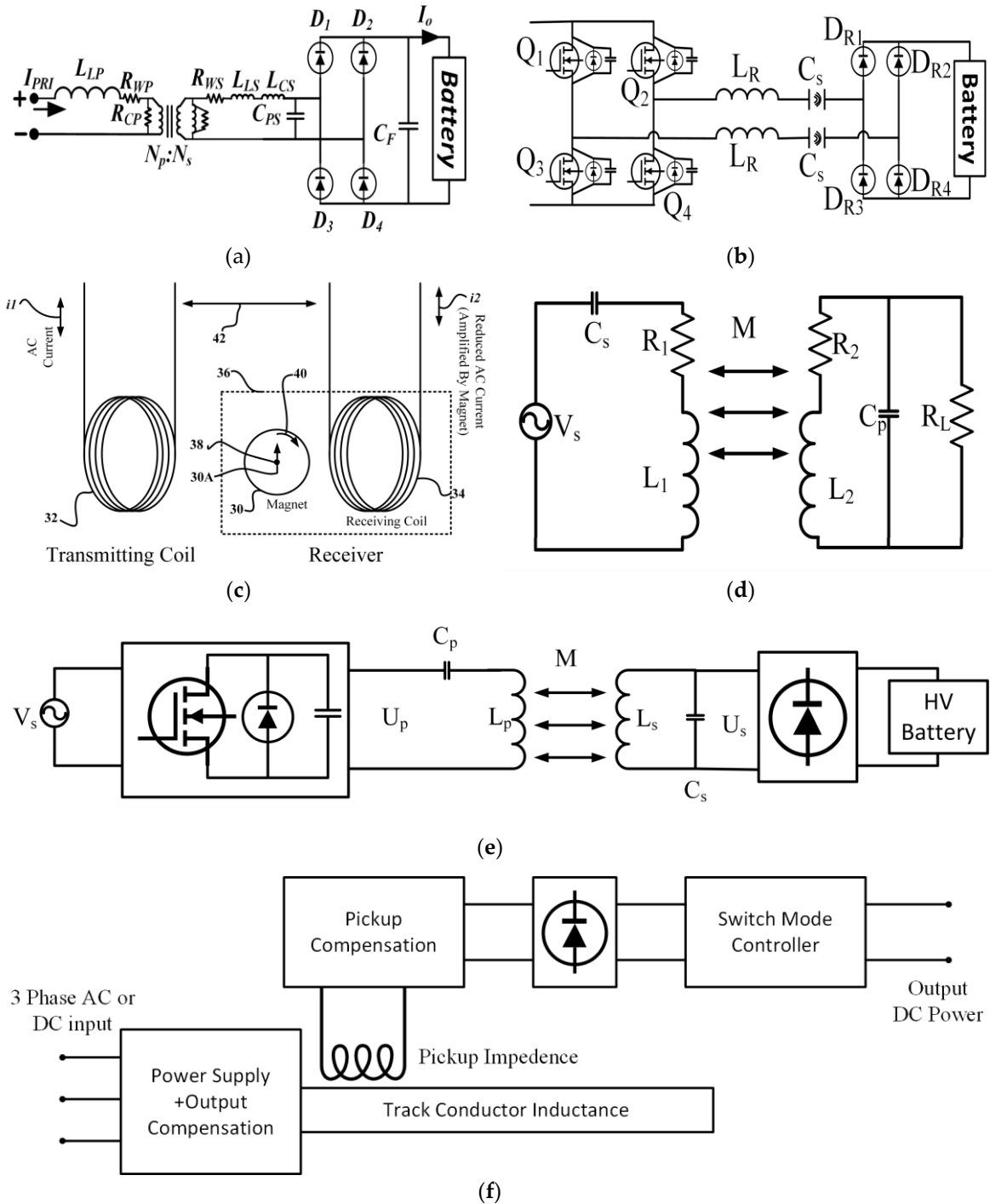


Figure 60. Different configurations used for wireless power transfer over the years: (a) Inductive WPT; (b) Capacitive WPT; (c) Low frequency permanent magnet coupling power transfer (PMPT); (d) Resonant antennae power transfer (RAPT); (e) Resonant inductive power transfer (RIPT); (f) Online power transfer (OLPT).

Table 25. Characteristics of wireless charging systems [87].

Technology	Characteristics
Inductive WPT	<p>7.2.1. It is not actually wireless, just does not require any connection.</p> <p>7.2.2. Primary and secondary coils are sealed in epoxy.</p> <p>7.2.3. Can provide power of either 6.6 kW or 50 kW.</p> <p>7.2.4. Coaxial winding transformer can be used to place all the transformer core materials off-board.</p> <ul style="list-style-type: none"> • Losses including geometric effects, eddy current loss, EMI are mainly caused by nonlinear flux distribution. • A piecewise assembly of ferrite core and dividing the secondary winding symmetrically can help minimizing the losses.
Capacitive WPT	<ul style="list-style-type: none"> • Capacitive power transfer or CPT interface is built with two coupling transformers at the center; the rest of the system is similar to inductive WPT. • Capacitive interface is helpful in reducing the size and cost of the required galvanic isolating parts. • Cheaper and smaller for lower power applications, but not preferred for high power usage. • Useful in consumer electronics, may not be sufficient for EV charging.
Low frequency permanent magnet coupling power transfer (PMPT)	<ul style="list-style-type: none"> • The transmitter is a cylinder-shaped, permanent magnet rotor driven by static windings placed on the rotor, inside it if the rotor is hollow, or outside the motor, separated by an air-gap. • The receiver is placed on the vehicle, similar to the transmitter in construction. • Transmitter and receiver have to be within 150 mm for charging. • Because of magnetic gear effect, the receiver rotor rotates at the same speed as the transmitter and energy is transferred. • The disadvantages may be the vibration, noise and lifetime associated with the mechanical components used.
Resonant inductive power transfer (RIPT)	<ul style="list-style-type: none"> • Most popular WPT system. • Uses two tuned resonant tanks or more, operating in the same frequency in resonance. • Resonant circuits enable maximum transfer of power, efficiency optimization, impedance matching, compensation of magnetic coupling and magnetizing current variation. • Can couple power for a distance of up to 40 cm. • Advantages include extended range, reduced EMI, operation at high frequency and high efficiency.
Online power transfer (OLPT)	<ul style="list-style-type: none"> • Has a similar concept like RIPT, but uses a lower resonant frequency. • Can be used for high power applications. • This system is proposed to be applied in public transport system in [87]. • The primary circuit—a combination of the input of resonant converter and distributed primary windings is integrated in the roadway. This primary side is called the ‘track’. • The secondary is placed in vehicles and is called the ‘pickup coil’. • Supply of this system is high voltage DC or 3-phase AC. • It can provide frequent charging of the vehicles while they are on the move, reducing the required battery capacity, which will reduce the cost and weight of the cars. • The costs associated with such arrangement may also make its implementation unlikely.

Resonant antennae power transfer (RAPT)

- This system uses two resonant antennas, or more, with integrated resonant inductances and capacitances. The antennas are tuned to identical frequencies.
- Large WPT coils are often used as antennas; resonant capacitance is obtained there by controlled separation in the helical structure.
- The frequencies used are in MHz range.
- Can transfer power efficiently for distances up to 10 m.
- The radiations emitted by most of such systems exceed the basic limits on human exposure and are difficult to shield without affecting the range and performance.
- Generating frequencies in the MHz range is also challenging and costly with present power electronics technologies.

8. Effects of EVs

Vehicles may serve the purpose of transportation, but they affect a lot of other areas. Therefore, the shift in the vehicle world created by EVs impacts the environment, the economy, and being electric, the electrical systems to a great extent. EVs are gaining popularity because of the benefits they provide in all these areas, but with them, there come some problems as well. Figure 61 illustrates the impacts of EVs on the power grid, environment and economy.

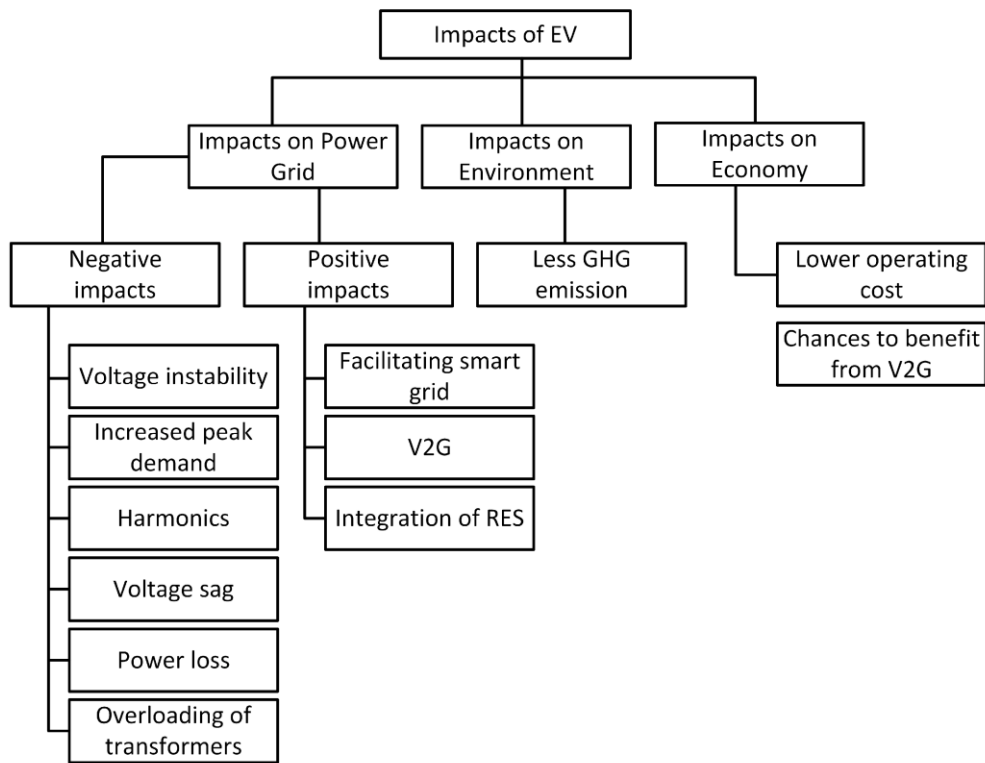


Figure 61. A short list of the impacts of EVs on the power grid, environment and economy.

8.1. Impact on the Power Grid

8.1.1. Negative Impacts

EVs are considered to be high power loads [114] and they affect the power distribution system directly; the distribution transformers, cables and fuses are affected by it the most [115,116]. A Nissan Leaf with a 24 kWh battery pack can consume power similar to a single European household. A 3.3 kW charger in a 220 V, 15 A system can raise the current demand by 17% to 25% [117]. The situation gets quite alarming if charging is done during peak hours, leading to overload on the system, damage of the system equipment, tripping of protection relays, and subsequently, an increase in the infrastructure cost [117]. Charging without any concern to the time of drawing power from the grid is denoted as uncoordinated charging, uncontrolled charging or dumb charging [117,118]. This can

lead to the addition of EV load in peak hours which can cause load unbalance, shortage of energy, instability, and decrease in reliability and degradation of power quality [116,119]. In case of the modified IEEE 23 kV distribution system, penetration of EVs can deviate voltage below the 0.9 p.u. level up to 0.83 p.u., with increased power losses and generation cost [118]. Level 1 charging from an 110 V outlet does not affect the power system much, but problems arise as the charging voltage increases. Adding an EV for fast charging can be equivalent to adding several households to the grid. The grid is likely to be capable of withstanding it, but distribution networks are designed with specific numbers of households kept into mind, sudden addition of such huge loads can often lead to problems. Reducing the charging time to distinguish their vehicles in the EV market has become the current norm among the manufacturers, and it requires higher voltages than ever. Therefore, mitigating the adverse effects is not likely by employing low charging voltages.

To avoid these effects, and to provide efficient charging with the available infrastructure, coordinated charging (also called controlled or smart charging) has to be adopted. In this scheme, the EVs are charged during the time periods when the demand is low, for example, after midnight. Such schemes are beneficial in a lot of ways. It not only prevents addition of extra load during peak hours, but also increases the load in valley areas of the load curve, facilitating proper use of the power plants with better efficiency. In [116], Richardson et al., showed that a controlled charging rate can make high EV penetration possible in the current residential power network with only a few upgrades in the infrastructure. Geng et al., proposed a charging strategy in [120] comprising of two stages aimed at providing satisfactory charging for all connected EVs while shifting the loads on the transformers. On the consumer side, it can reduce the electricity bill as the electricity is consumed by the EVs during off peak hours, which generally have a cheaper unit rate than peak hours. According to [121], smart charging systems can reduce the increase investment cost in distribution system by 60%–70%. The major problems that are faced in the power systems because of EVs can be charted as following:

- Voltage instability: Normally power systems are operated close to their stability limit. Voltage instabilities in such systems can occur because of load characteristics, and that instability can lead to blackouts. EV loads have nonlinear characteristics, which are different than the general industrial or domestic loads, and draw large quantities power in a short time period [81,122]. Reference [123] corroborated to the fact that EVs cause serious voltage instability in power systems. If the EVs have constant impedance load characteristics, then it is possible for the grid to support a lot of vehicles without facing any instability [81]. However, the EV loads cannot be assumed beforehand and thus their power consumptions stay unpredictable; addition of a lot of EVs at a time therefore can lead to violation of distribution constraints. To anticipate these loads properly, appropriate modeling methods are required. Reference [124] suggested tackling the instabilities by damping the oscillations caused by charging and discharging of EV batteries using a wide area control method. The situation can also be handled by changing the tap settings of transformers [125], by a properly planned charging system, and also by using control systems like fuzzy logic controllers to calculate voltages and SOC of batteries [81].
- Harmonics: The EV charger characteristics, being nonlinear, gives raise high frequency components of current and voltage, known as harmonics. The amount of harmonics in a system can be expressed by the parameters total current harmonic distortion (THD_i) and total voltage harmonic distortion (THD_v):

$$THD_i = \frac{\sqrt{\sum_{h=2}^H I_h^2}}{I_1} \times 100\% \quad (4)$$

$$THD_v = \frac{\sqrt{\sum_{h=2}^H V_h^2}}{V_1} \times 100\% \quad (5)$$

Harmonics distort the voltage and current waveforms, thus can reduce the power quality. It also causes stress in the power system equipment like cables and fuses [122]. The present cabling is capable of withstanding 25% EV penetration if slow charging is used, in case of rapid charging, the amount comes down to 15% [126]. Voltage imbalance and harmonics can also give rise to current flow in the neutral wire [127,128]. Different approaches have been adopted to determine the effects of harmonics due to EV penetration. Reference [127] simulated the effects of harmonics using Monte Carlo analysis to determine the power quality. In [129] the authors showed that THD_v can reach 11.4% if a few number of EVs are fast charging. This is alarming as the safety limit of THD_v is 8%. According to Melo et al. [130], THD_i also becomes high, in the range of 12% to 14%, in case of fast charging, though it remains in the safe limit during times of slow charging. Studies conducted in [131] show the modern EVs generate less THD_i than the conventional ones, though their THD_v values are higher. However, with increased number of EVs, there are chances of harmonics cancellation because of different load patterns [132,133]. Different EV chargers can produce different phase angles and magnitudes which can lead to such cancellations [133]. It is also possible to reduce, even eliminate harmonics by applying pulse width modulation in the EV chargers [132]. High THD_i can be avoided by using filtering equipment at the supply system [134].

- Voltage sag: A decrease in the RMS value of voltage for half a cycle or 1 min is denoted as voltagesag. It can be caused by overload or during the starting of electric machines. Simulation modeled with an EV charger and a power converter in [135] stated 20% EV penetration can exceed the voltage sag limit. Reference [136] stated that 60% EV penetration is possible without any negative impact is possible if controlled charging is employed. The amount, however, plummets to 10% in case of uncontrolled charging. Leemput et al., conducted a test employing voltage droop charging and peak shaving by EV charging [137]. This study exhibited considerable decrease in voltage sag with application of voltage droop charging. Application of smart grid can help in great extents in mitigating the sag [138].
- Power loss: The extra loss of power caused by EV charging can be formulated as:

$$PL_E = PL_{EV} - PL_{original} \quad (6)$$

$PL_{original}$ is the loss occurred when the EVs are not connected to the grid and PL_{EV} is the loss with EVs connected. Reference [121] charted the increased power loss as high as 40% in off peak hours considering 60% of the UK PEVs to be connected to distribution system. Uncoordinated charging, therefore, can increase the amount of loss furthermore. Taking that into account, a coordinated charging scheme, based on objective function, to mitigate the losses was proposed in [139]. Coordinated charging is also favored by [140,141] to reduce power losses significantly. Power generated in the near vicinity can also help minimizing the losses [142], and distributed generation can be quite helpful in this prospect, with the vehicle owners using energy generated at their home (by PV cells, CHP plants, etc.) to charge the vehicles.

- Overloading of transformers: EV charging directly affects the distribution transformers [81]. The extra heat generated by EV loads can lead to increased aging rate of the transformers, but it also depends on the ambient temperature. In places with generally cold weather like Vermont, the aging due to temperature is negligible [81]. Estimation of the lifetime of a transformer is done in [143], where factors taken into account are the rate of EV penetration, starting time of charging and the ambient temperature. It stated that transformers can withstand 10% EV penetration without getting any decrease in lifetime. The effect of level 1 charging, is in fact, has negligible effect on this lifetime, but significant increase in level 2 charging can lead to the failure of transformers [144]. Elnozahy et al., stated that overloading of transformer can happen with 20% PHEV penetration for level 1 charging, whereas level 2 does it with 10% penetration [145]. According to [122], charging that takes place right after an EV being plugged in can be detrimental to the transformers.
- Power quality degradation: The increased amount of harmonics and imbalance in voltage will degrade the power quality in case of massive scale EV penetration to the grid.

8.1.2. Positive Impacts

On the plus side, EVs can prove to be quite useful to the power systems in a number of ways:

- **Smart grid:** In the smart grid system, intelligent communication and decision making is incorporated with the grid architecture. Smart grid is highly regarded as the future of power grids and offers a vast array of advantages to offer reliable power supply and advanced control. In such a system, the much coveted coordinated charging is easily achievable as interaction with the grid system becomes very much convenient even from the user end. The interaction of EVs and smart grid can facilitate opportunities like V2G and better integration of renewable energy. In fact, EV is one the eight priorities listed to create an efficient smart grid [117].
- **V2G:** V2G or vehicle to grid is a method where the EV can provide power to the grid. In this system, the vehicles act as loads when they are drawing energy, and then can become dynamic energy storages by feeding back the energy to the grid. In coordinated charging, the EV loads are applied in the valley points of the load curve, in V2G; EVs can act as power sources to provide during peak hours. V2G is realizable with the smart grid system. By making use of the functionalities of smart grid, EVs can be used as dynamic loads or dynamic storage systems. The power flow in this system can be unidirectional or bidirectional. The unidirectional system is analogous to the coordinated charging scheme, the vehicles are charged when the load is low, but the time to charge the vehicles is decided automatically by the system. Vehicles using this scheme can simply be plugged in anytime and put there; the system will choose a suitable time and charge it. Smart meters are required for enabling this system. With a driver variable charging scheme, the peak power demand can be reduced by 56% [117]. Sortomme et al., found this system particularly attractive as it required little up gradation of the existing infrastructure; creating a communication system in-between the grid and the EVs is all that is needed [146]. The bidirectional system allows vehicles to provide power back to the grid. In this scenario, vehicles using this scheme will supply energy to the grid from their storage when it is required. This method has several appealing aspects. With ever increasing integration of renewable energy sources (RES) to the grid, energy storages are becoming essential to overcome their intermittency, but the storages have a very high price. EVs have energy storages, and in many cases, they are not used for a long time. Example for this point can be the cars in the parking lots of an office block, where they stay unused till the office hour is over, or vehicles that are used in a specific time of the year, like a beach buggy. Studies also revealed that, vehicles stay parked 95% of the time [117]. These potential storages can be used when there is excess generation or low demand and when the energy is needed, it is taken back to the grid. The vehicle owners can also get economically beneficial by selling this energy to the grid. In [147], Clement-Nyns et al., concluded that a combination of PHEVs can prove beneficial to distributed generation sources by providing storage for the excess generation, and releasing that to the grid later. Bidirectional charging, however, needs chargers capable of providing power flow in both directions. It also needs smart meters to keep track of the units consumed and sold, and advanced metering architecture (AMI) to learn about the unit charges in real time to get actual cost associated with the charging or discharging at the exact time of the day. The AMI system can shift 54% of the demand to off-peak periods, and can reduce peak consumption by 36% [117]. The bidirectional system, in fact, can provide 12.3% more annual revenue than the unidirectional one. But taking the metering and protections systems required in the bidirectional method, this revenue is nullified and indicates the unidirectional system is more practical. Frequent charging and discharging caused by bidirectional charging can also reduce battery life and increase energy losses from the conversion processes [81,117]. In a V2G scenario, operators with a vehicle fleet are likely to reduce their cost of operation by 26.5% [117]. Another concept is produced using the smart grid and the EVs, called virtual power plant (VPP), where a cluster of vehicles is considered as a power plant and dealt like one in the system. VPP architecture and control is shown in Figure 62. Table 26 shows the characteristics of unidirectional and bidirectional V2G.

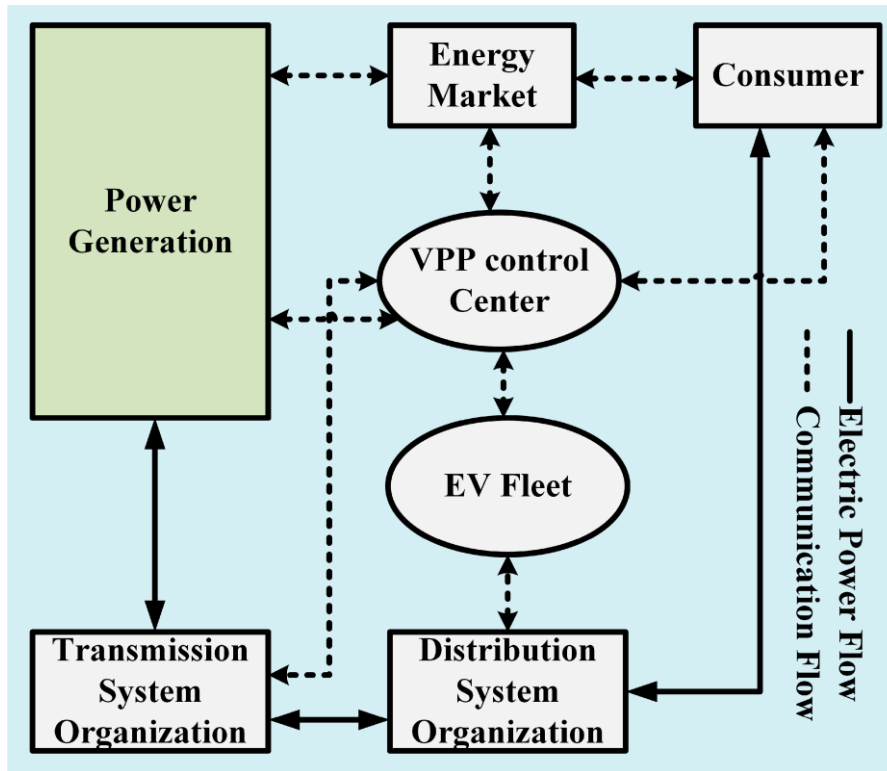


Figure 62. VPP architecture and control [117].

Table 26. Unidirectional and bidirectional V2G characteristics. Adapted from [1].

V2G System	Description	Services	Advantages	Limitations
Unidirectional	Controls EV charging rate with a unidirectional power flow directed from grid to EV based on incentive systems and energy scheduling	<ul style="list-style-type: none"> Ancillary service—load levelling 	<ul style="list-style-type: none"> Maximized profit Minimized power loss Minimized operation cost Minimized emission 	<ul style="list-style-type: none"> Limited service range
Bidirectional	Bidirectional power flow between grid and EV to attain a range of benefits	<ul style="list-style-type: none"> Ancillary service—spinning reserve Load leveling Peak power shaving Active power support Reactive power support/Power factor correction Voltage regulation Harmonic filtering Support for integration of renewable 	<ul style="list-style-type: none"> Maximized profit Minimized power loss Minimized operation cost Minimized emission Prevention of grid overloading Failure recovery Improved load profile Maximization of renewable energy generation 	<ul style="list-style-type: none"> Fast battery degradation Complex hardware High capital cost Social barriers

- Integration of renewable energy sources: Renewable energy usage becomes more promising with EVs integrated into the picture. EV owners can use RES to generate power locally to charge their EVs. Parking lot roofs have high potential for the placement of PV panels which can charge the vehicles parked underneath as well as supplying the grid in case of excess generation [148–150], thus serving the increase of commercial RES deployment. The V2G structure is further helpful to integrate RES for charging of EVs, and to the grid as well, as it enables the selling of energy to the grid when there is surplus, for example, when vehicles are parked and the system knows the user will not need the vehicle before a certain time. V2G can also enable increased penetration of wind energy (41%–59%) in the grid in an isolated system [121]. References [151–154] worked with different architectures to observe the integration scenario of wind energy with EV assistance. Figure 63 demonstrates integration of wind and solar farm with conventional coal

and nuclear power grid with EV charging station employing bidirectional V2G. Table 27 shows the types of assistance EVs can provide for integrating renewable energy sources to the grid.

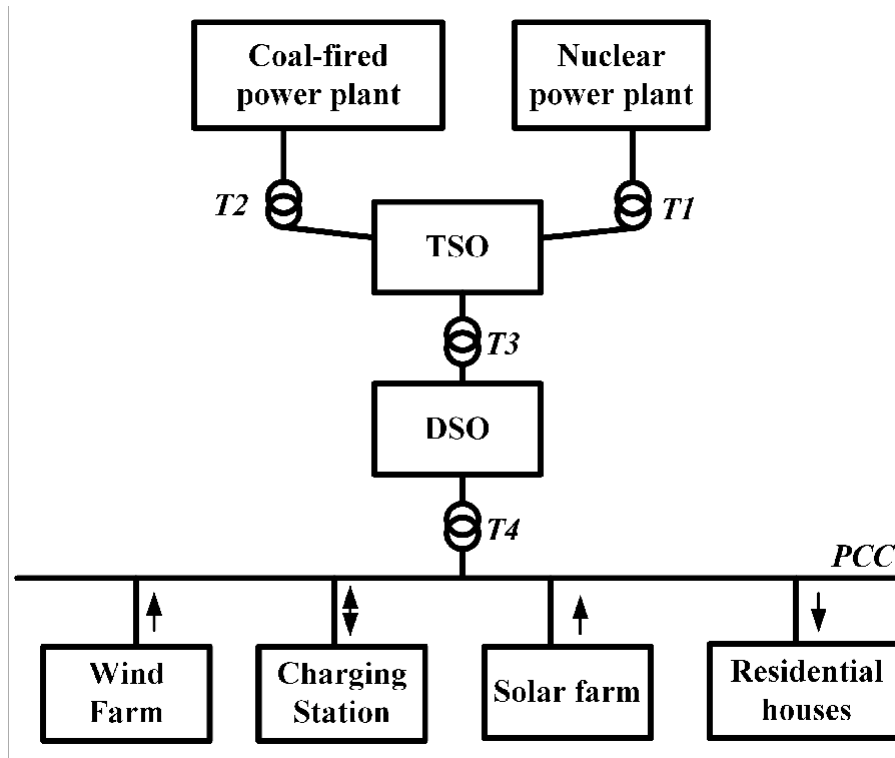


Figure 63. Wind and solar integration in the grid with the help of EV in V2G system. TSO stands for transmission system organization; DSO for distribution system organization; T1 to T4 represent the transformers coupling the generation, transmission, and distribution stages [117].

Table 27. Scopes of assisting renewable energy source (RES) integration using EV. Adapted from [1].

Interaction with RES	Field of Application	Contribution
Solar PV	Smart home	<ul style="list-style-type: none"> • Implementation of PV and EV in smart home to reduce emission • Development of stand-alone home EV charger based on solar PV system • Development of future home with uninterruptable power by implementing V2G with solar PV
	Parking lot	<ul style="list-style-type: none"> • Analysis of EV charging using solar PV at parking lots • Scheduling of charging and discharging for intelligent parking lot
	Grid distribution network	<ul style="list-style-type: none"> • Assessment of power system performance with integration of grid connected EV and solar PV • Development of EV charging control strategy for grid connected solar PV based charging station • Development of optimization algorithm to coordinate V2G services
	Micro grid	<ul style="list-style-type: none"> • Development of generation scheduling for micro grid consisting of EV and solar PV
Wind turbine	Grid distribution network	<ul style="list-style-type: none"> • Determination of EV interaction potential with wind energy generation • Development of V2G systems to overcome wind intermittency problems
	Micro grid	<ul style="list-style-type: none"> • Development of coordinating algorithm for energy dispatching of V2G and wind generation
Solar PV and wind turbine	Smart home	<ul style="list-style-type: none"> • Development of control strategy for smart homes with grid-interactive EV and renewable sources

Parking lot	<ul style="list-style-type: none"> • Design of intelligent optimization framework for integrating renewable sources and EVs
Grid distribution network	<ul style="list-style-type: none"> • Potential analysis of grid connected EVs for balancing intermittency of renewable sources • Emission analysis of EVs associated with renewable generation • Development of optimized algorithm to integrate EVs and renewable sources to the grid
Micro grid	<ul style="list-style-type: none"> • Development of V2G control for maximized renewable integration in micro grid

8.2. Impact on Environment

One of the main factors that propelled the increase of EVs' popularity is their contribution to reduce the greenhouse gas (GHG) emissions. Conventional internal combustion engine (ICE) vehicles burn fuels directly and thus produce harmful gases, including carbon dioxide and carbon monoxide. Though HEVs and PHEVs have IC engines, their emissions are less than the conventional vehicles. But there are also theories that the electrical energy consumed by the EVs can give rise to GHG emission from the power plants which have to produce more because of the extra load added in form of EVs. This theory can be justified by the fact that the peak load power plants are likely to be ICE type, or can use gas or coal for power generation. If EVs add excess load during peak hours, it will lead to the operation of such plants and will give rise to CO₂ emission [155]. Reference [156] also stated that power generation from coal and natural gas will produce more CO₂ from EV penetration than ICEs. However, all the power is not generated from such resources. There are many other power generating technologies that produce less GHG. With those considered, the GHG production from power plants because of EV penetration is less than the amount produced by equivalent power generation from ICE vehicles. The power plants also produce energy in bulk, thus minimizing the per unit emission. With renewable sources integrated properly, which the EVs can support strongly, the emission from both power generation and transportation sector can be reduced [115]. Over the lifetime, EVs cause less emission than conventional vehicles. This parameter can be denoted as well-to-wheel emission and it has a lower value for EVs [157]. In [158], well-to-wheel and production phases are taken into account to calculate the impact of EVs on the environment. This approach stated the EVs to be the least carbon intensive among the vehicles. Denmark managed to reduce 85% CO₂ emission from transportation by combining EVs and electric power. EVs also produce far less noise, which can highly reduce sound pollution, mostly in urban areas. The recycling of the batteries raises serious concerns though, as there are few organizations capable of recycling the lithium-ion batteries fully. However, like the previous nickel-metal and lead-acid ones, lithium-ion cells are not made of caustic chemicals, and their reuse can reduce 'peak lithium' or 'peak oil' demands [81].

8.3. Impact on Economy

From the perspective of the EV owners, EVs provide less operating cost because of their superior efficiency [22]; it can be up to 70% where ICE vehicles have efficiencies in the range of 60% to 70% [159]. The current high cost of EVs is likely to come down from mass production and better energy policies [3] which will further increase the economic gains of the owners. V2G also allows the owners to obtain a financial benefit from their vehicles by providing service to the grid [160]. The power service providers benefit from EV integration mainly by implementing coordinated charging and V2G. It allows them to adopt better peak shaving strategies as well as to integrate renewable sources. EV fleets can lead to \$200 to \$300 savings in cost per vehicle per year [161,162].

8.4. Impacts on Motor Sports

Hybrid technologies are not used extensively in motor sports to enhance the performance of the vehicles. Electric vehicles now have their own formula racing series named 'Formula E' [163] which started in Beijing in September 2014. Autonomous EVs are also being planned to take part in a segment of this series called 'Roborace'.

9. Barriers to EV Adoption

Although electric vehicles offer a lot of promises, they are still not widely adopted, and the reasons behind that are quite serious as well.

9.1. Technological Problems

The main obstacles that have frustrated EVs' domination are the drawbacks of the related technology. Batteries are the main area of concern as their contribution to the weight of the car is significant. Range and charging period also depend on the battery. These factors, along with a few others, are demonstrated below:

9.1.1. Limited Range

EVs are held back by the capacity of their batteries [4]. They have a certain amount of energy stored there, and can travel a distance that the stored energy allows. The range also depends on the speed of the vehicle, driving style, cargo the vehicle is carrying, the terrain it is being driven on, and the energy consuming services running in the car, for example air conditioning. This causes 'range anxiety' among the users [81], which indicates the concern about finding a charging station before the battery drains out. People are found to be willing to spend up to \$75 extra for an extra range of one mile [164]. Though even the current BEVs are capable of traversing equivalent or more distance than a conventional vehicle can travel with a full tank (Tesla Model S 100D has a range of almost 564 km on 19" wheels when the temperature is 70 °C and the air conditioning is off [24], the Chevrolet Bolt's range is 238 miles or 383 km [165]), range anxiety remains a major obstacle for EVs to overcome. This does not affect the use of EVs for urban areas though, as in most cases this range is enough for daily commutation inside city limits. Range extenders, which produce electricity from fuel, are also available with models like BMW i3 as an option. Vehicles with such facilities are currently being called as Extended Range Electric Vehicles (EREV).

9.1.2. Long Charging Period

Another major downside of EVs is the long time they need to get charged. Depending on the type of charger and battery pack, charging can take from a few minutes to hours; this truly makes EVs incompetent against the ICE vehicles which only take a few minutes to get refueled. Hidrue et al., found out that, to have an hour decreased from the charging time; people are willing to pay \$425–\$3250 [164]. A way to make the charging time faster is to increase the voltage level and employment of better chargers. Some fast charging facilities are available at present, and more are being studied. There are also the fuel cell vehicles that do not require charging like other EVs. Filling up the hydrogen tank is all that has to be done in case of these vehicles, which is as convenient as filling up a fuel tank, but FCVs need sufficient hydrogen refueling stations and a feasible way to produce the hydrogen in order to thrive.

9.1.3. Safety Concerns

The concerns about safety are rising mainly about the FCVs nowadays. There are speculations that, if hydrogen escapes the tanks it is kept into, can cause serious harm, as it is highly flammable. It has no color either, making a leak hard to notice. There is also the chance of the tanks to explode in case of a collision. To counter these problems, the automakers have taken measures to ensure the integrity of the tanks; they are wrapped with carbon fibers in case of the Toyota Mirai. In this car, the hydrogen handling parts are placed outside the cabin, allowing the gas to disperse easily in case of any leak, there are also arrangements to seal the tank outlet in case of high-speed collision [166].

9.2. Social Problems

9.2.1. Social Acceptance

The acceptance of a new and immature technology, along with its consequences, takes some time in the society as it means change of certain habits [167]. Using an EV instead of a conventional vehicle means change of driving patterns, refueling habits, preparedness to use an alternative transport in case of low battery, and these are not easy to adopt.

9.2.2. Insufficient Charging Stations

Though public charging stations have increased a lot in number, still they are not enough. Coupled with the lengthy charging time, this acts as a major deterrent against EV penetration. Not all the public charging stations are compatible with every car as well; therefore it also becomes a challenge to find a proper charging point when it is required to recharge the battery. There is also the risk of getting a fully occupied charging station with no room for another car. But, the manufacturers are working on to mitigate this problem. Tesla and Nissan have been expanding their own charging networks, as it, in turn means they can sell more of their EVs. Hydrogen refueling stations are not abundant yet as well. It is necessary as well to increase the adoption of FCVs. In [168], a placement strategy for hydrogen refueling stations in California is discussed. It stated that a total of sixty-eight such stations will be sufficient to provide service to FCVs in the area. To get the better out of the remaining stations, there are different trip planning applications, both web based and manufacturer provided, which helps to obtain a route so that there are enough charging facilities to reach the destination.

9.3. Economic Problems

High Price

The price of the EVs is quite high compared to their ICE counterparts. This is because of the high cost of batteries [81] and fuel cells. To make people overlook this factor, governments in different countries including the UK and Germany, have provided incentives and tax breaks which provide the buyers of EVs with subsidies. Mass production and technological advancements will lead to a decrease in the prices of batteries as well as fuel cells. Affordable EVs with a long range like the Chevrolet Bolt has already appeared in the market, while another vehicle with the same promises (the Tesla Model 3) is anticipated to arrive soon. Figure 64 shows the limitations of EVs in the three sectors. Table 28 demonstrates the drawbacks in key factors, while Table 29 suggests some solutions for the existing limitations.

10. Optimization Techniques

To make the best out of the available energy, EVs apply various aerodynamics and mass reduction techniques, lightweight materials are used to decrease the body weight as well. Regenerative braking is used to restore energy lost in braking. The restored energy can be stored in different ways. It can be stored directly in the ESS, or it can be stored by compressing air by means of hydraulic motor, springs can also be employed to store this energy in form of gravitational energy [169].

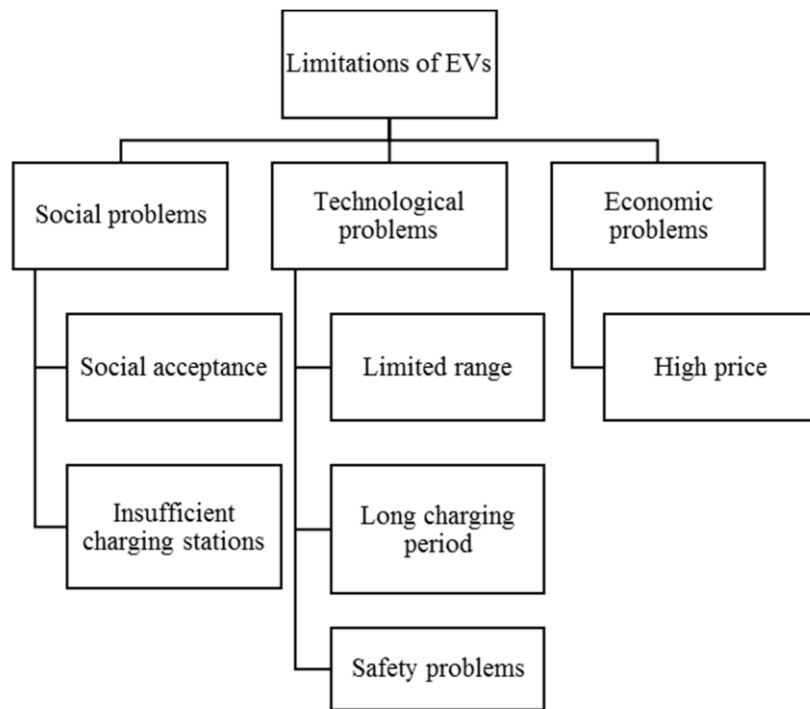


Figure 64. Social, technological, and economic problems faced by EVs.

Table 28. Hurdles in key EV factors. Adapted from [170].

Factor	Hurdles
Recharging	Weight of charger, durability, cost, recycling, size, charging time
Hybrid EV	Battery, durability, weight, cost
Hydrogen fuel cell	Cost, hydrogen production, infrastructure, storage, durability, reliability
Auxiliary power unit	Size, cost, weight, durability, safety, reliability, cooling, efficiency

Table 29. Tentative solutions of current limitations of EVs.

Limitation	Probable Solution
Limited range	Better energy source and energy management technology
Long charging period	Better charging technology
Safety problems	Advanced manufacturing scheme and build quality
Insufficient charging stations	Placement of sufficient stations capable of providing services to all kinds of vehicles
High price	Mass production, advanced technology, government incentives

Formula One vehicles employ kinetic energy recovery systems (KERSs) to use the energy gathered during braking to provide extra power during accelerating. The Porsche 911 GT3R hybrid uses a flywheel energy storage system to store this energy. The energy consuming accessories on a car include power steering, air conditioning, lights, infotainment systems etc. Operating these in an energy efficient way or turning some of these off can increase the range of a vehicle. LEDs can be used for lighting because of their high efficiency [169]. Table 30 shows different methods of recovering the energy lost during braking.

Table 30. Different methods of recovering energy during braking [169].

Storage System	Energy Converter	Recovered Energy	Application
Electric storage	Electric motor/generator	~50%	BEV, HEV
Compressed gas storage	Hydraulic motor	>70%	Heavy-duty vehicles
Flywheel	Rotational kinetic energy	>70%	Formula One (F1) racing
Gravitational energy storage	Spring storage system	-	Train

Aerodynamic techniques are used in vehicles to reduce the drag coefficient, which reduces the required power. Power needed to overcome the drag force is:

$$P_d = \frac{1}{2} \rho v^3 A C_d \quad (7)(7)$$

Here C_d is the drag coefficient, the power to overcome the drag increases if the drag coefficient's value increases. The Toyota Prius claims a drag coefficient of 0.24 for the 2017 model, the same as the Tesla Model S. The 2012 Nissan Leaf SL had this value set at 0.28 [171].

To ensure efficient use of the available energy, different energy management schemes can be employed [6]. Presented different control strategies for energy management which included systems using fuzzy logic, deterministic rule and optimization based schemes. Geng et al., worked on a plug-in series hybrid FCV. The objective of their control system was to consume the minimum amount of hydrogen while preserving the health of the proton exchange membrane fuel cell (PEMFC) [172]. The control system was comprised of two stages; the first stage determined the SOC and control references, whereas the second stage determined the PEMFC health parameters. This method proved to be capable of reducing the hydrogen consumption while increasing the life-time to the fuel cell. Another intelligent management system is examined in [173] by Murphey et al., which used machine learning combined with dynamic programming to determine energy optimization strategies for roadway and traffic-congestion scenarios for real-time energy flow control of a hybrid EV. Their system is simulated using a Ford Escape Hybrid model; it revealed the system was effective in finding out congestion level, optimal battery power and optimal speed. Geng et al., proposed a control mechanism for energy management for a PHEV employing batteries and a micro turbine in [174]. In this work, they introduced a new parameter, named the "energy ratio", to produce the equivalent factor (EF) which was used in the popular Equivalent Consumption Minimization Strategy (ECMS) to deduce the minimum driving cost by applying Pontryagin's minimum principle. This method claimed to reduce the cost by 7.7–21.6%. In [175], Moura et al., explored efficient ways to split power demand among different power sources of mid-sized sedan PHEVs. They used a number of drive cycles, rather than a single one, assessed the potential of depleting charge in a controlled manner, and considered relative pricing of fuel and electricity for optimal power management of the vehicle.

11. Control Algorithms

Control systems are crucial for proper functioning of EVs and associated systems. Sophisticated control mechanisms are required for providing a smooth and satisfactory ride quality, for providing the enough power when required, estimating the energy available from the on-board sources and using them properly to cover the maximum distance, charging in a satisfactory time without causing burden on the grid, and associated tasks. Different algorithms are used in these areas, and as the EV culture is becoming more mainstream, need for better algorithms are on the rise.

Driving control systems are required to assist the driver in keeping the vehicle in control, especially at high speeds and in adverse conditions such as slippery surfaces caused by rain or snow. Driving control systems such as traction control, cruise control, and different driving modes have been being applied in conventional vehicles for a long time. Application of such systems appeared more efficient in EVs as the driving forces of EVs can be controlled with more ease, with less conversion required in-between the mechanical and the electrical domains. In any condition, forces act on a vehicle at different directions; for a driving control system, it is essential to perfectly perceive these forces, along with other sensory inputs, and provide torques to the wheels to maintain desired stability. In Figure 65, the forces in different direction acting on each wheel of a car is shown in a horizontal plane. In [176], Magallan et al., proposed and simulated a control system to utilize the maximum torque in a rear-wheel-drive EV without causing the tires to skid. The model they worked on had independent driving systems for the two rear wheels. A sliding mode system, based on a *LuGre* dynamic friction model, was used to estimate the vehicle's velocity and wheel slip on unknown road surfaces. Utilizing these data, the control algorithm determined the maximum allowable traction force, which was applied to the road by torque controlling of the two rear motors. Juyong Kang et al.,

presented an algorithm aimed at driving control systems for four-wheel-drive EVs in [177]. Their vehicle model had two motors driving the front and the rear shafts. The algorithm had three parts: a supervisory level for determine the desirable dynamics and control mode, an upper level computing the yaw moment and traction force inputs, and a lower level determining the motor and braking commands. This system proved useful for enhancing lateral stability, maneuverability, and reducing rollover. Figure 66 shows the acting components of this system on a vehicle model while Figure 67 shows a detailed diagram of the system with the inputs, controller levels, and actuators. Tahami et al., introduced a stability system for driving assistance for all-wheel drive EVs in [25]. They trained a neural network to produce a reference yaw rate. A fuzzy logic controller dictated independent wheel torques; a similar controller was used for controlling wheel slip. This system is shown in Figure 68. In [178], Wang et al., showed a system to assist steering using differential drive for in-wheel drive system. A proportional integral (PI) closed loop control system was used here to monitor the reference steering position. It was achieved by distributing torque at the front wheels. Direct yaw moment control and traction control were also employed to make the differential drive system better. This approach maintained the lateral stability of the vehicle, and improved stability at high speeds. The structure of this system is shown in Figure 69. In a separate study conducted by Nam et al., lateral stability of an in-wheel drive EV was attained by estimating the sideslip angle of the vehicle employing sensors to measure lateral tire forces [179]. In this study, a state observer was proposed which was derived from extended-Kalman-filtering (EKF) method and was evaluated by implementing in an experimental EV alongside Matlab/Simulink-Carsim simulations.

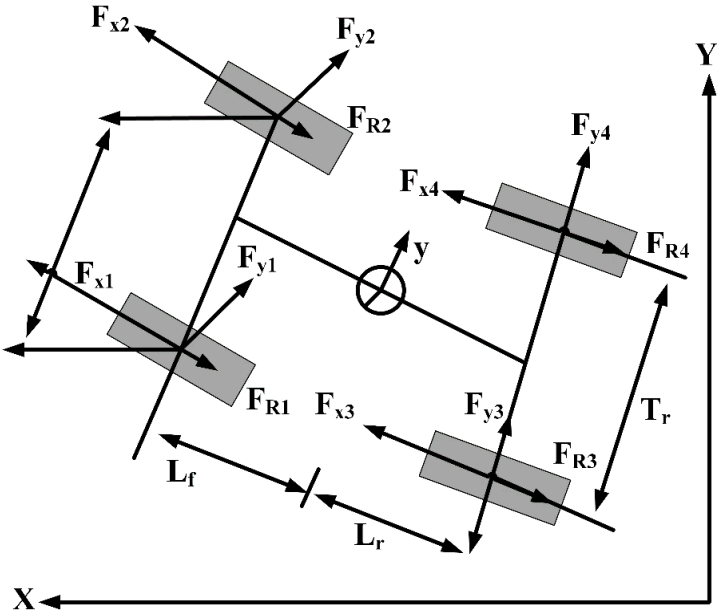


Figure 65. Forces acting on the wheels of a car. Each of the wheels experience forces in all three directions, marked with the 'F' vectors. L_f and L_r show the distances of front and rear axles from the center of the vehicle, while T_r shows the distance between the wheels of an axle. Adapted from [25].

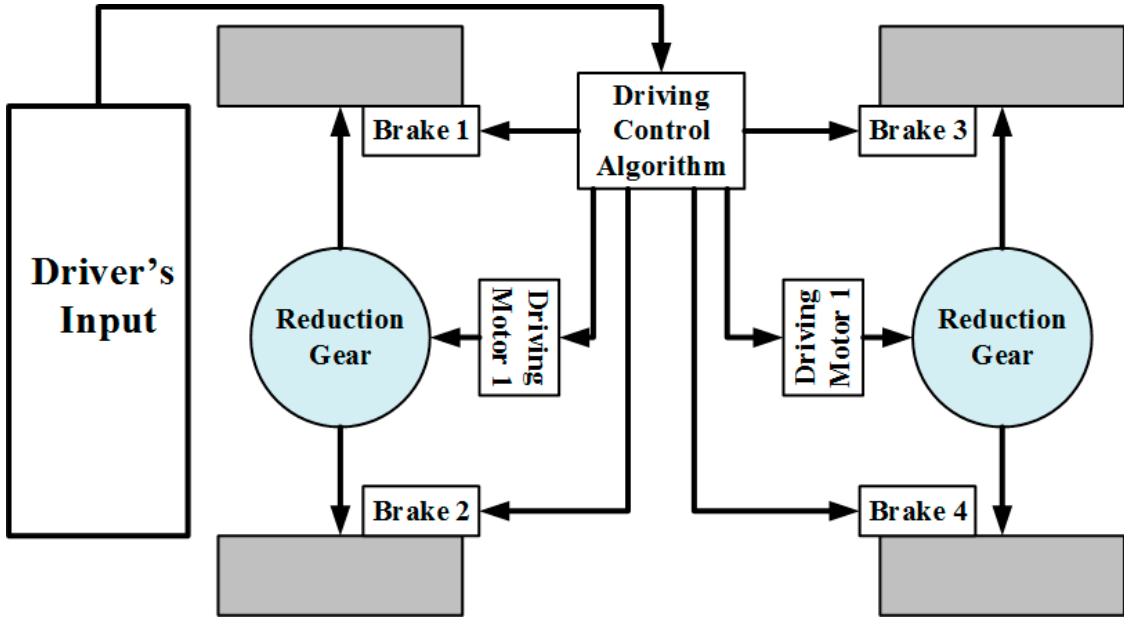


Figure 66. Main working components of the driving control system for four-wheel-drive EVs proposed by Juyong Kang et al. The driving control algorithm takes the driver's inputs, and then determines the actions of the brakes and the motors according to the control mode [177].

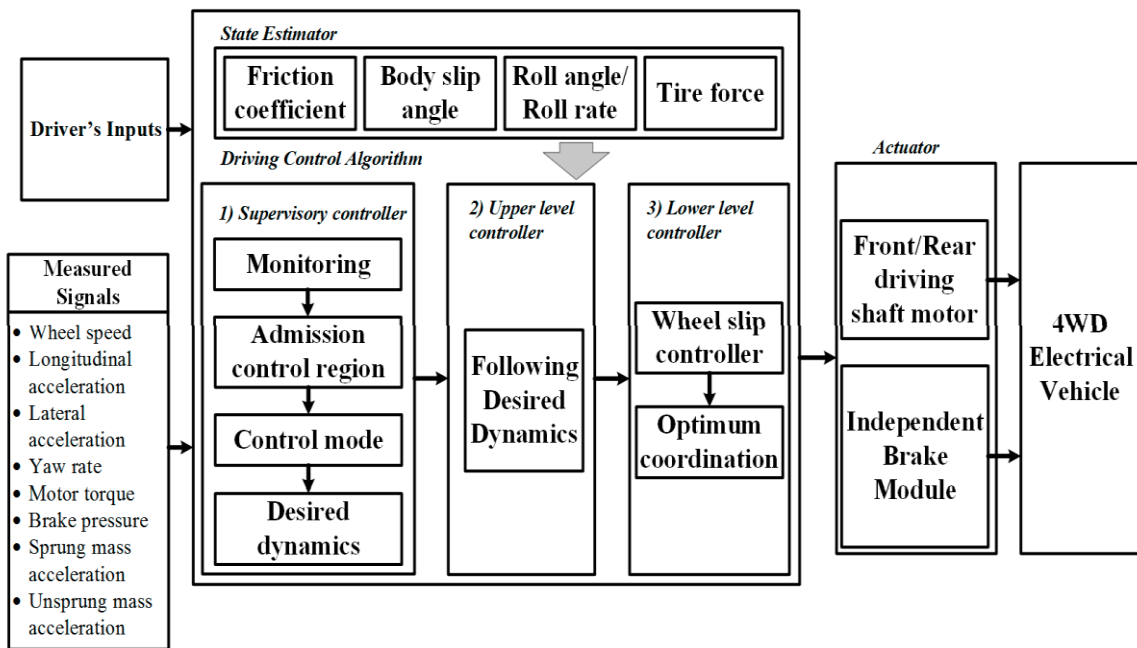


Figure 67. Working principle of the control system proposed by Kang et al. The system uses both the driver's commands and sensor measurements as inputs, and then drives the actuators as determined by the three level control algorithms. Adapted from [177].

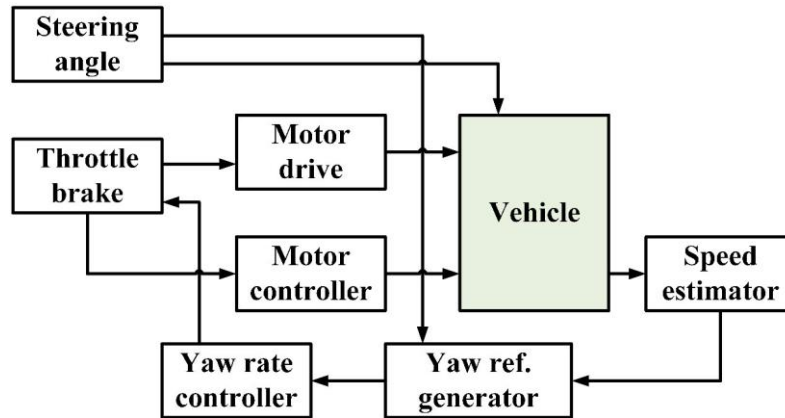


Figure 68. Working principle of vehicle stability system proposed by Tahami et al. A neural network was used in the yaw reference generator [25].

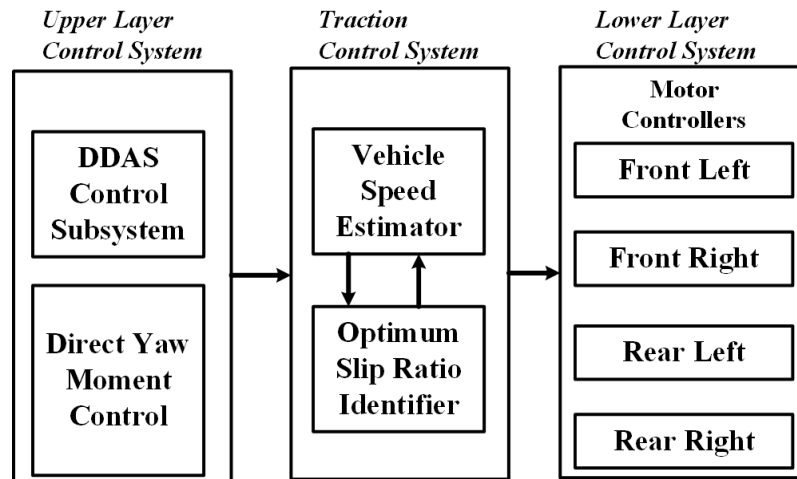


Figure 69. Independent torque control system proposed by Wang et al., Differential drive assisted steering (DDAS) subsystem and direct yaw moment control subsystem creates the upper layer. The traction control subsystem processes the inputs, and the controlling is done through the lower layer [178].

Energy management is a big issue for EVs. Proper measurement of the available energy is crucial for calculating the range and plans the driving strategy thereafter. For vehicles with multiple energy sources (e.g., HEVs), efficient energy management algorithms are required to make proper use of the energy on-board. Zhou et al., proposed a battery state-of-charge (SOC) measuring algorithm for lithium polymer batteries which made use of a combination of particle filter and multi-model data fusion technique to produce results real time and is not affected by measurement noise [180]. They used different battery models and presented the tuning strategies for each model as well. Their multi-model approach proved to be more effective than single model methods for providing real time results. Working principle of this system is shown in Figure 70. Moura et al., explored efficient ways to split power demand among different power sources of mid-sized sedan PHEVs in [175], which can be used for other vehicle configurations as well. Their method made use of different drive cycles, rather than using a single one; assessed the potential of depleting charge in a controlled manner; and considered relative pricing of fuel and electricity to optimally manage the power of the vehicle. In [181], Hui et al., presented a novel hybrid vehicle using parallel hybrid architecture which employed a hydraulic/electric synergy configuration to mitigate the drawbacks faced by heavy hybrid vehicles using a single energy source. Transition among the operating modes of such a vehicle is shown in Figure 71. They developed an algorithm to optimize the key parameters and adopted a logic

threshold approach to attain desired performance, stable SOC at the rational operating range constantly, and maximized fuel economy. The operating principle of this system is shown in Figure 72. Chen et al., proposed an energy management algorithm in [182] to effectively control battery current, and thus reduce fuel usage by allowing the engine operate more effectively. Quadratic programming was used here to calculate the optimum battery current. In [183], Li et al., used fuzzy logic to create a new quantity: battery working state or BWS which was used in an energy management system run by fuzzy logic to provide proper power division between the engine and the battery. Simulation results proved this approach to be effective in making the engine operate in the region of maximum fuel efficiency while keeping the battery away from excess discharging. Yuan et al., compared Dynamic Programming and Pontryagin’s Minimum Principle (PMP) for energy management in parallel HEVs using Automatic Manual Transmission. The PMP method proved better as it was more efficient to implement, required considerably less computational time, and both of the systems provided almost similar results [184]. In [185], Bernard et al., proposed a real time control system to reduce hydrogen consumption in FCEVs by efficiently sharing power between the fuel cell arrangement and the energy buffer (ultracapacitor or battery). This control system was created from an optimal control theory based non-causal optimization algorithm. It was eventually implemented in a hardware arrangement built around a 600 W fuel cell arrangement. In an attempt to create an energy management system for a still-not-commercialized PHEV employing a micro turbine, Geng et al., used an equivalent consumption minimization strategy (ECMS) in [174] to estimate the optimum driving cost. Their system used the battery SOC and the vehicle telemetry to produce the results, which were available in real time and provided driving cost reductions of up to 21.6%.

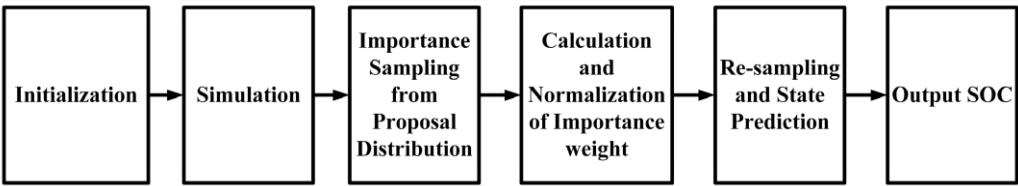


Figure 70. Working principle of the SOC measuring algorithm proposed by Zhou et al. [180].

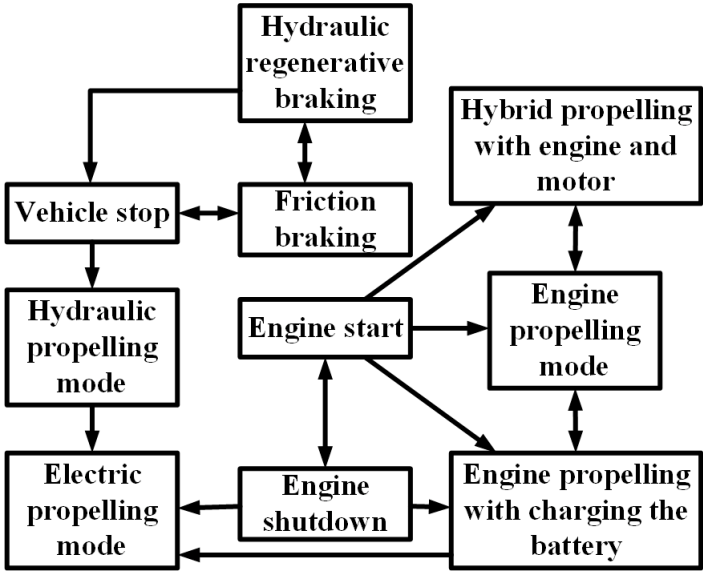


Figure 71. Transition of the operating modes of the vehicle used in [181] by Hui et al. From engine start to shutdown through stops, the vehicle can use either the hydraulic or the electric system, or it can use both.

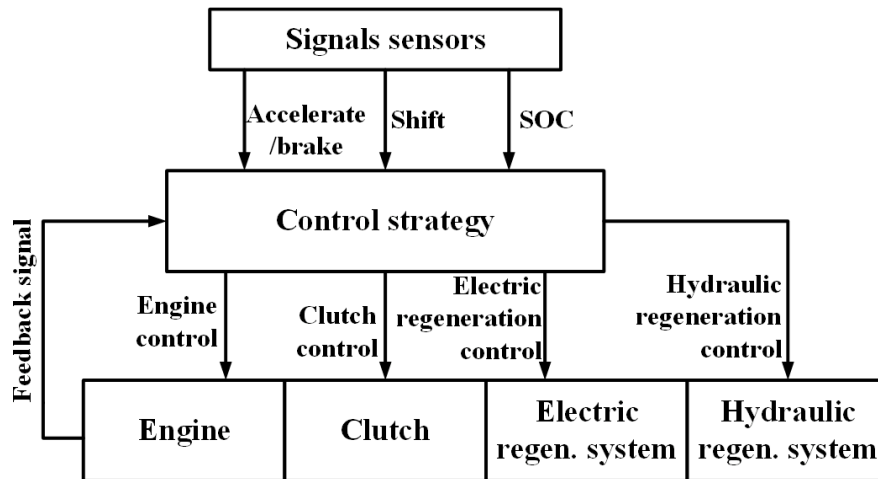


Figure 72. Operating principle of the control system proposed by Hui et al. The control strategy drives the actuating systems according to the decisions made from the sensor inputs. Adapted from [181].

As pointed out in Section 8, the grid is facing some serious problems with the current rise in EV penetration. Reducing the charging time of the vehicles while creating minimal pressure on the grid has become difficult goal to achieve. However, ample research has already been done on this matter and a number of charging system algorithms have been proposed to attain satisfactory charging performance.

In [186], Su et al., presented an algorithm (shown in Figure 73) capable of providing charge intelligently to a large fleet of PHEVs docked at a municipal charging station. This algorithm—which used the estimation of distribution (EDA) algorithm—considered real-world factors such as remaining charging time, remaining battery capacity, and energy price. The load management system proposed by Deilami et al., in [140] considered market energy prices that vary with time, time zones preferred by EV owners by priority selection, and random plugging-in of EVs—for providing coordinated charging in a smart grid system. It then used the maximum sensitivities selection (MSS) optimization technique to enable EVs charge as soon as possible depending on the priority time zones while maintaining the operation criteria of the grid such as voltage profile, limits of generation, and losses. This system was simulated using an IEEE 23 kV distribution system modified for this purpose. Mohamed et al., designed an energy management algorithm to be applied in EV charging parks incorporating renewable generation such as PV systems [187]. The system they developed used a fuzzy controller to manage the charging/discharging times of the connected EVs, power sharing among them, and V2G services. The goal of this system was to minimize the charging cost while reducing the impact on the grid as well as contributing to peak shaving. The flowchart associated to this system is shown in Figure 74.

To alleviate the problems at the distribution stage of the grid—which is highly affected by EV penetration—Geng et al., proposed a charging strategy comprising of two stages aimed at providing satisfactory charging for all connected EVs while shifting the loads on the transformers [120]. The first stage utilized Pontryagin’s minimum principle and was based on the concept of dynamic aggregator; it derived the optimal charging power for all the EVs in the system. The second stage used fuzzy logic to distribute the power calculated in the first stage among the EVs. According to the authors, the system was feasible to be implemented practically [120]. In [116], Richardson et al., employed a linear programming based technique to calculate the optimal rate of charging for each EV connected in a distribution network to enable maximized power delivery to the vehicles while maintaining the network limits. This approach can provide high EV penetration possible in existing residential power systems with no or a little upgrade. Sortomme et al., developed an algorithm to maximize profit from EV charging in a unidirectional V2G system where an aggregator is present to manage the charging [146]. Table 31 summarizes the algorithms presented in this section.

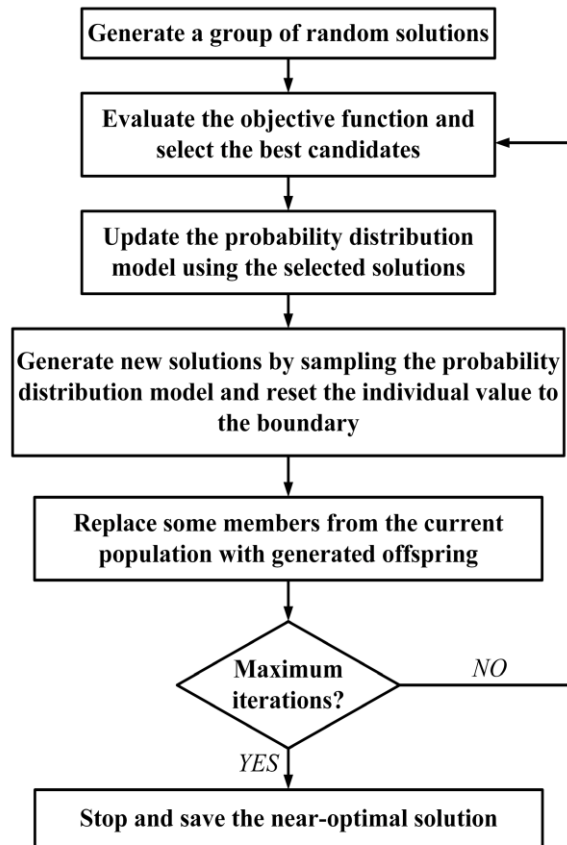


Figure 73. Intelligent charging algorithm proposed by Su et al., for a municipal charging station [186].

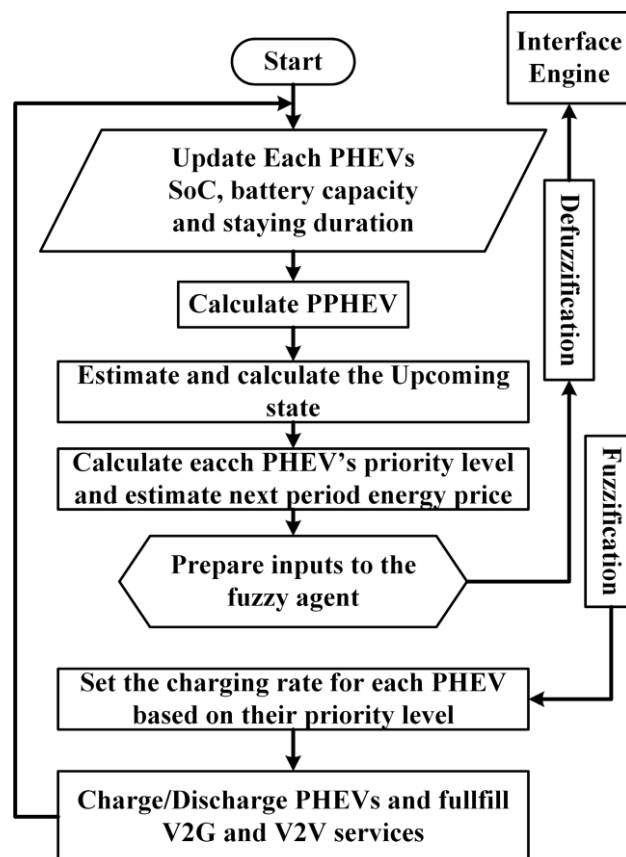


Figure 74. Flowchart of the management system proposed by Mohamed et al. [187].

Table 31. Summary of the control algorithms presented.

References	Algorithm Based on	Application
Magallan et al. [176]	<i>LuGre</i> dynamic friction model	Driving control system in rear-wheel-drive EV
Kang et al. [177]	Optimization-based control allocation strategy	Driving control system in four-wheel-drive EV
Tahami et al. [25]	Fuzzy logic	Driving control system in all-wheel-drive EV
Wang et al. [178]	Proportional-integral (PI) closed loop control system	Driving control system in in-wheel-drive EV
Nam et al. [179]	Extended Kalman filtering (EKF) method	Driving control system in in-wheel-drive EV
Zhou et al. [180]	Particle filter and multi-model data fusion	SOC measurement for lithium polymer batteries
Moura et al. [175]	Markov process	Power splitting in mid-sized sedan PHEV
Hui et al. [181]	Torque control strategy	Heavy hybrid vehicles using a single energy source
Chen et al. [182]	Quadratic programming	Reduction of fuel consumption by effective battery current control
Li et al. [183]	Fuzzy logic	Attaining maximum fuel efficiency without excess discharging of battery
Yuan et al. [184]	Dynamic Programming and Pontryagin's Minimum Principle	Efficient energy management in parallel HEV using Automatic Manual Transmission or AMT
Bernard et al. [185]	Non-causal optimization algorithm	Reduction of hydrogen consumption in FCEV
Geng et al. [174]	Equivalent consumption minimization strategy (ECMS)	Energy management in PHEV employing microturbine
Su et al. [186]	Estimation of distribution (EDA) algorithm	Intelligent charging of large fleet of PHEVs docked at a municipal charging station
Deilami et al. [140]	Maximum sensitivities selection (MSS) optimization	Load management system for intelligent charging
Mohamed et al. [187]	Fuzzy controller	V2G system for EV charging parks incorporating renewable generation
Geng et al. [120]	Pontryagin's minimum principle, fuzzy logic	Load shifting while charging EVs in the distribution network
Richardson et al. [116]	Linear programming	Enabling high EV penetration in existing residential power system network
Sortomme et al [146]	Preferred operating point (POP) algorithm	Maximizing profit from EV charging through an aggregator

12. Global EV Sales Figures

The electric vehicle market is growing much faster than the conventional vehicle market, and in some regions EVs are catching up with ICE vehicles in terms of the number of units sold. China has become the largest market for EVs, its market claiming 35.4% of the worldwide EV scene in 2017, an exorbitant rise from the mere 6.3% in 2013 [188]. Chinese consumers bought a world-topping 24.38 million passenger electric vehicles in 2016. China has the greatest number of manufacturers, led by BYD autos, which sold 96,000 EVs in 2016. This drive in China is fueled by government initiatives adopted to promote EV use to mitigate the country's serious air pollution. However, the majority of Chinese vehicles are in the \$36,000 range and offers limited range, but high-end vehicles manufacturing is on the rise in China too. This huge market has attracted major carmakers all over the world—Ford, Volkswagen, Volvo, and General Motors—who have their own EVs in the Chinese market and are poised to introduce more models in the coming years [189]. Figure 75 shows the ten highest selling EVs in China in 2016.

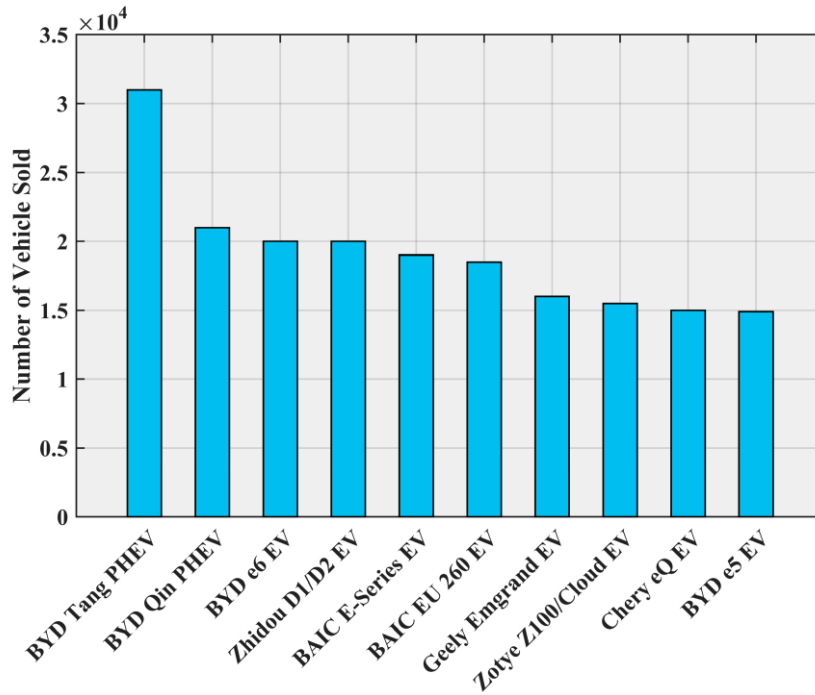


Figure 75. Top ten EVs in China in 2016 according to the number of units sold. Data from [190].

From a global perspective, sales of EV grew by 36% in the USA; Europe saw a growth of 13%, while Japan observed a decrease of 11% in the same period. BYD dominated the global market with a 13.2% share, followed by Tesla in second place (9.9%); the other major contributors can be listed as Volkswagen Group, BMW Group, Nissan, BAIC, and Zoyte. However, the Tesla Model S remained the best-selling EV in 2016 with 50,935 units sold, followed by the Nissan Leaf EV with 49,818 units [191]. The top ten best-selling vehicles around the globe in shown in Figure 76.

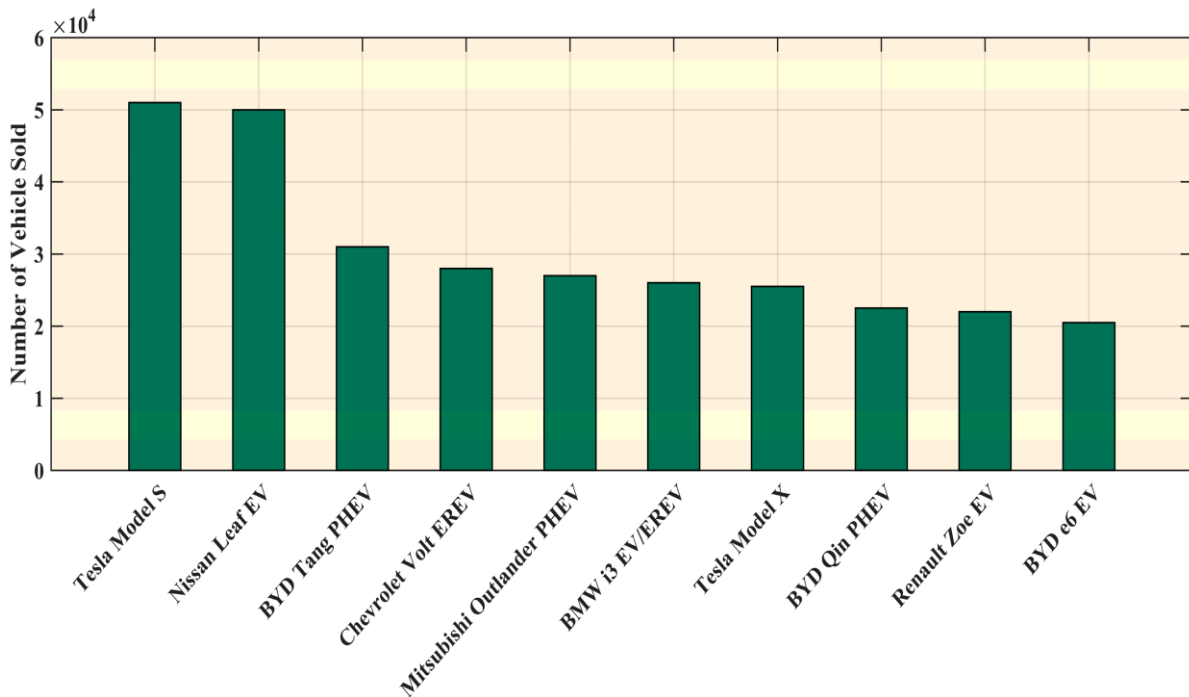


Figure 76. Top ten best-selling EVs globally in 2016. Data from [191].

The American market was dominated predictably by the Tesla Model S in 2016, 28,821 of these were sold; Chevrolet Volt EREV sold 24,739 units, thus securing the second place. The third place

was achieved by another Tesla, the Model X; 18,192 of these SUVs were sold in 2016 [192]. The ten best-selling EVs in the USA in 2016 are shown in Figure 77.

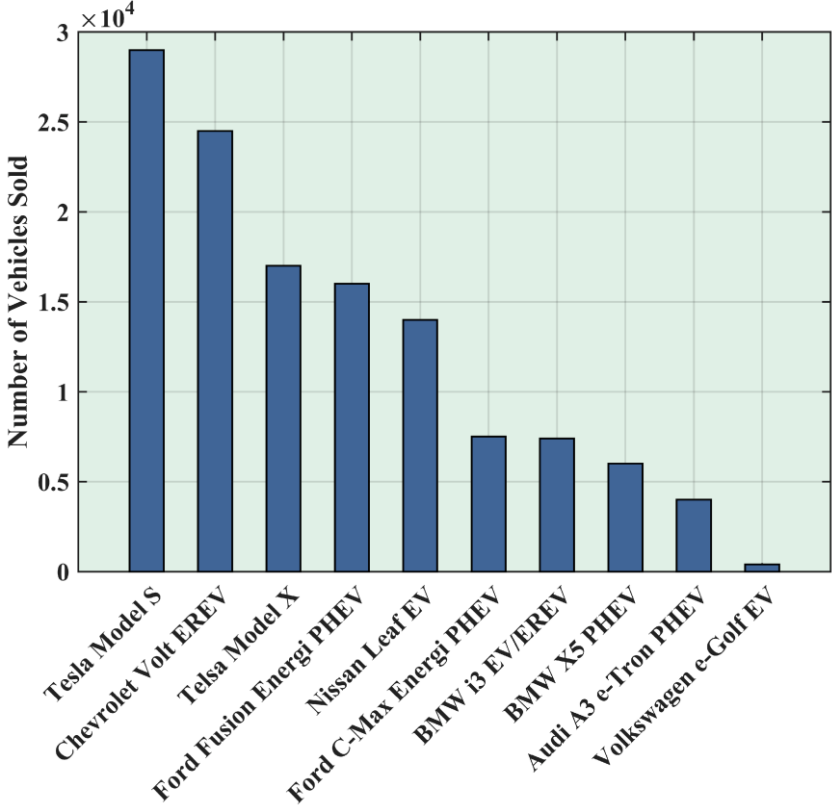


Figure 77. Top ten best-selling EVs in the USA in 2016. Data from [192].

The Renault Zoe was the best-selling BEV in Europe in 2016, with 21,338 units sold, followed by the Nissan Leaf with 18,614 units. In the PHEV segment, the Mitsubishi Outlander PHEV was the market leader in Europe in 2016, with 21,333 units sold; the Volkswagen Passat GTE held the second position with 13,330 units [193]. Figures 78 and 79 shows the BEV and PHEV market shares in Europe in 2016.

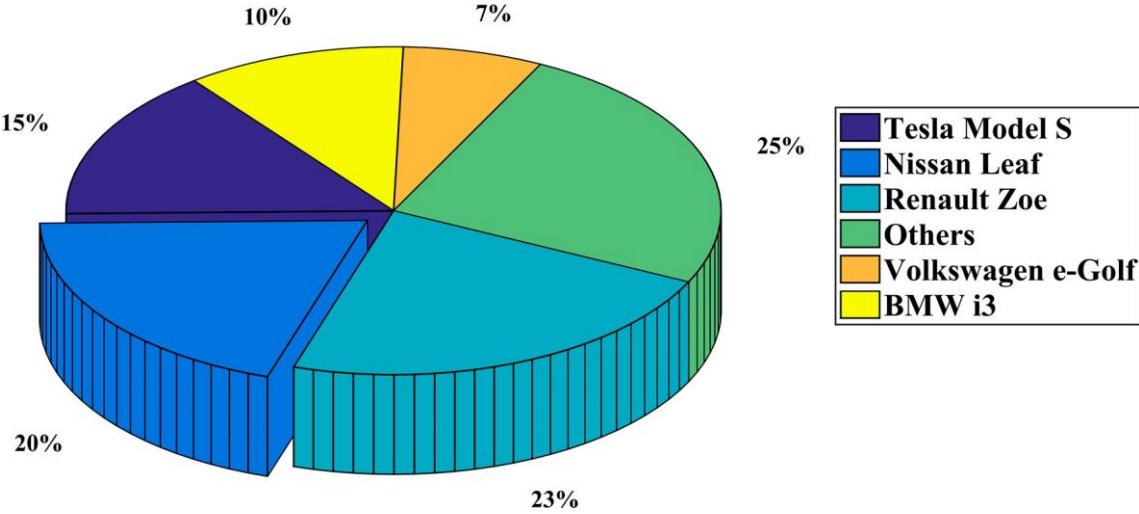


Figure 78. BEV market shares in Europe in 2016. Data from [193].

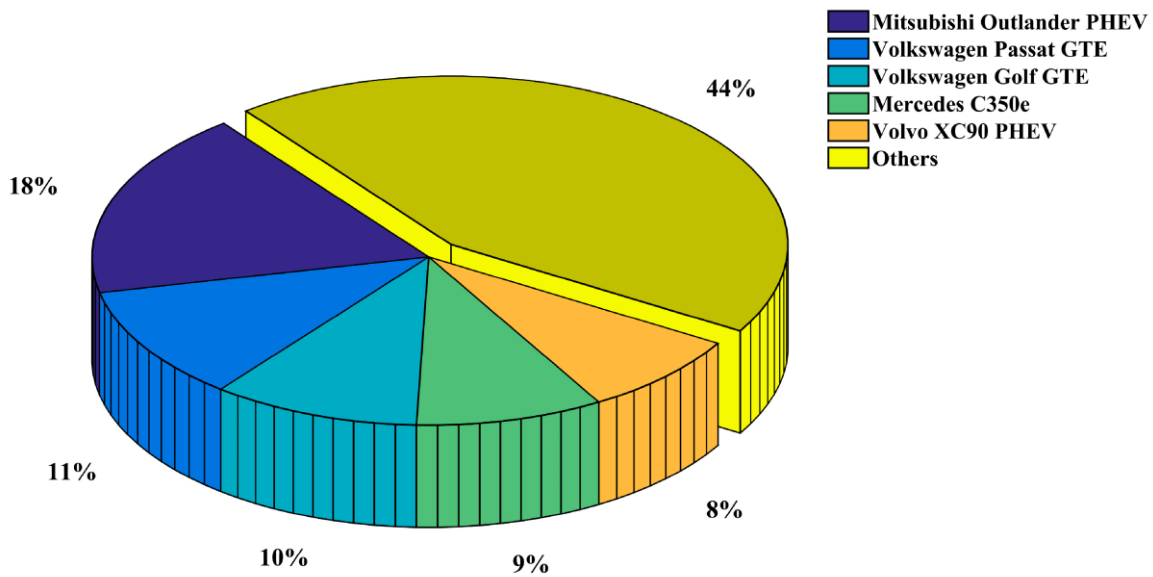


Figure 79. PHEV market shares in Europe in 2016. Data from [193].

13. Trends and Future Developments

The adoption of EVs has opened doors for new possibilities and ways to improve both the vehicles and the systems associated with it, the power system, for example. EVs are being considered as the future of vehicles, whereas the smart grid appears to be the grid of the future [194,195]. V2G is the link between these two technologies and both get benefitted from it. With V2G comes other essential systems required for a sustainable EV scenario—charge scheduling, VPP, smart metering etc. The existing charging technologies have to improve a lot to make EVs widely accepted. The charging time has to be decreased extensively for making EVs more flexible. At the same time, chargers and EVSEs have to be able to communicate with the grid for facilitating V2G, smart metering, and if needed, bidirectional charging [23]. Better batteries are a must to take the EV technology further. There is a need for batteries that use non-toxic materials and have higher power density, less cost and weight, more capacity, and needs less time to recharge. Though technologies better than Li-ion have been discovered already, they are not being pursued industrially because of the huge costs associated with creating a working version. Besides, Li-ion technology has the potential to be improved a lot more. Li-air batteries could be a good option to increase the range of EVs [23]. EVs are likely to move away from using permanent magnet motors which use rare-earth materials. The motors of choice can be induction motor, synchronous reluctance motor, and switched reluctance motor [23]. Tesla is using an induction motor in its models at present. Motors with internal permanent magnet may stay in use [23]. Wireless power transfer systems are likely to replace the current cabled charging system. Concepts revealed by major automakers adopted this feature to highlight their usefulness and convenience. The Rolls-Royce 103EX and the Vision Mercedes-Maybach 6 can be taken as example for that. Electric roads for wireless charging of vehicles may appear as well. Though this is not still viable, the situation may change in the future. Recent works in this sector includes the work of Electrode, an Israeli startup, which claims to be able to achieve this feat in an economic way. Vehicles that follow a designated route along the highway, like trucks, can get their power from overhead lines like trains or trams. It will allow them to gather energy as long as their route resides with the power lines, then carry on with energy from on-board sources. Such a system has been tested by Siemens using diesel-hybrid trucks from Scania on a highway in Sweden [196]. New ways of recovering energy from the vehicle may appear. Goodyear has demonstrated a tire that can harvest energy from the heat generated there using thermo-piezoelectric material. There are also chances of solar-powered vehicles. Until now, these have not appeared useful as installed solar cells only manage to convert up to 20% of the input power [70]. Much research is going on to make the electronics and sensors in EVs more compact, rugged and cheaper—which in many cases are leading

to advanced solid state devices that can achieve these goals with promises of cheaper products if they can be mass-produced. Some examples can be the works on gas sensors [197], smart LED drivers [198], smart drivers for automotive alternators [199], advanced gearboxes [200], and compact and smart power switches to weather harsh conditions [201]. The findings of [202–208] may prove helpful for studies regarding fail-proof on-board power supplies for EVs. The future research topics will of course, revolve around making the EV technology more efficient, affordable, and convenient. A great deal of research has already been conducted on making EVs more affordable and capable of covering more distance: energy management, materials used for construction, different energy sources etc. More of such researches are likely to go on emphasizing on better battery technologies, ultracapacitors, fuel cells, flywheels, turbines, and other individual and hybrid configurations. FCVs may get significant attention in military and utility-based studies, whereas the in-wheel drive configuration for BEVs may be appealing to researchers focusing on better urban transport systems. Better charging technologies will remain a crucial research topic in near future. This is one of the areas the EV technology is lacking very badly; wireless charging technologies are very likely to attract more researchers' attention. A lot of research has already been done incorporating EVs and the grid: the challenges and possibilities that the EVs bring with them to the existing grid and also to the grid of the future. With more implementation of smart grids, distributed generation, and renewable energy sources, researches in these fields are likely to increase. And as researches in the entire aforementioned field's increase, exploration for better algorithms to run the systems is bound to rise. Figure 80 shows the major trends and sectors for future developments for EVs.

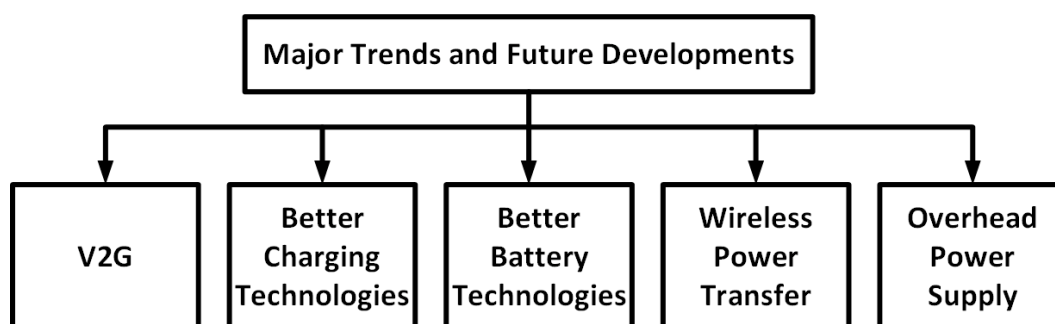


Figure 80. Major trends and sectors for future developments for EV.

14. Outcomes

The goal of this paper is to focus on the key components of EV. Major technologies in different sections are reviewed and the future trends of these sectors are speculated. The key findings of this paper can be summarized as follows:

- EVs can be classified as BEV, HEV, PHEV, and FCEV. BEVs and PHEVs are the current trends. FCEVs can become mainstream in future. Low cost fuel cells are the main prerequisite for that and there is need of more research to make that happen. There are also strong chances for BEVs to be the market dominators with ample advancement in key technologies; energy storage and charging systems being two main factors. Currently FCVs appear to have little chance to become ubiquitous, these may find popularity in niche markets, for example, the military and utility vehicles.
- EVs can be front wheel drive, rear wheel drive, even all-wheel drive. Different configurations are applied depending on the application of the vehicle. The motor can also be placed inside the wheel of the vehicle which offers distinct advantages. This configuration is not commercially abundant now, and has scopes for more study to turn it into a viable product.
- The main HEV configurations are classified as series, parallel, and series-parallel. Current vehicles are using the series-parallel system mainly as it can operate in both battery-only and ICE-only modes, providing more efficiency and less fuel consumption than the other two systems.

- Currently EVs use batteries as the main energy source. Battery technology has gone through significant changes, the lead-acid technology is long gone, as is the NiMH type. Li-ion batteries are currently in use, but even they are not capable enough to provide the amount of energy required to appease the consumers suffering from 'range anxiety' in most cases. Therefore the main focus of research in this area has to be creating batteries with more capacity, and also with better power densities. Metal-air batteries can be the direction where the EV makers will head towards. Lithium-sulfur battery and advanced rechargeable zinc batteries also have potential to provide better EVs. Nevertheless, low cost energy sources will be sought after always as ESS cost is one of the major contributors to high EV cost.
- Ultracapacitors are considered as auxiliary power sources because of their high power densities. If coupled with batteries, ultracapacitors produce a hybrid ESS that can satisfy some requirements demanded from an ideal source. Flywheels are also being used, especially because of their compact build and capability to store and discharge power on demand. Fuel cells can also be used more in the future if FCVs gain popularity.
- Different types of motors can be employed for EV use. The prominent ones can be listed as induction motor, permanent magnet synchronous motor, and synchronous reluctance motor. Induction motors are being extensively used these days, they can also dominate in the future because of their independence on rare-earth material permanent magnets.
- EVs can be charged with AC or DC supply. There are different voltage levels and they are designated accordingly. Higher voltage levels provide faster charging. DC supplies negate the need for rectification from AC, which reduces delay and loss. However, with increased voltage level, the pressure on the grid increases and can give rise to harmonics as well as voltage imbalance in an unsupervised system. Therefore, there are ample chances of research in the field of mitigating the problems associated with high-voltage charging.
- Two charger configurations are mainly available now: CCS and CHAdeMO. These two systems are not compatible with each other and each has a number of automakers supporting them. Tesla also brought their own 'supercharger' system, which provides a faster charging facility. It is not possible to determine now which one of these will prevail, or if both will co-exist, technical study is needed to find out the most useful one of these configurations or ways to make them compatible with each other.
- Whatever the charging system is, the charging time is still very long. This is a major disadvantage that is thwarting the growth of the EV market. Extensive research is needed in this sector to provide better technologies that can provide much faster charging and can be compatible with the small time required to refill an ICE vehicle. Wireless charging is also something in need of research. With all the conveniences it promises, it is still not in a viable form to commercialize.
- EV impacts the environment, power system, and economy alongside the transportation sector. It shows promise to reduce the GHG emissions as well as efficient and economical transport solutions. At the same time, it can cause serious problems in the power system including voltage instability, harmonics, and voltage sag, but these shortcomings may be short-lived if smart grid technologies are employed. There are prospects of research in the areas of V2G, smart metering, integration of RES, and system stability associated with EV penetration.
- EVs employ different techniques to reduce energy loss and increase efficiency. Reducing the drag coefficient, weight reduction, regenerative braking, and intelligent energy management are some of these optimization techniques. Further research directions can be better aerodynamic body designs, new materials with less weight and desired strength, ways to generate and restore the lost energy.
- Different control algorithms have been developed for driving assist, energy management, and charging. There is lots of room left for more research into charging and energy management algorithms. With increased EV penetration in the future, demands for efficient algorithms are bound to increase.

15. Conclusions

EVs have great potential of becoming the future of transport while saving this planet from imminent calamities caused by global warming. They are a viable alternative to conventional vehicles that depend directly on the diminishing fossil fuel reserves. The EV types, configurations, energy sources, motors, power conversion and charging technologies for EVs have been discussed in detail in this paper. The key technologies of each section have been reviewed and their characteristics have been presented. The impacts EVs cause in different sectors have been discussed as well, along with the huge possibilities they hold to promote a better and greener energy system by collaborating with smart grid and facilitating the integration of renewable sources. Limitations of current EVs have been listed along with probable solutions to overcome these shortcomings. The current optimization techniques and control algorithms have also been included. A brief overview of the current EV market has been presented. Finally, trends and ways of future developments have been assessed followed by the outcomes of this paper to summarize the whole text, providing a clear picture of this sector and the areas in need of further research.

Acknowledgments: No funding has been received in support of this research work.

Author Contributions: All authors contributed for bringing the manuscript in its current state. Their contributions include detailed survey of the literatures and state of art which were essential for the completion of this review paper.

Conflicts of Interest: The authors declare no conflict of interest.

References

1. Yong, J.Y.; Ramachandramurthy, V.K.; Tan, K.M.; Mithulananthan, N. A review on the state-of-the-art technologies of electric vehicle, its impacts and prospects. *Renew. Sustain. Energy Rev.* **2015**, *49*, 365–385.
2. Camacho, O.M.F.; Nørgård, P.B.; Rao, N.; Mihet-Popa, L. Electrical Vehicle Batteries Testing in a Distribution Network using Sustainable Energy. *IEEE Trans. Smart Grid* **2014**, *5*, 1033–1042.
3. Camacho, O.M.F.; Mihet-Popa, L. Fast Charging and Smart Charging Tests for Electric Vehicles Batteries using Renewable Energy. *Oil Gas Sci. Technol.* **2016**, *71*, 13–25.
4. Chan, C.C. The state of the art of electric and hybrid vehicles. *Proc. IEEE* **2002**, *90*, 247–275.
5. Grunditz, E.A.; Thiringer, T. Performance Analysis of Current BEVs Based on a Comprehensive Review of Specifications. *IEEE Trans. Transp. Electr.* **2016**, *2*, 270–289.
6. SAE International. SAE Electric Vehicle and Plug-in Hybrid Electric Vehicle Conductive Charge Coupler. In *SAE Standard J1772*; Society of Automotive Engineers (SAE): Warrendale, PA, USA, 2010.
7. Yilmaz, M.; Krein, P.T. Review of battery charger topologies, charging power levels, and infrastructure for plug-in electric and hybrid vehicles. *IEEE Trans. Power Electr.* **2013**, *28*, 2151–2169.
8. Bayindir, K.Ç.; Gözükcük, M.A.; Teke, A. A comprehensive overview of hybrid electric vehicle: Powertrain configurations, powertrain control techniques and electronic control units. *Energy Convers. Manag.* **2011**, *52*, 1305–1313.
9. Marchesoni, M.; Vacca, C. New DC–DC converter for energy storage system interfacing in fuel cell hybrid electric vehicles. *IEEE Trans. Power Electron.* **2007**, *22*, 301–308.
10. Schaltz, E.; Khaligh, A.; Rasmussen, P.O. Influence of battery/ultracapacitor energy-storage sizing on battery lifetime in a fuel cell hybrid electric vehicle. *IEEE Trans. Veh. Technol.* **2009**, *58*, 3882–3891.
11. Kramer, B.; Chakraborty, S.; Kroposki, B. A review of plug-in vehicles and vehicle-to-grid capability. In Proceedings of the 34th IEEE Industrial Electronics Annual Conference, Orlando, FL, USA, 10–13 November 2008; pp. 2278–2283.
12. Williamson, S.S. Electric drive train efficiency analysis based on varied energy storage system usage for plug-in hybrid electric vehicle applications. In Proceedings of the IEEE Power Electronics Specialists Conference, Orlando, FL, USA, 17–21 June 2007; pp. 1515–1520.
13. Wirasingha, S.G.; Schofield, N.; Emadi, A. Plug-in hybrid electric vehicle developments in the US: Trends, barriers, and economic feasibility. In Proceedings of the IEEE Vehicle Power and Propulsion Conference, Harbin, China, 3–5 September 2008; pp. 1–8.
14. Gao, Y.; Ehsani, M. Design and control methodology of plug-in hybrid electric vehicles. *IEEE Trans. Ind. Electron.* **2010**, *57*, 633–640.

**QUESTION BANK
PART - A**

Q.No	Questions	CO (L)
1.	List the type of EV system	CO2(L4)
2.	Justify why voltage equalizers are used in Battery.	CO2(L5)
3.	Compare the operational difference in resistive and capacitive voltage equalizer?	CO2(L4)
4.	Compare HEV and PHEV	CO2(L4)
5.	Discover the exclusive feature of ultra-capacitor from its operation.	CO2(L4)
6.	Justify why brushed DC motor not preferred for EV?	CO2(L5)
7.	Formulate Why PMSM is used in IWD vehicle	CO2(L6)
8.	Distinguish Compare AWD and IWD	CO2(L4)
9.	Compose the Reasons for squirrel cage rotor induction motors are preferred for EV?	CO2(L4)
10.	Justify why SRM called singly excited and doubly salient?	CO2(L5)
11.	Discover the feature of FCEV from its operation.	CO2(L4)
12.	Discuss the operation of three cruising mode of operation in HEV and compare with braking operation.	CO2(L6)

PART- B

Q.No	Questions	CO (L)
1.	With the help of a neat block diagram explain the different subsystem of electric vehicle. Also illustrate six different configurations of electric vehicle.	CO2(L4)
2.	Explain the fuel cell and flywheel as energy source elements in electric vehicle.	CO2(L4)
3.	Explain the battery and ultracapacitor as energy source elements in electric vehicle.	CO2(L4)
4.	Explain the operation any three converters for wired charging of electric vehicle.	CO2(L4)
5.	Compose comparative analysis of different motors are used in electric vehicle.	CO2(L4)
6.	Justify why voltage equalizers are used in Battery. Explain the operation of inductive voltage equalizer with neat sketch.	CO2(L4)



SATHYABAMA

INSTITUTE OF SCIENCE AND TECHNOLOGY
(DEEMED TO BE UNIVERSITY)

Accredited "A" Grade by NAAC | 12B Status by UGC | Approved by AICTE

www.sathyabama.ac.in

SCHOOL OF ELECTRICAL AND ELECTRONICS ENGINEERING

DEPARTMENT OF ELECTRICAL AND ELECTRONICS ENGINEERING

UNIT – III - Electric Vehicle – SEE1628/SEEA3028

Series Hybrid Electric Drive Train Design-Sizing of the Major Components- The Hybrid Electric Vehicle-
Energy Use in Conventional Vehicles-Energy Savings Potential of Hybrid Drive trains-HEV Configurations-
Series Hybrid System-Parallel Hybrid System-Series-Parallel System-Complex Hybrid System.

1. Hybrid Electric Vehicle (HEV)

What exactly is an HEV? The definition available is so general that it anticipates future technologies of energy sources. The term *hybrid vehicle* refers to a vehicle with at least two sources of power. A *hybrid-electric vehicle* indicates that *one source of power* is provided by an *electric motor*. The *other source of motive power* can come from a number of different technologies, but is typically provided by an *internal combustion engine* designed to run on either gasoline or diesel fuel. As proposed by Technical Committee (Electric Road Vehicles) of the International Electrotechnical Commission, *an HEV is a vehicle in which propulsion energy is available from two or more types of energy sources and at least one of them can deliver electrical energy*. Based on this general definition, there are many types of HEVs, such as:

- the gasoline ICE and battery
- diesel ICE and battery
- battery and FC
- battery and capacitor
- battery and flywheel
- battery and battery hybrid

Most commonly, the propulsion force in HEV is provided by a combination of electric motor and an ICE. The electric motor is used to improve the energy efficiency (improves fuel consumption) and vehicular emissions while the ICE provides extended range capability.

2. Energy Use in Conventional Vehicles

In order to understand how a HEV may save energy, it is necessary first to examine how conventional vehicles use energy. The breakdown of energy use in a vehicle is as follows:

- In order to maintain movement, vehicles must produce power at the wheels to overcome:
 - a. aerodynamic drag (air friction on the body surfaces of the vehicle, coupled with pressure forces caused by the air flow)
 - b. rolling resistance (the resistive forces between tires and the road surface)
 - b. resistive gravity forces associated with climbing a grade
- Further, to accelerate, the vehicle must overcome its inertia. Most of the energy

expended in acceleration is then lost as heat in the brakes when the vehicle is brought to a stop.

- The vehicle must provide power for accessories such as heating fan, lights, power steering, and air conditioning.
- Finally, a vehicle will need to be capable of delivering power for acceleration with very little delay when the driver depresses the accelerator, which may necessitate keeping the power source in a standby (energy-using) mode.

A conventional engine-driven vehicle uses its engine to translate fuel energy into shaftpower, directing most of this power through the drivetrain to turn the wheels. Much of the heat generated by combustion cannot be used for work and is wasted, both because heat engines have theoretical efficiency limit. Moreover, it is impossible to reach the theoretical efficiency limit because:

- some heat is lost through cylinder walls before it can do work
- some fuel is burned at less than the highest possible pressure
- fuel is also burned while the engine is experiencing negative load (during braking) or when the vehicle is coasting or at a stop, with the engine idling.

Although part of engine losses would occur under any circumstances, part occurs because in conventional drivetrains, engines are sized to provide very high levels of

peak power for the acceleration capability expected by consumers, about 10 times the power required to cruise at 100Km/h. However, the engines are operated at most times at a small fraction of peak power and at these operating points they are quite inefficient.

Having such a large engine also increases the amount of fuel needed to keep the engine operating when the vehicle is stopped or during braking or coasting, and increases losses due to the added weight of the engine, which increases rolling resistance and inertial losses. Even gradeability requirements (example: 55 mph up a 6.5% grade) require only about 60 or 70% of the power needed to accelerate from 0 to 100Km/h in under 12 seconds.

The **Figure 1** shows the translation of fuel energy into work at the wheels for a typical midsize vehicle in urban and highway driving. From **Figure 1** it can be observed that:

- At best, only 20% of the fuel energy reaches the wheels and is available to overcome the tractive forces, and this is on the highway when idling losses are at a minimum, braking loss is infrequent, and shifting is far less frequent.
- Braking and idling losses are extremely high in urban driving and even higher in more congested driving, e.g., within urban cores during rush hour. Braking loss represents 46% of all tractive losses in urban driving. Idling losses represent about one sixth of the fuel energy on this cycle.
- Losses to aerodynamic drag, a fifth or less of tractive losses in urban driving, are more than half of the tractive losses during highway driving.

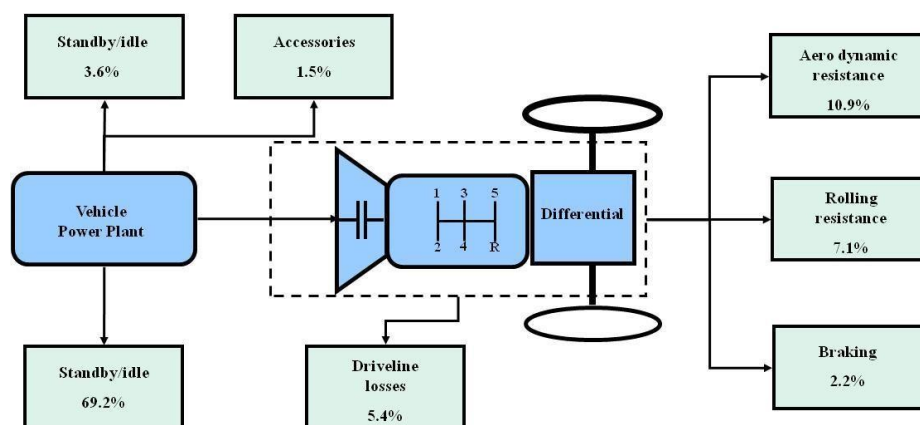


Figure 1: Translation of fuel energy into work in a vehicle

3. Energy Savings Potential of Hybrid Drivetrains

In terms of overall energy efficiency, the conceptual advantages of a hybrid over a conventional vehicle are:

- **Regenerative braking.** A hybrid can capture some of the energy normally lost as heat to the mechanical brakes by using its electric drive motor(s) in generator mode to brake the vehicle
- **More efficient operation of the ICE, including reduction of idle.** A hybrid can avoid some of the energy losses associated with engine operation at speed and load combinations where the engine is inefficient by using the energy storage device to either absorb part of the ICE's output or augment it or even substitute for it. This allows the ICE to operate only at speeds and loads where it is most efficient. When an HEV is stopped, rather than running the engine at idle, where it is extremely inefficient, the control system may either shut off the engine, with the storage device providing auxiliary power (for heating or cooling the vehicle interior, powering headlights, etc.), or run the engine at a higher-than-idle (more efficient) power setting and use the excess power (over auxiliary loads) to recharge the storage device. When the vehicle control system can shut the engine off at idle, the drivetrain can be designed so that the drive motor also serves as the starter motor, allowing extremely rapid restart due to the motor's high starting torque.
- **Smaller ICE:** Since the storage device can take up a part of the load, the HEV's ICE can be down sized. The ICE may be sized for the continuous load and not for the very high short term acceleration load. This enables the ICE to operate at a higher fraction of its rated power, generally at higher fuel efficiency, during most of the driving.

There are counterbalancing factors reducing hybrids' energy advantage, including:

- **Potential for higher weight.** Although the fuel-driven energy source on a hybrid generally will be of lower power and weight than the engine in a conventional vehicle of similar performance, total hybrid weight is

likely to be higher than the conventional vehicle it replaces because of the added weight of the storage device, electric motor(s), and other components. This depends, of course, on the storage mechanism chosen, the vehicle performance requirements, and so forth.

- **Electrical losses.** Although individual electric drivetrain components tend to be quite efficient for one-way energy flows, in many hybrid configurations, electricity flows back and forth through components in a way that leads to cascading losses. Further, some of the components may be forced to operate under conditions where they have reduced efficiency. For example, like ICEs, most electric motors have lower efficiency at the low-speed, low-load conditions often encountered in city driving. Without careful component selection and a control strategy that minimizes electric losses, much of the theoretical efficiency advantage often associated with an electric drivetrain can be lost.

4. HEV Configurations

The various possible ways of combining the power flow to meet the driving requirements are:

- i. powertrain 1 alone delivers power
- ii. powertrain 2 alone delivers power
- iii. both powertrain 1 and 2 deliver power to load at the same time
- iv. powertrain 2 obtains power from load (regenerative braking)
- v. powertrain 2 obtains power from powertrain 1
- vi. powertrain 2 obtains power from powertrain 1 and load at the same time
- vii. powertrain 1 delivers power simultaneously to load and to powertrain 2
- viii. powertrain 1 delivers power to powertrain 2 and powertrain 2 delivers power to load
- ix. powertrain 1 delivers power to load and load delivers power to powertrain 2.

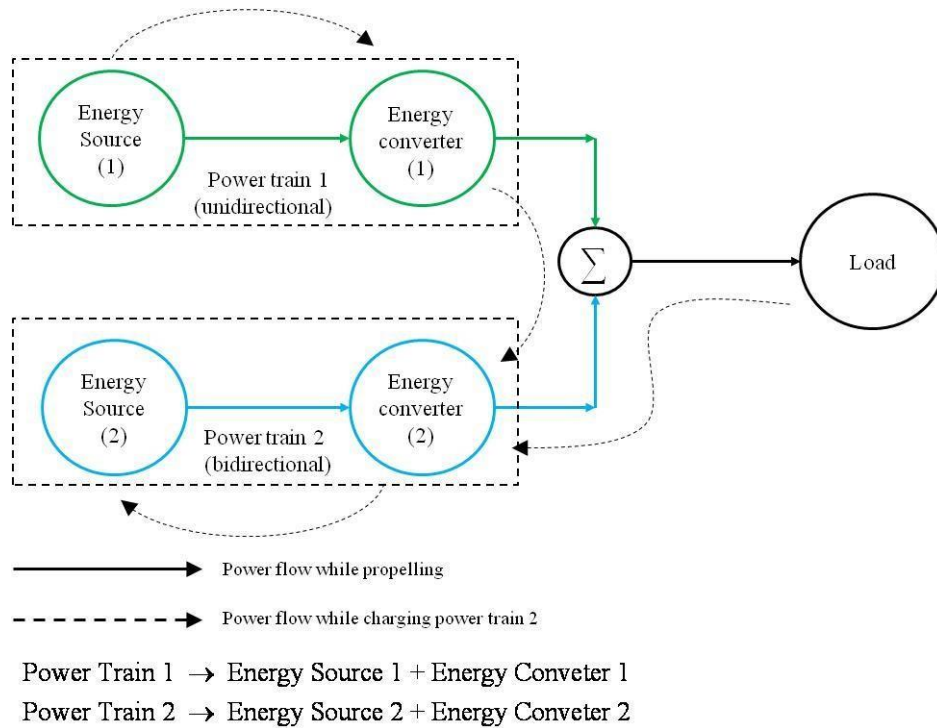


Figure 2: Generic Hybrid Drivetrain [1]

The load power of a vehicle varies randomly in actual operation due to frequent acceleration, deceleration and climbing up and down the grades. The power requirement for a typical driving scenario is shown in **Figure 3**. The load power can be decomposed into two parts:

- i. steady power, i.e. the power with a constant value
- ii. dynamic power, i.e. the power whose average value is zero

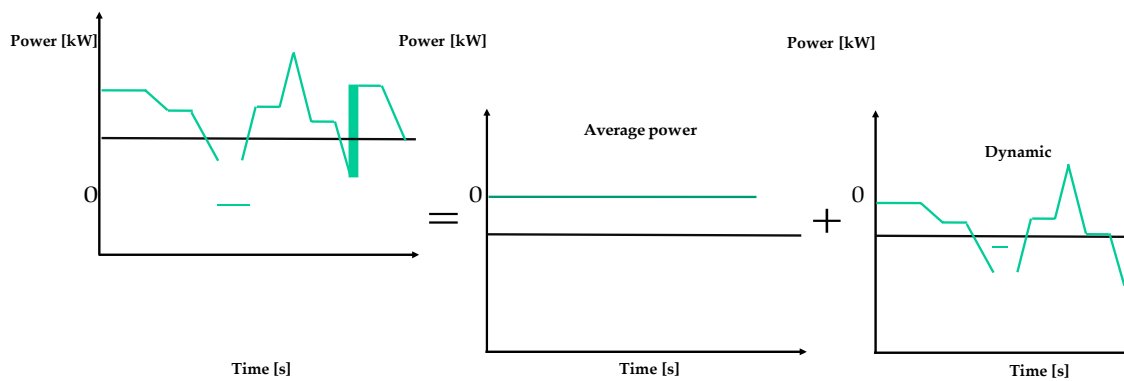


Figure 3: Load power decomposition

In HEV one powertrain favours steady state operation, such as an ICE or fuel cell. The other powertrain in the HEV is used to supply the dynamic power. The total energy output from the dynamic powertrain will be zero in the whole driving cycle. Generally, electric motors are used to meet the dynamic power demand. This hybrid drivetrain concept can be implemented by different configurations as follows:

- Series configuration
- Parallel configuration
- Series-parallel configuration
- Complex configuration

In **Figure 4** the functional block diagrams of the various HEV configurations is shown. From **Figure 4** it can be observed that the key feature of:

- series hybrid is to couple the ICE with the generator to produce electricity for pure electric propulsion.
- parallel hybrid is to couple both the ICE and electric motor with the transmission via the same drive shaft to propel the vehicle.

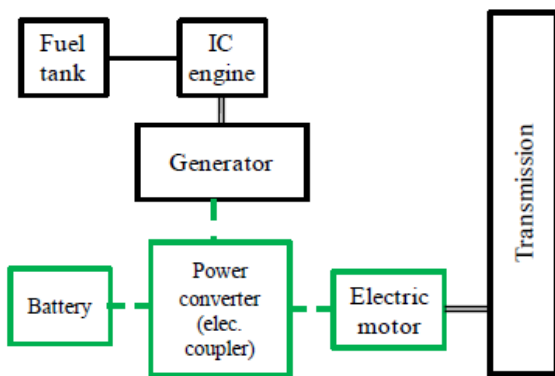


Figure 4a: Series hybrid [1]

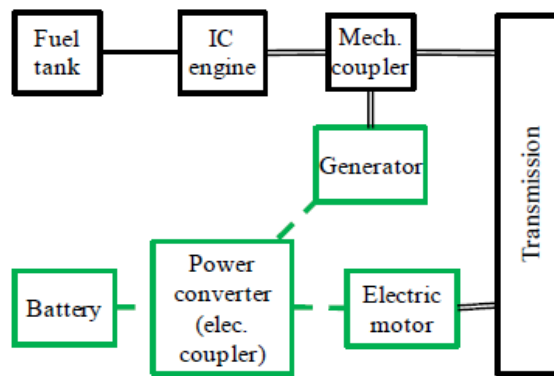


Figure 4b: Series-Parallel hybrid [1]

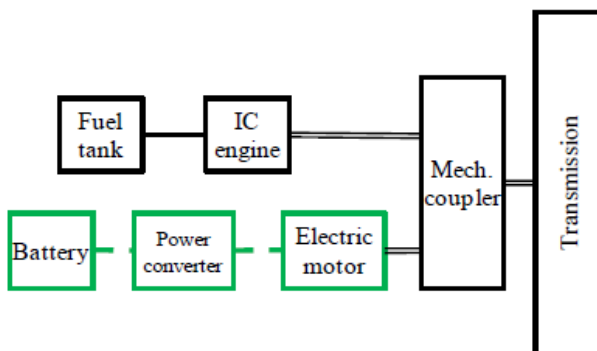


Figure 4c: Parallel hybrid [1]

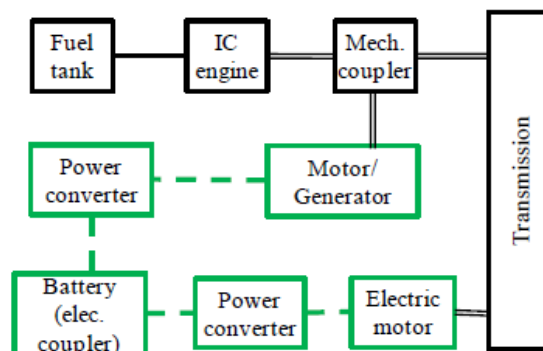


Figure 4d: Complex hybrid [1]

4.1 Series Hybrid System:

In case of series hybrid system (**Figure 4a**) the mechanical output is first converted into electricity using a generator. The converted electricity either charges the battery or can bypass the battery to propel the wheels via the motor and mechanical transmission. Conceptually, it is an ICE assisted Electric Vehicle (EV). The advantages of series hybrid drivetrains are:

- mechanical decoupling between the ICE and driven wheels allows the IC engine operating at its very narrow optimal region as shown in **Figure 5**.
- nearly ideal torque-speed characteristics of electric motor make multigear transmission unnecessary.

However, a series hybrid drivetrain has the following disadvantages:

- the energy is converted twice (mechanical to electrical and then to mechanical) and this reduces the overall efficiency.
- Two electric machines are needed and a big traction motor is required because it is the only torque source of the driven wheels.

The series hybrid drivetrain is used in heavy commercial vehicles, military vehicles and buses. The reason is that large vehicles have enough space for the bulky engine/generator system.

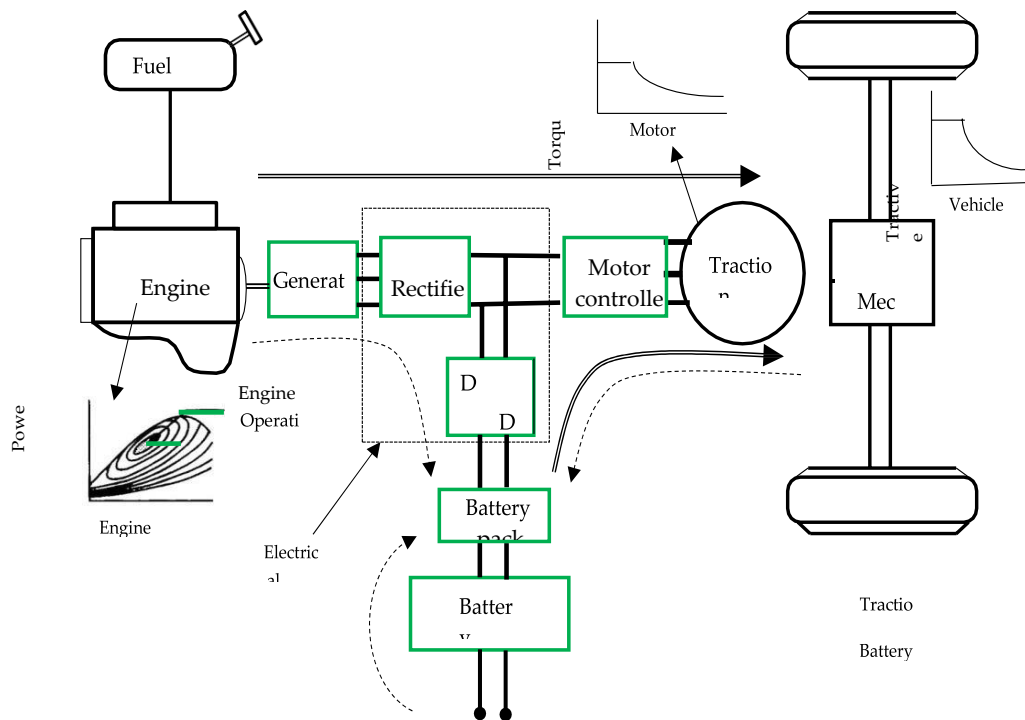


Figure 5: Detailed Configuration of Series Hybrid Vehicle [1]

4.1.1 Power Flow Control in Series Hybrid

In the series hybrid system there are four operating modes based on the power flow:

- **Mode 1:** During startup (**Figure 6a**), normal driving or acceleration of the series HEV, both the ICE and battery deliver electric energy to the power converter which then drives the electric motor and hence the wheels via transmission.
- **Mode 2:** At light load (**Figure 6b**), the ICE output is greater than that required to drive the wheels. Hence, a fraction of the generated electrical energy is used to charge the battery. The charging of the battery takes place till the battery capacity reaches a proper level.
- **Mode 3:** During braking or deceleration (**Figure 6c**), the electric motor acts as a generator, which converts the kinetic energy of the wheels into electricity and this, is used to charge the battery.
- **Mode 4:** The battery can also be charged by the ICE via the generator even when the vehicle comes to a complete stop (**Figure 6d**).

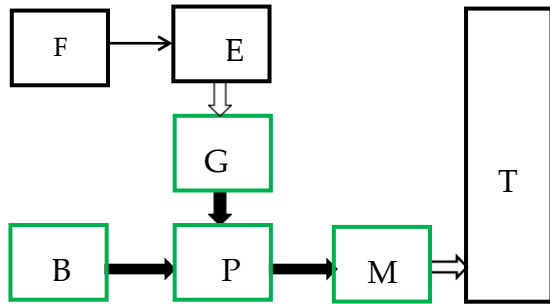


Figure 6a: Mode 1, normal driving or acceleration

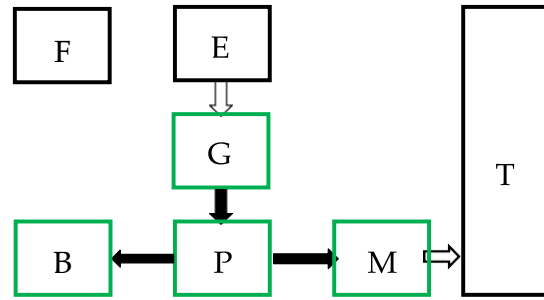


Figure 6b: Mode 2, light load

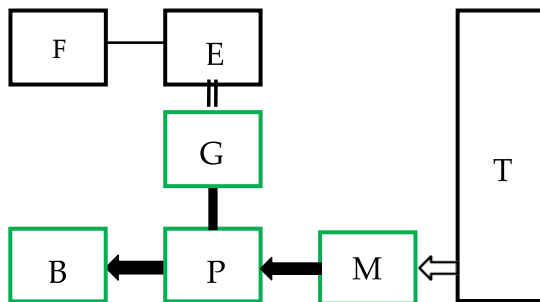


Figure 6c: Mode 3, braking or deceleration [1]

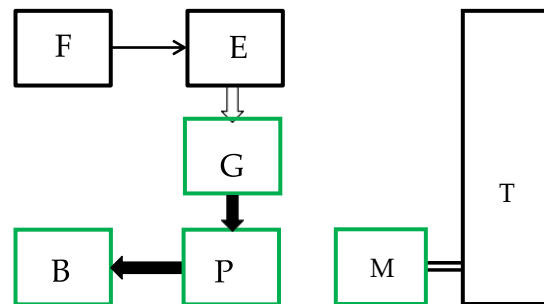


Figure 6d: Mode 4, vehicle at stop

B: Battery
 E: ICE
 F: Fuel tank
 G: Generator
 M: Motor
 P: Power Converter

— Electrical link
 — Hydraulic link
 = Mechanical link

4.2 Parallel Hybrid System:

The parallel HEV (**Figure 4b**) allows both ICE and electric motor (EM) to deliver power to drive the wheels. Since both the ICE and EM are coupled to the drive shaft of the wheels via two clutches, the propulsion power may be supplied by ICE alone, by EM only or by both ICE and EM. The EM can be used as a generator to charge the battery by regenerative braking or absorbing power from the ICE when its output is greater than that required to drive the wheels. The advantages of the parallel hybrid drivetrain are:

- both engine and electric motor directly supply torques to the driven wheels and no energy form conversion occurs, hence energy loss is less
 - compactness due to no need of the generator and smaller traction motor.
- The drawbacks of parallel hybrid drivetrains are:

- mechanical coupling between the engines and the driven wheels, thus the engine operating points cannot be fixed in a narrow speed region.
- The mechanical configuration and the control strategy are complex

compared to series hybrid drivetrain.

Due to its compact characteristics, small vehicles use parallel configuration. Most passenger cars employ this configuration.

4.2.1 Power Flow Control in Parallel Hybrid

The parallel hybrid system has four modes of operation. These four modes of operation are

- **Mode 1:** During start up or full throttle acceleration (**Figure 7**); both the ICE and the EM share the required power to propel the vehicle. Typically, the relative distribution between the ICE and electric motor is 80-20%.
- **Mode 2:** During normal driving (**Figure 7**), the required traction power is supplied by the ICE only and the EM remains in off mode.
- **Mode 3:** During braking or deceleration (**Figure 7**), the EM acts as a generator to charge the battery via the power converter.
- **Mode 4:** Under light load condition (**Figure 7**), the traction power is delivered by the ICE and the ICE also charges the battery via the EM.

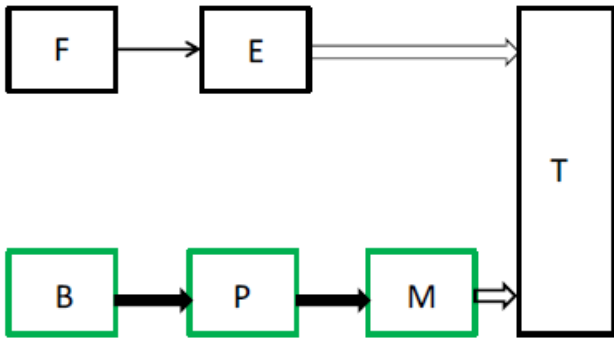


Figure 2a: Mode 1, start up

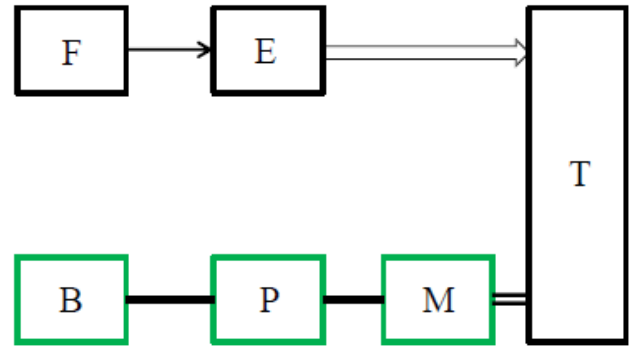


Figure 2b: Mode 2, normal driving

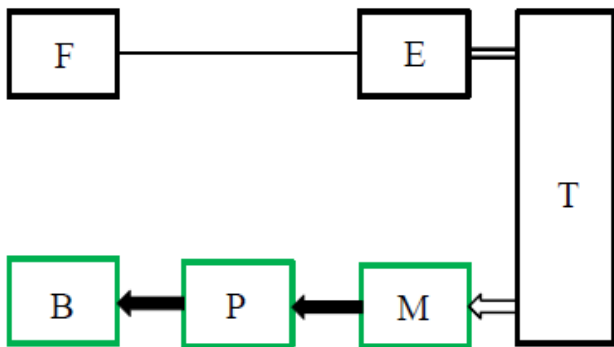


Figure 2c: Mode 3, braking or deceleration [1]

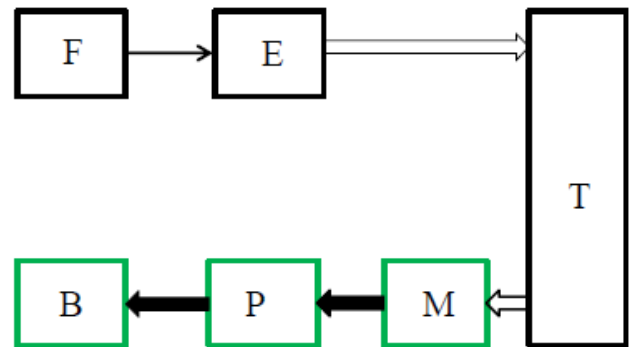


Figure 2d: Mode 4, light load

B: Battery
 E: ICE
 F: Fuel tank
 G: Generator
 M: Motor
 P: Power Converter

— Electrical link
 — Hydraulic link
 = Mechanical link

T: Transmission (including brakes, clutches and gears)

Figure.7 Mode diagram of Parallel hybrid system

4.3 Series-Parallel System

In the series-parallel hybrid, the configuration incorporates the features of both the series and parallel HEVs. However, this configuration needs an additional electric machine and a planetary gear unit making the control complex.

4.3.1 Power Flow Control Series-Parallel Hybrid

The series-parallel hybrid system involves the features of series and parallel hybrid systems. Hence, a number of operation modes are feasible. Therefore, these hybrid systems are classified into two categories: **the ICE dominated** and the **EM dominated**.

The various operating modes of **ICE dominated** system are:

- **Mode 1:** At startup (**Figure 8**), the battery solely provides the necessary power to propel the vehicle and the ICE remains in off mode.
- **Mode 2:** During full throttle acceleration (**Figure 8**), both the ICE and the EM share the required traction power.
- **Mode 3:** During normal driving (**Figure 8**), the required traction power is provided by the ICE only and the EM remains in the off state.
- **Mode 4:** During normal braking or deceleration (**Figure 8**), the EM acts as a generator to charge the battery.
- **Mode 5:** To charge the battery during driving (**Figure 8**), the ICE delivers the required traction power and also charges the battery. In this mode the EM acts as a generator.
- **Mode 6:** When the vehicle is at standstill (**Figure 8**), the ICE can deliver power to charge the battery via the EM

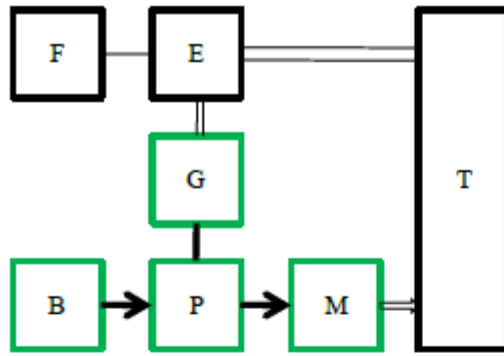


Figure 3a: Mode 1, start up [1]

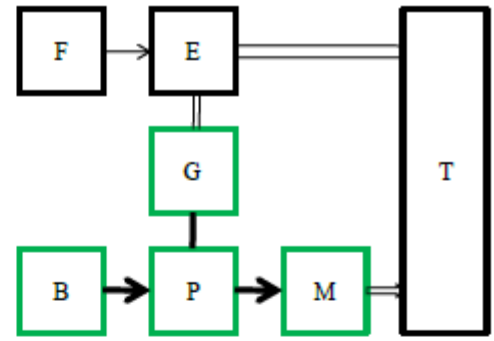


Figure 3b: Mode 2, acceleration [1]

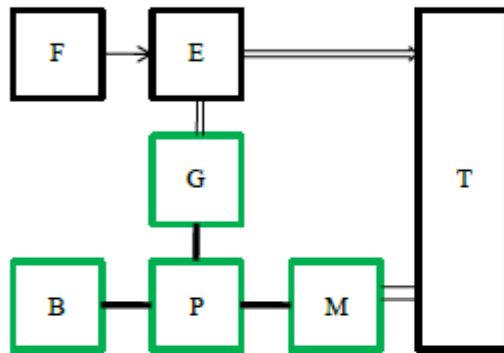


Figure 3c: Mode 3, normal drive [1]

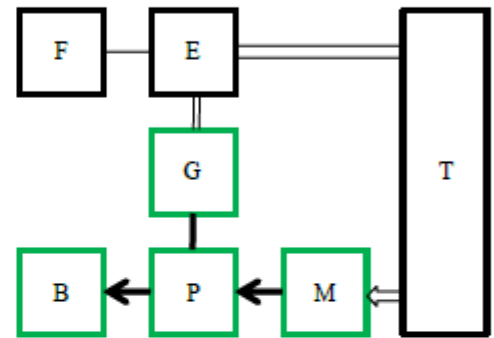


Figure 3d: Mode 4, braking or deceleration [1]

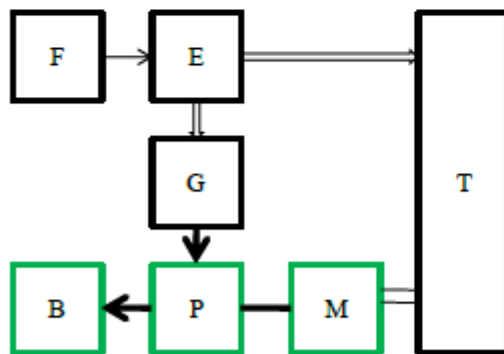


Figure 3e: Mode 5, battery charging during driving [1]

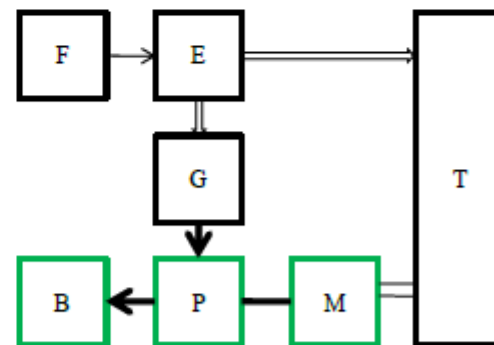


Figure 3f: Mode 6, battery charging during standstill [1]

B : Battery
 E : ICE
 F : Fuel Tank
 G : Generator
 M : Motor
 P : Power Converter
 T : Transmission(including brakes, clutches and gears)

— Electrical link
 — Hydraulic link
 = Mechanical link

Figure 8 series and parallel hybrid system with ICE dominated

The operating modes of **EM dominated** system are:

- **Mode 1:** During startup (**Figure 9**), the EM provides the traction power and the ICE remains in the off state.
- **Mode 2:** During full throttle (**Figure 9**), both the ICE and EM provide the traction power.
- **Mode 3:** During normal driving (**Figure 9**), both the ICE and EM provide the traction power.
- **Mode 4:** During braking or deceleration (**Figure 9**), the EM acts as a generator to charge the battery.
- **Mode 5:** To charge the battery during driving (**Figure 9**), the ICE delivers the required traction power and also charges the battery. The EM acts as a generator.
- **Mode 6:** When the vehicle is at standstill (**Figure 9**), the ICE can deliver power to charge the battery via the EM

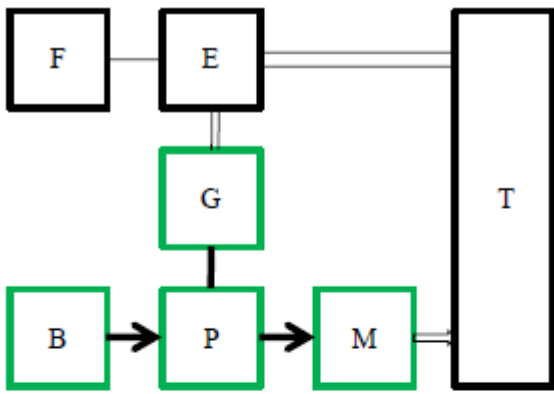


Figure 4a: Mode 1, start up [1]

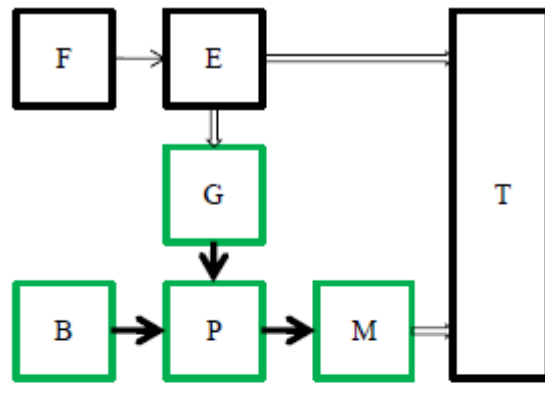


Figure 4b: Mode 2, acceleration [1]

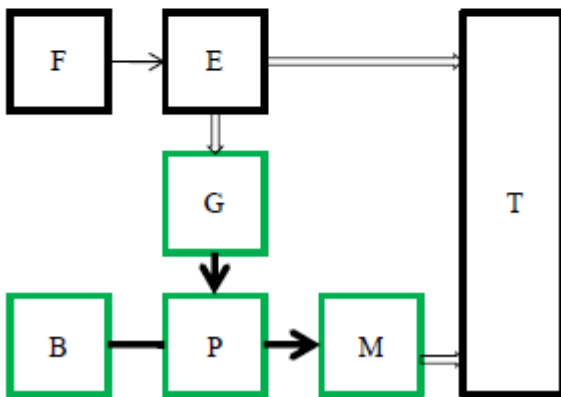


Figure 4c: Mode 3, normal drive [1]

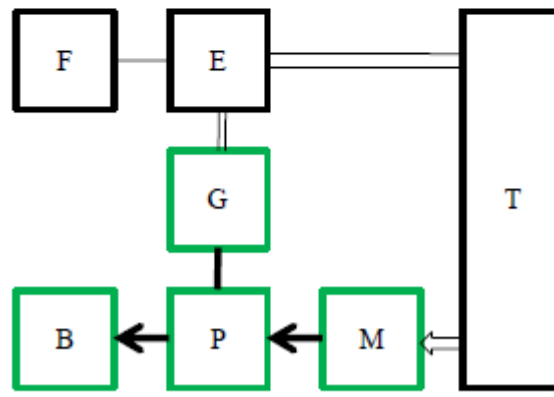


Figure 4d: Mode 4, braking or deceleration [1]

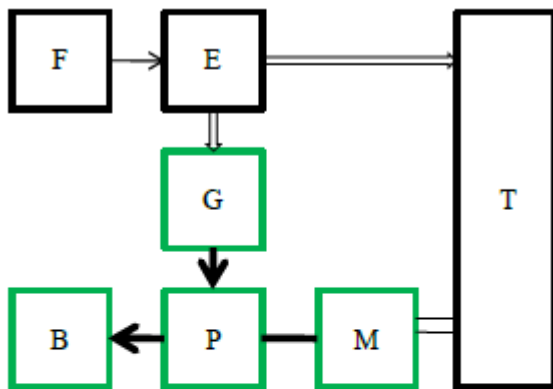


Figure 4e: Mode 5, battery charging during driving [1]

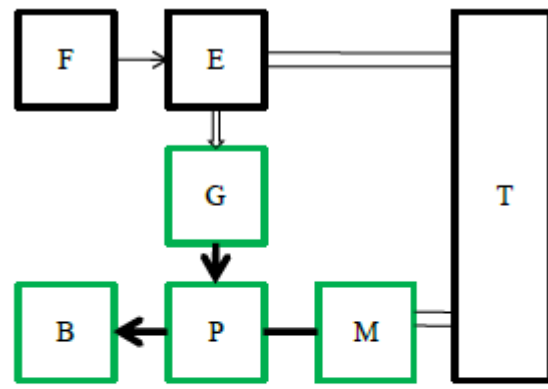


Figure 4f: Mode 6, battery charging during standstill [1]

B : Battery
 E : ICE
 F : Fuel Tank
 G : Generator
 M : Motor
 P : Power Converter
 T : Transmission(including brakes, clutches and gears)

— Electrical link
 — Hydraulic link
 — Mechanical link

Figure 9 series and parallel hybrid system with EM dominated

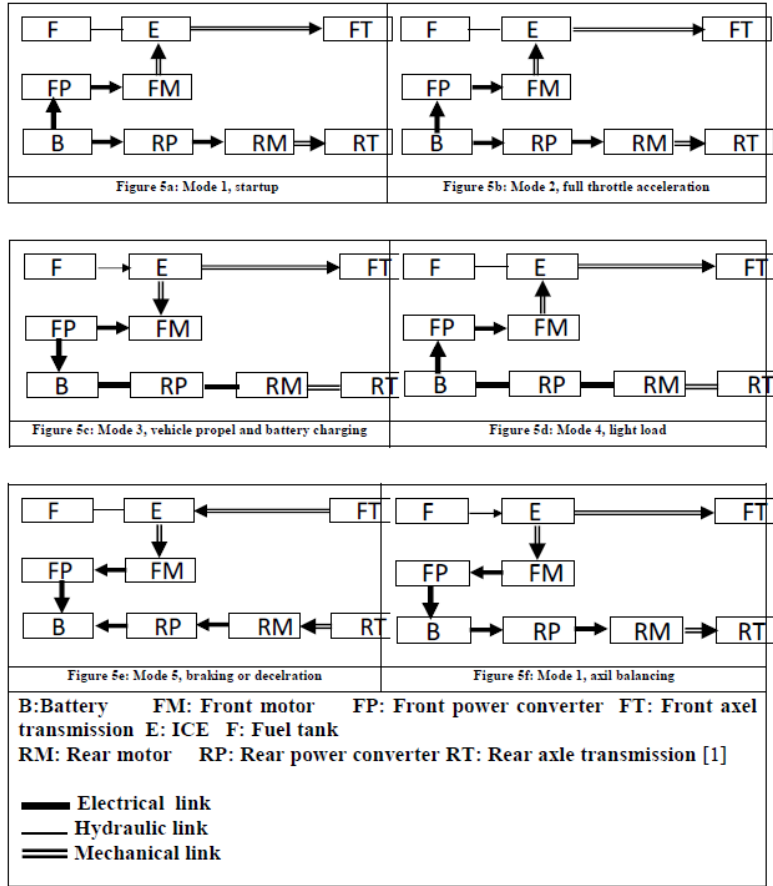
4.4 Complex Hybrid Control

The complex hybrid vehicle configurations are of two types:

- Front hybrid rear electric
- Front electric and rear hybrid

Both the configurations have six modes of operation:

- **Mode 1:** During startup (**Figure 10**), the required traction power is delivered by the EMs and the engine is in off mode.
- **Mode 2:** During full throttle acceleration (**Figure 10**), both the ICE and the front wheel EM deliver the power to the front wheel and the second EM delivers power to the rear wheel.
- **Mode 3:** During normal driving (**Figure 10**), the ICE delivers power to propel the front wheel and to drive the first EM as a generator to charge the battery.
- **Mode 4:** During driving at light load (**Figure 10**) first EM delivers the required traction power to the front wheel. The second EM and the ICE are in off state.
- **Mode 5:** During braking or deceleration (**Figure 10**), both the front and rear wheel EMs act as generators to simultaneously charge the battery.
- **Mode 6:** A unique operating mode of complex hybrid system is **axial balancing**. In this mode (**Figure 10**) if the front wheel slips, the front EM works as a generator to absorb the change of ICE power. Through the battery, this power difference is then used to drive the rear wheels to achieve the axle balancing.



**Figure.10 Mode diagram of Front hybrid
and rear electric**

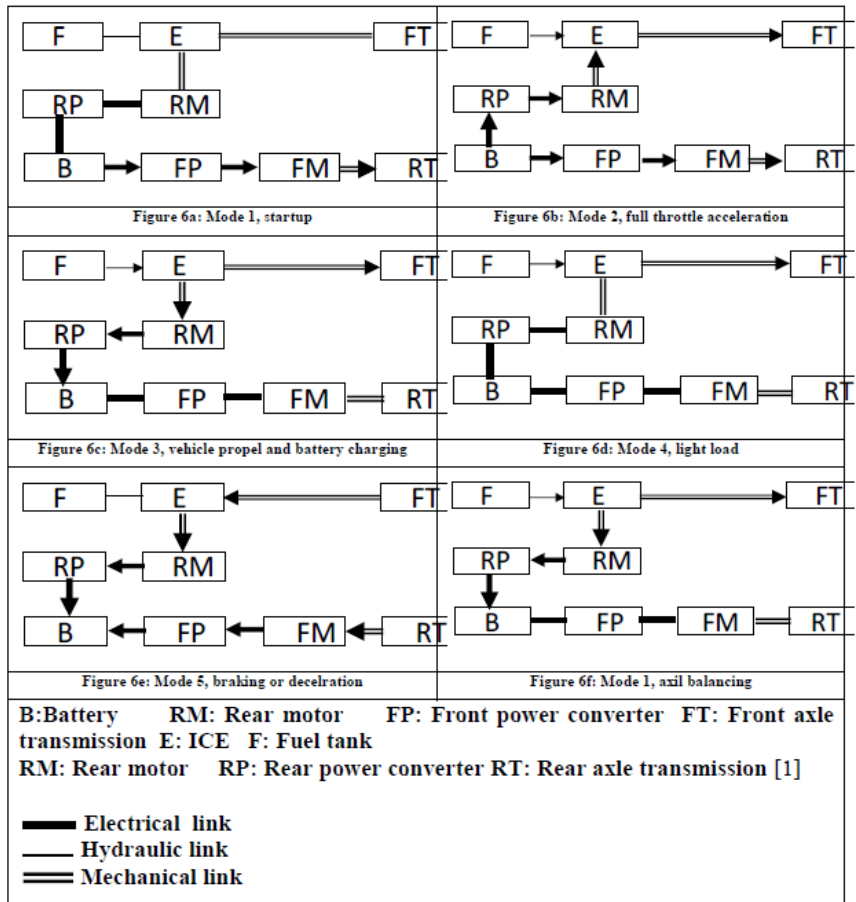


Figure.11 Mode diagram of Front hybrid and rear electric

4.5 Series Hybrid Electric Drive Train Design

The concept of a series hybrid electric drive train was developed from the electric vehicle drive train.¹ As mentioned in Chapter 4, electric vehicles, compared with conventional gasoline or diesel-fueled vehicles, have the advantages of zero mobile pollutant emissions, multienergy sources, and high efficiency. However, electric vehicles using present technologies have some disadvantages: a limited drive range due to the shortage of energy storage in the on-board batteries, limited payload and volume capacity due to heavy and bulky batteries, and a longer battery charging time. The initial objective of developing a series hybrid electric vehicle (S-HEV) was aimed at extending the drive range by adding an engine/alternator system to charge the batteries on-board.

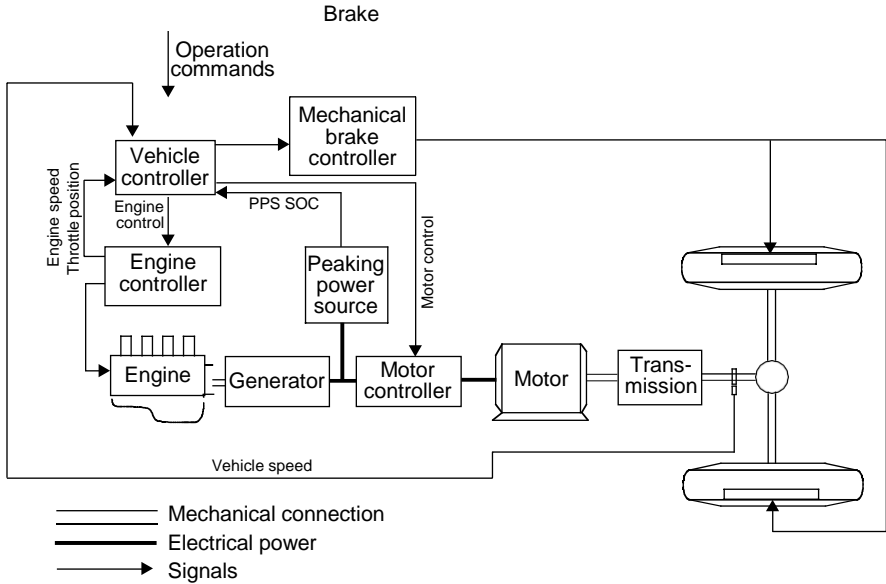


FIGURE. 12
Configuration of a typical series hybrid electric drive train

A typical series hybrid electric drive train configuration is shown in Figure 12. The vehicle is propelled by a traction motor. The traction motor is powered by a battery pack and/or an engine/generator unit. The engine/generator unit either helps the batteries to power the traction motor when load power demand is large or charges the batteries when load power demand is small. The motor controller is to control the traction motor to produce the power required by the vehicle.

Vehicle performance (acceleration, gradeability, and maximum speed) is completely determined by the size and characteristics of the traction motor drive. The determination of the size of the motor drive and gears of transmission is the same as in the electric vehicle design discussed in Chapter 4. However, the drive train control is essentially different from the pure electric drive train due to the involvement of an additional engine/generator unit. This chapter focuses on the design of the engine/alternator system, operation control strategy, and battery size design. Also, the term “peak power source” will replace “battery pack,” because, in HEVs, the major function of batteries is to supply peaking power. They can be replaced with other kinds of sources such as ultracapacitors and flywheels.

4.5.1 Operation Patterns

In series hybrid electric drive trains, the engine/generator system is mechanically decoupled from the driven wheels as shown in Figure 12.

The speed and torque of the engine are independent of vehicle speed and traction torque demand, and can be controlled at any operating point on its speed–torque plane.^{3,4} Generally, the engine should be controlled in such a way that it always operates in its optimal operation region, where fuel consumption and emissions of the engine are minimized (see Figure 13). Due to the mechanical decoupling of the engine from the drive wheels, this optimal engine operation is realizable. However, it heavily depends on the operating modes and control strategies of the drive train.

The drive train has several operating modes, which can be used selectively according to the driving condition and desire of the driver. These operating modes are:

1. Hybrid traction mode: When a large amount of power is demanded, that is, the driver depresses the accelerator pedal deeply, both engine/generator and peaking power source (PPS) supply their powers to the electric motor drive. In this case, the engine should be controlled to operate in its optimal region for efficiency and emission reasons as shown in Figure 7.2. The PPS supplies the additional power to meet the traction power demand. This operation mode can be expressed as

$$P_{demand} = P_{elg} + P_{pps} \tag{3.1}$$

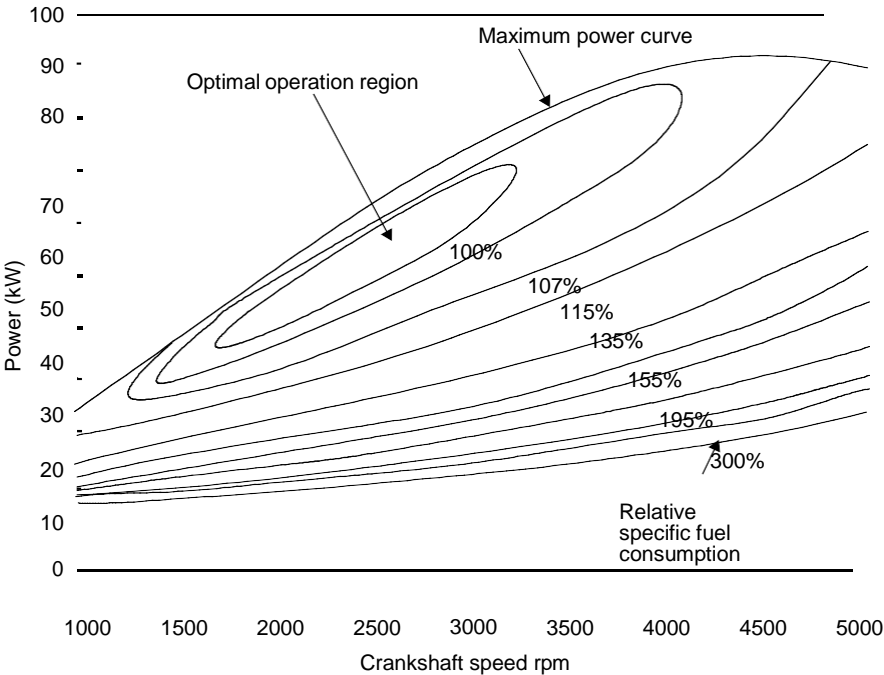


FIGURE 13
Example of engine characteristics and optimal operating region

where P_{demand} is the power demanded by the driver, $P_{e/g}$ is the engine/generator power, and P_{pps} is the PPS power.

2. Peak Power Source-Alone Traction Mode: In this operating mode, the peak power source alone supplies its power to meet the power demand, that is,

$$P_{demand} = P_{pps}. \quad (3.2)$$

3. Engine/Generator-Alone Traction Mode: In this operating mode, the engine/generator alone supplies its power to meet the power demand, that is,

$$P_{demand} = P_{e/g}. \quad (3.3)$$

4. PPS Charging from the Engine/Generator: When the energy in the PPS decreases to a bottom line, the PPS must be charged. This can be done by regenerative braking or by the engine/generator. Usually, engine/generator charging is needed, since regenerative braking charging is insufficient. In this case, the engine power is divided into two parts: one is used to propel the vehicle and the other is used to charge the PPS. That is,

$$P_{demand} = P_{e/g} - P_{pps}. \quad (3.4)$$

It should be noticed that the operation mode is only effective when the power of the engine/generator is greater than the load power demand.

5. Regenerative Braking Mode: When the vehicle is braking, the traction motor can be used as a generator, converting part of the kinetic energy of the vehicle mass into electric energy to charge the PPS.

As shown in Figure 12, the vehicle controller commands the operation of each component according to the traction power (torque) command from the driver, the feedback from each of the components, and also the drive train and the preset control strategy. The control objectives are to (1) meet the power demand of the driver, (2) operate each component with optimal efficiency, (3) recapture braking energy as much as possible, and (4) maintain the state-of-charge (SOC) of the PPS in a preset window.

4.6 Control Strategies

A control strategy is a control rule that is preset in the vehicle controller and commands the operating of each component. The vehicle controller receives

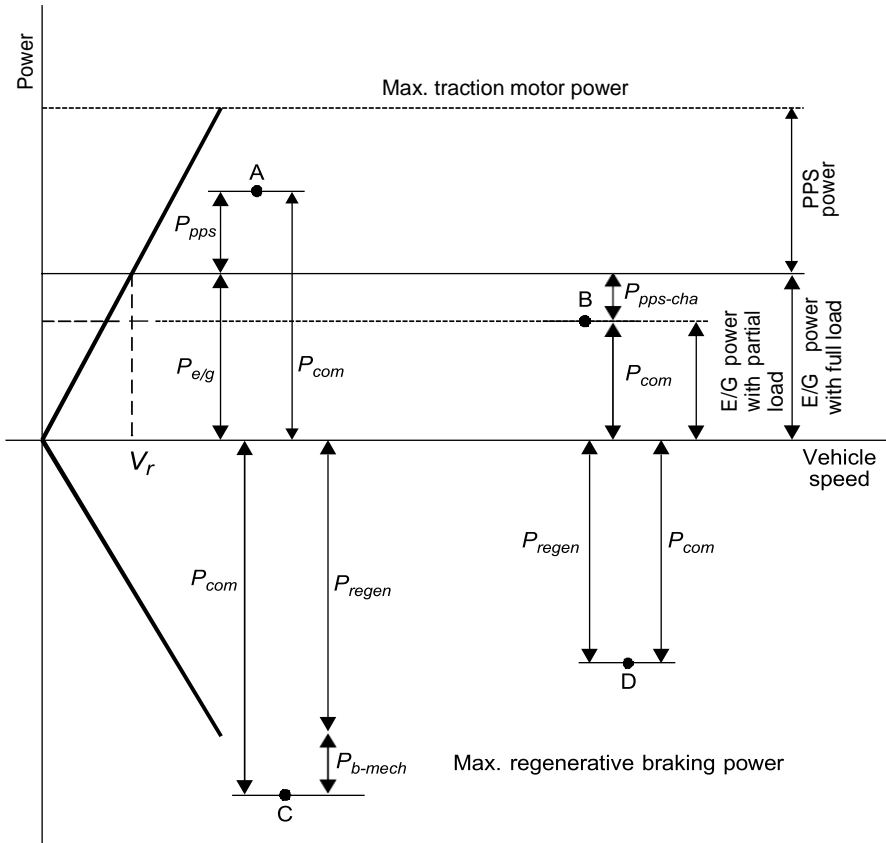
the operation commands from the driver and the feedback from the drive train and all the components, and then makes the decisions to use proper operation modes. Obviously, the performance of the drive train relies mainly on the control quality, in which the control strategy plays a crucial role.

In practice, there are a number of control strategies that can be used in a drive train for vehicles with different mission requirements. In this chapter, two typical control strategies are introduced: (1) maximum state-of-charge of peaking power source (Max. SOC-of-PPS) and (2) engine turn-on and turn-off (engine-on-off) control strategies.²

4.6.1 Max. SOC-of-PPS Control Strategy

The target of this control strategy is to meet the power demand commanded by the driver and, at the same time, maintain the SOC of the PPS at its high level. This control strategy is considered to be the proper design for vehicles for which the performance relies heavily on the peak power source. This includes vehicles with frequent stop-go driving patterns, and military vehicles for which carrying out their mission is the most important. A high SOC level will guarantee the high performance of the vehicles at any time.

The Max. SOC-of-PPS control strategy is depicted in Figure 14 in which points A, B, C, and D represent the power demands that the driver commands in either traction mode or braking mode. Point A represents the commanded traction power that is greater than the power that the engine/generator can produce. In this case, the PPS must produce its power to make up the power shortage of the engine/generator. Point B represents the commanded power that is less than the power that the engine/generator produces when operating in its optimal operation region (refer to Figure 13). In this case, two operating modes may be used, depending on the SOC level of PPS. If the SOC of the PPS is below its top line, the PPS charging mode is applied — that is, the engine/generator is operated within its optimal operating region and part of its power goes to the traction motor to propel the vehicle and the other part goes to the PPS. On the other hand, if the SOC of the PPS has already reached its top line, the engine/generator traction mode alone is supplied, that is, the engine/generator is controlled to produce power equal to the demanded power, and the PPS is set at idle. Point C represents the commanded braking power that is greater than the braking power that the motor can produce (maximum regenerative braking power). In this case, the hybrid braking mode is used, in which the electric motor produces its maximum braking power and the mechanical braking system produces the remaining braking power. Point D represents the commanded braking power that is less than the maximum braking power that the motor can produce. In this case, only regenerative braking is used. The control flowchart of Max. SOC-of-PPS is illustrated in Figure 15.



- A — Hybrid traction mode
 - P_{com} — Commanded power
 - P_{pps} — Power of the peaking power source
 - $P_{e/g}$ — Power of engine/generator
- B — Engine/generator-alone traction mode or PPS charging mode
 - $P_{pps-cha}$ — PPS charging power
- C — Hybrid braking mode
 - P_{regen} — Regenerative braking power
 - P_{b-mech} — Mechanical braking power
- D — Regenerative braking mode

FIGURE 14
Illustration of the Max. SOC-of-PPS control strategy

4.6.2 Thermostat Control Strategy (Engine-On-Off)

The Max. SOC-of-PPS control strategy emphasizes maintaining the SOC of the PPS at a high level. However, in some driving conditions such as long

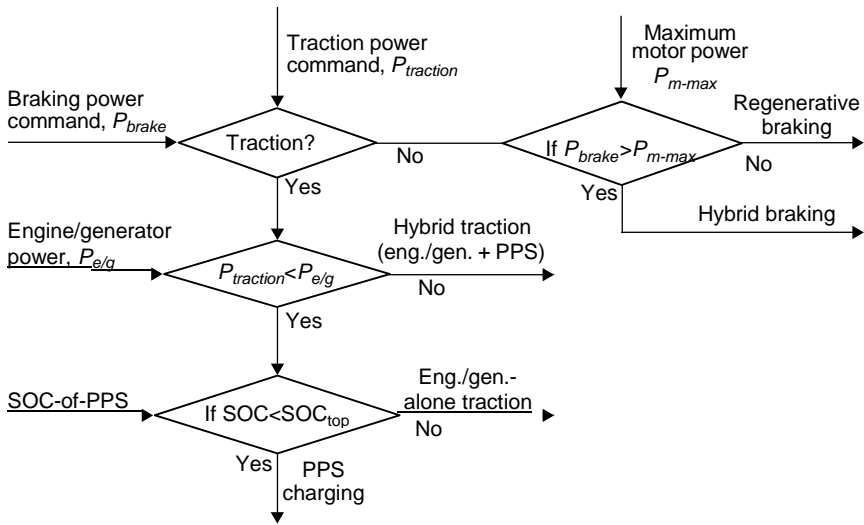


FIGURE 15
Control flowchart of the Max. SOC-of-PPS control strategy

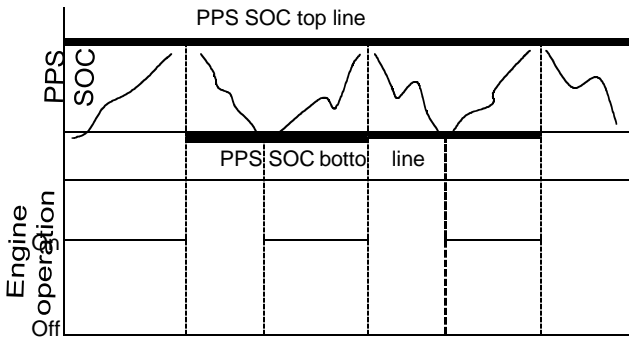


FIGURE 16
Illustration of thermostat control

time driving with a low load on a highway at constant speed, the PPS can be easily charged to its full level, and the engine/generator is forced to operate with a power output smaller than its optimum. Hence, the efficiency of the drive train is reduced. In this case, engine-on-off or thermostat control of the engine/generator would be appropriate. This control strategy is illustrated in Figure 16. The operation of the engine/generator is completely controlled by the SOC of the PPS. When the SOC of the PPS reaches its preset top line, the engine/generator is turned off and the vehicle is propelled only by the PPS. On the other hand, when the SOC of the PPS reaches its bottom line, the engine/generator is turned on. The PPS gets its charging from the

engine/generator. In this way, the engine can always be operated within its optimal deficiency region.

4.7 Sizing of the Major Components

The major components in a series hybrid drive train include traction motor, engine/generator, and PPS. The design of the power ratings of these components is the first and most important step in the whole system design. In the design of these parameters, some design constraints must be considered, which include (1) acceleration performance, (2) highway driving and urban driving, and (3) energy balance in the PPS.

4.7.1 Power Rating Design of the Traction Motor

The power rating of the electric motor drive in series HEV is completely determined by vehicle acceleration performance requirements, motor characteristics, and transmission characteristics (refer to Chapter 4). At the beginning of the design, the power rating of the motor drive can be estimated, according to the acceleration performance (time used to accelerate the vehicle from zero speed to a given speed), using the following equation:

$$P = \frac{\delta M_v}{2t_a} (V_b^2 - V_f^2) + M g f_r V + \frac{1}{5} \rho C_D A V^3, \tag{3.5}$$

where M_v is the total vehicle mass in kg, t_a is the expected acceleration time in sec, V_b is the vehicle speed in m/s, corresponding to the motor-based speed, V_f is the final speed of the vehicle accelerating in m/s, g is gravity acceleration in 9.80 m/s², f_r is the tire rolling resistance coefficient, ρ_a is the air density in 1.202 kg/m³, A_f is the front area of the vehicle in m², and C_D is the aerodynamic drag coefficient. The first term in equation (3.5) represents the power used to accelerate the vehicle mass, and the second and third terms represent the average power for overcoming the tire rolling resistance and aerodynamic drag.

Figure 17 shows the tractive effort and traction power vs. vehicle speed with a two-gear transmission. During acceleration, starting from low gear, the tractive effort follows the trace of a–b–d–e and $V_b = V_{b1}$. However, when a single-gear transmission is used, that is, only when a high gear is available, the tractive effort follows the trace of c–d–e and $V_b = V_{b2}$.

Figure 18 shows an example of the power rating of motor vs. speed ratio, which is defined as the ratio of maximum speed to the base speed as shown in Figure 17.

It should be noted that the rated motor power determined by equation (3.5) is only an estimate for meeting the acceleration performance. In order to accurately determine the rated motor power, verification would be necessary.

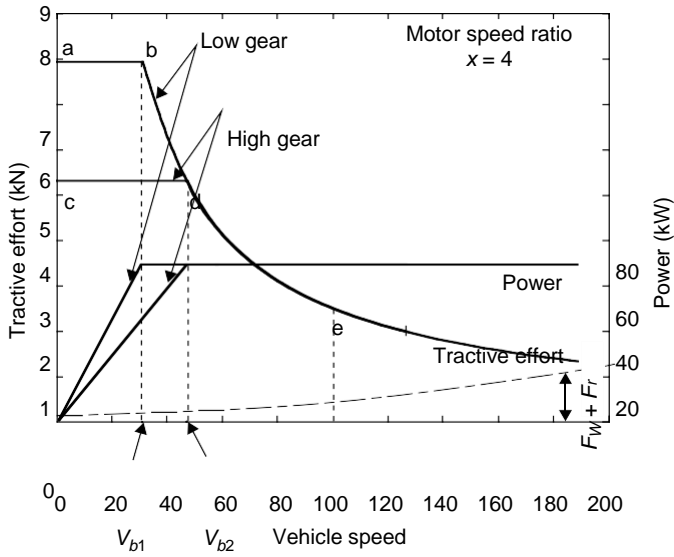


FIGURE 16
Speed-torque (power) characteristics of an electric motor

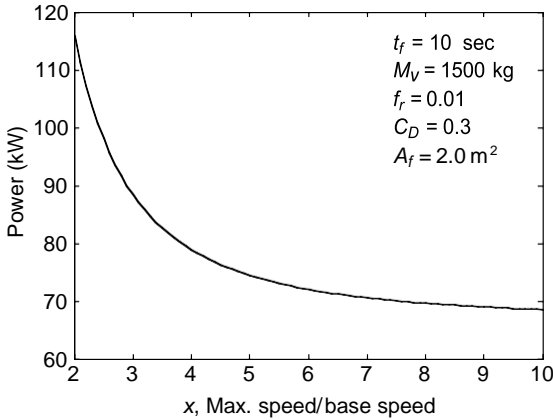


FIGURE 17
Power rating of the traction power vs. speed ratio of drive train

The calculation of vehicle performance, such as acceleration time, acceleration distance, and gradeability, is exactly the same as that of a pure electric vehicle.

4.7.2 Power Rating Design of the Engine/Generator

As discussed in Chapter 5, the engine/generator in a series hybrid drive train is used to supply steady-state power in order to prevent the PPS from being

discharged completely. In the design of the engine/generator, two driving conditions should be considered: driving for a long time with constant

speed, such as highway driving between cities, and driving with a frequent stop-go driving pattern, such as driving in cities. With the former driving pattern (long time at a constant speed), the engine/generator and drive train should not rely on the PPS to support the operation at a high speed of, for example, 130 km/h or 80 mph. The engine/generator should be able to produce sufficient power to support this speed. For a frequent stop-go driving pattern, the engine/generator should produce sufficient power to maintain the energy storage of the PPS at a certain level, so that enough power can be drawn to support vehicle acceleration. As mentioned above, the energy consumption in the PPS is closely related to the control strategy.

At a constant speed and on a flat road, the power output from the power source (engine/generator and/or the PPS) can be expressed as

$$P_{e/g} = \frac{V}{1000\eta_t\eta_m} \left(M_v g f_r + \frac{1}{2} \rho_a C_D A_f V^2 \right) \text{(kW)}, \tag{3.6}$$

where η_t and η_m are the efficiency of transmission and traction motor, respectively. Figure 18 shows an example of the load power (not including η_t and η_m curve vs. vehicle speed) for a 1500 kg passenger car. It indicates that the power demand at constant speed is much less than that for acceleration (refer to Figure 18). In this example, about 35 kW are needed at 130 km/h of constant speed driving.

Considering the inefficiency of the motor drive and transmission (η_t and η_m equation [3.7]), the power output of the engine/generation system is about 20 to 25% more than that shown in Figure 17

When the vehicle is driving in a stop-and-go pattern in urban areas, the power that the engine/generator produces should be equal to or slightly greater than the average load power in order to maintain balanced PPS energy storage. The average load power can be expressed as

$$P_{ave} = \frac{1}{T} \int_0^T \left(M_v g f_r + \frac{1}{2} \rho_a C_D A_f V^2 \right) V dt + \frac{1}{T} \int_0^T \delta M_v \frac{dV}{dt} dt, \tag{3.7}$$

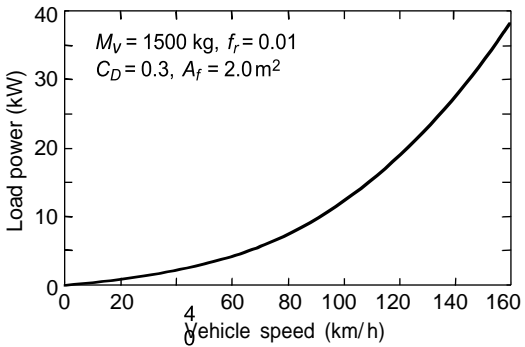


FIGURE 18
Load power of a 1500 kg passenger car at constant speed

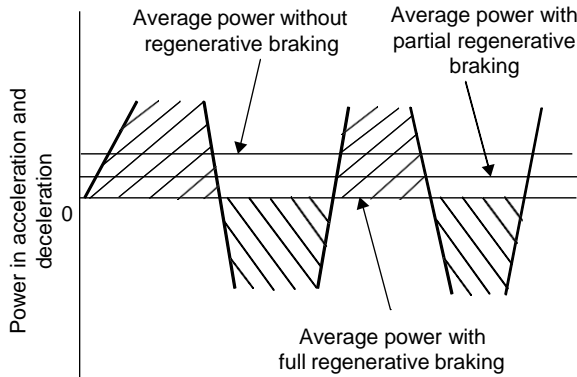


FIGURE 19 Average power consumed in acceleration and deceleration with full, partial, and zero regenerative braking

where δ is the vehicle mass factor (refer to Chapter 4) and dV/dt is the acceleration of the vehicle. The first term in equation (3.8) is the average power that is consumed to overcome the tire rolling resistance and aerodynamic drag. The second term is the average power consumed in acceleration and deceleration. When the vehicle has the ability to recover all of the kinetic energy of the vehicle, the average power consumed in acceleration and deceleration is zero. Otherwise, it will be greater than zero, as shown in Figure 19.

In the design of an engine/generator system, the power capability should be greater than, or at least not less than, the power that is needed to support the vehicle driving at a constant speed (highway driving) and at average power when driving in urban areas. In actual design, some typical urban drive cycles may be used to predict the average power of the vehicle, as shown in Figure 20.

4.7.3 Design of PPS

The PPS must be capable of delivering sufficient power to the traction motor at any time. At the same time, the PPS must store sufficient energy to avoid failure of power delivery due to too-deep discharging.

5.3.4 Power Capacity of PPS

To fully utilize the electric motor power capacity, the total power of the engine/generator and PPS should be greater than, or at least equal to, the rated maximum power of the electric motor. Thus, the power capacity of the PPS can be expressed as

$$P_{pps} \geq \frac{P_{m,max}}{\eta_m} - P_{e/g} \tag{3.8}$$

where $P_{m,max}$ is the maximum rated power of the motor, η_m is the efficiency of the motor, and $P_{e/g}$ is the power of the engine/generator system.

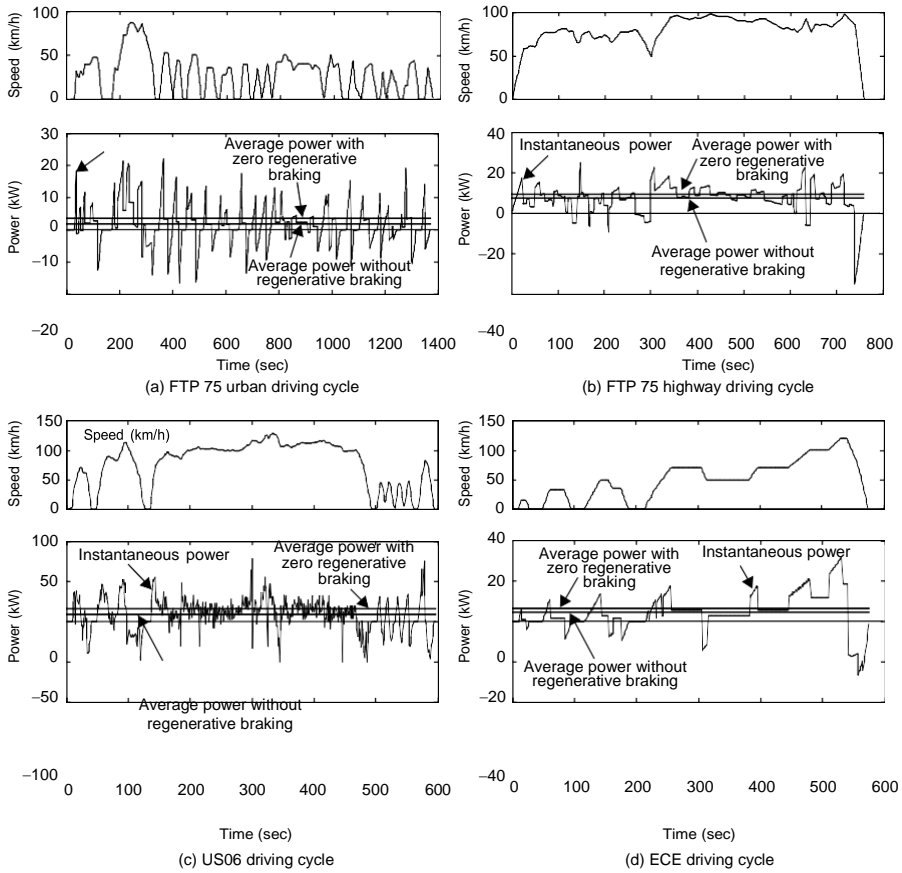


FIGURE 20 Instantaneous power and average power with full and zero regenerative braking in typical drive cycles

4.7.3.1 Energy Capacity of PPS

In some driving conditions, a frequent accelerating/decelerating driving pattern would result in a low SOC in the PPS, thus losing its delivery power. In order to properly determine the energy capacity of the PPS, the energy changes in the PPS in some typical drive cycles must be known. The energy changes in the PPS can be expressed as

$$\Delta E = \int_0^T P_{pps} dt, \quad (3.9)$$

where P_{pps} is the power of the PPS. Positive P_{pps} represents charging power, and negative P_{pps} represents discharging power. Figure 7.11 shows an example in which the energy changes in the peaking power vary with driving time. Figure 21 also shows the maximum amount of energy changes, ΔE_{max} in the whole drive cycle, if the SOC of the PPS is allowed in the operating range between SOC_{top} and SOC_{bott} . The whole energy capacity of the peaking power

can be calculated using equation (3.10). The operating range of PPS SOC depends upon the operating characteristics of the PPS. For example, for efficiency reasons chemical batteries would have an optimal operating range in

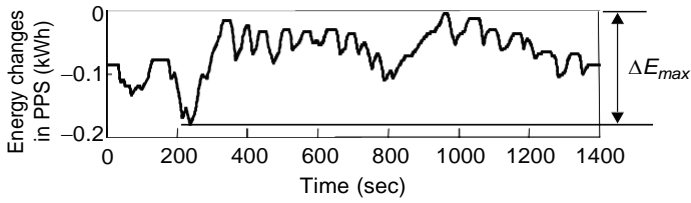


FIGURE 21
Energy changes in a typical urban drive cycle with Max. SOC control strategy

the middle (0.4–0.7), and for limited voltage variation reasons, ultracapacitors would only have a very limited energy change range (0.8–1.0).

$$E_{cap} = \frac{\Delta E_{max}}{SOC_{top} - SOC_{bott}} \cdot \quad (3.10)$$

4.8 Design Example

Design specification:

Parameters

Vehicle total mass	1500 kg
Rolling resistance coefficient	0.01
Aerodynamic drag coefficient	0.3
Front area	2.0 m ²
Transmission efficiency (single gear)	0.9

Performance speciation:

Acceleration time (from 0 to 100 km/h)	10±1 sec
Maximum gradeability	> 30% at low speed and > 5 at 100 km/h
Maximum speed	160 km/h

4.8.1 Design of Traction Motor Size

Using equation (7.5) and supposing the motor drive has a speed ratio of $x = 4$, the motor drive power rating can be obtained as 82.5 kW for the specified acceleration time of 10 sec from zero to 100 km/h. Figure 22 shows the speed–torque and speed–power profiles of the motor.

4.8.2 Design of the Gear Ratio

The gear ratio is designed such that the vehicle reaches its maximum speed at the motor maximum speed, that is,

$$\frac{\pi n_{m, max} r}{g} \equiv \quad (3.11)$$

$$30V'_{max}$$

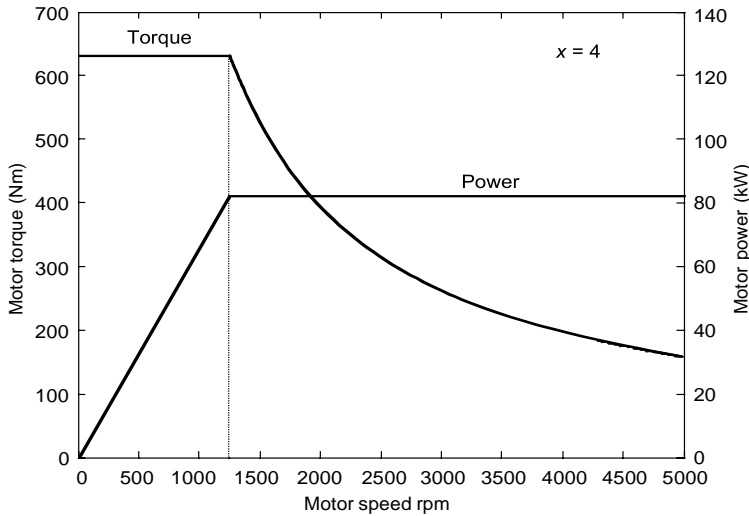


FIGURE 22
 Characteristics of traction motor vs. motor rpm and vehicle speed

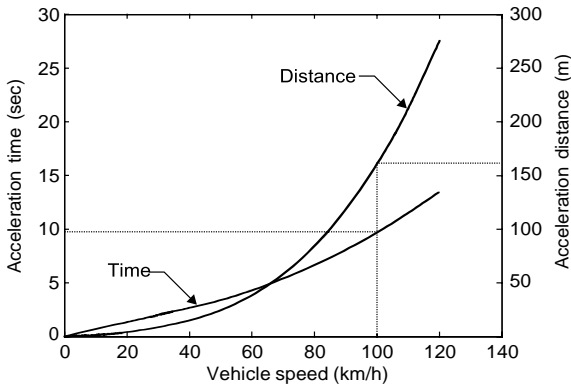


FIGURE 23
 Accelerating time and distance vs. vehicle speed

where $n_{m,max}$ is the maximum motor rpm and V_{max} is the maximum speed of the vehicle in m/s. Suppose $n_{m,max} = 5000$ rpm, $V_{max} = 44.4$ m/s (160 km/h or 100 mph), and $r = 0.2794$ m (11 in.); $i_g = 3.29$ is obtained.

4.8.3 Verification of Acceleration Performance

Based on the torque–speed profile of the traction motor, gear ratio, and the vehicle parameters, and using the calculation method the vehicle acceleration performance (acceleration time and distance vs. vehicle speed) can be obtained as shown in Figure 23. If the acceleration

time obtained does not meet the design specification, the motor power rating should be redesigned.

4.8.4 Verification of Gradeability

Using the motor torque–speed profile, gear ratio and vehicle parameters, the tractive effort and resistance vs. vehicle speed can be calculated and drawn in a diagram, as shown in Figure 24(a). Further, the gradeability of the vehicle can be calculated as shown in Figure 24(b). Figure 24 indicates that the gradeability calculated is much greater than that specified in the design specification. This result implies that for a passenger car, the power needed

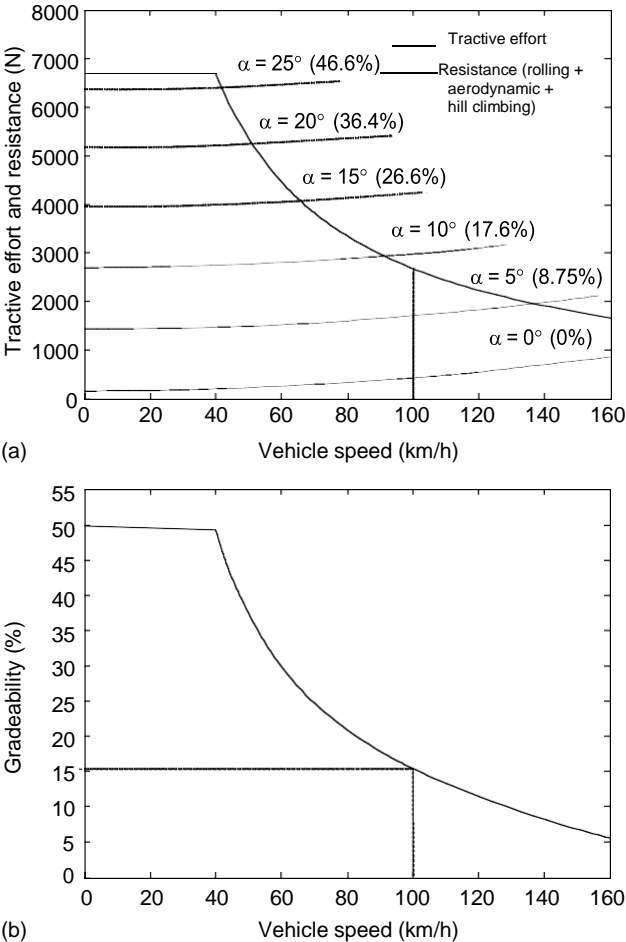


FIGURE 24 Traction effort and resistance of the vehicle vs. speed

for acceleration performance is usually larger than that needed for grade-ability; the former determines the power rating of the traction motor.

5.4.5 Design of Engine/Generator Size

The power rating of the engine/generator is designed to be capable of supporting the vehicle at a regular highway speed (130 km/h or 81 mph) on a flat road. Figure 7.15 shows that the engine power needed at 130 km/h or 81 mph is 32.5 kW, in which energy losses in transmission (90% of efficiency), motor drive (85% of efficiency), and generator (90% of efficiency) are involved. Figure 7.15 also indicates that 32.5 kW of engine power can be capable of supporting a vehicle driving at 78 km/h (49 mph) on a 5% grade road.

Another consideration in the design of the power rating of the engine/generator is the average power when driving with some typical stop-and-go driving patterns as illustrated in Figure 7.10. The typical data in these drive cycles are listed in Table 7.1.

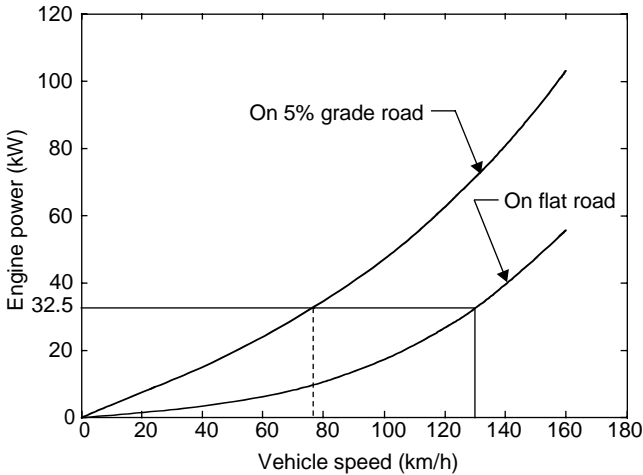


FIGURE 25
Engine power vs. vehicle constant speed on a flat road and a 5% grade road

TABLE 3.1
Typical Data of Different Drive Cycles

	Max. Speed (km/h)	Average Speed (km/h)	Average Power with Full Regen. Braking (kW)	Average Power with No Regen. Braking (kW)
FTP 75 urban	86.4	27.9	3.76	4.97
FTP 75 highway	97.7	79.6	12.6	14.1
US06	128	77.4	18.3	23.0
ECE-1	120	49.8	7.89	9.32

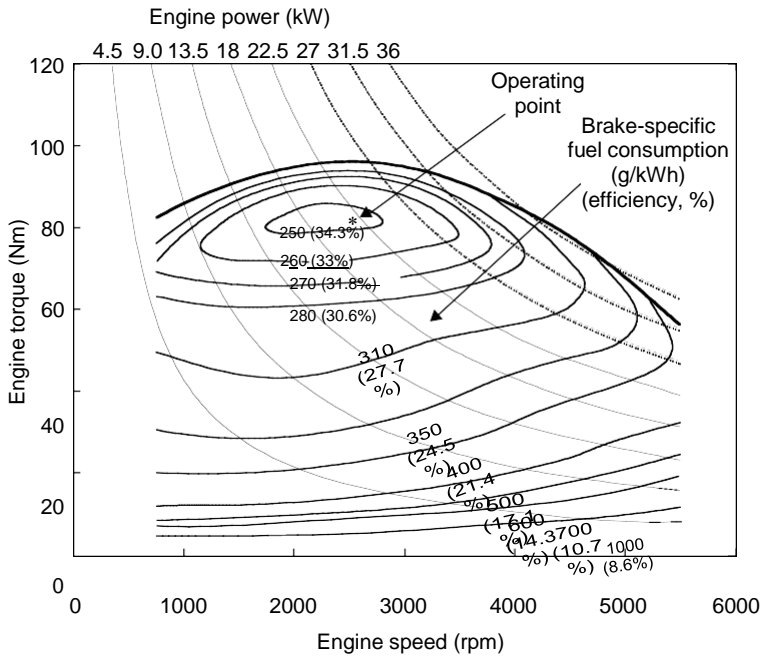


FIGURE 26
Engine characteristics and operating points

Compared with the power needed in Figure 7.14, the average power in these drive cycles is smaller. Hence, 32.5 kW of engine power can meet the power requirement in these drive cycles. Figure 7.16 shows the engine characteristics.

4.8.5 Design of the Power Capacity of PPS

The sum of the output power of the engine/generator PPS should be greater than, or at least equal to, the input power of the traction motor. That is,

$$P_{pps} = \frac{P_{motor}}{\eta_{motor}} - P_{e/g} = \frac{82.5}{0.85} - 32.5 \times 0.9 = 67.8 \text{ kW.} \quad (3.12)$$

4.8.6 Design of the Energy Capacity of PPS

The energy capacity of the PPS heavily depends on the drive cycle and overall control strategy. In this design, because the power capacity of the engine/generator is much greater than the average load power and average traction power, the thermostat control strategy (engine-on-off) is considered to be appropriate.

Figure 27 shows simulation results of the above vehicle with engine-on-off control strategy in the FTP 75 urban drive cycle. In the simulation,

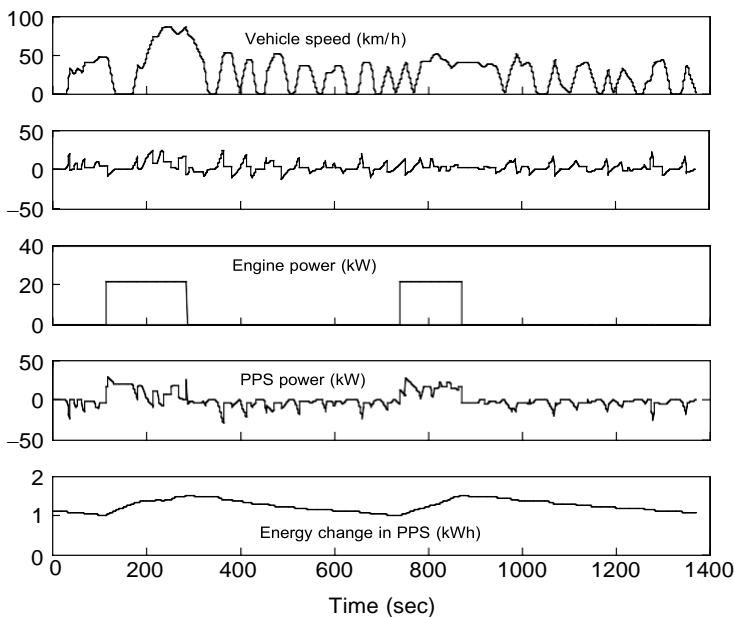


FIGURE 27
Simulation results in the FTP 75 urban drive cycle

regenerative braking is involved. In the control, the allowed maximum energy variation in the PPS is 0.5 kWh. Suppose that the peaking power allowed to operate in the SOC range is 0.2. Using batteries as the PPS, operating in the range of 0.4 to 0.6 of SOC will have optimal efficiency. Using ultracapacitors, 0.2 variation of SOC will limit the terminal voltage to 10%. The total storage energy in the PPS can be calculated by

$$E_{pps} = \frac{\Delta E_{max}}{\Delta SOC} = \frac{0.5}{0.2} = 2.5 \text{ kWh.} \quad (3.13)$$

5.4.8 Fuel Consumption

The fuel consumption for various drive cycles can be calculated by simulation. In the FTP 75 urban drive cycle (Figure 28), the designed drive train has the fuel economy of 17.9 km/l or 42.4 mpg, and in the FTP highway drive cycle (Figure 28), it is 18.4 km/l or 43.5 mpg. It is clear that a hybrid vehicle with performance similar to a conventional vehicle is much more efficient, especially in a frequent stop-and-go environment. The main reasons are the high operating efficiency of the engine and the significant amount of braking energy recovered by regenerative braking.

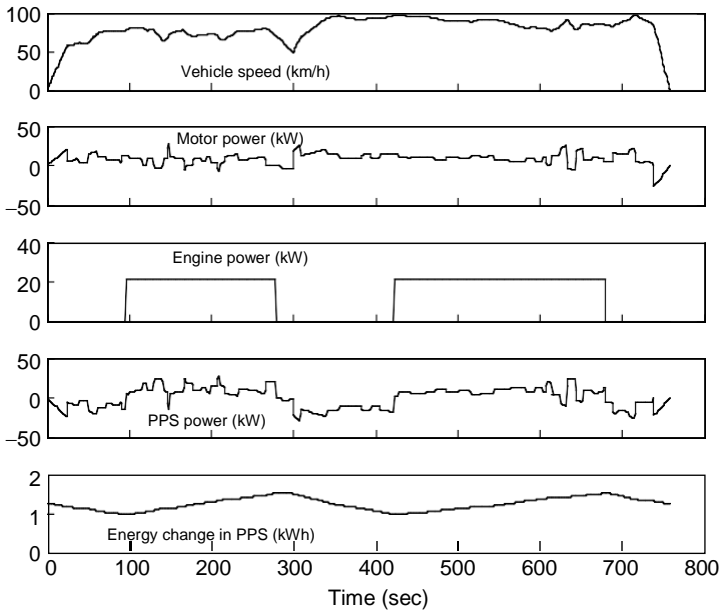


FIGURE 28
Simulation results in the FTP 75 highway drive cycle

References

- [1] C.C. Chan and K.T. Chau, *Modern Electric Vehicle Technology*, Oxford University Press, New York, 2001.
- [2] M. Ehsani, Y. Gao, and K. Butler, Application of electric peaking hybrid (ELPH) propulsion system to a full size passenger car with simulation design verification, *IEEE Transactions on Vehicular Technology*, 48, 1779–1787, 1999.
- [3] C.G. Hochgraf, M.J. Ryan, and H.L. Wiegman, Engine control strategy for a series hybrid electric vehicle incorporating load-leveling and computer controlled energy management, *Society of Automotive Engineers (SAE) Journal*, Paper No. 960230, Warrendale, PA, 2002.
- [4] M. Ender and P. Dietrich, Duty cycle operation as a possibility to enhance the fuel economy of an SI engine at part load, *Society of Automotive Engineers (SAE) Journal*, Paper No. 960227, Warrendale, PA, 2002.
- [5] I. Husain, *Electric and Hybrid Electric Vehicles*, CRC Press, 2003.
- [6] M. Ehsani, *Modern Electric, Hybrid Electric and Fuel Cell Vehicles: Fundamentals, Theory and Design*, CRC Press, 2005



SATHYABAMA

INSTITUTE OF SCIENCE AND TECHNOLOGY
(DEEMED TO BE UNIVERSITY)

Accredited "A" Grade by NAAC | 12B Status by UGC | Approved by AICTE

www.sathyabama.ac.in

SCHOOL OF ELECTRICAL AND ELECTRONICS ENGINEERING

DEPARTMENT OF ELECTRICAL AND ELECTRONICS ENGINEERING

UNIT – IV - Electric Vehicle – SEE1628/SEEA3028

DC motor drive-Chopper control of DC motor drive- multi-quadrant control of Chopper fed drive Induction motor drive-constant v/f control-power electronics control-FOC-VSI for FOC. PMBLDC motor drive-basic principle – construction-classification-performance and control of PMBLDC machine. SRM drive-basic magnetic structure-SRM drive converter-modes of operation-generating modes of operation.

1 DC Motor Drives

DC motor drives have been widely used in applications requiring adjustable speed, good speed regulation, and frequent starting, braking and reversing. Various DC motor drives have been widely applied to different electric traction applications because of their technological maturity and control simplicity.

1.1 Principle of Operation and Performance

The operation principle of a DC motor is straightforward. When a wire carrying electric current is placed in a magnetic field, a magnetic force acting on the wire is produced. The force is perpendicular to the wire and the magnetic field as shown in Figure 6.3. The magnetic force is proportional to the wire length, magnitude of the electric current, and the density of the magnetic field; that is,

$$F = BIL. \tag{4.1}$$

When the wire is shaped into a coil, as shown in Figure 1, the magnetic forces acting on both sides produce a torque, which is expressed as

$$T = BIL \cos \alpha, \tag{4.2}$$

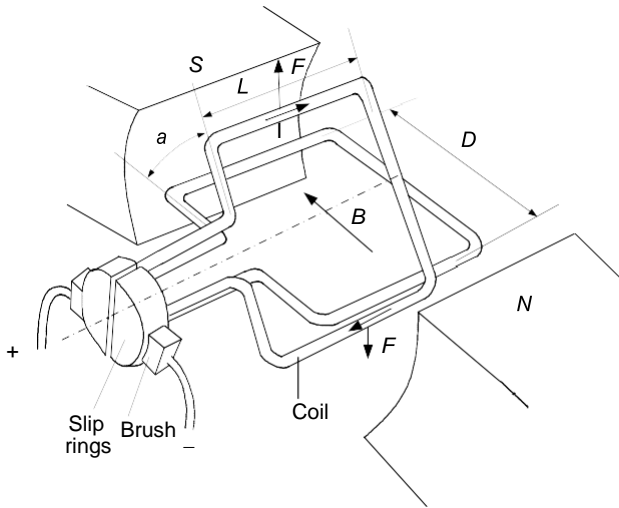


FIGURE 1
Operation principle of a DC motor

where α is the angle between the coil plane and magnetic field as shown in Figure 6.3. The magnetic field may be produced by a set of windings or permanent magnets. The former is called wound-field DC motor and the latter is called the PM DC motor. The coil carrying the electric current is called the armature. In practice, the armature consists of a number of coils. In order to obtain continuous and maximum torque, slip rings and brushes are used to conduct each coil at the position of $\alpha = 0$.

Practically, the performance of DC motors can be described by the armature voltage, back electromotive force (EMF), and field flux.

Typically, there are four types of wound-field DC motors, depending on the mutual interconnection between the field and armature windings. They are separately excited, shunt excited, series excited, and compound excited as shown in Figure 2. In the case of a separately excited motor, the field and armature voltage can be controlled independently of one another. In a shunt motor, the field and armature are connected in parallel to a common source. Therefore, an independent control of field current and armature or armature voltage can be achieved by inserting a resistance into the appropriate circuit. This is an inefficient method of control. The efficient method is to use power electronics-based DC-DC converters in the appropriate circuit to replace the resistance. The DC-DC converters can be actively controlled to produce proper armature and field voltage. In the case of a series motor, the field current is the same as the armature current; therefore, field flux is a function of armature current. In a cumulative compound motor, the magnetomotive force (mmf) of a series field is a function of the armature current and is in the same direction as the mmf of the shunt field.²

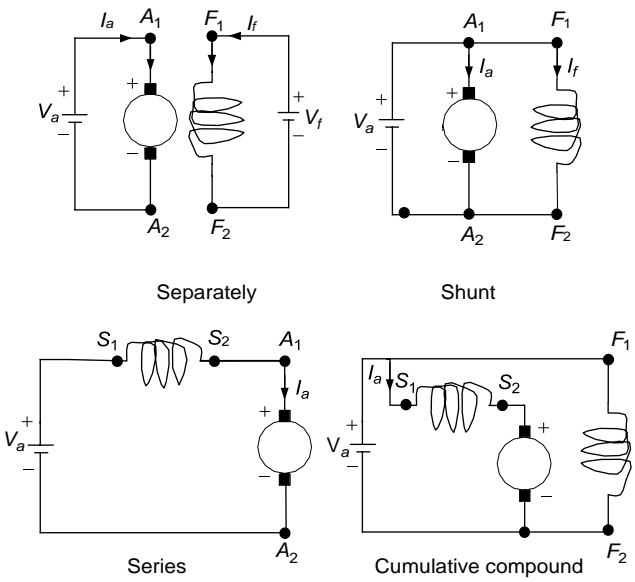


FIGURE 2
Wound-field DC motors

The steady-state equivalent circuit of the armature of a DC motor is shown in Figure 3. The resistor R_a is the resistance of the armature circuit. For separately excited and shunt DC motors, it is equal to the resistance of the armature windings; for the series and compound motors, it is the sum of armature and series field winding resistances. Basic equations of a DC motor are

$$V_a = E + R_a I_a, \quad E = K \phi \omega_m \tag{4.3}$$

$$T = K_e \phi I_a \tag{4.4}$$

where ϕ is the flux per pole in Webers, I_a is the armature current in A, V_a is the armature voltage in volt, R_a is the resistance of the armature circuit in ohms, ω_m is the speed of the armature in rad/sec, T is the torque developed by the motor in Nm, and K_e is constant.

From equations (6.3)–(6.4), one can obtain

$$T = \frac{K \phi}{R_a} V - \frac{(K \phi)^2}{R_a} \omega_m \tag{4.5}$$

Equations (4.3)–(4.5) are applicable to all the DC motors, namely, separately (or shunt) excited, series, and compound motors. In the case of separately excited motors, if the field voltage is maintained as constant, one can assume the flux to be practically constant as the torque changes. In this case, the speed–torque characteristic of a separately excited motor is a straight line, as shown in Figure 3. The nonload speed ω_{m0} is determined by the values of the armature voltage and the field excitation. Speed decreases as torque increases, and speed regulation depends on the armature circuit resistance. Separately excited motors are used in applications requiring good speed regulation and proper adjustable speed.

In the case of series motors, the flux is a function of armature current. In an unsaturated region of the magnetization characteristic, ϕ can be assumed to be proportional to I_a . Thus,

$$\phi = K_f I_a \tag{4.6}$$

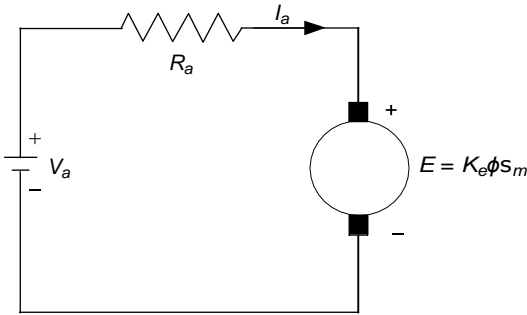


FIGURE 3
Steady-state equivalent circuit of the armature circuit of a DC motor

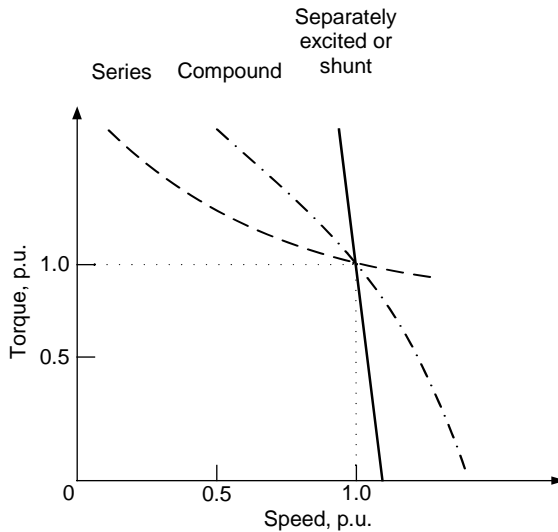


FIGURE 4
Speed characteristics of DC motors

A speed–torque characteristic of a series DC motor is shown in Figure 4. In the case of series, any increase in torque is accompanied by an increase in the armature current and, therefore, an increase in magnetic flux. Because flux increases with the torque, the speed drops to maintain a balance between the induced voltage and the supply voltage. The characteristic, therefore, shows a dramatic drop. A motor of standard design works at the knee point of the magnetization curve at the rated torque. At heavy torque (large current) overload, the magnetic circuit saturates and the speed–torque curve approaches a straight line.

Series DC motors are suitable for applications requiring high starting torque and heavy torque overload, such as traction. This was just the case for electric traction before the power electronics and microcontrol era. However, series DC motors for traction application have some disadvantages. They are not allowed to operate without load torque with full supply voltage. Otherwise, their speed will quickly increase up to a very high value. Another disadvantage is the difficulty in regenerative braking.

Performance equations for cumulative compound DC motors can be derived from equations (4.3) to (4.4). The speed–torque characteristics are between series and separately excited (shunt) motors, as shown in Figure 4.

1.2 Combined Armature Voltage and Field Control

The independence of armature voltage and field provides more flexible control of the speed and torque than other types of DC motors. In EV and HEV applications, the most desirable speed–torque characteristic is to have a constant torque below a certain speed (base speed), with the torque dropping parabolically with the increase of speed (constant power) in the range above the base speed, as shown in Figure 5. In the range of lower than base speed, the armature current and field are set at their rated values, producing the rated torque. From equations (4.3) to (4.4), it is clear that the armature voltage must be increased proportionally with the increase of the speed. At the base speed, the armature voltage reaches its rated value (equal to the source voltage) and cannot be increased further. In order to further increase the speed, the field must be weakened with the increase of the speed, and then the back EMF E and armature current must be maintained constant. The torque produced drops parabolically with the increase in the speed and the output power remains constant, as shown in Figure 5.

1.3 Chopper Control of DC Motors

Choppers are used for the control of DC motors because of a number of advantages such as high efficiency, flexibility in control, light weight, small size, quick response, and regeneration down to very low speeds. Presently, the separately excited DC motors are usually used in traction, due to the control flexibility of armature voltage and field.

For a DC motor control in open-loop and closed-loop configurations, the chopper offers a number of advantages due to its high operation frequency.

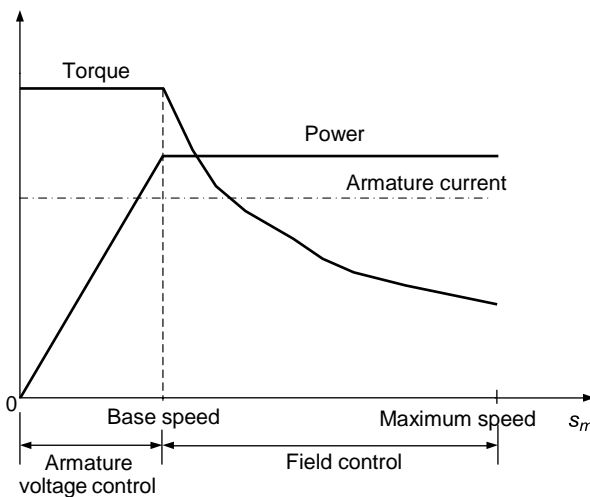


FIGURE 5

Torque and power limitations in combined armature voltage and field control

High operation frequency results in high-frequency output voltage ripple and, therefore, less ripples in the motor armature current and a smaller region of discontinuous conduction in the speed–torque plane. A reduction in the armature current ripple reduces the armature losses. A reduction or elimination of the discontinuous conduction region improves speed regulation and the transient response of the drive.

The power electronic circuit and the steady-state waveform of a DC chopper drive are shown in Figure 6. A DC voltage source, V , supplies an inductive load through a self-commutated semiconductor switch S . The symbol of a self-commutated semiconductor switch has been used because a chopper can be built using any device among thyristors with a forced commutation circuit: GTO, power transistor, MOSFET, and IGBT. The diode shows the direction in which the device can carry current. A diode D_F is connected in parallel with the load. The semiconductor switch S is operated periodically over a period T and remains closed for a time $t_{on} = \delta T$ with $0 < \delta < 1$. The variable $\delta = t_{on}/T$ is called the duty ratio or duty cycle of a chopper. Figure 6.8 also shows the waveform of control signal i_c . Control signal i_c will be the base current for a transistor chopper, and a gate current for the GTO of a GTO

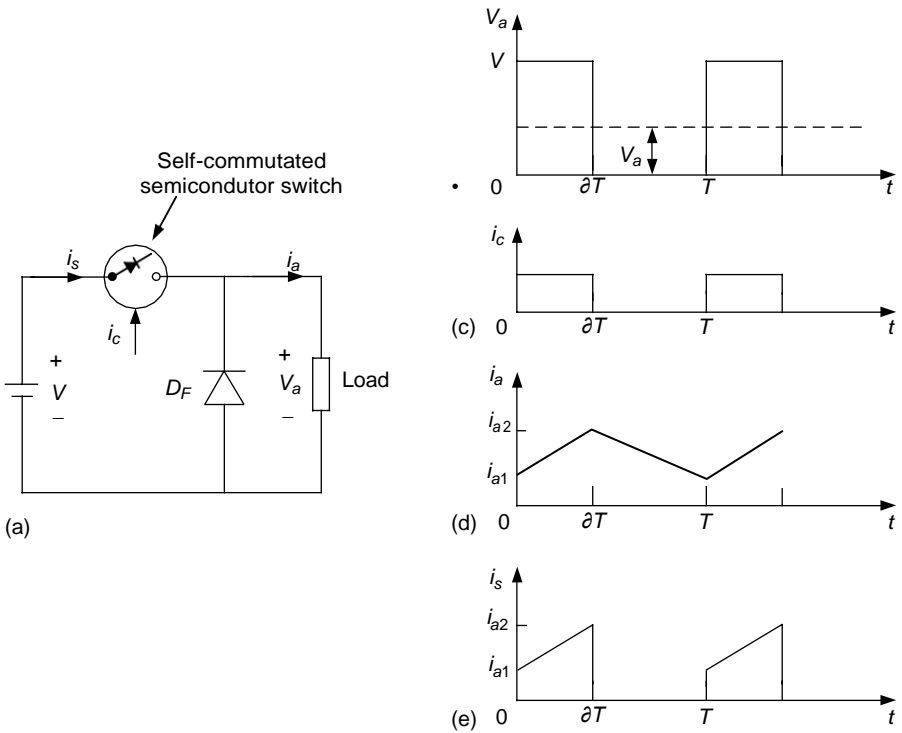


FIGURE 6 Principle of operation of a step down (or class A) chopper: (a) basic chopper circuit; (b) to (e) waveforms

chopper or the main thyristor of a thyristor chopper. If a power MOSFET is used, it will be a gate to the source voltage. When the control signal is present, the semiconductor switch S will conduct, if forward biased. It is assumed that the circuit operation has been arranged such that the removal of i_c will turn off the switch.

During the on interval of the switch ($0 \leq t \leq \delta T$), the load is subjected to a voltage V and the load current increases from i_{a1} to i_{a2} . The switch is opened at $t = \delta T$. During the off period of the switch ($\delta T \leq t \leq T$), the load inductance maintains the flow of current through diode D_F . The load terminal voltage remains zero (if the voltage drop on the diode is ignored in comparison to V) and the current decreases from i_{a2} to i_{a1} . The interval $0 \leq t \leq \delta T$ is called the duty interval and the interval $\delta T \leq t \leq T$ is known as the freewheeling interval. Diode D_F provides a path for the load current to flow when switch S is off, and thus improves the load current waveform. Furthermore, by maintaining the continuity of the load current at turn off, it prevents transient voltage from appearing across switch S , due to the sudden change of the load current. The source current waveform is also shown in Figure 6.8e. The source current flows only during the duty interval and is equal to the load current. By controlling δ between 0 and 1, the load voltage can be varied from 0 to V ; thus, a chopper allows a variable DC voltage to be obtained from a fixed voltage DC source.

The switch S can be controlled in various ways for varying the duty ratio δ . The control technologies can be divided into the following categories:

1. Time ratio control (TRC).
2. Current limit control (CLC).

In TRC, also known as pulse width control, the ratio of on time to chopper period is controlled. The TRC can be further divided as follows:

1. Constant frequency TRC: The chopper period T is kept fixed and the on period of the switch is varied to control the duty ratio δ .
2. Varied frequency TRC: Here, δ is varied either by keeping t_{on} constant and varying T or by varying both t_{on} and T .

In variable frequency control with constant on-time, low-output voltage is obtained at very low values of chopper frequencies. The operation of a chopper at low frequencies adversely affects the motor performance. Furthermore, the operation of a chopper with variable frequencies makes the design of an input filter very difficult. Thus, variable frequency control is rarely used.

In current limit control, also known as point-by-point control, δ is controlled indirectly by controlling the load current between certain specified maximum and minimum values. When the load current reaches a specified maximum value, the switch disconnects the load from the source and reconnects it when the current reaches a specified minimum value. For a DC motor load, this type of control is, in effect, a variable frequency variable ontime control.

The following important points can be noted from the waveform of Figure 6:

1. The source current is not continuous but flows in pulses. The pulsed current makes the peak input power demand high and may cause fluctuation in the source voltage. The source current waveform can be resolved into DC and AC harmonics. The fundamental AC harmonic frequency is the same as the chopper frequency. The AC harmonics are undesirable because they interfere with other loads connected to the DC source and cause radio frequency interference through conduction and electromagnetic radiation. Therefore, an L-C filter is usually incorporated between the chopper and the DC source. At higher chopper frequencies, harmonics can be reduced to a tolerable level by a cheaper filter. From this point, a chopper should be operated at the highest possible frequency.
2. The load terminal voltage is not a perfect direct voltage. In addition to a direct component, it has harmonics of the chopping frequency and its multiples. The load current also has an AC ripple.

The chopper of Figure 6 is called a class A chopper. It is one of a number of chopper circuits that are used for the control of DC motors. This chopper is capable of providing only a positive voltage and a positive current. It is therefore called a single-quadrant chopper, capable of providing DC separately excited motor control in the first quadrant, positive speed, and positive torque. Since it can vary the output voltage from V to 0, it is also a step-down chopper or a DC to DC buck converter. The basic principle involved can also be used to realize a step-up chopper or DC to DC boost converter.

The circuit diagram and steady-state waveforms of a step-up chopper are shown in Figure 7. This chopper is known as a class B chopper. The presence of control signal i_c indicates the duration for which the switch can conduct if forward-biased. During a chopping period T , it remains closed for an interval $0 \leq t \leq \delta T$ and remains open for an interval $\delta T \leq t \leq T$. During the on period, i_s increases from i_{s1} to i_{s2} , thus increasing the magnitude of energy stored in inductance L . When the switch is opened, current flows through the parallel combination of the load and capacitor C . Since the current is forced against the higher voltage, the rate of change of the current is negative. It decreases from i_{s2} to i_{s1} in the switch's off period. The energy stored in the inductance L and the energy supplied by the low-voltage source are given to the load. The capacitor C serves two purposes. At the instant of

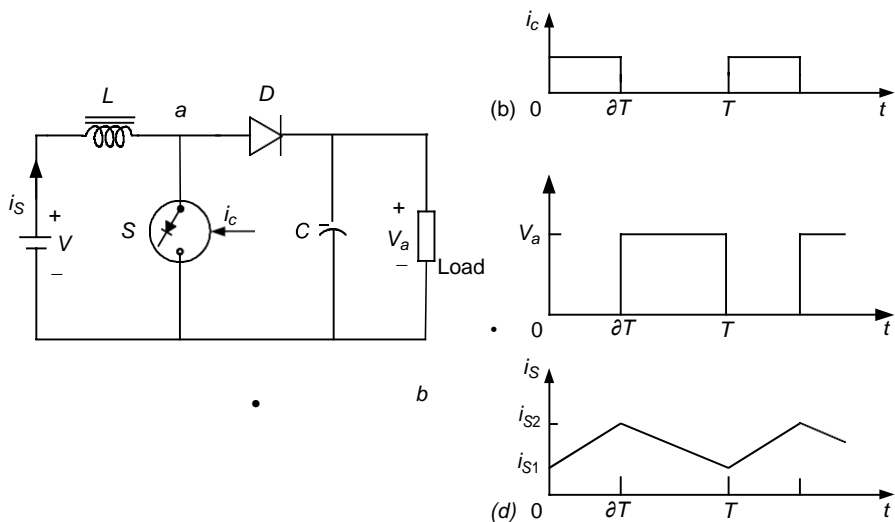


FIGURE 7

Principle of operation of a step-up (or class B) chopper: (a) basic chopper circuit; (b) to (d) waveforms

opening of switch S , the source current, i_s , and load current, i_a , are not the same. In the absence of C , the turn off of S will force the two currents to have the same values. This will cause high induced voltage in the inductance L and the load inductance. Another reason for using capacitor C is to reduce the load voltage ripple. The purpose of the diode D is to prevent any flow of current from the load into switch S or source V .

For understanding the step-up operation, capacitor C is assumed to be large enough to maintain a constant voltage V_a across the load. The average voltage across the terminal a, b is given as

$$V_{ab} = \frac{1}{T} \int_0^T v_{ab} dt = V(1 - \delta) \quad (4.6)$$

The average voltage across the inductance L is

$$V_L = \frac{1}{T} \int_0^T \left(L \frac{di_s}{dt} \right) dt = L \int_0^T i_s di_s = 0 \quad (4.7)$$

The source voltage is

$$V = V_L + V_{ab} \quad (4.8)$$

Substituting from equations (6.9) and (6.10) into (6.11) gives

$$V = V_a(1 - \delta) \text{ or } V_a = \frac{V}{1 - \delta} \quad (4.9)$$

According to (6.12), theoretically the output voltage V_a can be changed from

V to ∞ by controlling δ from 0 to 1. In practice, V_a can be controlled from V

to a higher voltage, which depends on the capacitor C , and the parameters of the load and chopper.

The main advantage of a step-up chopper is the low ripple in the source current. While most applications require a step-down chopper, the step-up chopper finds application in low-power battery-driven vehicles. The principle of the step-up chopper is also used in the regenerative braking of DC motor drives.

1.4 Multiquadrant Control of Chopper-Fed DC Motor Drives

The application of DC motors on EVs and HEVs requires the motors to operate in multiquadrants, including forward motoring, forward braking, backward motoring, and backward braking, as shown in Figure 6.10. For vehicles with reverse mechanical gears, two-quadrant operation (forward motoring and forward braking, or quadrant I and quadrant IV) is required. However, for vehicles without reverse mechanical gears, four-quadrant operation is needed. Multiquadrant operation of a separately excited DC motor is implemented by controlling the voltage poles and magnitude through power electronics-based choppers.

Two-Quadrant Control of Forward Motoring and Regenerative Braking

A two-quadrant operation consisting of forward motoring and forward regenerative braking requires a chopper capable of giving a positive voltage and current in either direction. This two-quadrant operation can be realized in the following two schemes.²

Single Chopper with a Reverse Switch

The chopper circuit used for forward motoring and forward regenerative braking is shown in Figure 9, where S is a self-commutated semi-conductor switch, operated periodically such that it remains closed for a duration of δT and remains open for a duration of $(1-\delta)T$. C is the manual switch. When C is closed and S is in operation, the circuit is similar to that of

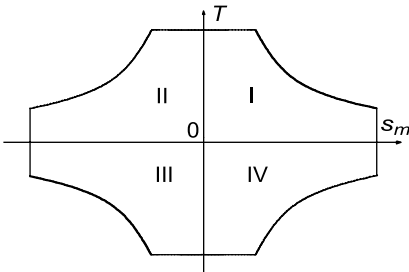


FIGURE 8
Speed–torque profiles of multiquadrant operation

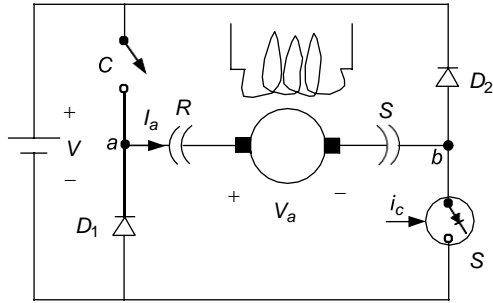


FIGURE 9
Forward motoring and regenerative braking control with a single chopper

Figure 4, permitting the forward motoring operation. Under these conditions, terminal a is positive and terminal b is negative.

Regenerative braking in the forward direction is obtained when C is opened and the armature connection is reversed with the help of the reversing switch RS , making terminal b positive and terminal a negative. During the on-period of the switch S , the motor current flows through a path consisting of the motor armature, switch S , and diode D_1 , and increases the energy stored in the armature circuit inductance. When S is opened, the current flows through the armature diode D_2 , source V , diode D_1 and back to the armature, thus feeding energy into the source.

During motoring, the changeover to regeneration is done in the following steps. Switch S is deactivated and switch C is opened. This forces the armature current to flow through diode D_2 , source V , and diode D_1 . The energy stored in the armature circuit is fed back to the source and the armature current falls to zero. After an adequate delay to ensure that the current has indeed become zero, the armature connection is reversed and switch S is reactivated with a suitable value of d to start regeneration.

Class C Two-Quadrant Chopper

In some applications, a smooth transition from motoring to braking and vice versa is required. For such applications, the class C chopper is used as shown in Figure 10. The self-commutated semiconductor switch S_1 and diode D_1 constitute one chopper and the self-commutator switch S_2 and diode D_2 form another chopper. Both the choppers are controlled simultaneously, both for motoring and regenerative braking. The switches S_1 and S_2 are closed alternately. In the chopping period T , S_1 is kept on for a duration δT , and S_2 is kept on from δT to T . To avoid a direct short-circuit across the source, care is taken to ensure that S_1 and S_2 do not conduct at the same time. This is generally achieved by providing some delay between the turn off of one switch and the turn on of another switch.

The waveforms of the control signals v_a , i_a , and i_s and the devices under conducting during different intervals of a chopping period are shown in

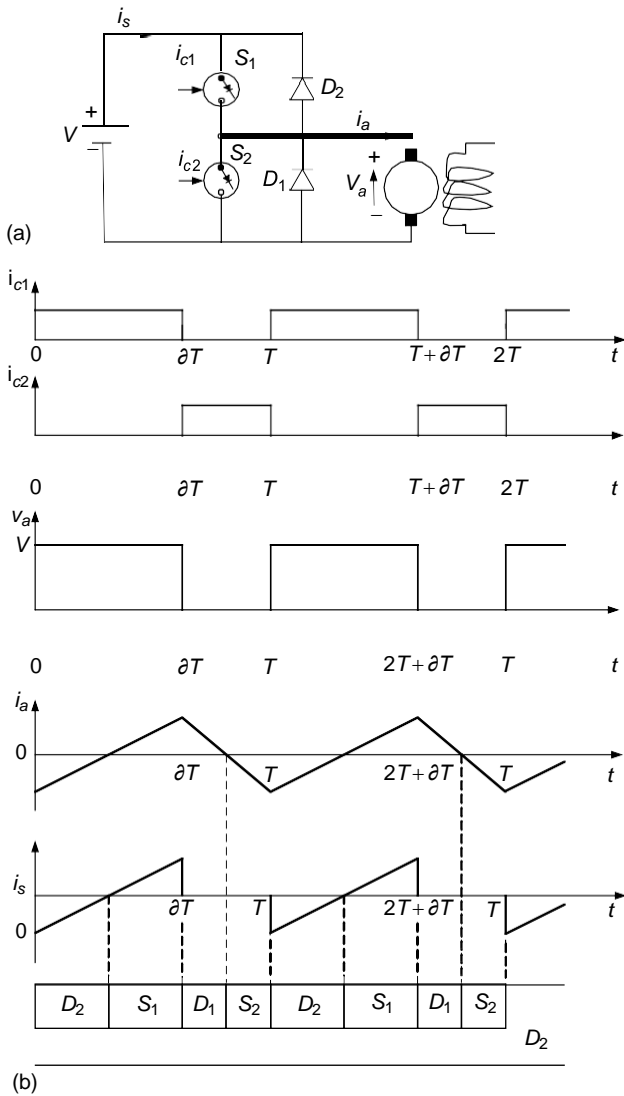


FIGURE 10
 Forward motoring and regenerative braking control using class C two-quadrant chopper:
 (a) chopper circuit and (b) waveforms

Figure 10(b). In drawing these waveforms, the delay between the turn off of one switch and the turn on of another switch has been ignored because it is usually very small. The control signals for the switches S_1 and S_2 are denoted by i_{c1} and i_{c2} , respectively. It is assumed that a switch conducts only when the control signal is present and the switch is forward biased.

The following points are helpful in understanding the operation of this two-quadrant circuit:

1. In this circuit, discontinuous conduction does not occur, irrespec-

tive of its frequency of operation. Discontinuous conduction occurs

when the armature current falls to zero and remains zero for a finite interval of time. The current may become zero either during the freewheeling interval or in the energy transfer interval. In this circuit, freewheeling will occur when S_1 is off and the current is flowing through D_1 . This will happen in interval $\delta T \leq t \leq T$, which is also the interval for which S_2 receives the control signal. If i_a falls to zero in the freewheeling interval, the back EMF will immediately drive a current through S_2 in the reverse direction, thus preventing the armature current from remaining zero for a finite interval of time. Similarly, energy transfer will be present when S_2 is off and D_2 is conducting — that is, during the interval $0 \leq t \leq \delta T$. If the current falls to zero during this interval, S_1 will conduct immediately because i_c is present and $V > E$. The armature current will flow, preventing discontinuous conduction.

2. Since discontinuous conditions are absent, the motor current will be flowing all the time. Thus, during the interval $0 \leq t \leq \delta T$, the motor armature will be connected either through S_1 or D_2 . Consequently, the motor terminal voltage will be V and the rate of change of i_a will be positive because $V > E$. Similarly, during the interval $\delta T \leq t \leq T$, the motor armature will be shorted either through D_1 or S_2 . Consequently, the motor voltage will be zero and the rate of change of i_a will be negative.
3. During the interval $0 \leq t \leq \delta T$, the positive armature current is carried by S_1 and the negative armature current is carried by D_2 . The source current flows only during this interval and it is equal to i_a . During the interval $\delta T \leq t \leq T$, the positive current is carried by D_1 and the negative current is carried by S_2 .
4. From the motor terminal voltage waveform of Figure 6.12(b), $V_a = \delta V$. Hence,

$$I_a = \frac{\delta V - E}{R_a} \quad (4.10)$$

Equation (6.13) suggests that the motoring operation takes place when $\delta > E/V$, and that regenerative braking occurs when $\delta < E/V$. The no-load operation is obtained when $\delta = E/V$.

Four-Quadrant Operation

The four-quadrant operation can be obtained by combining two class C choppers (Figure 6.12[a]) as shown in Figure 11, which is referred to as a class E chopper. In this chopper, if S_2 is kept closed continuously and S_1 and S_4 are controlled, a two-quadrant chopper is obtained, which provides positive terminal voltage (positive speed) and the armature current in either direction (positive or negative torque), giving a motor control in quadrants I and IV. Now if S_3 is kept closed continuously and S_1 and S_4 are controlled, one obtains a two-quadrant chopper, which can supply a variable negative terminal voltage (negative

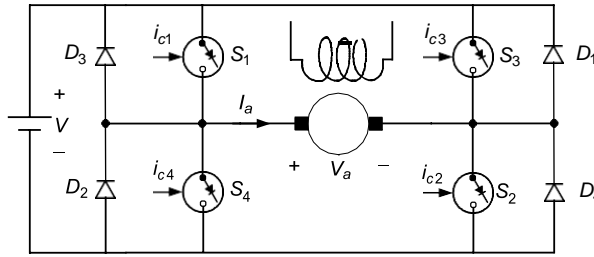


FIGURE 11
Class E four-quadrant chopper

speed) and the armature current can be in either direction (positive or negative torque), giving a motor control in quadrants II and III.

This control method has the following features: the utilization factor of the switches is low due to the asymmetry in the circuit operation. Switches S_3 and S_2 should remain on for a long period. This can create commutation problems when the switches use thyristors. The minimum output voltage depends directly on the minimum time for which the switch can be closed, since there is always a restriction on the minimum time for which the switch can be closed, particularly in thyristor choppers.⁴⁷ The minimum available output voltage, and therefore the minimum available motor speed, is restricted.

To ensure that switches S_1 and S_4 , or S_2 and S_3 are not on at the same time, some fixed time interval must elapse between the turn off for one switch and the turn on of another switch. This restricts the maximum permissible frequency of operation. It also requires two switching operations during a cycle of the output voltage.

Reference² provides other control methods to solve the problems mentioned above.

2 Induction Motor Drives

Commutatorless motor drives offer a number of advantages over conventional DC commutator motor drives for the electric propulsion of EVs and HEVs. At present, induction motor drives are the mature technology among commutatorless motor drives. Compared with DC motor drives, the AC induction motor drive has additional advantages such as lightweight nature, small volume, low cost, and high efficiency. These advantages are particularly important for EV and HEV applications.

There are two types of induction motors, namely, wound-rotor and squirrel-cage motors. Because of the high cost, need for maintenance, and lack of sturdiness, wound-rotor induction motors are less attractive than their squirrel-cage counterparts, especially for electric propulsion in EVs and HEVs. Hence, squirrel-cage induction motors are loosely termed as induction motors.

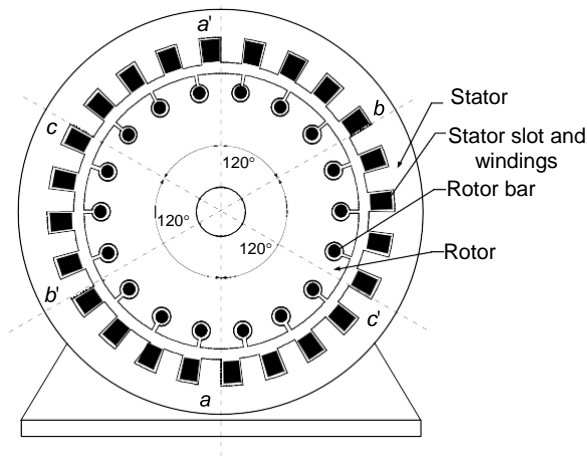


FIGURE 12
Cross-section of an induction motor

A cross section of a two-pole induction motor is shown in Figure 12. Slots in the inner periphery of the stator are inserted with three phase windings, $a-a'$, $b-b'$, and $c-c'$. The turns of each winding are distributed such that the current in the winding produces an approximately sinusoidally distributed flux density around the periphery of the air gap. The three windings are spatially arranged by 120° as shown in Figure 12.

The most common types of induction motor rotors are the squirrel cage in which aluminum bars are cast into slots in the outer periphery of the rotor. The aluminum bars are short-circuited together at both ends of the rotor by cast aluminum end rings, which can also be shaped into fans.

2.1 Basic Operation Principles of Induction Motors

Figure 6.15 shows, schematically, a cross section of the stator of a three-phase, two-pole induction motor. Each phase is fed with a sinusoidal AC current, which has a frequency of ω and a 120° phase difference between each other as shown in Figure 13. Current i_{as} , i_{bs} , and i_{cs} in the three stator coils $a-a'$, $b-b'$, and $c-c'$ produce alternative mmfs, F_{as} , F_{bs} , and F_{cs} , which are space vectors. The resultant stator mmf vector F^s , constitutes a vector sum of the phase mmf vectors.

The mmfs produced by the phase currents can be written as

$$F_{as} = F_{as} \sin \omega t, \quad (4.11)$$

$$F_{bs} = F_{bs} \sin (\omega t - 120^\circ), \quad (4.12)$$

$$F_{cs} = F_{cs} \sin (\omega t - 240^\circ). \quad (4.13)$$

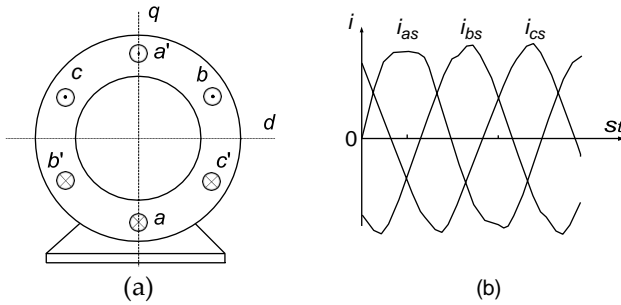


FIGURE 13

Induction motor stator and stator winding current: (a) spatially symmetric three-phase stator windings; (b) phase currents

The resultant stator mmf vector, F_s^s is expressed as

$$F_s^s = F_s e^{j0^\circ} + F_s e^{j120^\circ} + F_s e^{j240^\circ} \quad (4.14)$$

$\begin{matrix} s & as & bs & cs \end{matrix}$

Assuming that the magnitude of the three phase mmfs are identical, equal to F_s , equation (6.17) can be further expressed as

$$F_s^s = \frac{3F_s}{2} e^{j(\omega t - 90^\circ)} \quad (4.15)$$

Equation indicates that the resultant stator mmf vector is rotating with a frequency of the angular velocity of ω , and its magnitude is $(3/2)F_s$. Figure 14 graphically shows the stator mmf vectors at $\omega t = 0$ and $\omega t = 90^\circ$; here, ωt is the angle in (6.12) to (6.18), rather than the resultant stator mmf vector relative to the d -axis. Actually, if the ωt in equations is taken as the reference, the resultant stator mmf vector is a 90° delay to the phase $a-a'$ mmf.

The reaction between the rotating stator mmf and the rotor conductors induces a voltage in the rotor, and hence electric current in the rotor. In turn, the rotating mmf produces a torque on the rotor, which is carrying the induced current. It is clear that the induced current in the rotor is essential for producing the torque, and in turn the induced current depends on the relative movements between the stator mmf and the rotor. This is why there must exist a difference between the angular velocity of the rotating stator mmf and the angular velocity of the rotor.

The frequency ω , or angular velocity of the rotating stator mmf in the equation depends only on the frequency of the alternative current of the stator; thus, it is referred to as electrical angular velocity. For a machine with two poles, the electrical angular velocity is identical to the mechanical angular velocity of the rotating stator mmf.

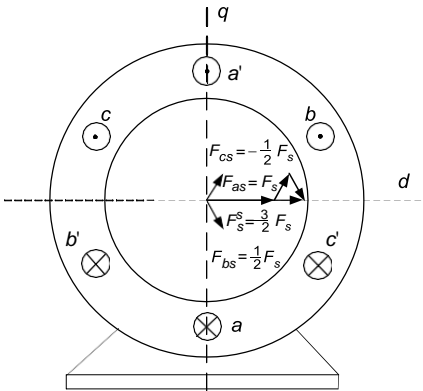
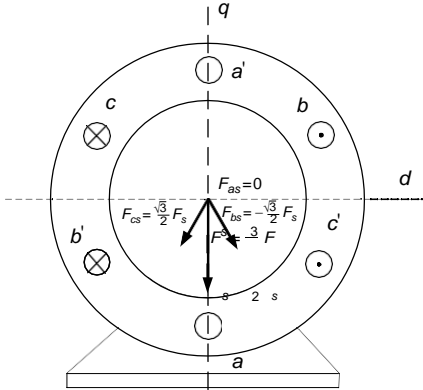
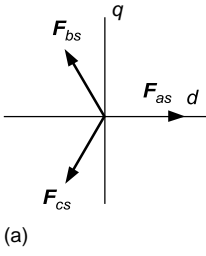


FIGURE 14

Stator mmf vectors: (a) positive direction of each phase (b) stator mmf vectors at $\omega t = 0$ and (c) stator mmf vectors at $\omega t = 90^\circ$

where f is the frequency of the alternative current or angular velocity of the rotating stator mmf in cycles/sec. When the angular velocity of the rotor is equal to the mechanical angular velocity of the rotating stator mmf, there will be no induced current in the rotor, and then no torque is produced. Thus, the mechanical angular velocity of the rotating stator mmf is also called synchronous speed.

If the rotor speed is ω_m rad/sec, then the relative speed between the stator rotating field and the rotor is given by

$$\omega_{sl} = \omega_{ms} - \omega_m = s\omega_{ms} \quad (4.16)$$

where ω_{sl} is called slip speed. The parameter s , known as slip, is given by

$$s = \frac{\omega_{ms} - \omega_m}{\omega_{ms}} = \frac{\omega_{sl}}{\omega_{ms}}. \tag{4.17}$$

Because of the relative speed between the stator field and the rotor, balanced three-phase voltages are induced in the rotor mentioned before. The frequency of these voltages is proportional to the slip speed. Hence,

$$\omega_r = \frac{\omega_{sl}}{\omega_{ms}} \omega = s\omega, \tag{4.18}$$

where ω_r is the frequency of the rotor voltage induced.

For $\omega_m < \omega_{ms}$, the relative speed is positive; consequently, the rotor-induced voltages have the same phase sequence as the stator voltages. The three-phase current flowing through the rotor produces a magnetic field that moves with respect to the rotor at the slip speed in the same direction as the rotor speed. Consequently, the rotor field moves in space at the same speed as the stator, and a steady torque is produced. For $\omega_m = \omega_{ms}$ the relative speed between the rotor and stator field becomes zero. Consequently, no voltages are induced and no torque is produced by the motor. For $\omega_m < \omega_{ms}$, the relative speed between the stator field and the rotor speed reverses. Consequently, the rotor-induced voltages and currents also reverse and have a phase sequence opposite to that of the stator. Moreover, the developed torque has a negative sign, suggesting generator operation. (The generator is used to produce regenerative braking.)

2.2 Steady-State Performance

A per phase equivalent circuit of an induction motor is shown in Figure 6.15(a). The fields produced by the stator and rotor are linked together by an ideal transformer. a_{T1} is the transformer factor, which is equal to n_s/n_r , where n_s and n_r are the number of turns of stator and rotor windings, respectively. For a squirrel-cage rotor, $n_r = 1$. The equivalent circuit can be simplified by referring the rotor quantities to the stator frequency and number of turns. The resultant equivalent circuit is shown in Figure 6.15(b) where R'_r and X'_r are the rotor resistance and reactance referred to the stator and are given by the following equations:

$$R'_r = a^2_{T1} R_r \quad \text{and} \quad X'_r = a^2_{T1} X_r. \tag{4.19}$$

The stator reactance, mutual reactance, and rotor reactance referred to the stator can be expressed by the stator frequency and their inductances, L_s , L_m , and L_r , as shown in Figure 6.17. The impedances of stator, field, and rotor can be expressed as

$$Z_s = R_s + jL_s \omega, \tag{4.20}$$

$$Z_m = \bar{K}_r jL_m \omega, \tag{4.21}$$

$$Z_r = \frac{\bar{K}_r}{s} jL_r \omega. \tag{4.22}$$

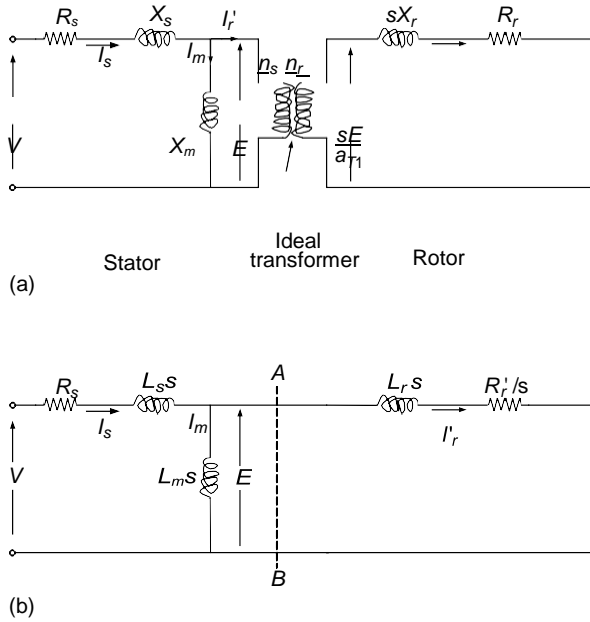


FIGURE 15
 Per phase equivalent circuit of an induction motor: (a) per phase equivalent circuit and (b) per phase equivalent circuit refer to the stator

The driving-point impedance of the circuit is

$$Z = Z_s + \frac{Z_m Z_r}{Z_m + Z_r} \tag{4.23}$$

Hence, the current I_s and I_r' can be calculated as

$$I_s = \frac{V}{Z} \tag{4.24}$$

and

$$I_r' = \frac{Z_m}{Z} \frac{Z_r}{Z_r + Z_m} I_s \tag{4.25}$$

The total electrical power supplied to the motor for three phase is

$$P_{elec} = 3 I_r'^2 \frac{R_r'}{s} \tag{4.26}$$

The mechanical power of the rotor can be obtained by subtracting the total power loss in the stator as

$$P_{mech} = P_{elec} - 3 I_r'^2 R_r' \tag{4.27}$$

The angular velocity of the rotor, ω_m , is

$$\omega_m = \frac{2}{p} \omega (1-s). \quad (4.28)$$

The torque developed by the motor can be determined by

$$T = \frac{P_{mech}}{\omega_m} \tag{4.29}$$

Figure 16 shows the torque–slip characteristics of an induction motor, which has fixed voltage and frequency. In the region of $0 < s < s_{m'}$ where $s_{m'}$ is the rated slip of the motor, the torque increases approximately linearly with the increase of slip until reaching its maximum at $s = s_{m'}$; then it decreases as the slip further increases. At $s = 1$, the rotor speed is zero and the corresponding torque is the starting torque, which is less than its torque at $s = s_{m'}$. The region of $0 < s < 1$ is the forward motoring region. In the region of $s > 1$, the rotor torque further decreases with the increase of slip, and rotor speed is negative, according to (6.21). Thus, in this region, the operation of the motor is reverse braking. In the region of $s < 0$, that is, when the rotor speed is greater than the synchronous speed, the motor produces a negative torque.

It is clear that the speed–torque characteristics of a fixed voltage and frequency induction motor are not appropriate to vehicle traction applications. This is due to the low starting torque, limited speed range, and unstable operation in the range of $s > s_{m'}$ in which any additional disturbing torque in the load will lead the machine to stop as the torque decreases with the speed-decreasing characteristics. High slip also results in high current, which may cause damage to the stator windings. Actually, the operation of the fixed voltage and frequency induction motor are usually operated in the narrow slip range of $0 < s < s_{m'}$. Thus, for traction application, an induction motor must be controlled to provide proper speed–torque characteristics.

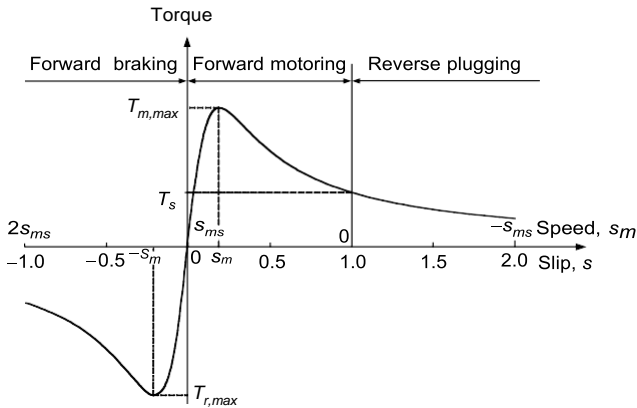


FIGURE 16 Torque–slip characteristics of an induction motor with fixed stator frequency and voltage

2.3 Constant Volt/Hertz Control

For traction application, the torque–speed characteristic of an induction motor can be varied by simultaneously controlling the voltage and frequency, which is known as constant volt/hertz control. By emulating a DC motor at low speed, the flux may be kept constant. According to Figure 6.17(b), the field current I_m should be kept constant and equal to its rated value. That is,

$$I_{mr} = \frac{E}{X_m} = \frac{E_{rated}}{\omega_r L_m}, \quad (4.30)$$

where I_{mr} is the rated field current, and E_{rated} and ω_r are the rated mmf and frequency of the stator, respectively. To maintain the flux at constant, E/ω should be kept constant and equal to E_{rated}/ω_r . Ignoring the voltage drop in the stator impedance Z_s results in a constant V/ω until the frequency and voltage reach their rated values. This approach is known as constant volt/hertz control.²

From Figure 6.17(b), the rotor current can be calculated as

$$I_r' = \frac{(\omega/\omega_r) E_{rated}}{jL(\omega) \frac{R_r'}{R_r} + \omega_r + j\omega_r s} \quad (4.31)$$

The torque produced can be obtained as

$$T = \frac{3}{\omega} I_r'^2 R_r' / s = \frac{3}{\omega} \left[\frac{(\omega_r)^2 \omega_{rated} R_r' / s}{(R_r' / s)^2 + (L \omega)^2} \right]. \quad (4.32)$$

The slip s_m corresponding to the maximum torque is

$$s_m = \pm \frac{R_r'}{L_r \omega}. \quad (4.33)$$

And then, the maximum torque is

$$T_{max} = \frac{3}{2} \frac{E^2}{L_r \omega^2}. \quad (4.34)$$

Equation (4.34) indicates that with the constant E/ω , the maximum torque is constant with varying frequency. Equation (4.33) indicates that $s_m \omega$ is constant, resulting in constant slip speed, ω_{sl} . In practice, due to the presence of stator impedance and the voltage drop, the voltage should be somewhat higher than that determined by constant E/ω , as shown in Figure 17.

When motor speed is beyond its rated speed, the voltage reaches its rated value and cannot be increased with the frequency. In this case, the voltage is fixed to its rated value and the frequency continuously increases with the motor speed. The motor goes into the field weakening operation. The slip s is fixed to its rated value corresponding to the rated frequency, and the slip speed ω_{sl} increases linearly with motor speed. This control approach results

in constant power operation as shown in Figure 17.

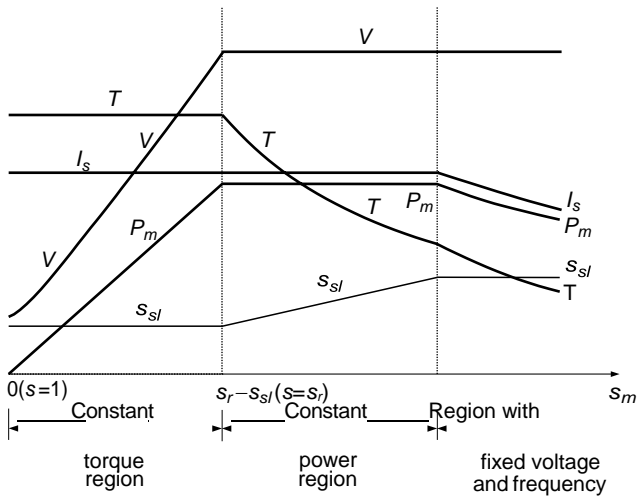


FIGURE 17
Operating variables varying with motor speed

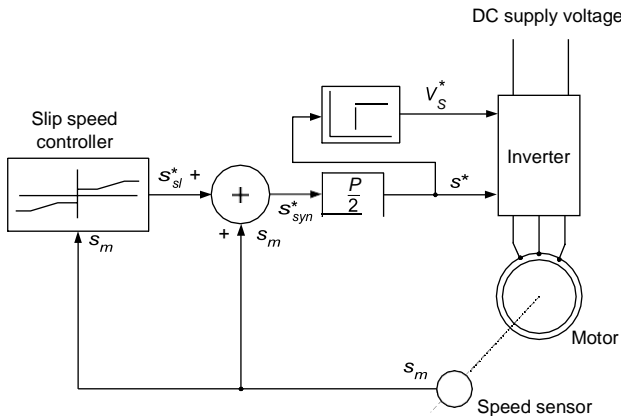


FIGURE 18
General configuration of constant V/f control

In traction application, speed control in a wide range is usually required and the torque demand in the high-speed range is low. Control beyond constant power range is required. To prevent the torque from exceeding the breakdown torque, the machine is operated at a constant slip speed and the machine current and power are allowed to decrease as shown in Figure 17. Figure 18 shows a general block diagram where constant V/f control is implemented.

2.4 Power Electronic Control

As EV and HEV propulsion, an induction motor drive is usually fed with a DC source (battery, fuel cell, etc.), which has approximately constant

terminal voltage. Thus, a variable frequency and variable voltage DC/AC inverter is needed to feed the induction motor. The general DC/AC inverter is constituted by power electronic switches and power diodes. The commonly used topology of a DC/AC inverter is shown in Figure 6.21(a), which has three legs (S_1 and S_4 , S_3 and S_6 , and S_5 and S_2), feeding phase a , phase b , and phase c of the induction motor, as shown in Figure 6.19(a). When switches S_1 , S_3 , and S_5 are closed, S_4 , S_6 , and S_2 are opened, and phases a , b , and c are supplied with a positive voltage ($V_d/2$). Similarly, when S_1 , S_3 , and S_5 are opened and S_4 , S_6 , and S_2 are closed, phases a , b , and c are supplied with a negative voltage. All the diodes provide a path for the reverse current of each phase.

For constant volt/hertz control of an induction motor, sinusoidal pulse-width modulation (PWM) is used exclusively. Three-phase reference voltages V_a , V_b , and V_c of variable amplitudes A_a , A_b , and A_c are compared with a common isosceles triangular carrier wave V_{tr} of a fixed amplitude A_m as shown in Figure 6.21(c). The outputs of comparators 1, 2, and 3 form the control signals for the three legs of the inverter. When the sinusoidal reference voltage V_a , V_b , and V_c at a time t is greater than the triangular waved voltage, turn-on signals are sent to the switches S_1 , S_3 , and S_5 and turn-off signals are sent to S_4 , S_6 , and S_2 . Thus, the three phases of the induction motor have a positive voltage. On the other hand, when the reference sinusoidal voltage is smaller than the triangular wave voltage, turn-on signals are sent to the switches S_1 , S_3 , and S_5 and turn-off signals are sent to S_4 , S_6 , and S_2 . The three phases of the induction motor then have a negative voltage. The voltages of the three phases are shown in Figure 6.21(d) to (f).

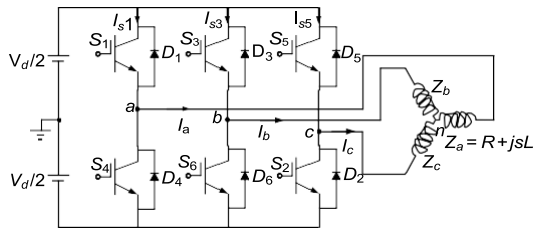
The frequency of the fundamental component of the motor terminal voltage is the same as that of the reference sinusoidal voltage. Hence, the frequency of the motor voltage can be changed by the frequency of the reference voltage. The ratio of the amplitude of the reference wave to that of the triangular carrier wave, m , is called the modulation index; therefore,

$$m = \frac{A}{A_m}, \tag{4.35}$$

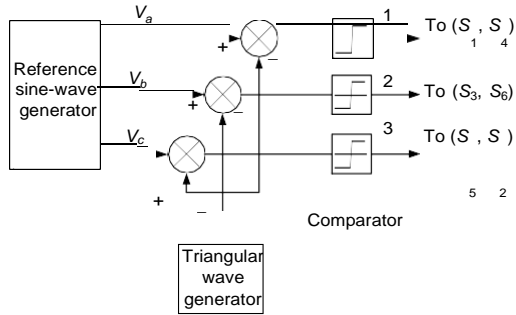
where A is the multitude of the reference sinusoidal voltage, V_a , V_b , or V_c , and A_m is the multitude of angular carrier voltage. The fundamental (rms) component in the phase waveform, V_{aor} , V_{bor} , or V_{cor} is given by

$$V = \frac{mV_d}{2\sqrt{2}}. \tag{4.36}$$

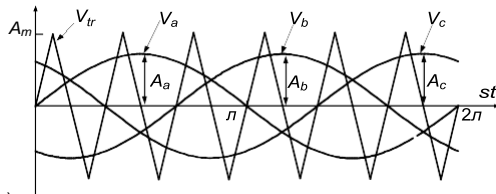
Thus, the fundamental voltage increases linearly with m until $m = 1$ (that is, when the amplitude of the reference wave becomes equal to that of the carrier wave). For $m > 1$, the number of pulses in V_{aor} , V_{bor} , or V_{cor} becomes less and the modulation ceases to be sinusoidal.²



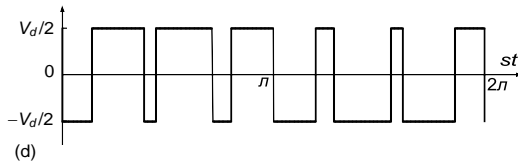
(a)



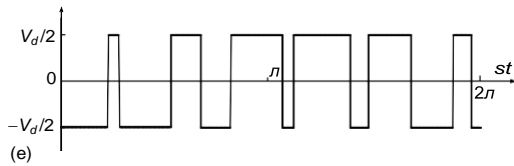
(b)



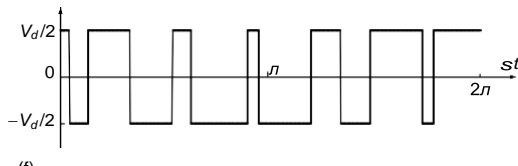
(c)



(d)



(e)



(f)

FIGURE 19

DC/AC inverter with sinusoidal PWM: (a) inverter topology; (b) control signals; (c) three phase reference voltage and a common isosceles triangular carrier wave; (d) voltage of phase *a*; (e) voltage of phase *b*; and (f) voltage of phase *c*

Field Orientation control

- AC **Induction motors** offer desirable operational characteristics such as robustness, reliability and ease of control.
- They are extensively used in various applications ranging from industrial motion control systems to home appliances.
- However, the use of induction motors at its highest efficiency is a challenging task because of their complex mathematical model and non-linear characteristic during saturation.
- These factors make the control of induction motor difficult and call for the use of a high performance control algorithms such as vector control.

Introduction of Field Oriented Control

- The scalar control method for induction motors generates oscillations on the produced torque. Hence to achieve better dynamic performance, a more superior control scheme is needed for Induction Motor.
- With the mathematical processing capabilities offered by the micro-controllers, digital signal processors and FPGA, advanced control strategies can be implemented to decouple the torque generation and the magnetization functions in an AC induction motor.
- This **decoupled torque** and **magnetization flux** is commonly called rotor **Flux Oriented Control (FOC)**.
- **Field Oriented Control** describes the way in which the control of torque and speed are directly based on the electromagnetic state of the motor, similar to a **DC motor**.
- FOC is the first technology to control the “real” motor control variables of torque and **flux**.

- With decoupling between the stator **current** components, the torque producing component of the stator flux can be controlled independently.
- FOC has been solely developed for high-performance motor applications which can operate smoothly over the wide speed range, can produce full torque at zero speed, and is capable of quick acceleration and deceleration.

Working Principle of Field Oriented Control

- The **field oriented control** consists of controlling the stator currents represented by a vector. This control is based on projections that transform a three phase time and speed dependent system into a two coordinate (d and q frame) time invariant system.
- These transformations and projections lead to a structure similar to that of a DC machine control.
- FOC machines need two constants as input references: the torque component (aligned with the **q coordinate**) and the flux component (aligned with **d coordinate**).

-

The three-phase voltages, currents and **fluxes** of AC-motors can be analyzed in terms of complex space vectors. If we take i_a , i_b , i_c as instantaneous currents in the stator phases, then the stator **current** vector is defined as follow:

$$\vec{i}_s = i_a + i_b e^{j2\pi/3} + i_c e^{j4\pi/3}$$

Where, (a, b, c) are the axes of **three phase system**.

This **current** space vector represents the three phase sinusoidal system.

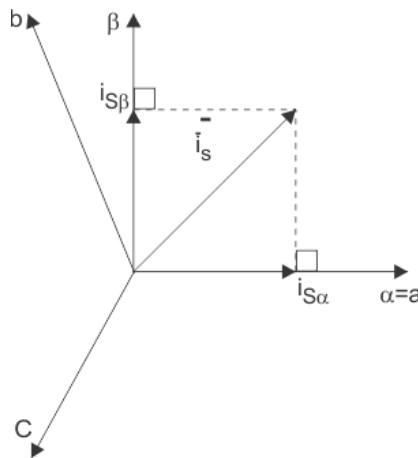
It needs to be transformed into a two time invariant coordinate system. This transformation can be divided into two steps: (a, b, c) \rightarrow (α , β) (the Clarke transformation), which gives outputs of two coordinate time variant system. (a, β) \rightarrow (d, q) (the Park transformation), which gives outputs of two coordinate time invariant system.

The (a, b, c) → (α, β) Projection (Clarke transformation)

Three-phase quantities either voltages or currents, varying in time along the axes a, b, and c can be mathematically transformed into two-phase voltages or currents, varying in time along the axes α and β by the following transformation matrix:

$$i_{\alpha\beta 0} = \frac{2}{3} * \begin{bmatrix} 1 & -\frac{1}{2} & -\frac{1}{2} \\ 0 & \frac{\sqrt{3}}{2} & -\frac{\sqrt{3}}{2} \\ \frac{1}{2} & \frac{1}{2} & \frac{1}{2} \end{bmatrix}$$

Assuming that the axis a and the axis α are along same direction and β is orthogonal to them, we have the following vector diagram:



The above projection modifies the three phase system into the (α, β) two dimension orthogonal system as stated below:

$$\begin{aligned} i_{s\alpha} &= i_a \\ i_{s\beta} &= i_a/\sqrt{3} + 2i_b/\sqrt{3} \end{aligned}$$

But these two phase (α, β) currents still depends upon time and

speed.

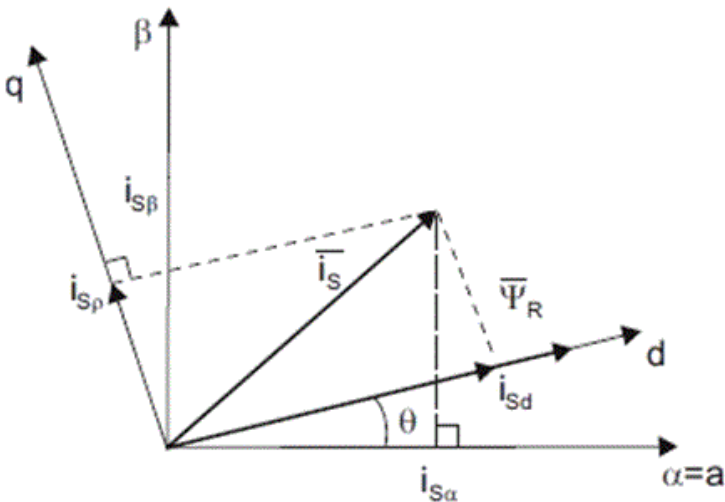
The $(\alpha, \beta) \rightarrow (d,q)$ projection (Park transformation)

This is the most important transformation in the FOC. In fact, this projection modifies the two phase fixed orthogonal system (α, β) into d, q rotating reference system. The transformation matrix is given below:

$$i_{dq0} = 2/3 * \begin{bmatrix} \cos\theta & \cos\left(\theta - \frac{2\pi}{3}\right) & \cos\left(\theta + \frac{2\pi}{3}\right) \\ \sin\theta & \sin\left(\theta - \frac{2\pi}{3}\right) & \sin\left(\theta + \frac{2\pi}{3}\right) \\ \frac{1}{2} & \frac{1}{2} & \frac{1}{2} \end{bmatrix}$$

Where, θ is the angle between the rotating and fixed coordinate system.

If you consider the d axis aligned with the rotor flux, Figure 2 shows the relationship from the two reference frames for the **current** vector:



Where, θ is the rotor flux position. The torque and flux

components of the **current** vector are determined by the following equations:

$$\begin{aligned}i_{sq} &= i_{s\alpha}\sin\theta + i_{s\beta}\cos\theta \\i_{sd} &= i_{s\alpha}\cos\theta + i_{s\beta}\sin\theta\end{aligned}$$

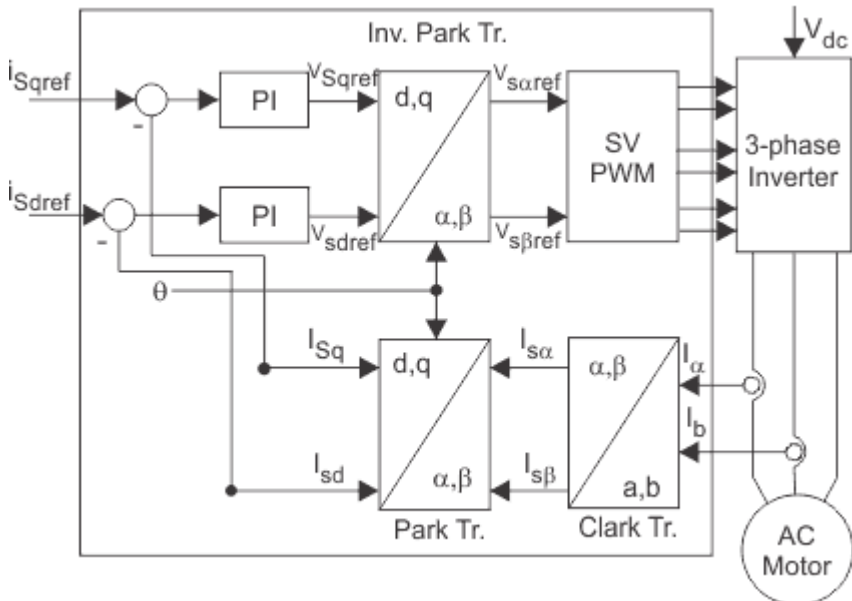
These components depend on the current vector (α, β) components and on the rotor flux position. If you know the accurate rotor flux position then, by above equation, the d, q component can be easily calculated. At this instant, the torque can be controlled directly because flux component (i_{sd}) and torque component (i_{sq}) are independent now.

Basic Module for Field Oriented Control

Stator phase currents are measured. These measured currents are fed into the Clarke transformation block. The outputs of this projection are entitled $i_{s\alpha}$ and $i_{s\beta}$. These two components of the current enter into the Park transformation block that provide the **current** in the d, q reference frame. The i_{sd} and i_{sq} components are contrasted to the references: i_{sdref} (the flux reference) and i_{sqref} (the torque reference). At this instant, the control structure has an advantage: it can be used to control either synchronous or induction machines by simply changing the flux reference and tracking rotor flux position. In case of PMSM the rotor flux is fixed determined by the magnets so there is no need to create one. Therefore, while controlling a PMSM, i_{sdref} should be equal to zero. As **induction motors** need a rotor flux creation in order to operate, the flux reference must not be equal to zero. This easily eliminates

one of the major shortcomings of the “classic” control structures: the portability from asynchronous to synchronous drives. The outputs of the PI controllers are V_{sdref} and V_{sqref} . They are applied to the inverse Park transformation block. The outputs of this projection are $V_{s\alpha ref}$ and $V_{s\beta ref}$ are fed to the space vector pulse width modulation (SVPWM) algorithm block. The outputs of this block provide signals that drive the inverter. Here both Park and inverse Park transformations need the rotor flux position. Hence rotor flux position is essence of FOC. The evaluation of the rotor flux position is different if we consider the synchronous or induction motor.

- In case of **synchronous motor(s)**, the rotor speed is equal to the rotor flux speed. Then rotor flux position is directly determined by position **sensor** or by integration of rotor speed.
- In case of **asynchronous motor(s)**, the rotor speed is not equal to the rotor flux speed because of slip; therefore a particular method is used to evaluate rotor flux position (θ). This method utilizes **current model**, which needs two equations of the **induction motor** model in d,q rotating reference frame.



Simplified Indirect FOC Block Diagram

Classification of Field Oriented Control

FOC for the **induction motor drive** can be broadly classified into two types: Indirect FOC and Direct FOC schemes. In DFOC strategy rotor flux vector is either measured by means of a flux sensor mounted in the air-gap or by using the **voltage** equations starting from the electrical machine parameters. But in case of IFOC rotor flux vector is estimated using the **field oriented control** equations (current model) requiring a rotor speed measurement. Among both schemes, IFOC is more commonly used because in closed-loop mode it can easily operate throughout the speed range from zero speed to high-speed field-weakening.

Advantages of Field Oriented Control

1. Improved torque response.
2. Torque control at low frequencies and low speed.
3. Dynamic speed accuracy.
4. Reduction in size of motor, cost and power consumption.
5. Four quadrant operation.
6. Short-term overload capability.

3 PMBLDC motor drive

The conventional DC motors are highly efficient and their characteristics make them suitable for use as servomotors. But the only drawback is that they need a commutator and brushes which are subjected to wear and requires maintenance. In a conventional DC motor, commutation is undertaken by brushes and commutator but in brushless DC motor, it is done by using semiconductor devices such as transistors. The commutation refers to the process which converts the input direct current to an alternating current and properly distributes it to each winding in the armature.

3.1 Construction

- The construction of modern brushless DC motor is very similar to the AC motor. It consists of two important main parts (ie) stator and rotor.
- The stator which is the stationary parts has got stator frame which encloses the internal parts of the motor and protects it and it is made up of cast iron (or) steel.
- Beneath the stator frame, stator poles are fixed which are of projective type which may be laminated or solid piece and it is mostly made of silicon steel material.
- The stator windings are placed on the stator poles .They may be copper windings and may be single (or) Double layer winding.
- The stator windings are excited by the DC supply through the controllable switches.
- The rotor construction is very simple (ie) it has permanent magnets of one (or) two number with their poles, which may be projecting pole type.
- The rotor doesn't carry any winding, brushes (or) commutator segments. The maintenance is less and inertia is low.
- The rotor positions are sensed by position sensors such as Hall elements (or) optical encoders which are fixed on the shaft of the motor.
- The constructional details are shown in the figure 4.1

3.3 Basic Principle of operation of PMBLDC Motor

- The basic principle of operation of motor can be easily understand by considering simple three phase unipolar motor as shown in the figure 4.2
- It uses optical sensors (photo transistors) as position detectors. Three photo transistors PT_1 , PT_2 , and PT_3 are placed on the end plates at 120° interval and they are exposed to light in sequence through a revolving shutter coupled to the motor shaft.

- As shown in the figure 4.2, the south pole of the rotor now faces the salient pole P_2 of the stator, and the phototransistor PT_1 detects the light and turns transistor Tr_1 ON.
- In this state, the south pole which is created by the salient pole P_1 by the electrical current flowing through the winding w_1 is attracting the north pole of the rotor to move it in the direction of the arrow (CCW).

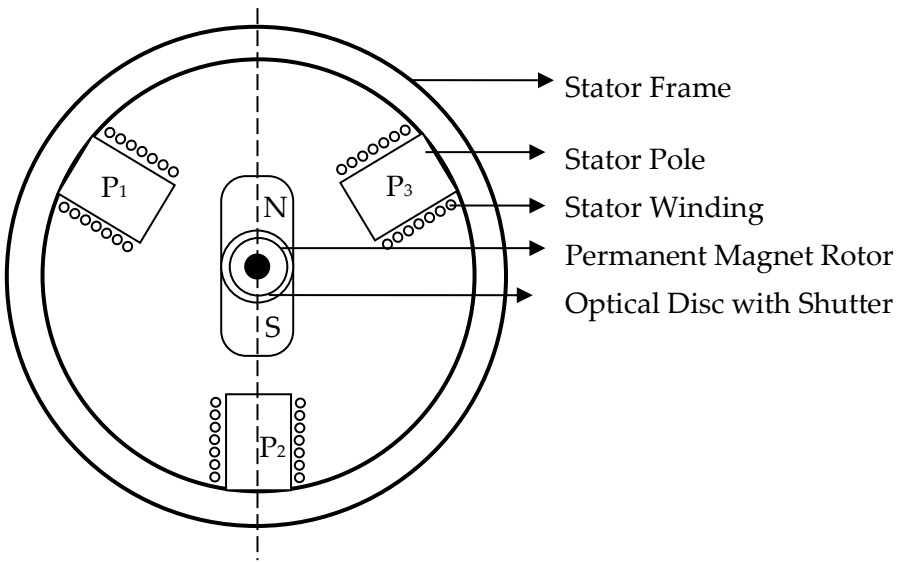


Fig 4.1 constructional details

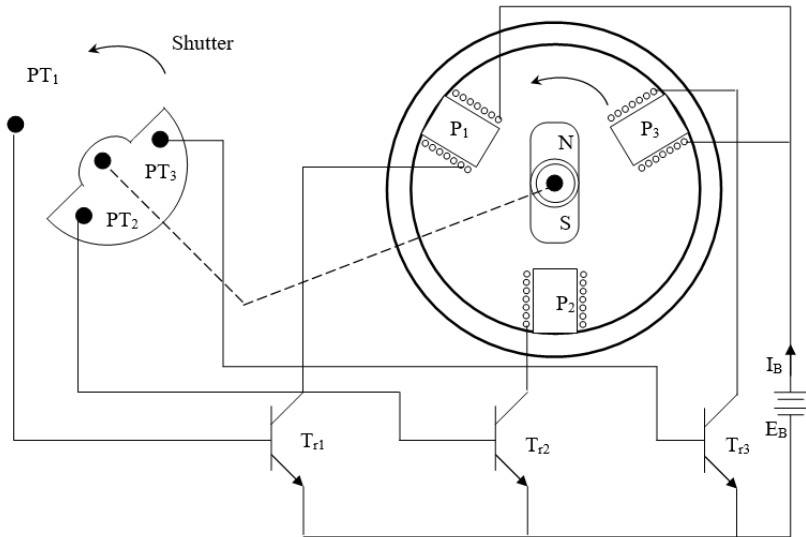


Fig 4.2 Rotor construction

- When the south pole comes to the position to face the pole P₁ the shutter which is coupled to rotor shaft will shade PT₁ and PT₂ will be exposed to the light and current will flow through the transistor Tr₂.
- When a current flows through the winding W₂ and creates a south pole on pole P₂, then the north pole of the rotor will revolve in the direction of the arrow and face the pole P₂. At this moment, the shutter shades PT₂ and PT₃ is exposed to light.
- Thus the P₂ is de-energised and P₃ is energized. By repeating such a switching action in the sequence the permanent magnet rotor revolves continuously.
- In order to reverse the direction of rotation of the motor, we can't change the supply terminal because most of the semiconductor devices are unidirectional switches.
- Therefore some circuit is necessary when the motor is to be driven in either direction. So we go for circuit connections change between the phototransistors and the transistors as given below.

For CCW rotation

PT1 → TR1

PT2 → TR2

PT3 → TR3

For CW rotation

PT1 → TR3

PT2 → TR2

PT3 → TR1

The switching sequence for CCW & CW is given below.

	CCW				CW			
PT ₁	1	0	0	1	1	0	0	1
PT ₂	0	1	0	0	0	1	0	0
PT ₃	0	0	1	0	0	0	1	0
TR ₁	1	0	0	1	0	0	1	0
TR ₂	0	1	0	0	0	1	0	0
TR ₃	0	0	1	0	1	0	0	1

The above switching sequences between the phototransistors and the transistors can be implemented by using integrated logic gate circuits. The rotation of stator magnetic field with respect to the excitation of the winding and the respective photo transistor waveforms are shown in the figure 4.3 for CCW rotational direction.

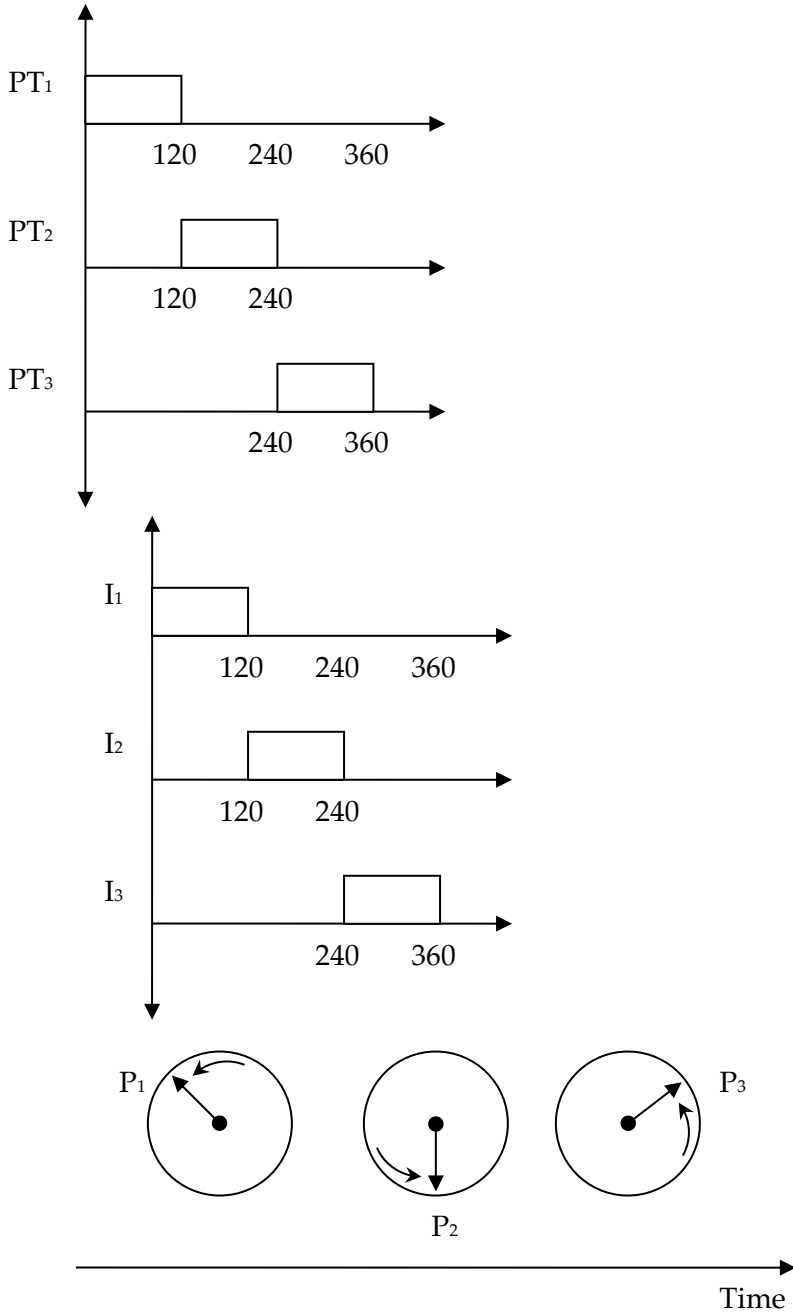


Fig 4.3 photo transistor waveforms

3.3 Comparison of Conventional and Brushless DC Motor:

Description	Conventional Motor	Brushless Motor
-------------	--------------------	-----------------

Mechanical structure	Field magnets on the stator	Field magnets on the rotor
Distinctive features	Quick response and excellent controllability	Long lasting, easy maintenance
Winding connection	Ring (or) Δ connection	Δ (or) Y connected three phase winding (or) Two phase winding
Commutation methods	Mechanical contact between brushes and commutator	Electronic switching using transistors
Detecting method of rotor's position	Automatically detected by brushes	Hall elements optical encoders etc.,
Reversing method	By reversal of terminal voltage	Rearranging the logic sequences

Advantages

1. Brushes maintenance is no longer required and many problems associated with brushes are eliminated
2. Radio-frequency interference and the sparking associated with the brushes are eliminated.
3. The conduction of heat through the frame is improved.
4. Increase in the electric loading is possible by providing greater specific torque.
5. The efficiency is likely to be higher than that of DC motor of equal size.
6. Motor length is reduced.
7. The maximum speed of brushless motor is limited by the retention of the magnets against centrifugal force.
8. Better efficiency, power factor and greater output power.

Disadvantages

1. The need for shaft position sensing

2. Increased complexity in the electronic controller.
3. It is difficult to operate the motor in Field weakening mode providing a constant power capability at high speed.
4. In very large motors, PM excitation does not make sense because the magnet weight becomes excessive.
5. Design of logical control circuit is somewhat complex and costlier.

3.4 TORQUE-SPEED CHARACTERISTICS OF BLDC MOTOR

The torque speed characteristics of the ideal brushless motor can be derived from the following equations. If the commutation is perfect and the current waveforms are exactly rectangular and if the converter is supplied from an ideal direct voltage source V , then at any instant the following equation can be written for the DC terminal voltage.

$$V = E + RI$$

Where R is the sum of two phase resistance in series and E is the sum of two phase Emf's in series. This equation is exactly the same as that of the commutator motor.

The voltage drops across two converter switches in series are omitted, but they correspond exactly to the two brush voltage drops in series in the commutator motor.

The torque speed equation is written as

$$\omega = \omega_o \left[1 - \frac{T}{T_o} \right]$$

Where the no load speed is $\omega_o = \frac{V}{k\phi}$ rad/sec

and the stall torque is given by $T_o = K\phi I_o$

This is the torque with the motor stalled (ie) at zero speed.

The stalling current is given by

$$I_o = \frac{V}{R}$$

This characteristic is shown in Figure 4.13

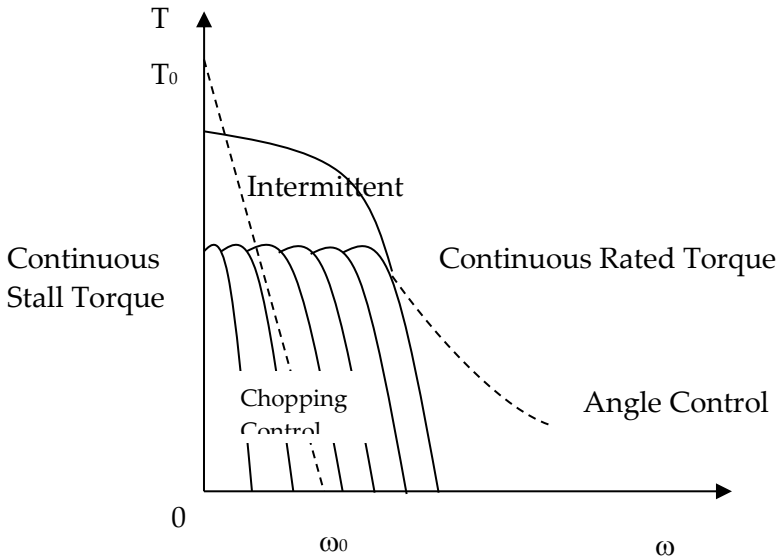


Fig 4.13

If the phase resistance is small, as it should be an efficient design, then characteristic is similar to that of a DC shunt Motor. The speed is essentially controlled by the voltage V , and may be varied by varying the supply voltage. The motor then draws just enough current to drive the torque at this speed. As the load torque is increased, the speed drops and the drop is directly proportional to the phase resistance and the torque.

The voltage is usually controlled by chopping or PWM. This gives rise to a family of the torque-speed curve as shown. Note the boundaries of continuous and intermittent operation. The continuous limit is usually determined by heat transfer and temperature rise. The intermittent limit may be determined by the maximum rating of semiconductor Devices in the controller (or) by temperature rise.

In practice the torque speed curve deviates from the ideal form because of the effects of inductance and other parasitic influences. The curve also shows the possibility of extending the speed range by advancing the phase (or) the dwell of the conduction period relative to the rotor position (ie) Angle control.

3.5 TORQUE AND EMF EQUATION OF BLDC MOTOR

The basic Torque & Emf equations of the BLDC motor are quite simple and resemble those of the DC commutator Motor.

A simple concept machine is shown in figure 4.14 Note that the two pole magnet has a pole arc of 180° instead of 120° analyzed in the previous section.

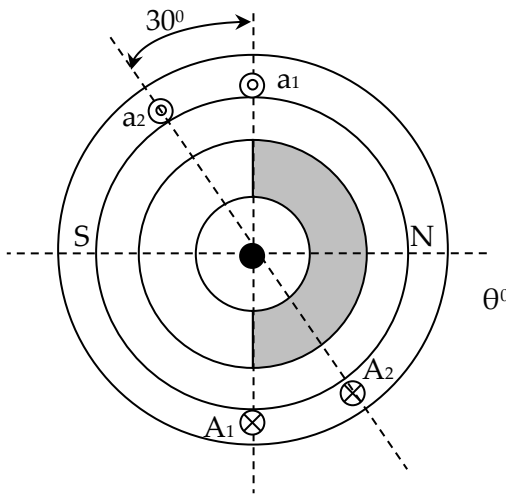


Fig 4.14

The airgap flux density waveform is ideally a square wave as shown 4.15a. In practice, fringing causes to be somewhat rounded. The coordinate axes have been chosen so that the centre of a north pole of the magnet is aligned with x-axis (ie) at $\theta = 0$. The stator has 12 slots and three phase winding. Thus there are two slots per pole per phase. Each phase winding consists of two adjacent full pitch coils of N_1 turns each, whose axes are displaced from one another by 30 degree.

The winding is a single layer winding. This winding is equivalent with only one coil per pole per phase having a fractional pitch of 5/6. This is more practical winding than the one analyzed because it has less bulky end windings and is generally easier to assemble and its copper losses are lower.

Consider the flux linkage ψ_1 of coil a_1A_1 as the rotor rotates. This is shown in the figure 4.14 Note that θ now represents the movements of the rotor from the reference position in the figure 4.14 The flux linkage varies linearly with rotor position because the airgap flux density is constant over each pole pitch of the rotor. Maximum positive flux linkage occurs at 0° and maximum negative flux linkage at 180° . By integrating the flux density around the airgap, the maximum flux linkage of the coil can be found as

$$\begin{aligned}\Psi_{1\max} &= N_1 \int_0^\pi B(\theta) r_1 l d\theta \\ &= N_1 B_g \pi r_1 l\end{aligned}$$

The variation of flux linkage with θ as the rotor rotates from 0° to 180° is given by

$$\psi_1(\theta) = \left[1 - \frac{\theta}{\pi/2} \right] \psi_{1\max}$$

The emf induced in coil a_1A_1 is given by

$$e_1 = -\frac{d\psi_1}{dt} = -\frac{d\psi_1}{d\theta} \times \frac{d\theta}{dt} = -\omega \frac{d\psi_1}{d\theta}$$

which gives

$$e_1 = 2N_1 B_g l r_1 \omega \quad (\text{volts})$$

Where $2N_1$ = Number of turns per Coil-1 = N_{ph}

Therefore $e_1 = N_{ph} B_g l r_1 \omega$ volts

Similarly $e_2 = N_{ph} B_g l r_1 \omega$ Volts

The sum of the EMFs $e_{ph} = e_1 + e_2 = 2N_{ph} B_g l r_1 \omega$ volts

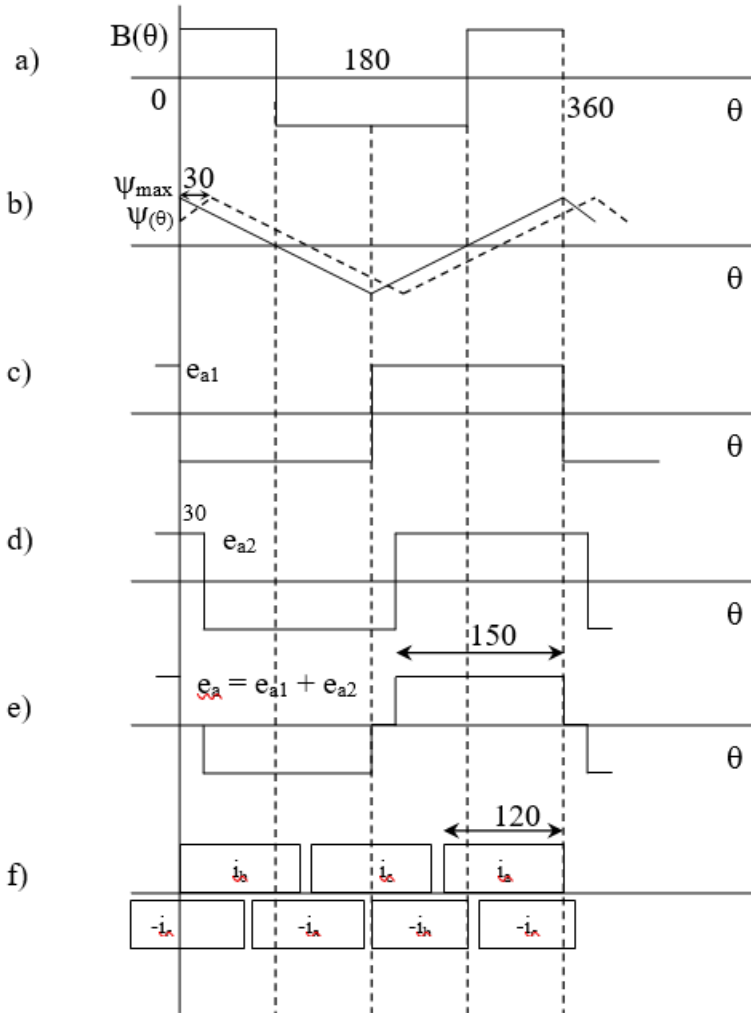


Fig 4.15

This represents the magnitude of the square wave Emf e_{a1} shown in the figure 4.15c. The Emf induced in the second coil of phase A is identical, but rotated in phase by 30° . If the two coils are connected in series, the total phase voltage is sum of the two separate coil voltages and

this is shown in figure 4.15e. The basic effect of distributing the winding into two coils is to produce a stepped Emf waveform. In practice, fringing causes its corners to be rounded. The wave form then has the "trapezoidal" shape, i.e., characteristics of the brushless DC Motor. With 180° magnet arcs and two slots per pole per phase, the flat top of this waveform is ideally 150° wide but in practice the fringing field reduces this to smaller value (i.e.) 120°. The magnitude of the flat topped phase emf is given by

$$e_{ph} = e_1 + e_2 = 2N_{ph} B_g l r_1 \omega \quad \text{volts}$$

where $N_{ph} = 2N_1$ because two coils are assumed to be in series.

In a machine with P pole pairs, the equation remains valid provided N_{ph} is the number of turns in series per phase and ω is in mechanical radians per second.

In the figure 4.15f shows an ideal rectangular waveform of phase current, in which the current pulses are 120° electrical degree wide and of magnitude I . The positive direction of current is motoring current. The conduction periods of the three phases are symmetrically phased so as to produce a three phase set of balanced 120° square waves.

If the phase windings are star connected as shown, then at any time there are just two phases and two transistors conducting.

During any 120° interval of phase current, the instantaneous power being converted from electrical to Mechanical is

$$P = \omega T_e = 2 e I$$

The number 2 in this equation arises from the fact that two phases are conducting.

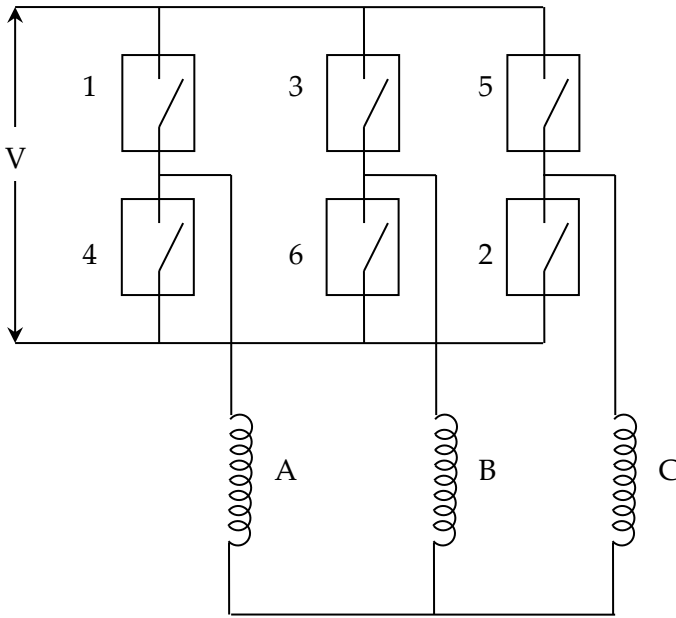
$$T_e = 4N_{ph} B_g l r_1 I \quad (\text{Nm})$$

The above equation is valid for any number of pole pairs. The similarity between the brushless motor and the commutator motor can now be seen. Writing $E = 2 e$ to represent the combined Emf of two phases in series, the Emf and torque equations can be written in the form

$$E = K \phi \omega \text{ and } T = K \phi I$$

Where $K = 4 N_{ph} \text{ and } \phi = B_g r_1 \pi l$

Where K is the armature constant and ϕ is the flux. In practice, of course, none of the ideal conditions can be perfectly realized. The main result of this is to introduce ripple torque but the basic relationships of Emf proportional to speed and torque proportional to current remain unchanged.



3.6 Control of BLDC Motor Drives

In vehicle traction application, the torque produced is required to follow the torque desired by the driver and commanded through the accelerator and brake pedals. Thus, torque control is the basic requirement.

Figure 6.51 shows a block diagram of a torque control scheme for a BLDC motor drive. The desired current I^* is derived from the commanded torque T^* through a torque controller. The current controller and commutation sequencer receive the desired current I^* position information from the position sensors, and perhaps the current feedback through current transducers, and then produces gating signals. These gating signals are sent to the three-phase inverter (power converter) to produce the phase current desired by the BLDC machine.

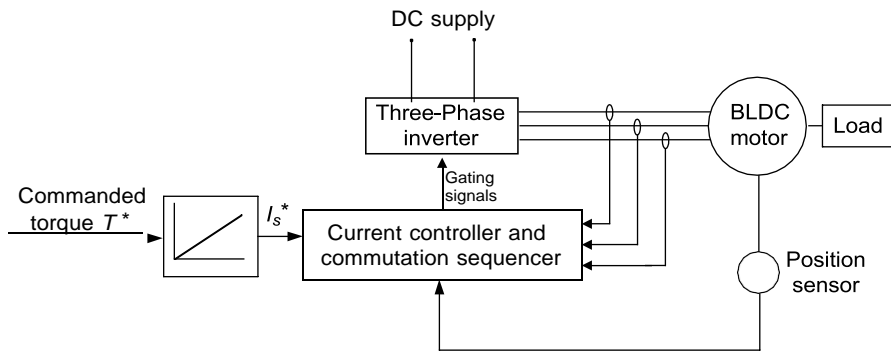


FIGURE 6.51
Block diagram of the torque control of the BLDC motor

In traction application, speed control may be required, cruising control operation, for example (see Figure 6.52). Many high-performance applications include current feedback for torque control. At the minimum, a DC bus current feedback is required to protect the drive and machine from over-currents. The controller blocks, “speed controller” may be any type of classical controller such as a PI controller, or a more advanced controller such as an artificial intelligence control. The “current controller and commutation sequencer” provides the properly sequenced gating signals to the “three-phase inverter” while comparing sensed currents to a reference to maintain a constant peak current control by hysteresis (current chopping) or with a voltage source (PWM)-type current control. Using position information, the commutation sequencer causes the inverter to “electronically commute,” acting as the mechanical commutator of a conventional DC machine. The commutation angle associated with a brush-less motor is normally set so that the motor will commute around the peak of the torque angle curve. Considering a three-phase motor, connected in delta or wye, commutation occurs at electrical angles, which are $\pm 30^\circ$ (electrical) from the peaks of the torque-angle curves. When the motor position moves beyond the peaks by an amount equal to 30° (electrical), then the commutation sensors cause the stator phase excitation to switch to move the motor suddenly to -30° relative to the peak of the next torque-angle curve.⁷⁷

3.7 Extension of Speed Technology

As discussed above, PM BLDC machines inherently have a short constant power range due to their rather limited field weakening capability. This is a result of the presence of the PM field, which can only be weakened through

the production of a stator field component that opposes the rotor magnetic field. The speed ratio, x , is usually less than 2.⁸

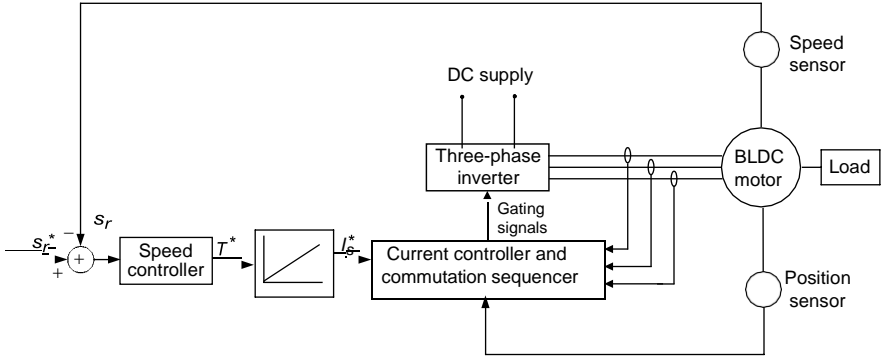


FIGURE 6.52
Block diagram of the speed control of the BLDC motor

Recently, the use of additional field windings to extend the speed range of PM BLDC motors has been developed.¹ The key is to control the field current in such a way that the air gap field provided by PMs can be weakened during high-speed constant-power operation. Due to the presence of both PMs and the field windings, these motors are called PM hybrid motors. The PM hybrid motor can achieve a speed ratio of around 4. The optimal efficiency profiles of a PM hybrid motor drive are shown in Figure 6.53.¹ However, the PM hybrid motors have the drawback of a relatively complex structure. The speed ratio is still not enough to meet the vehicle performance requirement, especially in an off-road vehicle. Thus, a multigear transmission is required.

2. Switched Reluctance Motor

- The Switched Reluctance Motor is a doubly salient, singly excited motor. Which means that it has salient poles on both the rotor and the stator, but only one member carries winding (ie) stator winding.
- The rotor has no windings (or) magnets but it is built up from a stack of salient pole laminations.
- Basically two important parts are Stator & Rotor.
- The Stator has a laminated construction made up of stampings.
- The stampings are slotted on its inner periphery to carry the winding called as stator winding.

- The laminated construction keeps eddy current losses to minimum. The stampings are made up of material like silicon steel which minimizes the hysteresis losses.
- The stator winding are concentrated and it is wound for certain definite number of poles.
- The rotor is also made up of stack of laminations with projecting poles.
- Due to rotor shape, the air gap between the stator and rotor is not uniform and no DC supply is given to the rotor.
- The rotor is free to rotate. Because of non-uniformity in the air gap, the reluctance also varies in the air gap.
- The stator and rotor are designed in such a manner that the variation of the inductance of the winding is sinusoidal with respect to the rotor position sensed by the rotor position encoder.
- The constructional details are shown in the fig 3.1

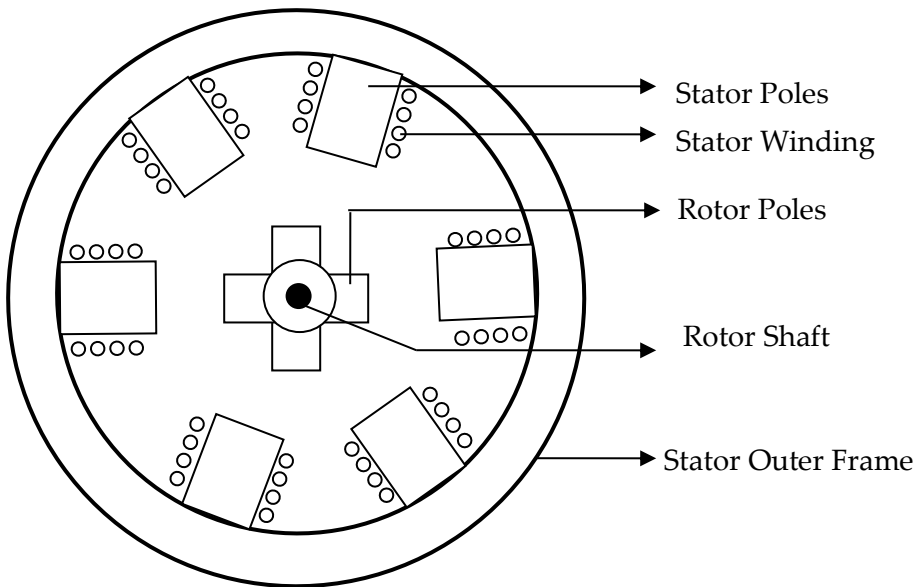


Fig 3.1

4.1 Working Principle

- When the stator windings are excited by the unidirectional supply system, the magnetic field will be produced by the opposite stator pole pair in the air gap
- The rotor starts rotating through an angle and the rotor position is sensed by the rotor position encoder .
- If an iron piece is placed in a magnetic field, it aligns itself in a minimum reluctance position and gets locked magnetically.
- Similarly in the SRM, the rotor tries to align itself with the axis of magnetic field in the minimum reluctance position.
- The other phases of the stator windings are excited sequentially by the unidirectional current by synchronism with the rotor position. So that the rotor starts rotating continuously by sequential excitation of the stator pole pairs by producing unidirectional torque.
- The torque which is exerted on the rotor is called as reluctance Torque

Advantages

1. No DC supply is necessary for rotor.
2. Constant speed characteristics.
3. Robust construction.
4. Less maintenance.

Limitations

1. Less efficiency.
2. Poor power factor
3. Need of very low inertia rotor.
4. Less capacity to drive the loads.

Applications

- Signaling Devices, Control Apparatus.
- Automatic regulators, Recording Instruments.
- Digital Clocks, Tele-printers, Gramophones, etc.,

4.2 Difference between SRM & Stepper Motor

1. The conduction angle for phase current is controlled & synchronized with the rotor position usually by means of a shaft position sensor. In this respect the SRM is exactly like the PM brushless DC motor. But the stepper motor which is usually fed with a square wave of phase current without rotor position feedback.
2. The SRM is designed for efficient power conversion at high speeds comparable with those of PMBLDC motor. Whereas the stepper motor is usually designed as a torque motor with limited speed range.
3. SRM requires a rotor position sensor whereas it is not needed in the VR Stepper Motor.
4. SRM is designed for continuous rotation whereas the VR stepper motor is designed to rotate in steps.

Advantages of SRM

1. The rotor is simple and requires relatively few manufacturing steps, which tends to have a low inertia.
2. The stator is simple to wind, the end turns are short & robust and have no phase crossovers.
3. In most applications the bulk of the losses appear on the stator, which is relatively easy to cool.
4. Because there are no magnets the maximum permissible rotor temperature may be higher than in PM motors.

5. The torque is independent of the polarity of phase current, for certain applications this permits a reduction in the number of semiconductor switches needed in the controller.
6. Under fault conditions, the open circuit voltage & short circuit current are zero (or) very small.
7. The most converter circuits used with SRM are immune from shoot through faults.
8. Starting torque can be very high, without the problem of excessive inrush current.
9. Extremely high speeds are possible.
10. The speed / Torque characteristics can be 'tailored' to the application requirement more easily than the I.M (or) PM motor.
11. There is no magnetic flux fixed value, so the maximum speed at constant power is not restricted by controller voltage as in PM motors.

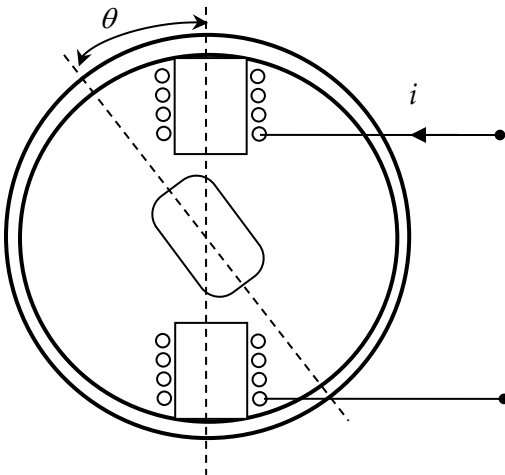
Disadvantages of SRM

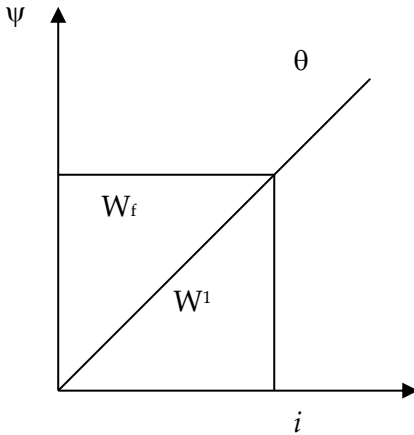
1. Absence of free PM excitation imposes the burden of excitation on the stator windings and the controller.
2. Increase in per unit copper loss and limits the efficiency and torque per ampere.
3. The pulsed or non-uniform torque production which leads to torque ripple and may contribute to acoustic noise.
4. It is very difficult (or) impossible to maintain very low torque ripple level over a wide speed Range.
5. Acoustic noise is very severe in large machines where ultrasonic chopping frequencies are not possible.
6. The noise level is sensitive to the size, mechanical construction and precession of firing angles.

7. As the torque ripple is larger , larger filter capacitance is required. This will cause significant Ac line harmonics in the systems operating from rectified Ac source.
8. The SRM typically requires more turns of thinner wire than the A.C motors wound for the same voltage.
9. For small drives with wide speed range, the SRM requires lower minimum duty cycle with high chopping frequency. So special high frequency pulse techniques and very fast power switches and diodes are necessary, which increase the cost.
10. The SRM cannot start (or) run from an ac voltage source and it is not normally possible to operate more than one motor from one inverter.
11. Cabling for SRM is typically more complex than for I.M Drives, a minimum of four wires and usually six are required for a three phase motor in addition to the sensor cabling.

4.3 Static Torque Production of SRM

Consider the primitive Reluctance motor as shown below.





When current is passed through the phase winding of the stator, the rotor tends to align with the stator poles, ie it produces a torque that tends to move the rotor to a minimum reluctance position. In such a case, the most general expression for the instantaneous torque is

$$T = \left[\frac{\partial W^1}{\partial \theta} \right]_{i = \text{constant}}$$

Where w^1 = co-energy of the magnetic field

The Co-energy is defined as $W^1 = \int_0^i \psi \, di$

An equivalent expression is $T = - \left[\frac{\partial w_f}{\partial \theta} \right]_{\psi = \text{constant}}$

Where w_f is the stored field energy and it is defined as

$$w_f = - \int_0^{\Psi} i \, d\Psi$$

When evaluating the partial derivatives it is necessary to keep the indicated variables constant. If the differentiation is done analytically, then w_f must first be expressed as a function of flux or flux linkage and rotor position only with current i is absent

from the expression. Similarly w^1 must first be expressed as a function of current and rotor position only with flux (or) flux linkage absent from the expression.

If magnetic saturation is negligible, then the relationship between flux linkage & current at the instantaneous rotor position θ is a straight line whose slope is the instantaneous inductance L . Thus

$$\psi = Li$$

$$\therefore w^1 = w_f = \frac{1}{2} Li^2$$

$$\therefore T = \frac{1}{2} i^2 \frac{dL}{d\theta} \quad (Nm)$$

If there is magnetic saturation this formula is invalid and the torque should be derived as the derivative of co-energy (or) field energy.

SRM Drive Converter

It can be seen from Figure 6.61 that the torque developed by the motor can be controlled by varying the amplitude and the timing of the current pulses

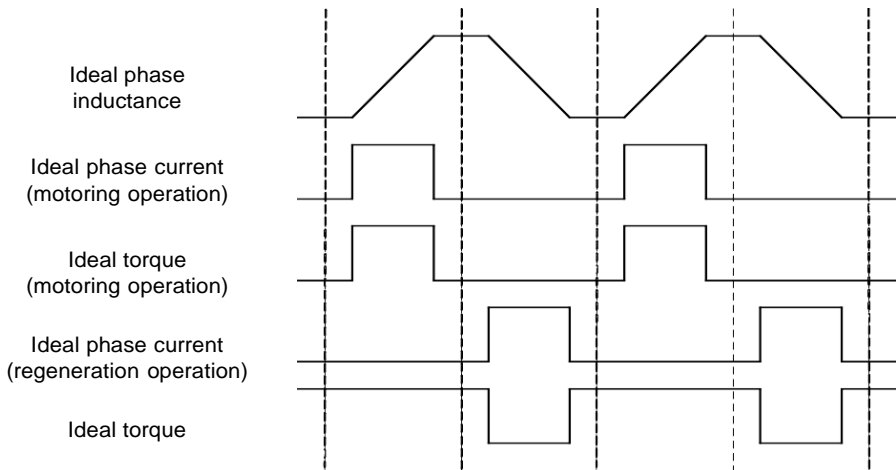


FIGURE 6.61

Idealized inductance, current, and torque profiles of the SRM

in synchronism with the rotor position. In order to control the amplitude and pulse width of the phase current, a certain type of inverter should be used.

The input to the SRM drive is DC voltage, which is usually derived from the utility through a front-end diode rectifier or from batteries. Unlike other AC machines, the currents in SR motors can be unidirectional. Hence, conventional bridge inverters used in AC motor drives are not used in SRM drives. Several configurations have been proposed for an SRM inverter in the literature;^{45,46} some of the most commonly used ones are shown in Figure 6.62.

The most commonly used inverter uses two switches and two freewheeling diodes per phase and is called the classic converter. The configuration of the classic converter is shown in Figure 6.62(a). The main advantage of the classic converter is its flexibility in control. All the phases can be controlled independently, which is essential for very high-speed operations where there will be a considerable overlap between the adjacent phase currents.⁵

The operation of the classic converter is shown in Figure 6.63 by taking phase-1 as an example. When the two switches S_1 and S_2 are turned on as in

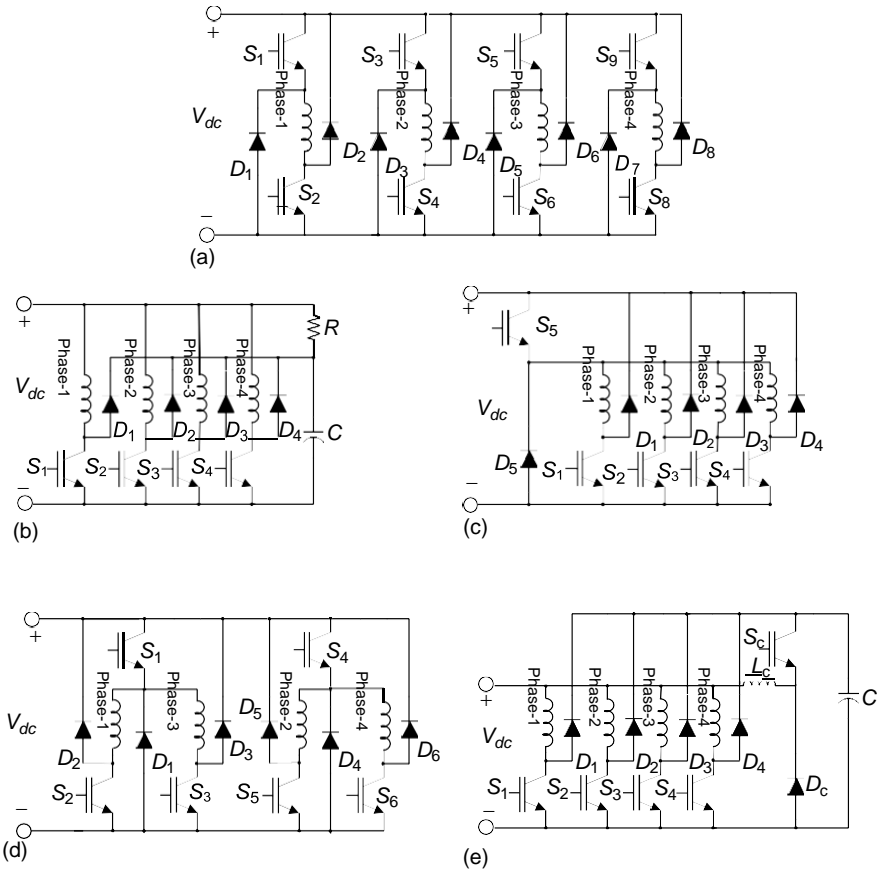


FIGURE 6.62

Different inverter topologies for SRM drives: (a) classical half bridge converter; (b) R-dump;

(c) $n+1$ switch (Miller converter); (d) $1.5n$ switch converter; and (e) C-dump

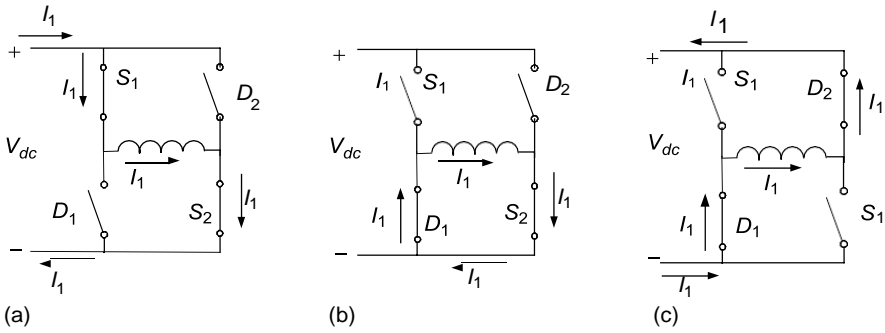


FIGURE 6.63

Modes of operation for the classic converter: (a) turning on phase mode; (b) zero voltage mode; and (c) turning off mode

Figure 6.63(a), the DC bus voltage, V_{dc} , will be applied to the phase-1 winding. Phase-1 current will increase as it flows through the path consisting of V_{dc} positive terminal, S_1 , phase-1 winding, S_2 , and V_{dc} negative terminal. By turning off S_1 and holding on S_2 (i.e., Figure 6.63[b]), when the phase is energized, the current freewheels through S_2 and D_1 . In this mode, phase-1 is not getting or giving energy to the power supply. When S_1 and S_2 are turned off (Figure 6.63[c]), the phase-1 current will flow through D_2 , V_{dc} positive terminal, V_{dc} negative terminal, D_1 , and phase-1 winding. During this time, the motor phase is subjected to negative DC bus voltage through the free-wheeling diodes. The energy trapped in the magnetic circuit is returned to the DC link. The phase current drops due to the negative applied phase voltage. By turning S_1 and S_2 on and off, the phase-1 current can be regulated.

The half bridge converter uses $2n$ switches and $2n$ diodes for an n -phase machine. There are several configurations that use fewer switches: for example, the R-dump-type inverter (Figure 6.62[b]) uses one switch and one diode per phase. This drive is not efficient; during turn off, the stored energy of the phase is charging capacitor C to the bus voltage and dissipating in resistor R . Also, zero voltage mode does not exist in this configuration.

An alternative configuration is an $(n + 1)$ switch inverter. In this inverter, all the phases are sharing a switch and diode so that overlapping operation between phases is not possible, which is inevitable in the high-speed operation of this motor. This problem has been solved by sharing switches of each couple of nonadjacent phases, as shown in Figure 6.62(d). This configuration is limited to an even number of phases of switched reluctance motor drives.

One of the popular inverter configurations is C-dump (Figure 6.62[e]), which has the advantage of less switches and of allowing independent phase current control. In this configuration, during the turn-off time, the stored magnetic energy is charging capacitor C , and if the voltage of the capacitor reaches a certain value, for example V_c , it is transferred to the supply through switch S_c . The main disadvantage of this configuration is that the

negative voltage across the phase coil is limited to the difference between the voltage across the capacitor V_c and the system power supply voltage.

Modes of Operation

For SRM, there is a speed at which the back EMF is equal to the DC bus voltage. This speed is defined as the base speed. Below the base speed, the back EMF is lower than the DC bus voltage. From equation (6.125), it can be seen that when the converter switches are turned on or off to energize or de-energize the phase, the phase current will rise or drop accordingly. The phase current amplitude can be regulated from 0 to the rated value by turning the switches on or off. Maximum torque is available in this case when the phase is turned on at an unaligned position and turned off at the aligned position, and the phase current is regulated at the rated value by hysteresis or PWM control. The typical waveforms of the phase current, voltage, and flux linkage of the SRM below base speed are shown in Figure 6.64.

Above the base speed, the back EMF is higher than the DC-bus voltage. At the rotor position — where the phase has a positive inductance slope with respect to the rotor position — the phase current may drop even if the switches of the power inverter are turned on. The phase current is limited by the back EMF. In order to build high current and therefore produce high motoring torque in the SRM, the phase is usually excited ahead of the unaligned position, and the turn-on position is gradually advanced as the rotor speed increases. The back EMF increases with the rotor speed. This leads to a decrease in the phase current and hence the torque drops. If the turn-on position is advanced for building as high as possible a current in the SRM phase, the maximum SRM torque almost drops as a linear function of the reciprocal of the rotor speed. The maximum power of the SRM drive is

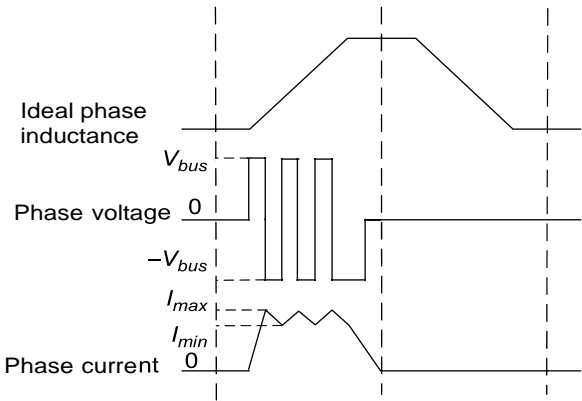


FIGURE 6.64 Low-speed (below the base speed) operation of SRM

almost constant. The typical waveforms at high-speed operations are shown in Figure 6.65.

The advancing of the phase turn-on position is limited to the position at which the phase inductance has a negative slope with respect to the rotor position. If the speed rotor further increases, no phase advancing is available for building higher current in the phase, and the torque of the SRM will drop significantly.⁷⁷ The mode is referred to as the natural mode operation. The torque–speed characteristic of the SRM is shown in Figure 6.66.

Generating Mode of Operation (Regenerative Braking)

Torque in the SR machines is created based on the principle of reaching the minimum reluctance for the excited phase. Therefore, if the rotor pole is approaching the excited phase, which means the bulk inductance is increasing, the torque produced is in the direction of the rotor and it is in motoring mode. But if the rotor pole is leaving the stator phase – which means the negative slope of the bulk inductance – the stator tries to keep it in alignment; the torque produced is then in the opposite direction of the movement of the rotor, and the SSR works in generating mode.

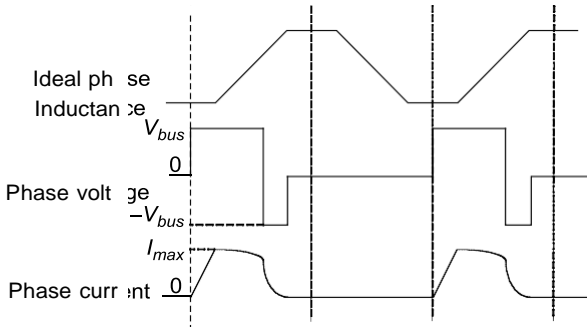


FIGURE 6.65 High-speed (above the base speed) operation of SRM

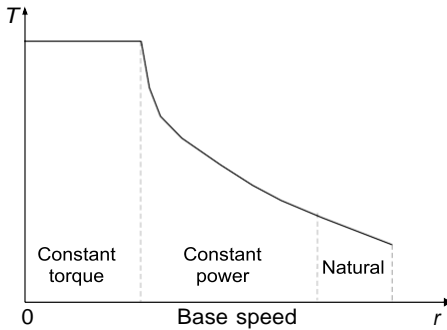


FIGURE 6.66 Torque–speed characteristic of SRM

Regenerative braking is an important issue in the propulsion drive of EVs and HEVs. There is a duality in operation of generating and motoring modes and the current waveforms in the generating modes are simply the mirror images of the waveforms in the motoring region around the alignment rotor position.⁵² The SRG is a singly excited machine; thus, in order to obtain power from it, it should be excited near the rotor aligned position and then turned off before the unaligned region (Figure 6.67).

As in motoring operations, the current can be controlled by changing the turn-on and turn-off angles and current level while in low speed. Alternatively, in speeds higher than the base speed, only the turn-on and turn-off angles can be used for control.

The driving circuit for SRG is similar to the SRM's; one of the common configurations is shown in Figure 6.68. When the switches are turned on, the phase gets energy from the supply and capacitor. During the turn-off period, the freewheeling current from the motor charges up the capacitor and delivers energy to the load. Since there is no PM in this motor, during the start-up and initial condition, it needs an external source such as a battery to deliver energy to the phase; after taking transient time, the capacitor is then charged up to the output voltage. Depending on the output voltage during phase on time, both the capacitor and external source or just the capacitor provide the current to the load and the phase coil. The external source can be designed

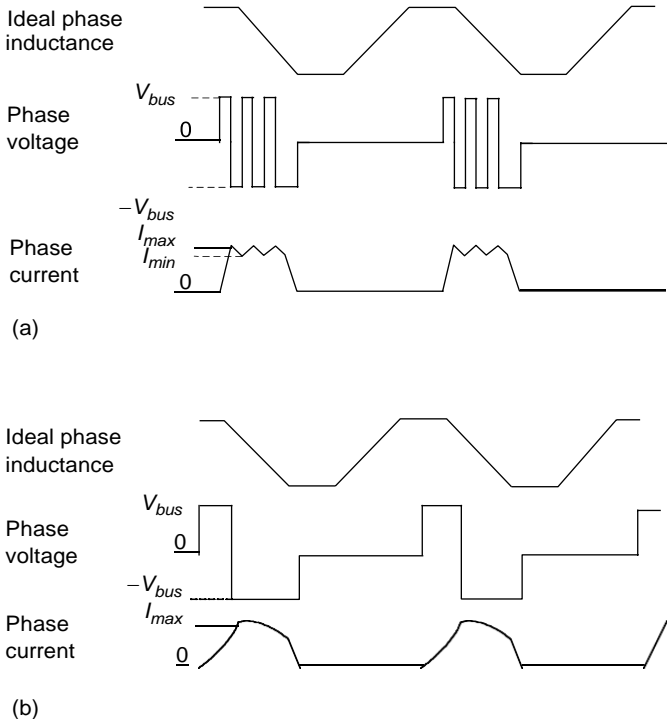


FIGURE 6.67 Low- and high-speed operation in generating mode: (a) low-speed operation in generating

mode and (b) high-speed operation in generating mode

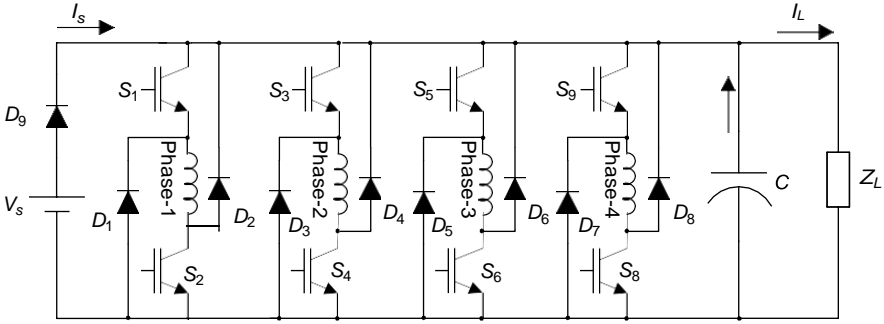


FIGURE 6.68
A driving circuit example for switched reluctance generator

to be charged, or can be disconnected from the system after the system reaches its operating point.

In the generating region, the back EMF is negative and thus it helps the phase to be charged very fast; then, during turn-off, the back EMF opposes the negative supply voltage and decreases slowly.

$$V_c - e = L \frac{di}{dt} + Ri, \quad e > 0 \quad (\text{during phase on period}), \quad (6.132)$$

$$-V_c - e = L \frac{di}{dt} + Ri, \quad e > 0 \quad (\text{during phase off period}). \quad (6.133)$$

In (6.132) and (6.133), V_c is the bus voltage of the inverter or, equivalently, the voltage of the bus capacitor and e is back EMF voltage.

In certain conditions such as high speed and high loads, the back EMF voltage is greater than the bus supply voltage; thus, the current increases even after turning off the phase. In addition to uncontrollable torque, this necessitates an oversized converter, thereby adding to the cost and overall size of the system. Due to variations in speed of the prime mover, the power electronic converter should be designed for the worst possible case. This will magnify the additional cost and size issues. By properly selecting the turn-off angle, this maximum generating current can be coaxed into the safe region.⁴⁹ Figure 6.69 shows the effect of turn-off angle in the maximum generating current.

References

- [1] C.C. Chan and K.T. Chau, *Modern Electric Vehicle Technology*, Oxford University Press, Oxford, 2001.
- [2] G.K. Dubey, *Power Semiconductor Controlled Drives*, Prentice-Hall Inc., Englewood Cliffs, NJ, 1989.
- [3] A.M. Trzynadlowski, *The Field Orientation Principle in Control of Induction Motor*, Kluwer Academic Publishers, Dordrecht, 1994.
- [4] D.W. Novotny and T.A. Lipo, *Vector Control and Dynamics of AC Drives*, Oxford Science Publications, London, 1996.
- [5] N. Mohan, T.M. Undeland, and W.P. Robbins, *Power Electronics — Converters, Applications, and Design*, John Wiley & Sons, New York, 1995.

**Question bank
PART A**

Q.No	Questions	CO (L)
1.	List the types of DC motor from its excitation	CO4(L4)
2.	Formulate Why DC series motor suitable for traction applications.	CO4 (L6)
3.	Discuss the significance of back emf.	CO4 (L6)
4.	Formulate the factors affect the controlling the speed of DC motor.	CO4 (L6)
5.	Discuss the braking methods used in DC motor.	CO4 (L6)
6.	Relate the switched reluctance motor as doubly salient motor.	CO4(L5)
7.	Argue on the Switched reluctance motor is singly excited motor.	CO4(L5)
8.	Describe the modes of operation of SRM.	CO4(2)
9.	Argue on the type of commutation is used in PMBLDC motors.	CO4(5)
10.	Compare conventional DC motor and PMBLDC motor.	CO4(4)
11.	Justify why induction motor mature technology among commutatorless motor drives.	CO4(L5)
12.	Justify why squirrel cage induction motor more attractive in EV	CO4(L5)

PART B

Q.No	Questions	CO (L)
1.	Explain the multi-quadrant control of DC motor with suitable chopper circuit diagram.	CO4(L5)
2.	With necessary equations Explain the operation of V/F controlled induction motor drive.	CO4(L5)
3.	With necessary equations Explain the operation of field oriented controlled induction motor drive.	CO4(L5)
4.	Examine the performance and control of PMBLDC motor for vehicle traction application.	CO4(L5)
5.	With necessary diagram Examine the regenerative braking control of SRM for low and high speed operation.	CO4(L5)



SATHYABAMA

INSTITUTE OF SCIENCE AND TECHNOLOGY
(DEEMED TO BE UNIVERSITY)

Accredited "A" Grade by NAAC | 12B Status by UGC | Approved by AICTE

www.sathyabama.ac.in

SCHOOL OF ELECTRICAL AND ELECTRONICS ENGINEERING

DEPARTMENT OF ELECTRICAL AND ELECTRONICS ENGINEERING

UNIT – V - Electric Vehicle – SEE1628/SEEA3028

Batteries-Overview-Types of battery-Fuel Cell-Super capacitor -Flywheel. Charging, standards and infrastructure-Wireless power transfer-Solar charging case study. Case studies-General motor EV-1 and Tesla roadster

Batteries

5.1 Overview

5.1.1 Battery range

The main thing that affects the range of an EV is your right foot! Smooth driving with gentle acceleration and minimal braking has the most impact on range – as it does in any vehicle. However, the range is also affected by cold weather as well as the use of air conditioning (heating or cooling) and other items (such as lights). This is because these systems use battery energy. Vehicle manufacturers are using solutions such as LED exterior lights to reduce consumption. Control systems can also minimize the energy used by additional items. Mains powered pre-heating (or cooling) is now common, allowing the driver to start their journey with the interior at a comfortable temperature without draining the battery. One plus point is that EVs don't need a warm-up period like many conventional ICE vehicles in the winter.



Figure 5.1 Battery pack for the Chevrolet Spark (Source: General Motors)

5.1.2 Battery life and recycling

Manufacturers usually consider the end of life for a battery to be when the battery capacity drops to 80% of its rated capacity. This means that if the original battery has a range of 100 km from a full charge, after 8–10 years of use the range may reduce to 80 km. However, batteries can still deliver usable power below 80% charge capacity. A number of vehicle manufacturers have designed the battery to last the lifetime of the car. The main sources of lithium for EV batteries are salt lakes and salt pans, which produce the soluble salt lithium chloride. The main producers of lithium are South America (Chile, Argentina and Bolivia), Australia, Canada and China. Lithium can also be extracted from seawater.

It is expected that recycling will become a major source of lithium. Worldwide

reserves are estimated to be about 30 million tons. Around 0.3 kg of lithium is required per kWh of battery storage. There is a range of opinion but many agree reserves will last over a thousand years! The volume of lithium recycling at the time of writing is relatively small, but it is growing. Lithium-ion cells are considered non-hazardous and they contain useful elements that can be recycled. Lithium, metals (copper, aluminium, steel), plastic, cobalt and lithium salts can all be recovered.

All battery suppliers must comply with 'The Waste Batteries and Accumulators Regulations 2009'. This is a mandatory requirement, which means manufacturers take batteries back from customers to be reused, recycled or disposed of in an appropriate way.

The main sources of lithium for EV batteries are salt lakes and salt pans, which produce the soluble salt lithium chloride. The main producers of lithium are South America (Chile, Argentina and Bolivia), Australia, Canada and China. Lithium can also be extracted from sea water. It is expected that recycling will become a major source of lithium. Worldwide reserves are estimated to be about 30 million tons. Around 0.3 kg of lithium is required per kWh of battery storage. There is a range of opinion but many agree reserves will last over a thousand years. The volume of lithium recycling at the time of writing is relatively small, but it is growing. Lithium-ion cells are considered non-hazardous and they contain useful elements that can be recycled. Lithium, metals (copper, aluminium, steel), plastic, cobalt and lithium salts can all be recovered. Lithium-ion batteries have a lower environmental impact than other battery technologies, including lead-acid, nickel-cadmium and nickel-metal hydride. This is because the cells are composed of more environmentally benign materials. They do not contain heavy metals (cadmium for example) or compounds that are considered toxic, such as lead or nickel. Lithium iron phosphate is essentially a fertilizer. As more recycled materials are used, the overall environmental impact will be reduced.

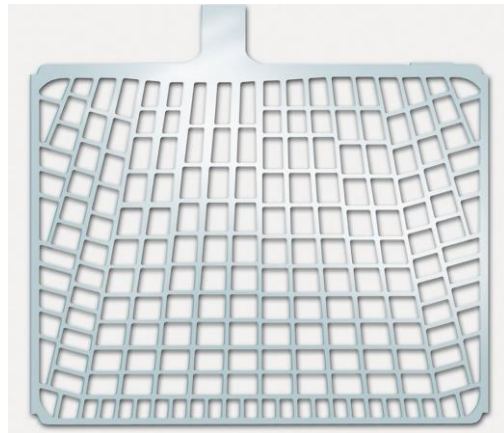
Types of battery

5.1.3 Lead–acid batteries(Pb–PbO₂)

Even after about 150 years of development and much promising research into other techniques of energy storage, the lead–acid battery is still the best choice for low-voltage motor vehicle use. This is particularly so when cost and energy density are taken into account.

Incremental changes over the years have made the sealed and maintenance-free battery now in common use very reliable and long lasting. This may not always appear to be the case to some end-users, but note that quality is often related to the price the

customer pays. Many bottom-of-the-range cheap batteries, with a 12-month guarantee, will last for 13 months! The basic construction of a nominal 12 V lead–acid battery consists of six cells connected in series. Each cell, producing about 2 V, is housed in an individual compartment within a polypropylene, or similar, case. [Figure 5.2](#) depicts a cut-away battery showing the main component parts. The active material is held in grids or baskets to form the positive and negative plates. Separators made from a micro-porous plastic insulate these plates from each other.



[Figure 5.2](#) Battery grid before the active materials are added

However, even modern batteries described as sealed do still have a small vent to stop the pressure build-up due to the very small amount of gassing. A further requirement of sealed batteries is accurate control of charging voltage.

In use, a battery requires very little attention other than the following when necessary:

- Clean corrosion from terminals using hot water.
- Terminals should be smeared with petroleum jelly or Vaseline, not ordinary grease.
- Battery tops should be clean and dry.
- If not sealed, cells should be topped up with distilled water 3 mm above the plates.

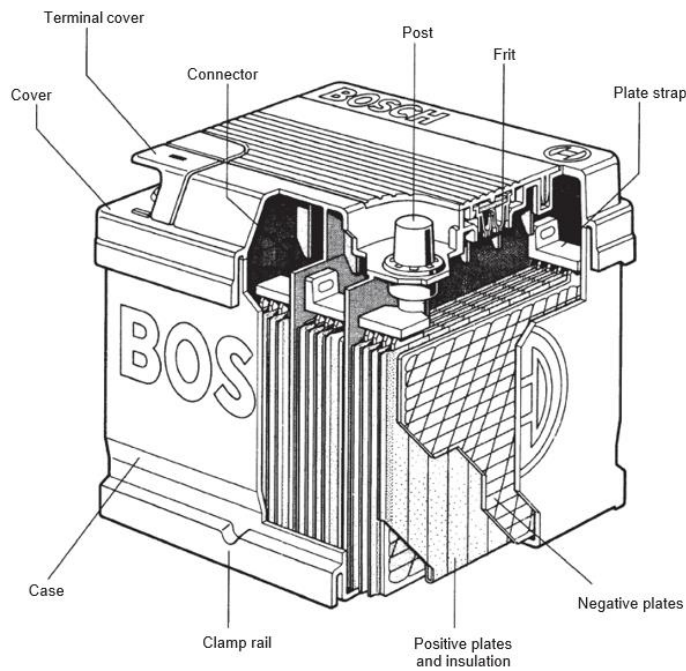


Figure 5.3 Lead-acid battery

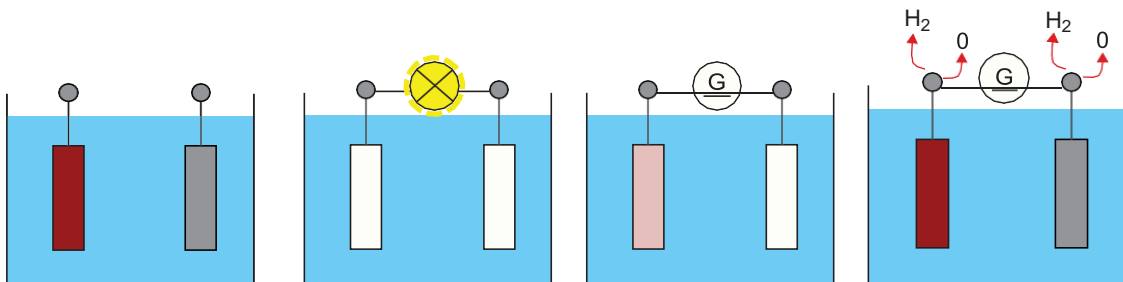


Figure 5.4 Battery discharge and charging process (left to right): Fully charged; discharging; charging; charging and gassing



Figure 5.5 Modern vehicle battery

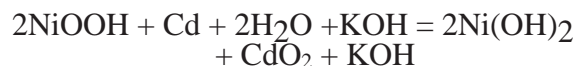
- The battery should be securely clamped in position.

5.2.2 Alkaline (Ni–Cad, Ni–Fe and Ni–MH)

The main components of the nickel–cadmium (Ni–Cad or NiCad) cell for vehicle use are as follows:

- positive plate – nickel hydrate (NiOOH)
- negative plate – cadmium (Cd)
- electrolyte – potassium hydroxide (KOH) and water (H₂O).

The process of charging involves the oxygen moving from the negative plate to the positive plate, and the reverse when discharging. When fully charged, the negative plate becomes pure cadmium and the positive plate becomes nickel hydrate. A chemical equation to represent this reaction is given next, but note that this is simplifying a more complex reaction.



The 2H₂O is actually given off as hydrogen (H) and oxygen (O₂) because gassing takes place all the time during charge. It is this use of water by the cells that indicates they are operating, as will have been noted from the equation. The electrolyte does not change during the reaction. This means that a relative density reading will not indicate the state of charge. Nickel–metal hydride (Ni–MH or NiMH) batteries are used by some electric vehicles and have proved to be very effective. Toyota in particular has developed these batteries. The components of NiMH batteries include a cathode of nickel–hydroxide, an anode of hydrogen absorbing alloys and a potassium–hydroxide (KOH) electrolyte. The energy density of NiMH is more than double that of a lead–acid battery but less than lithium-ion batteries.

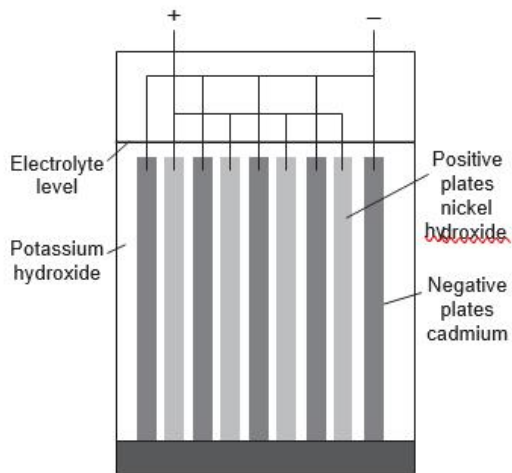


Figure 5.6 Simplified representation of a NiCad alkaline battery cell

Key Fact

NiMH batteries are used by some electric vehicles and have proved to be very effective.



Figure 5.7 Toyota NiMH battery and management components (Source: Toyota)



Figure 5.8 Third-generation NiMH battery (Source: Toyota)

Toyota developed a cylindrical NiMH battery in 1997 that powered the Rav4EV as well as the e-com electric vehicle. Since then, Toyota has continually improved its NiMH batteries by reducing size, improving power density, lowering weight, improving the battery pack/case and lowering costs. The current NiMH battery, which powers the third-generation Prius, costs 25% that of the battery used in the first generation. Nickel-metal batteries are ideal for mass-producing affordable conventional hybrid vehicles because of their low cost, high reliability and high durability. There are first-generation Prius batteries still on the road with over 200,000 miles and counting. That is why NiMH remains the battery of choice for Toyota's conventional hybrid line up.



Figure 5.8 Third-generation NiMH battery(Source: Toyota)

5.2.3 Sodium–nickel chloride(Na–NiCl₂)

Molten salt batteries (including liquid metal batteries) are a class of battery that uses molten salts as an electrolyte and offers both a high energy density and a high power density. Traditional ‘use-once’ thermal batteries can be stored in their solid state at room temperature for long periods of time before being activated by heating. Rechargeable liquid metal batteries are used for electric vehicles and potentially also for grid energy storage, to balance out intermittent renewable power sources such as solar panels and wind turbines. Thermal batteries use an electrolyte that is solid and inactive at normal ambient temperatures. They can be stored indefinitely (over 50 years) yet provide full power in an instant when required. Once activated, they provide a burst of high power for a short period (a few tens of seconds) to 60 minutes or more, with output ranging from a few watts to several kilowatts. The high power capability is due to the very high ionic conductivity of the molten salt, which is three orders of magnitude (or more) greater than that of the sulfuric acid in a lead–acid car battery.

There has been significant development relating to rechargeable batteries using sodium (Na) for the negative electrodes. Sodium is attractive because of its high potential of 2.71 V, low weight, non-toxic nature, relative abundance and ready availability, and its low cost. In order to construct practical batteries, the sodium must be used in liquid form. The melting point of sodium is 98°C (208°F). This means that sodium-based batteries must operate at high temperatures between 400 and 700°C, with newer designs running at temperatures between 245 and 350°C.

5.2.4 Sodium–sulphur (Na–S)

The sodium–sulphur or Na–S battery consists of a cathode of liquid sodium into which is placed a current collector. This is a solid electrode of alumina (a form of aluminium oxide). A metal can that is in contact with the anode (a sulphur electrode) surrounds the whole assembly. The major problem with this system is that the running temperature needs to be 300–350°C. A heater rated at a few hundred watts forms part of the charging circuit. This maintains the battery temperature when the vehicle is not running. Battery temperature is maintained when in use due to current flowing through the resistance of the battery (often described as I^2R power loss).

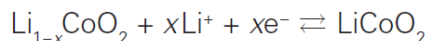
Each cell of this battery is very small, using only about 15 g of sodium. This is a safety feature because, if the cell is damaged, the sulphur on the outside will cause the potentially dangerous sodium to be converted into polysulphides, which are comparatively harmless. Small cells also have the advantage that they can be distributed around the car.

The capacity of each cell is about 10 Ah. These cells fail in an open circuit condition and hence this must be taken into account, as the whole string of cells used to create the required voltage would be rendered inoperative. The output voltage of each cell is about 2 V.

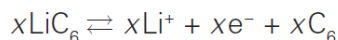
5.2.5 Lithium-ion (Li-ion)

Lithium-ion technology is becoming the battery technology of choice, but it still has plenty of potential to offer. Today's batteries have an energy density of up to 140 Wh/kg or more in some cases, but have the potential to go as high as 280 Wh/kg. Much research in cell optimization is taking place to create a battery with a higher energy density and increased range. Lithium-ion technology is currently considered the safest.

The cathode (marked +) half-reaction is:



The anode (marked –) half-reaction is:



One issue with this type of battery is that in cold conditions the lithium-ions' movement is slower during the charging process. This tends to make them reach the electrons on the surface of the anode rather than inside it. Also, using a charging current that is too high creates elemental lithium. This can be deposited on top of the anode covering the surface, which can seal the passage. This is known as lithium plating. Research is ongoing and one possible solution could be to warm up the battery before charging

The Li-ion battery works as follows. A negative pole (anode) and a positive pole (cathode) are part of the individual cells of a lithium-ion battery together with the electrolyte and a separator. The anode is a graphite structure and the cathode is layered metal oxide. Lithium-ions are deposited between these layers. When the battery is charging, the lithium-ions move from the anode to the cathode and take on electrons. The number of ions therefore determines the energy density. When the battery is discharging, the lithium-ions release the electrons to the anode, and move back to the cathode. Useful work is performed when electrons flow through a closed external circuit. The following equations show one example of the chemistry, in units of moles, making it possible to use coefficient X.

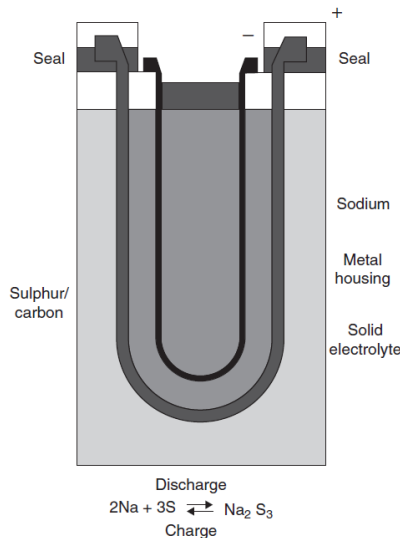


Figure 5.9 Sodium–sulphur battery

Bosch is working on post-lithium-ion batteries, such as those made using lithium–sulphur technology, which promises greater energy density and capacity. The company estimates that the earliest the lithium–sulphur battery will be ready for series production is the middle of the 2020s. There are several ways to improve battery performance. For example, the material used for the anode and cathode plays a major role in the cell chemistry. Most of today’s cathodes consist of nickel–cobalt–manganese (NCM) and nickel carboxyanhydrides (NCA), whereas anodes are made of graphite, soft or hard carbon, or silicon carbon. High-voltage electrolytes can further boost battery performance, raising the voltage within the cell from 4.5 to 5 volts. The technical challenge lies in guaranteeing safety and longevity while improving performance. Sophisticated battery management can further increase the range of a car by up to 10%, without altering the cell chemistry.

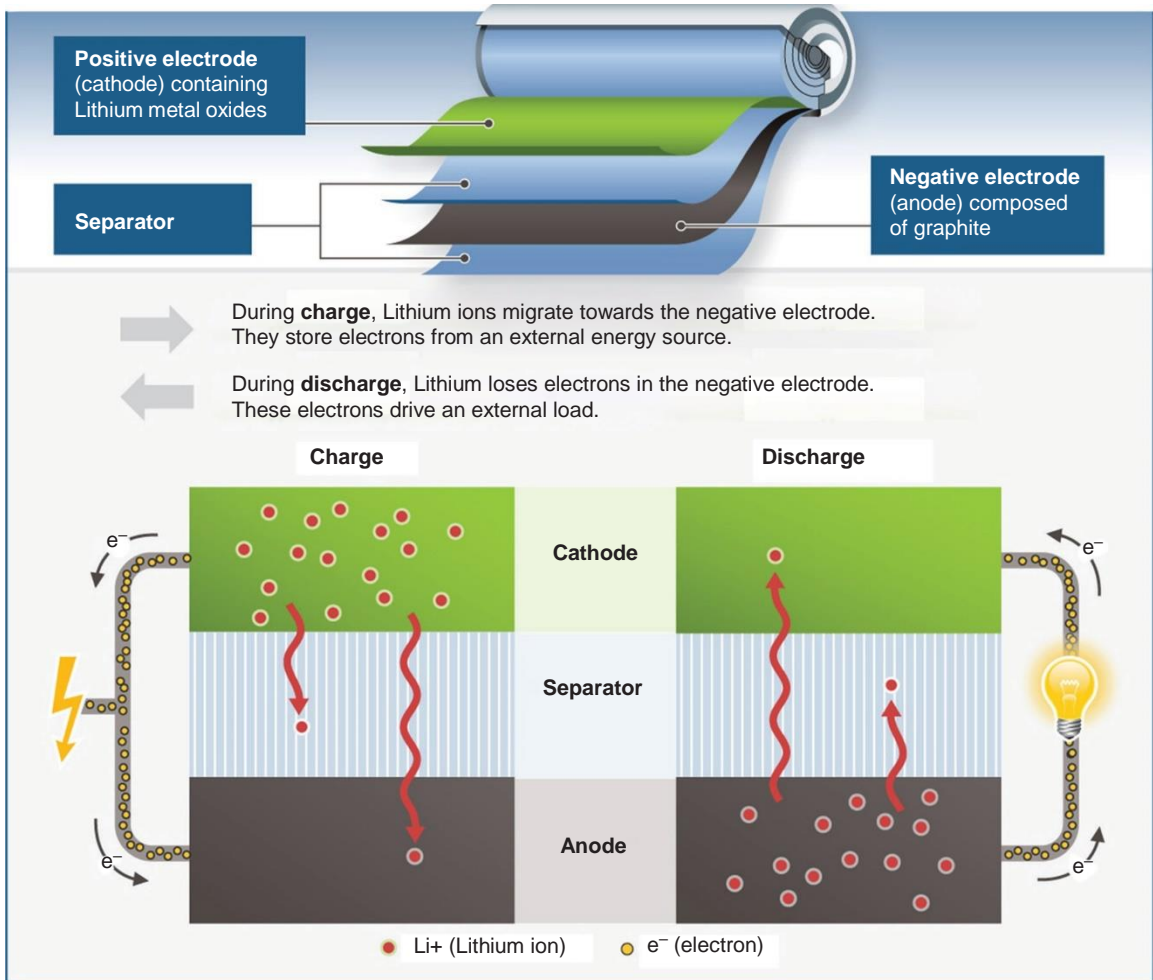


Figure 5.10 Basic operation of a lithium-ion battery (Source: Bosch Media)



Figure 5.11 Battery developments are ongoing(Source: Bosch Media)

5.2.6 Fuel cells

The energy of oxidation of conventional fuels, which is usually manifested as heat, can be converted directly into electricity in a fuel cell. All oxidations involve a transfer of electrons between the fuel and oxidant, and this is employed in a fuel cell to convert the energy directly into electricity. All battery cells involve an oxidation at the positive pole and a reduction at the negative during some part of their chemical process. To achieve the separation of these reactions in a fuel cell, an anode, a cathode and electrolyte are required. The electrolyte is fed directly with the fuel.

It has been found that a fuel of hydrogen when combined with oxygen proves to be a most efficient design. Fuel cells are very reliable and silent in operation, but are quite expensive to construct. Operation of a fuel cell is such that as hydrogen is passed over an electrode (the anode), which is coated with a catalyst, the hydrogen diffuses into the electrolyte. This causes electrons to be stripped off the hydrogen atoms. These electrons then pass through the external circuit. Negatively charged hydrogen anions (OH^-) are formed at the electrode over which oxygen is passed such that it also diffuses into the solution. These anions move through the electrolyte to the anode. Water is formed as the by-product of a reaction involving the hydrogen ions, electrons and oxygen atoms. If the heat generated by the fuel cell is used, an efficiency of over 80% is possible, together with a very good energy density figure. A unit consisting of many individual fuel cells is often referred to as a stack. The working temperature of these cells varies but about 200°C is typical. High pressure is also used and this can be of the order of 30 bar. It is the pressures and storage of hydrogen that are the main problems to be overcome before the fuel cell will be a realistic alternative to other forms of storage for the mass market.

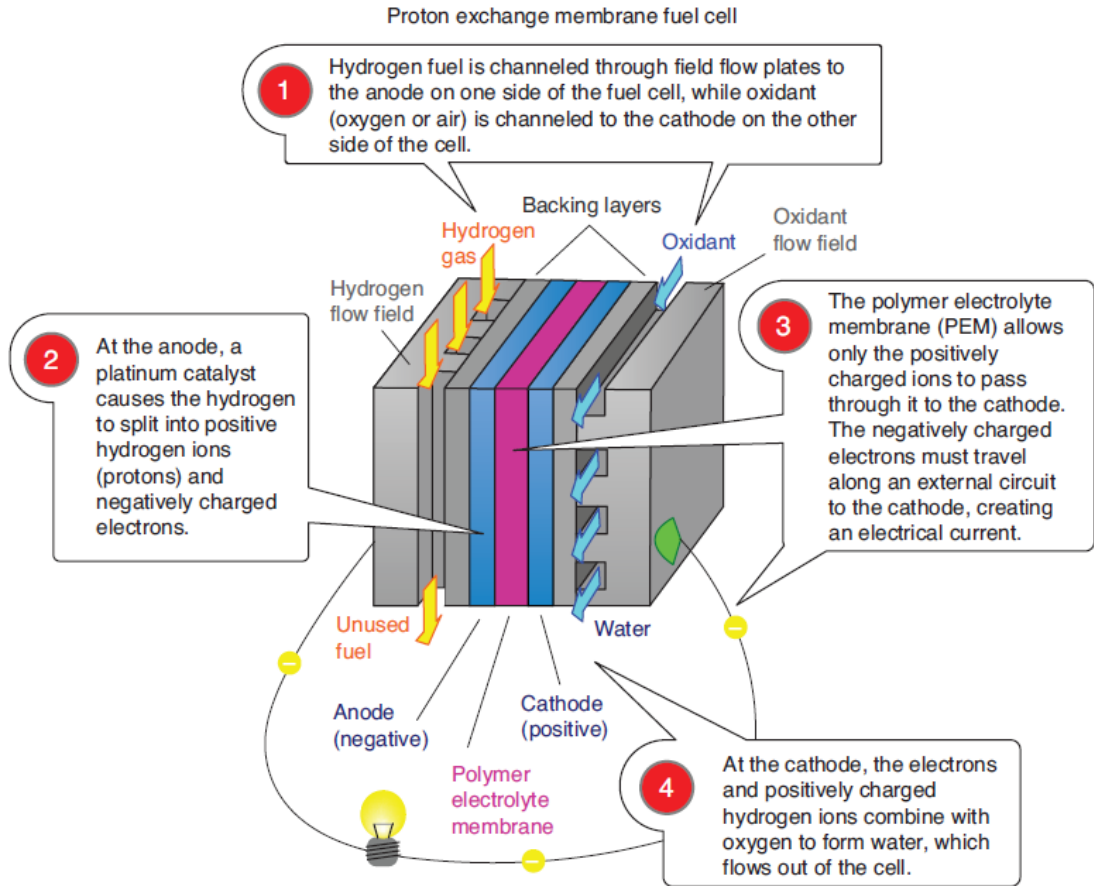


Figure 5.12 Proton exchange membrane fuel cell operation

Many combinations of fuel and oxidant are possible for fuel cells. Though hydrogen–oxygen is conceptually simple, hydrogen has some practical difficulties, including that it is a gas at standard temperature and pressure and that there does not currently exist an infrastructure for distributing hydrogen to domestic users. More readily usable, at least in the short term, would be a fuel cell powered by a more easily handled fuel. To this end, fuel cells have been developed that run on methanol. There are two types of fuel cell that use methanol:

- reformed methanol fuel cell (RMFC)
- direct methanol fuel cell (DMFC).

In the RMFC, a reaction is used to release hydrogen from the methanol, and then the fuel cell runs on hydrogen. The methanol is used as a carrier for hydrogen. The DMFC uses methanol directly.

RMFCs can be made more efficient in the use of fuel than DMFCs, but are more

complex. DMFCs are a type of proton exchange membrane fuel cell (PEMFC). The membrane in a PEMFC fulfills the role of the electrolyte, and the protons (positively charged hydrogen ions) carry electrical charge between the electrodes.

Because the fuel in a DMFC is methanol, not hydrogen, other reactions take place at the anode. Methanol is a hydrocarbon (HC) fuel, which means that its molecules contain hydrogen and carbon (as well as oxygen in the case of methanol). When HCs burn, the hydrogen reacts with oxygen to create water and the carbon reacts with oxygen to create carbon dioxide. The same general process takes place in a DMFC, but in the process the hydrogen crosses the membrane as an ion, in just the same way as it does in a hydrogen-fuelled PEMFC.

The real benefit of methanol is that it can easily fit into the existing fuel infrastructure of filling stations and does not need highly specialized equipment or handling. It is easy to store on-board the vehicle, unlike hydrogen, which needs heavy and costly tanks.

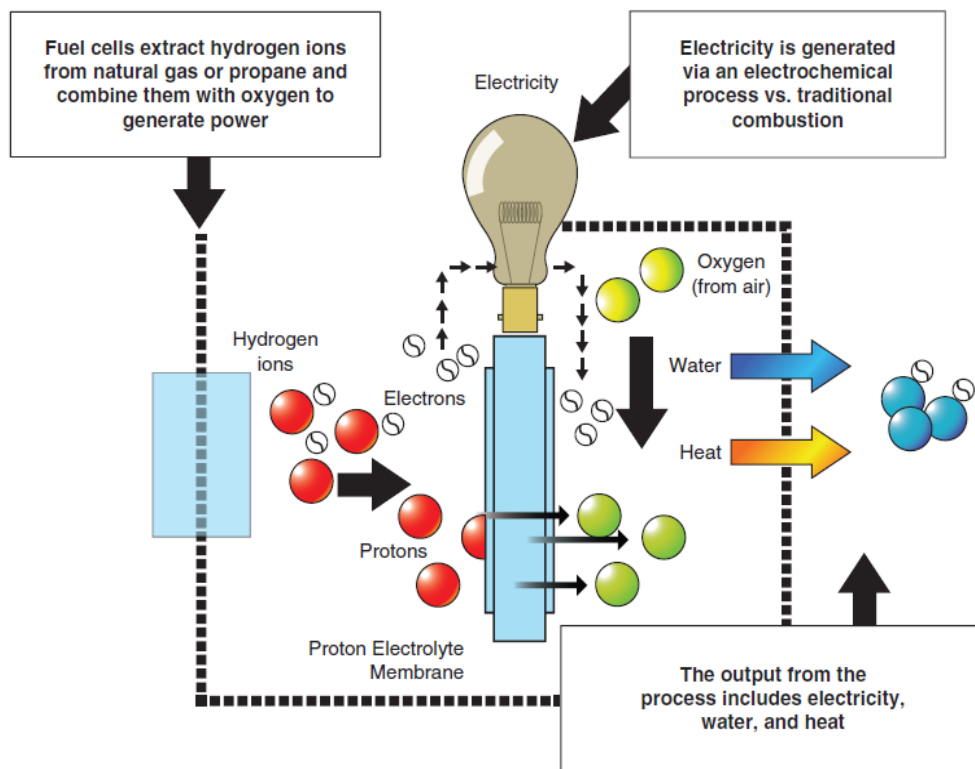


Figure 5.13 Fuel-cell operation (Source: Dana)

5.2.7 Super-capacitors

Super- or ultra-capacitors are very high-capacity but (relatively) low-size capacitors. These two characteristics are achieved by employing several distinct electrode materials prepared using special processes. Some state-of-the-art ultra-capacitors are based on high surface area, ruthenium dioxide (RuO_2) and carbon electrodes. Ruthenium is extremely expensive and available only in very limited amounts.

Electrochemical capacitors are used for high-power applications such as cellular electronics, power conditioning, industrial lasers, medical equipment and power electronics in conventional, electric and hybrid vehicles. In conventional vehicles, ultra-capacitors could be used to reduce the need for large alternators for meeting intermittent high-peak power demands related to power steering and braking. Ultra-capacitors recover braking energy dissipated as heat and can be used to reduce losses in electric power steering.

One system in use on a hybrid bus uses 30 ultra-capacitors to store 1600 kJ of electrical energy (20 farads at 400 V). The capacitor bank has a mass of 950 kg. Use of this technology allows recovery of energy when braking, which would otherwise have been lost because the capacitors can be charged in a very short space of time. The energy in the capacitors can also be used very quickly for rapid acceleration.

5.2.8 Flywheels

As discussed previously, recovering the energy that would otherwise be lost when a vehicle brakes is an extremely effective way to improve fuel economy and reduce emissions. However, there are some concerns about the environmental impact of widespread battery manufacture and end-of-life disposal. Flywheel technology is one possible answer. A company known as Flybrid produces a mechanically compact kinetic energy recovery system (KERS).

Flywheel technology itself is not new. Flywheel energy storage has been used in hybrid vehicles such as buses, trams and prototype cars before, but the installation tended to be heavy and the gyroscopic forces of the flywheel were significant. The new system overcomes these limitations with a compact and relatively lightweight carbon and steel flywheel.



Figure 5.14 Carbon fibre flywheel (Source:Flybrid)

KERS captures and stores energy that is otherwise lost during vehicle deceleration events. As the vehicle slows, kinetic energy is recovered through the KERS continuously variable transmission (CVT) or clutched transmission (CFT) and stored by accelerating a flywheel. As the vehicle gathers speed, energy is released from the flywheel, via the CVT or CFT, back into the driveline. Using this stored energy to reaccelerate the vehicle in place of energy from the engine reduces engine fuel consumption and CO₂ emissions. Flywheel systems offer an interesting alternative to batteries or super-capacitors. In a direct comparison they are less complex, more compact and lighter weight. However, the technology challenges involved in a flywheel that can rotate at speeds up to 64,000 rpm, extracting the energy and keeping it safe, should not be underestimated.



Figure 5.15 The Flybrid® hybrid system (Source: <http://www.flybridsystems.com>)

5.2.7 Summary

As a summary to this section, the following table compares the potential energy density of several types of battery. Wh/kg means watt-hours per kilogram. This is a measure of the power it will supply, and for how long, per kilogram.¹

Key Points:

1. EV range is affected by cold weather and the use of air conditioning and lights.
2. Manufacturers usually consider the end of life for a battery to be when the battery capacity drops to 80% of its rated capacity.
3. Gaston Planté was the French physicist who invented the lead–acid battery in 1859.
4. Lithium-ion cells are considered non-hazardous and they contain useful elements that can be recycled.
5. NiCad batteries do not suffer from over-charging because once the cadmium oxide has changed to cadmium, no further reaction can take place.
6. NiMH batteries are used by some electric vehicles and have proved to be very effective.
7. Thermal batteries use an electrolyte that is solid and inactive at normal ambient temperatures.
8. Sodium-based batteries must operate at high temperatures between 400 and 700°C, with newer designs running at temperatures between 245 and 350°C.
9. Today's batteries have an energy density of approximately 140 Wh/kg or more in some cases, but have the potential to go as high as 280 Wh/kg.
10. Lithium-ion movement is slower during the charging process if the battery is cold.
11. Sophisticated battery management can further increase the range of a car by up to 10%, without altering the cell chemistry.
12. The energy of oxidation of conventional fuels can be converted directly into electricity in a fuel cell.
13. A unit consisting of many individual fuel cells is often referred to as a stack.
14. The working temperature of fuel cells varies but about 200°C is typical. High pressure is also used and this can be of the order of 30 bar.
15. Super- or ultra-capacitors are very high capacity but (relatively) low-size capacitors.
16. Flywheel systems offer an interesting alternative to batteries or super-capacitors.

Charging

6.1 Charging, standards and infrastructure

6.1.1 Infrastructure

Most electric cars will be charged at home, but national infrastructures are developing. There are, however, competing organizations and commercial companies, so it is necessary to register with a few different organizations to access their charging points. Many businesses now also provide charging stations for staff and visitors. Some are pay in advance, some are pay as you go, and others require a monthly subscription. Many apps and websites are available for locating charge points. One of the best I have found is <https://www.zap-map.com>

Interestingly, having just completed a roundtrip UK journey in my PHEV of about 600 miles, I did not find any charging points on the main roads and would have had to search local towns for the facilities. I wonder why they are not available in service areas where fuel is sold by multinational oil companies...

Safety note:

Although the rechargeable electric vehicles and equipment can be recharged from a domestic wall socket, a charging station has additional current or connection-sensing mechanisms to disconnect the power when the EV is not charging. There are two main types of safety sensor:

- Current sensors, which monitor the power consumed and only maintain the connection if the demand is within a predetermined range.
- Additional sensor wires, which provide a feedback signal that requires special powerplug fittings.

The majority of public charge points are lockable, meaning passers-by cannot unplug the cable. Some charge points can send a text message to the car owner if the vehicle is unexpectedly unplugged, or tell you when the vehicle is fully charged.

It is safe to charge in wet weather. When you plug in the charge lead, the connection to the supply is not made until the plug is completely in position. Circuit breaker devices are also used for additional safety. Clearly some common sense is necessary, but EV charging is very safe.

Domestic charge points: It is strongly recommended that home charging sockets and wiring are installed and approved by a qualified electrician. A home charge point with its own dedicated circuit is the best way of charging an EV safely. This will ensure the circuit can manage the electricity demand from the vehicle and that the circuit is activated only when the charger communicates with the vehicle, known as the ‘handshake’. For rapid charging, special equipment and an upgraded electrical supply would be required and is therefore unlikely to be installed at home, where most consumers will charge overnight.



Figure 6.2 Charging point (Source: RichardWebb, <http://www.geograph.ie>)



Figure 6.1 Charging point on the roadside
(Source: Rod Allday, <http://www.geograph.org.uk>)



Figure 6.3 Charging at home



Figure 6.4 Domestic charging point

6.1.2 Charging time

How long it takes to charge an EV depends on the type of vehicle, how discharged the battery is and the type of charge point used. Typically, pure-electric cars using standard charging will take between 6 and 8 hours to charge fully and can be ‘opportunity charged’ whenever possible to keep the battery topped up. Pure-EVs capable of using rapid chargepoints could be fully charged in around 30 minutes and can be topped up in around 20 minutes, depending on the type of charge point and available power. PHEVs take approximately 2 hours to charge from a standard electricity supply. E-REVs take approximately 4 hours to charge from a standard electricity supply. PHEVs and E-REVs require less time to charge because their batteries are smaller.

Table 6.1 Estimated charging times

Charging time for 100-km range	Power supply	Power	Voltage	Max. current
6–8 hours	Single phase	3.3 kW	230 V AC	16 A
3–4 hours	Single phase	7.4 kW	230 V AC	32 A
2–3 hours	Three phase	10 kW	400 V AC	16 A
1–2 hours	Three phase	22 kW	400 V AC	32 A
20–30 minutes	Three phase	43 kW	400 V AC	63 A
20–30 minutes	Direct current	50 kW	400–500 V DC	100–125 A
10 minutes	Direct current	120 kW	300–500 V DC	300–350 A

6.1.3 Cost

The cost of charging an EV depends on the size of the battery and how much charge is left in the battery before charging. As a guide, charging an electric car from flat to full will cost from as little as £1 to £4. This is for a typical pure-electric car with a 24 kWh battery that will offer around 100-mile range. This results in an average cost of a few pence per mile.

If you charge overnight you may be able to take advantage of cheaper electricity rates when there is surplus energy. The cost of charging from public points will vary; many will offer free electricity in the short term. It is also possible to register with supply companies who concentrate on energy from renewable sources.

6.1.4 Standardization

So that electric vehicles can be charged everywhere with no connection problems, it was necessary to standardize charging cables, sockets and methods. The IEC publishes the standards that are valid worldwide, in which the technical requirements have been defined. [Table 7.2](#) below lists some of the most important standards associated with the charging of EVs:

Types of charging cables: IEC 61851-1 defines the different variants of the connection configuration:

Table 6.2 Charging standards

IEC 62196-1	IEC 62196-2	IEC 62196-3	IEC 61851-1	IEC 61851-21-1	IEC 61851-21-2	HD 60364-7-722
Plugs, socket-outlets, Vehicle connectors and vehicle inlets. Conductive Charging of electric Vehicles	Dimensional compatibility and interchangeability requirements for AC pin and contact tube accessories. The permissible plug and socket types are described	Dimensional compatibility and interchangeability requirements for dedicated DC and combined AC/DC pin and contact-tube vehicle couplers	Electric vehicle Conductive Charging system. Different variants of the Connection configuration, as well as the basic Communication with the vehicle, are defined in this Standard	Electric vehicle conductive charging systems. Electric vehicle on-board charger EMC requirements For conductive connection to an AC/DC supply	Electric vehicle conductive charging systems EMC requirements for off-board electric vehicle charging systems	Low-voltage electrical installations. Requirements for special Installations supply of Electric Vehicles

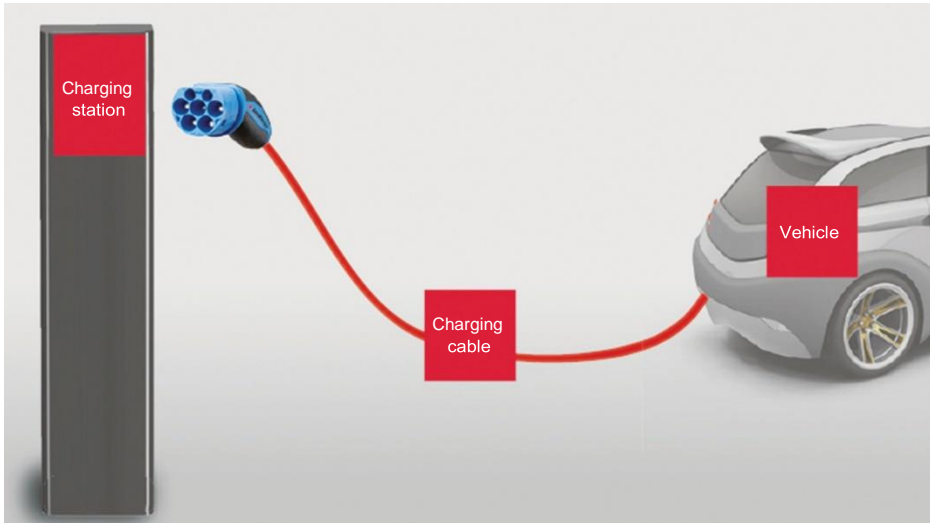


Figure 6.5 Case A: The charging cable is permanently connected to the vehicle (Source: Mennekes)

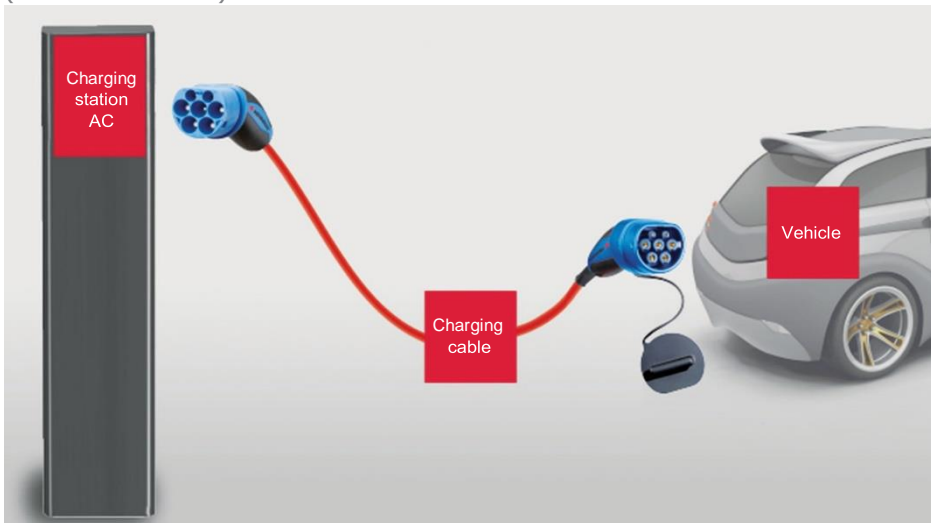


Figure 6.6 Case B: The charging cable is not permanently connected to the vehicle or the charging station (Source: Menneke)



Figure 6.7 Case C: The charging cable is permanently connected to the charging station
 (Source: Mennekes)

6.1.5 Charging methods

AC charging: Alternating current charging has now established itself as the standard charging method. It is possible in the private sector, as well as at charging stations in the semi-public and public sector, with relatively low investments. Consequently, this charging method also has a long-term future. Standard charging occurs via an alternating current connection and is the most common and most flexible charging method. In charging modes 1 and 2, charging is possible on household sockets or on CEE sockets. On the household socket, charging can take up to several hours due to the power limited through the socket, depending on rechargeable battery capacity, fill level and charging current. In charging mode 3 a vehicle can be charged at a charging station where power of up to 43.5 kW is possible with a significantly reduced charging time. Particularly in the private sector, the usable power is limited by the fuse protection of the building connection. Charging powers to maximum 22 kW at 400 V AC are usually the high power limit for home charging stations.

The charging device is permanently installed in the vehicle. Its capacity is adjusted to the vehicle battery. Compared with other charging methods, the investment costs for AC charging are moderate

DC charging: With direct current charging there is a distinction between

- DC low charging: up to 38 kW with type 2 plugs
- DC high charging: up to 170 kW.

The charging device is part of the charging station, so DC charging stations are significantly more expensive as compared with AC charging stations. The prerequisite for DC charging is an appropriate network of charging stations, which due to the high power require high infrastructure investments. Fast charging with high currents requires appropriately dimensioned line cross-sections that make connecting the vehicle to the charging station more cumbersome. Standardization of the DC charging connection has not yet been concluded and market availability is still uncertain. In practice, vehicles with a DC charging connection have an additional connection for standard charging so that the vehicle can also be charged at home.

Inductive charging: Charging occurs without contacts via inductive loops. The technical complexity and thus the costs are considerable, for the charging stations as well as the vehicle. This system is not yet ready for the market or for large-scale production.

Battery replacement: The vehicle's rechargeable battery is replaced with a fully charged battery at the change station. In this case you can continue driving after a few minutes. The prerequisite for this concept would be that vehicle manufacturers would have to install standardized rechargeable batteries at standardized positions in the vehicle. However, such standardization would hardly be possible due to the different vehicle types and uses. The charge stations would have to keep battery types for the different vehicles on hand, which in practice would be equally difficult. Consequently, battery replacement could only be implemented today in closed fleets.

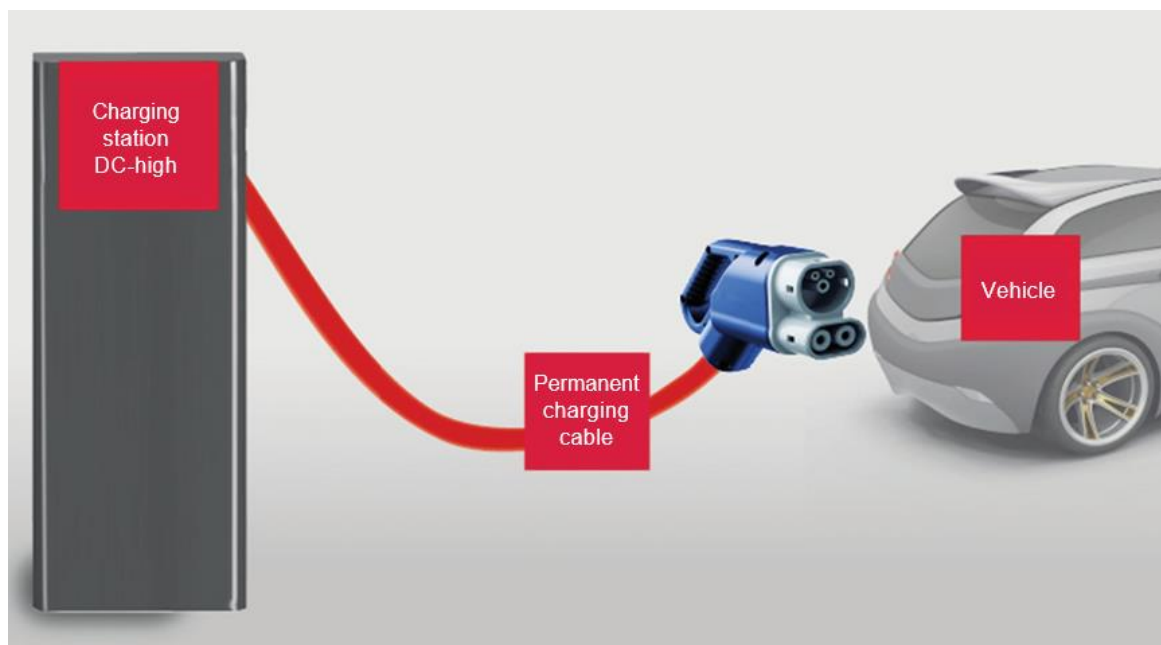


Figure 6.8 DC high charging

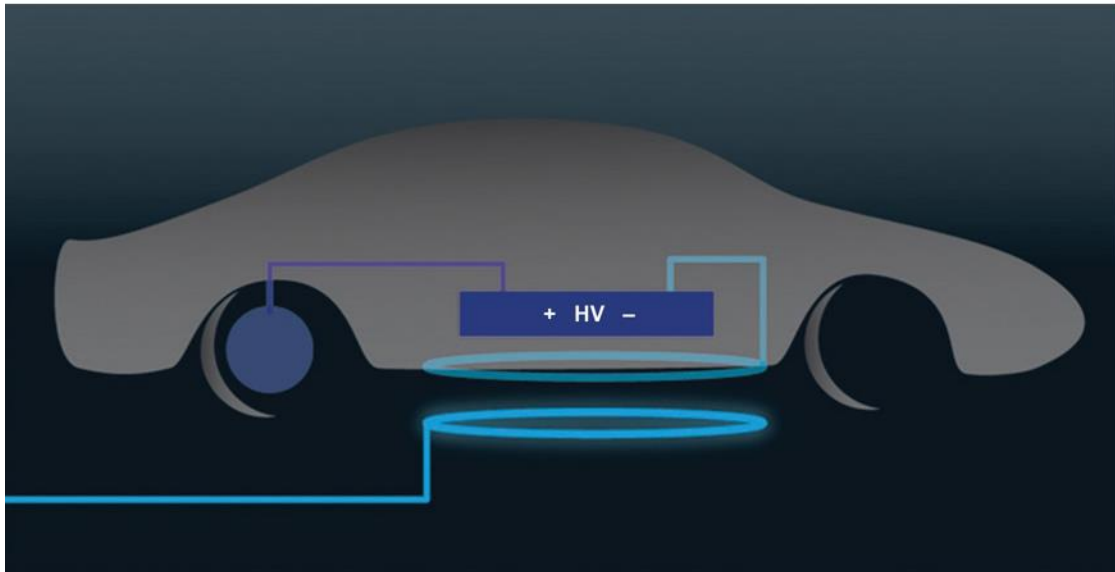


Figure 6.9 Inductive charging

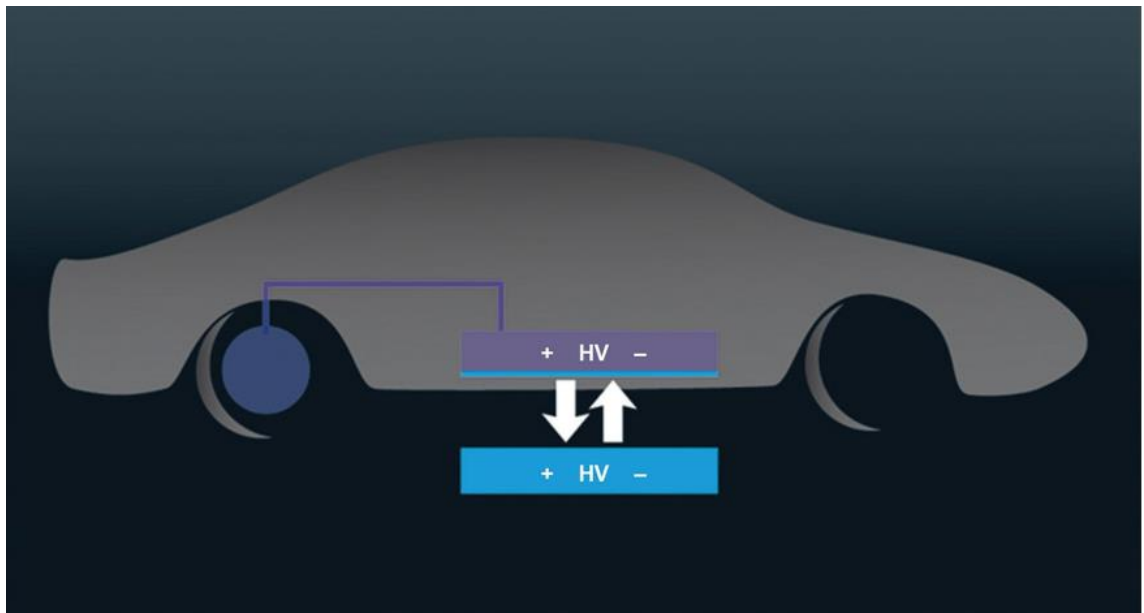


Figure 6.10 Replacement batteries

6.1.6 Charging modes

Four different charging modes have been defined for safe charging of electric vehicles in line with demand. These charging modes differ relative to the power source used (protective contact, CEE, AC or DC charging socket), and they differ relative to the maximum charging power and the communication possibilities.

Mode 1: Charging from a socket to max 16 A three-phase without communication with the vehicle. The charging device is integrated in the vehicle. Connection to the energy network occurs via an off-the-shelf, standardized plug and socket that must be fused via a residual current protective device. This method is not recommended because mode 2 offers greater safety thanks to communication with the vehicle.

Mode 2: Mode for charging from a socket to max. 32 A, three-phase with a control function and protective function integrated in the cable or the wall-side plug. The charging device is installed in

the vehicle. Connection to the energy network occurs via an off-the-shelf, standardized plug and socket. For mode 2 the standard prescribes a mobile device to increase the level of protection. Moreover, for the power setting and to satisfy the safety requirements, a communication device is required with the vehicle. These two components are combined in the In-Cable Control Box (ICCB).



Figure 6.11 In-Cable Control Box (ICCB)

Mode 3: Mode for charging at AC charging stations. The charging device is a fixed component of the charging station and includes protection. In the charging station PWM communication, residual current device (RCD), overcurrent protection, shutdown, as well as a specific charging socket are prescribed. In mode 3 the vehicle can be charged three-phase with up to 63 A so a charging power of up to 43.5 kW is possible. Depending on rechargeable battery capacity and charge status, charges in less than 1 hour are possible.

Mode 4: Mode for charging at DC charging stations. The charging device is a component of the charging station and includes protection. In mode 4 the vehicle can be charged with two plug-and-socket systems, both of which are based on the Type 2 plug geometry.

The 'Combined Charging System' has two additional DC contacts to 200 A and up to 170 kW charging power. The other option is a plug and socket with lower capacity for a charge to 80 A and up to 38 kW in Type 2 design. Standards continue to be reviewed and changed to improve safety and ease of use as well as compatibility.

6.1.7 Communication

Basic communication: Safety check and charging current limitation is determined. Even before the charging process starts, in charging modes 2, 3 and 4 PWM communication with the vehicle occurs via a connection known as the control pilot (CP) line. Several parameters are communicated and coordinated. The charging will only begin if all security queries clearly correspond to the specifications and the maximum permissible charging current has been communicated. These test steps are always executed:

- 1 The charging station locks the infrastructure side charging coupler.
- 2 The vehicle locks the charging coupler and requests start of charging.
- 3 The charging station (in mode 2 the control unit in the charging cable) checks the connection of the protective conductor to the vehicle and communicates the available charging current.
- 4 The vehicle sets the charger accordingly.

If all other prerequisites are met, the charging station switches the charging socket on.

For the duration of the charging process, the protective conductor is monitored via the PWM connection and the vehicle has the possibility of having the voltage

supply switched off by the charging station. Charging is ended and the plugs and sockets are

unlocked via a stop device (in the vehicle).

Limitation of the charging current: The vehicle's charging device determines the charging process. To prevent the vehicle charging device from overloading the capacity of the charging station or of the charging cable, the power data of the systems is identified and adjusted to match. The CP box reads the power data of the cable from the cable. Before the charging process is started, the box communicates the power data to the vehicle via PWM signal, the vehicle's charging device is adjusted accordingly and the charging process can begin, without the possibility of an overload situation occurring.

The weakest link in the charging chain determines the maximum charging current: The charging current in the charger is limited depending on the power of the charging station and the resistance coding in the plug of the charging cable.

6.1.7.1 EU system

Due to the communication and safety devices used, charging couplers do not need a shutter. However, in some European countries national regulations for household couplers are applied to these charging couplers for charging of electric vehicles. Mennekes has developed an add-on for Type 2. Thus a modular system has been produced that enables the Type 2 socket to be equipped with a shutter. In countries that do not have these requirements, the shutter is simply omitted. Thus Type 2 is a solution for all of Europe.

6.1.7.2 Charging plugs

Worldwide, three different plug-and-socket systems are standardized in IEC 62196-2 for connection of electric vehicles; these three systems are not compatible. Basically, all three standardized systems meet the high safety requirements for the consumer. Voltage is only switched on when the system has detected that the plugs on the vehicle side and infrastructure side are completely plugged in, that the plugs are locked, and that the protective conductor connection is correct. As long as one of these conditions is not satisfied, the contacts will remain de-energized.

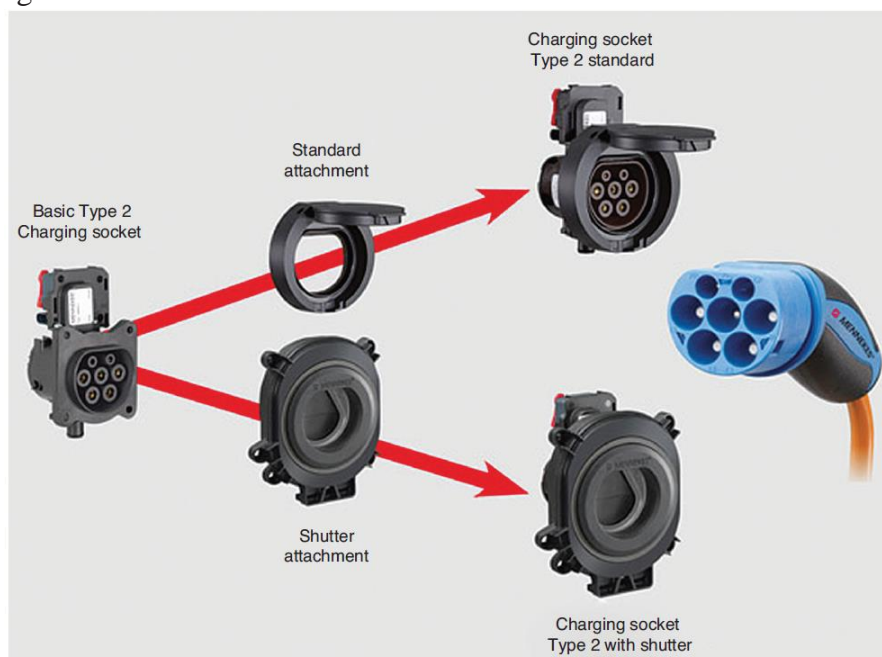


Figure 6.12 Type 2 system with and without shutter (Source: Mennekes)

Type 1 is a single phase charging plug developed in Japan exclusively for the vehicle-side charging connection. The maximum charging power is 7.4 kW at 230 V AC. Type 1 offers insufficient possibilities for the three-phase European networks.



Figure 6.13 Type 1 plug

Type 2 is the EU charging plug developed in Germany by Mennekes. This is appropriate to single phase alternating current in the private household to the powerful three-phase connection with 63 A. With the EU charging plug at a connection voltage of 230 V single phase, or 400 V three-phase, charging powers from 3.7 kW to 43.5 kW can be transmitted – with identical plug geometry. Type 2 is also the basis for the combined charging system for DC charging. Type 2 plugs and sockets can be used on the vehicle-side as well as on the infrastructure-side. Due to the extensive electronic safety architecture, there is no need for a mechanical touch guard in the charging plug or charging connector.



Figure 6.14 Type 2 plug. The pins from the top left and clockwise are: Proximity (PP), Control pilot (CP), Neutral (N), L3, L2, L1 and the Earth pin in the centre (Source: Mennekes)

Type 3 variant was developed in Italy. It is suitable for a connection voltage of 30 V single phase or 400 V three-phase for charging powers from 3.7 kW to 43.5 kW. However, three different plug geometries that are not compatible with each other are required for the different power levels. For the information in the previous sections I am most grateful to Mennekes (<http://www.mennekes.de>)



Figure 6.15 Type 3 plug

6.1.8 Vehicle-to-grid technology

Vehicle-to-grid (V2G) is a system that uses bidirectional power from the car to the grid as well as the normal charging routine of grid to car. If this system is employed the car battery can be used as a power back-up for the home or business. If the car is primarily charged from renewable sources such as PV panels or wind generation then returning this to the grid is not only ecologically beneficial, it is also an ideal way of stabilizing fluctuations of demand in the grid. The potential problem is managing inrush currents if lots of vehicles fast charge at the same time. This notion is a little way into the future at the time of writing (2015), but the concept of the ‘smart grid’ using techniques such as this is not far off.

6.1.9 Tesla Powerwall

While not an EV technology, the Tesla Powerwall is a spin-off and if combined with home solar charging it could have a significant impact on EV use. Powerwall is a home battery that charges using electricity generated from solar panels, or when utility rates are low, and powers your home in the evening. It also safeguards against power outages by providing a back-up electricity supply. Automated, compact and simple to install, Powerwall offers independence from the utility grid and the security of an emergency back-up. The average home uses more electricity in the morning and evening than during the day when solar energy is plentiful. Without a home battery, excess solar energy is often sold to the power company and purchased back in the evening. This mismatch adds demand on power plants and increases carbon emissions. Powerwall bridges this gap between renewable energy supply and demand by making your home’s solar energy available to you when you need it. Home solar installations consist of a solar panel, an electrical inverter, and now a home battery to store surplus solar energy for later use.

- ▶ Solar panel: Installed in an array on your roof, solar panels convert sunlight into electricity.
- ▶ Home battery: Powerwall stores surplus electricity generated from solar panels during the day or from the utility grid when rates are low.
- ▶ Inverter: Converts direct current electricity from solar panels or a home battery into the alternating current used by your home’s lights, appliances and devices.

Contained within Powerwall's outdoor-rated enclosure is a rechargeable lithium-ion battery, a liquid thermal management system, a battery management system and a smart DC-DC converter for controlling power flow. The batteries are 7 or 10 kW/h.

6.2 Wireless power transfer

6.2.1 Introduction

Range anxiety continues to be an issue to EV acceptance. Wireless power transfer (WPT) is a means to increase the range of an electric vehicle without substantial impact on the weight or cost. WPT is an innovative system for wirelessly charging the batteries in electric vehicles. There are three categories:

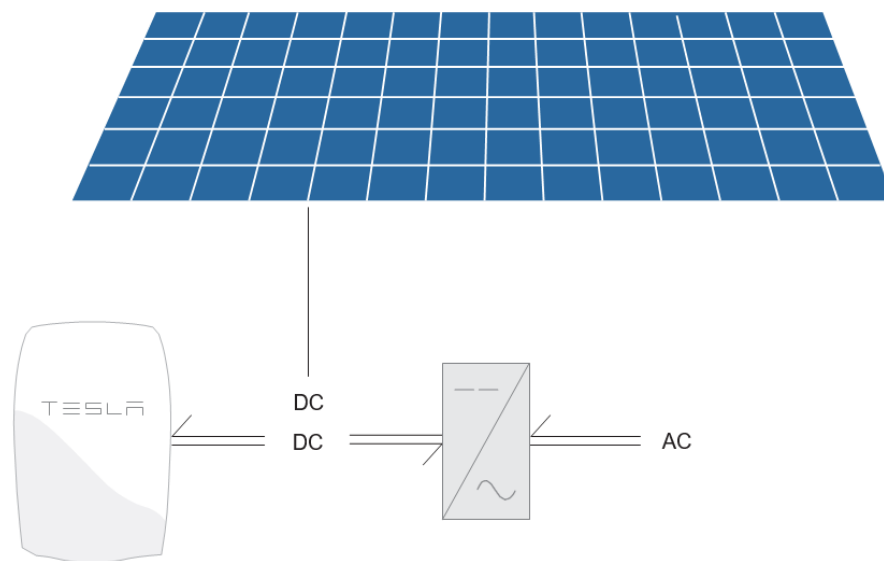


Figure 6.16 Tesla Powerwall System (Source: Tesla)



Figure 6.17 Powerwall (Source: Tesla)

- stationary WPT: vehicle is parked, no driver is in the vehicle
- quasi-dynamic WPT: vehicle stopped, driver is in the vehicle
- dynamic WPT: vehicle is in motion.

There are also three WPT power classes (SAEJ2954):

- Light Duty Home: 3.6 kW

- Light Duty Fast Charge: 19.2 kW
- High Duty: 200–250 kW.

With stationary charging, the electric energy is transferred to a parked vehicle (typically without passengers on board). It is important to keep the geometrical alignment of primary and secondary within certain tolerance values in order to ensure a sufficient efficiency rate of the energy transfer.

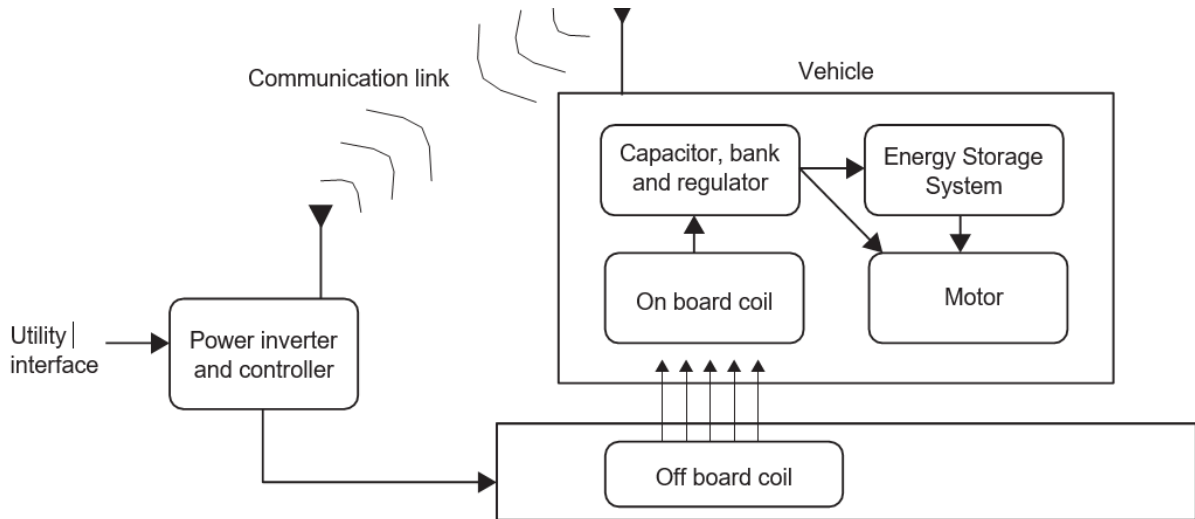


Figure 6.18 WPT principle (Source: CuiCAR)

With quasi-dynamic wireless charging the energy is transferred from the road-side primary coil system of limited length to the secondary coil of a slowly moving, or in stop-and-go mode moving, vehicle (with passengers).

With dynamic wireless charging the energy is transferred via a special driving lane equipped with a primary coil system at a high power level to a secondary coil of a vehicle moving with medium to high velocity.

Stationary WPT

Electric vehicles simply park over an induction pad and charging commences automatically. WPT requires no charging poles or associated cabling. It can accommodate differing rates of charge from a single on-board unit and the rate of charge or required tariff can be set from within the vehicle. It has no visible wires or connections and only requires a charging pad buried in the pavement and a pad integrated on to the vehicle.

The system works in a range of adverse environments including extremes of temperature, while submerged in water or covered in ice and snow. It will operate under asphalt or embedded in concrete and is also unaffected by dust or harsh chemicals. WPT systems can be configured to power all road-based vehicles from small city cars to heavy goods vehicles and buses.

A company called haloIPT (inductive power transfer) developed a technique where power at a frequency, usually in the range 20–100 kHz, can be magnetically coupled across IPT pads, which are galvanically isolated from the original source of power. A conceptual system is shown below. This comprises two separate elements. A primary-side power supply, with track and a secondary-side pick-up pad, with controller.

The power supply takes electrical power from the mains supply and energizes a lumped coil, with a current typically in the range 5–125 A. Since the coil is inductive, compensation using series or parallel capacitors may be required to reduce the working voltages and currents in the supply circuitry. These capacitors also ensure an appropriate power factor.

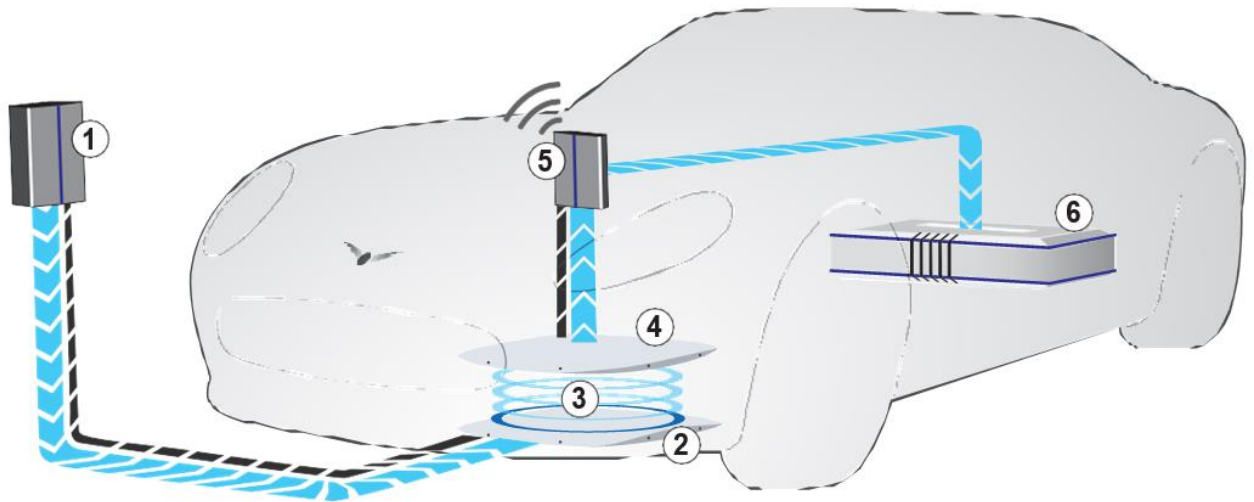


Figure 6.19 An inductive wireless charging system for statically charging an EV: 1, power supply; 2, transmitter pad; 3, wireless electricity and data transfer; 4, receiver pad; 5, system controller; 6, battery (Source: haloIPT)

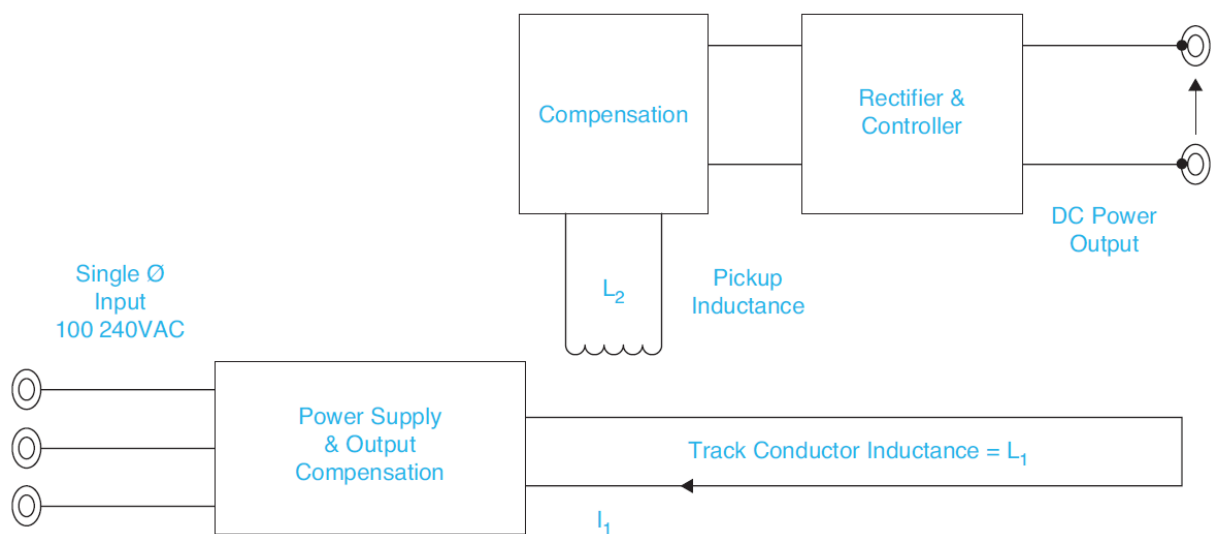


Figure 6.20 Conceptual wireless IPT charging system (Source: haloIPT)

Pick-up coils are magnetically coupled to the primary coil. Power transfer is achieved by tuning the pick-up coil to the operating frequency of the primary coil with a series or parallel capacitor. The power transfer is controllable with a switch-mode controller.

A block diagram for a single-phase wireless charger is shown as [Figure 7.21](#). The main supply is rectified with a full bridge rectifier

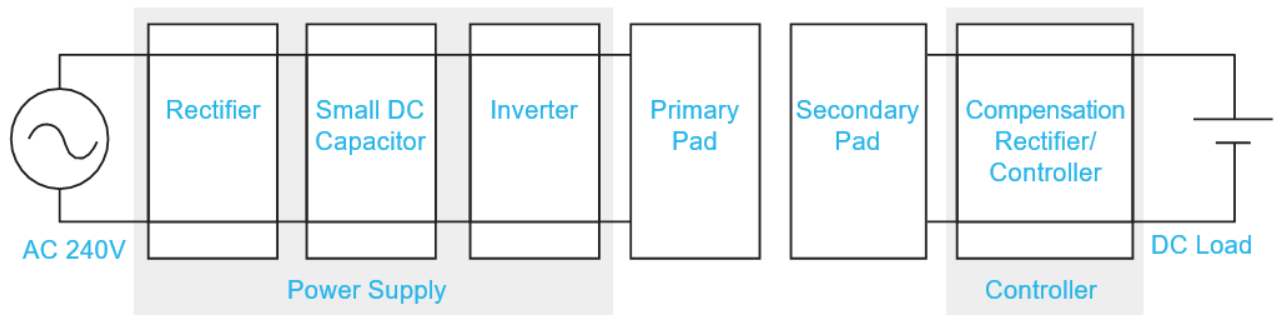


Figure 6.21 IPT (WPT) system components (Source: haloIPT)

followed by a small DC capacitor. Keeping this capacitor small helps the overall power factor and allows the system to have a fast start-up with a minimal current surge. The inverter consists of an H-bridge to energize the tuned primary pad with current at 20 kHz. The 20 kHz current also has a 100 Hz/120 Hz envelope as a result of the small DC bus capacitor. Power is coupled to the secondary tuned pad. This is then rectified and controlled to a DC output voltage appropriate to the vehicle and its batteries. The conversion from AC to DC and back to AC, in the power supply side, is necessary so the frequency can be changed

The system includes three distinct hardware components:

- 1 High-frequency generator or power supply.
- 2 Magnetic coupling system or transmitter/receiver pads.
- 3 Pick-up controller/compensation.

The high-frequency generator takes a mains voltage input (240 V AC at 50/60 Hz) and produces high-frequency current (>20 kHz). The output current is controlled and the generator may be operated without a load. The efficiency of the generator is high at over 94% at 2 kW. The generator comprises the following:

- mains filter (to reduce EMI)
- rectifier
- bridge (MOSFETs) converting DC to high-frequency
- combined isolating transformer/AC inductor
- tuning capacitors (specified for frequency and output current)
- control electronics (microcontroller, digital logic, feedback and protection circuits).

The design and construction of the transmitter and receiver pads gives important improvements over older pad topologies. This results in better coupling, lower weight and a smaller footprint, for a given power transfer and separation. The pads can couple power over gaps of up to 400 mm. The coupling circuits are tuned through the addition of compensation capacitors.

A pick-up controller takes power from the receiver pad and provides a controlled output to the batteries, typically ranging from 250 V to 400 V DC. The controller is required to provide an output that remains independent of the load and the separation between pads. Without a controller, the voltage would rise as the gap decreased and fall as the load current increased.

6.2.2 Dynamic WPT

It seems illogical in many ways but the prospect of wirelessly charging an EV as it drives along a road is already possible and being trialled in a number of countries. The principle is fundamentally the same as static wireless charging but even more complex.

The technology is known as wireless power transfer (WPT).

The challenges with this technology are:

- synchronization of energizing coils (timing of power transfer)
- acceptable power levels
- vehicle alignment
- allowable speed profiles
- multiple vehicles on charging lane.

A number of feasibility studies and trials are ongoing (2015) and it is expected that this system will be available in the near future. The following image shows the principle of dynamic WPT.

Driver assistance systems may play a role in combination with wireless charging. With stationary wireless charging, a system could be developed where the vehicle is parked automatically and at the same time primary and secondary coils are brought into perfect alignment. With quasi-dynamic and dynamic charging the vehicle speed as well as horizontal and vertical alignment could be automatically adapted by dynamic cruise control and lane assist. This would increase the efficiency rate of the energy transfer because of the need to synchronize energy transfer via the coil systems.

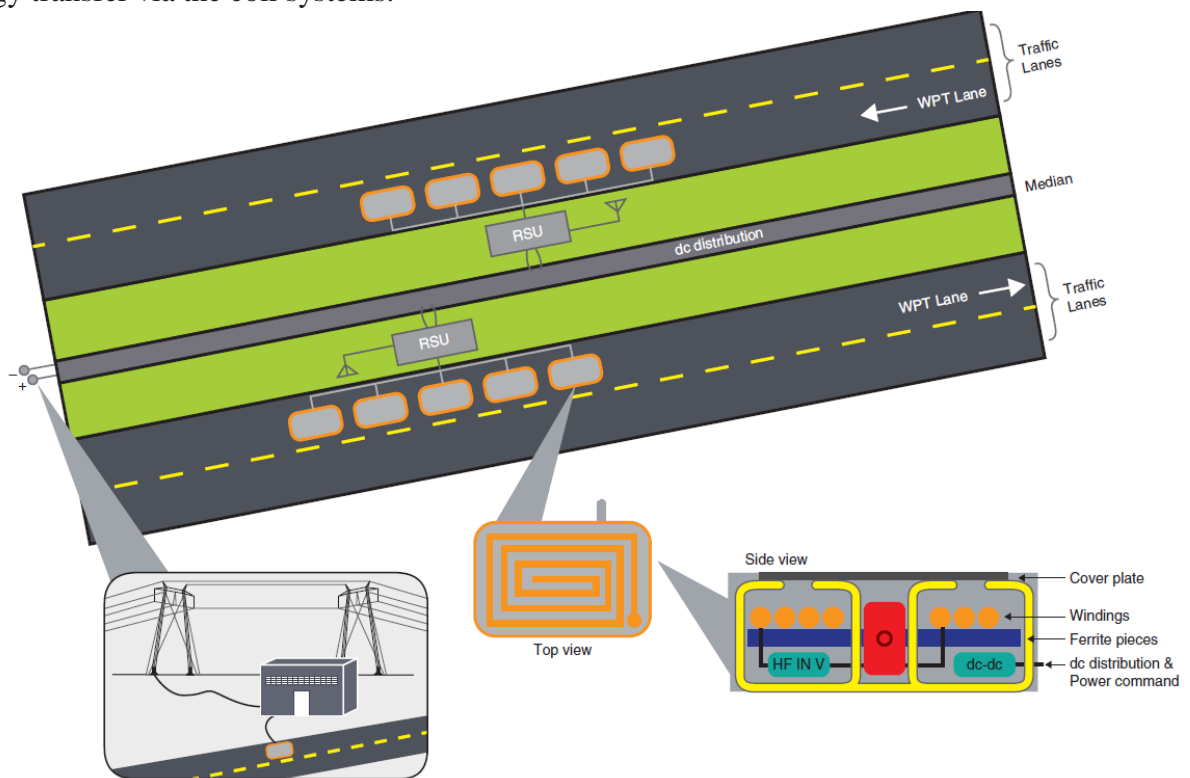


Figure 6.22 Principle of dynamic wireless charging – RSU is a road side unit (Source: OakridgeNational Lab)

Communication will be essential to exchange standardized control commands in real time between the grid and the vehicle control systems. For safety reasons, vehicles in other lanes and other users of the main coil system in the charging lane need to be monitored in real time. Dedicated short-range communication (IEEE 802.11p) is a likely technology that will be used for low-latency wireless communication in this context.

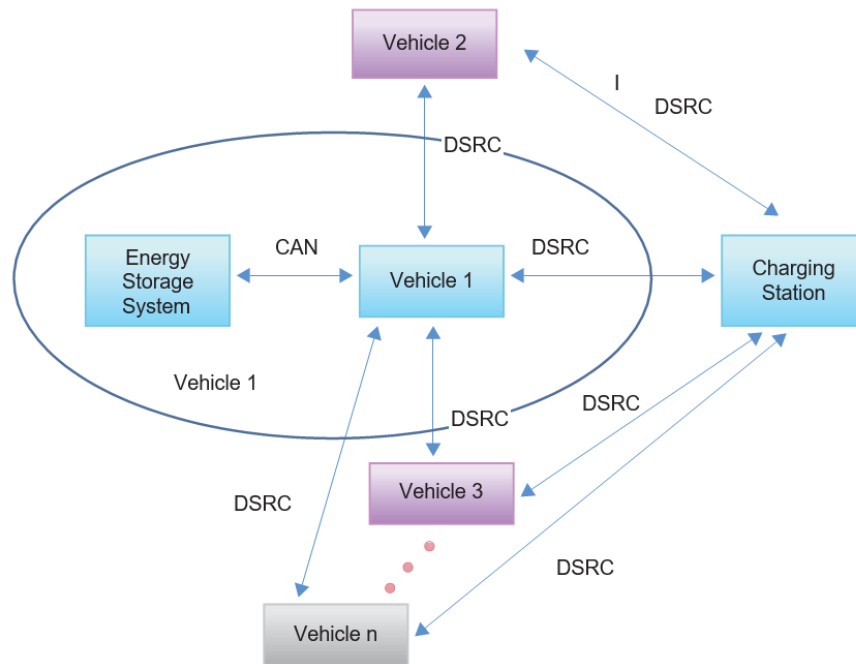


Figure 6.23 Communication is essential for dynamic WPT

Finally, powerful electromagnetic fields are used in the active charging zone between primary and secondary coils. For human safety in this respect, compliance with international standards needs to be achieved.

6.3 Solar charging case study

In January 2015 I started running an experiment using domestic solar panels, energy saving and monitoring systems, and a plug-in hybrid car. The key part of the plan was to see if I could run the car for free – or at least at very low cost. The 4-kW array of panels was fitted and commissioned on 16 January 2015.

The following charts will show how much electricity (in kilowatt hours; kWh) my panels generated each week compared with my electricity use from the grid, and in due course, the amount used to charge the car. At the end of week 1, they generated 22 kWh; considering the snow and the time of year, I was reasonably impressed!

On 31 January I generated over 1 kW, even with snow, and was generating about 25 kWh a week. The solar plot on [Figure 7.27](#) is effectively a measure of the amount of weekly sunshine. The other interesting issue is a matter of timing, because if you use electricity during the night it will come from the grid regardless of how much was generated by the panels during the day. This was something to consider when the car arrived.

My PV array has saved me buying a lot of electricity and has further resulted in an income. Over a period of six months I have received about £400 by selling the excess energy back to the grid (using what is known as a feed-in tariff). In addition, my electricity bill has reduced considerably.

As you would expect, we pay much more for the electricity we use than the price we get when selling it (something like 14p per unit when buying and 3p per unit – a kWh – when selling). The way the feed-in tariff works is that the electricity generation company pays us for 50% of the amount generated by the PV panels. So the more we generate the more we get, but of course the other advantage is gained because the more of the PV energy we use, the less electricity we purchase.



Figure 6.24 DC panel connections

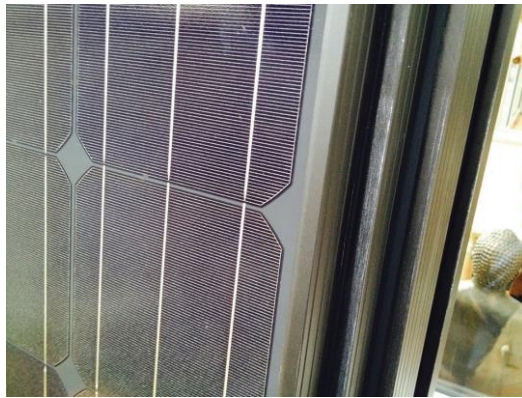


Figure 6.25 Photo voltaic (PV) cell arrangement



Figure 6.26 A 4kW array of PV panels (ten front and six more at the back)

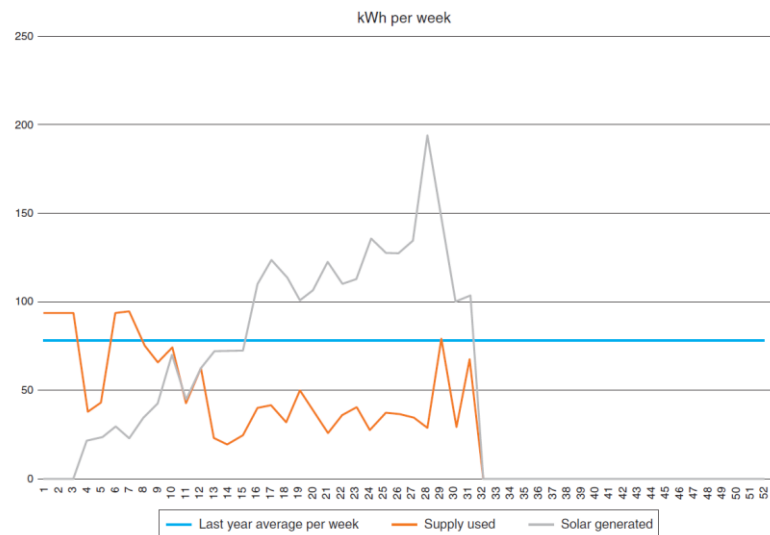


Figure 6.27 Over time it is clear how the solar generated increased and my use from the grid decreased

References

Denton, T. (2013) *Automobile Electrical and Electronic Systems*. Routledge, London.

Larminie, J. and Lowry, J. (2012) *Electric Vehicle Technology Explained, Second Edition*. John Wiley & Sons, Chichester.

Bosch (2011) *Automotive Handbook*. SAE Electrical installations and shock information:

<http://www.electrical-installation.org/enwiki/> Electric_shock

Flybrid flywheel systems: <http://www.flybridsystems.com>

Health and Safety Executive UK: <https://www.hse.gov.uk>

Institute of the Motor Industry (IMI): <http://www.theimi.org.uk>

Mennekes (charging plugs): <http://www.mennekes.de>

Mi, C., Abul Masrur, M. and Wenzhong Gao, D. (2011) *Hybrid Electric Vehicles*. John Wiley & Sons, Chichester.

Picoscope: <https://www.picoauto.com>

Renesas motor and battery control system: <http://www.renesas.eu>

Society of Automotive Engineers (SAE): <http://www.sae.org>

Society of Motor Manufacturers and Traders(SMMT): <http://www.smmt.co.uk>

Tesla Motors first responder information: <https://www.teslamotors.com/firstresponders>

Wireless power transfer: <https://www.qualcomm.com/products/halo>

ZapMap charging point locations: <https://www.zap-map.com>

Question Bank

Short Answer

Q.No	Questions	CO (L)
1	Choose the factors that affect the EV range.	CO5(L5)
2	Justify why Lithium-ion battery considered as non-hazardous	CO5(L5)
3	Value end of life for the battery is decided by manufacturer	CO5(L5)
4	List the types of batteries are used in the storage system	CO5(L4)
5	Justify why NiCad batteries do not suffer from over-charging	CO5(L5)
6	List the main components of the nickel-cadmium battery	CO5(L4)
7	Justify why battery management system is required in electric vehicle.	CO5(L5)
8	List the types of fuel cell that use methanol	CO5(L4)
9	List the safety measures are used in charging station	CO6(L4)
10	List the charging methods of the electric vehicle	CO6(L4)
11	Discuss the term V2G in electric vehicle	CO6 (L6)
12	List the WPT power classes	CO6(L4)

Long Answer

Q.No	Questions	CO (L)
1	Explain the stationary and dynamic WPT of charging a battery compare them in detail.	CO6(L5)
2	With necessary diagram explain each part of the Tesla Roadster electric vehicle	CO6(L5)
3	Explain the different modes of charging a battery compare them in detail.	CO6 L5)
4	Justify why Lithium-ion battery is used in EV? Explain the storage technology with neat sketch.	CO5(L5)
5	Justify why Lead-acid battery is used in EV? Explain the storage technology with neat sketch.	CO5(L5)
6	With necessary diagram explain each part of the General motor EV-1 electric vehicle	CO6(L5)
7	Explain the fuel cell energy production technology in electric vehicle with neat sketch.	CO5(L5)
8	With necessary diagram explain each part of the V2G electric vehicle	CO6(L5)